Ethnopharmacological survey and phytochemical investigation of Maasai traditional medicinal plants from north-eastern Tanzania

Dissertation

Submitted to the Faculty of Chemistry and Pharmacy,

University of Regensburg for the degree of

Doctor of Natural Sciences (Dr. rer. nat.)

Presented by

Edna Makule

From Arusha, Tanzania

2015

Gedruckt mit Unterstutzung des Deutschen Akademischen Austauschdienstes.

The present work was carried out from October, 2012 until November, 2015 under the supervision of Prof. Dr. Jörg Heilmann and Dr. Birgit Kraus at the Institute of Pharmacy, Faculty of Chemistry and Pharmacy, University of Regensburg.

Dissertation submitted on: 16. 11. 2015

Oral presentation on: 21. 12. 2015

Examination committee:	PD Dr. Sabine Amslinger	(Chairperson)
	Prof. Dr. Jörg Heilmann	(First examiner)
	Prof. Dr. Ulrike Lindequist	(Second examiner)
	Prof. Dr. Gerhard Franz	(Third examiner)

Acknowledgements

First and foremost, I would like to thank the almighty GOD who is the essence of everything for giving me life and immense strength throughout the course of this PhD work. For him all things are possible.

I am sincerely grateful to my supervisor Prof. Dr. Jörg Heilmann, for having trust in me in the first place and giving me an opportunity to pursue my PhD studies under his supervision. His expertise, generous support, guidance, valuable ideas and suggestions, have made it possible for me to accomplish the work on the topic that was interesting for me.

My heartfelt gratitude to my co-supervisor Dr. Birgit Kraus, for her kind supervision, tireless guidance, encouragement, problems solving ability, valuable suggestions, constructive ideas throughout the time of my doctorial research. Besides, a friend to rely on. I am indebted to her more than she knows.

I am thankful to Dr. Guido Jürgenliemk for introducing me to the first analytics procedures, his willingness to help, advice, comments, corrections, as well as for providing tips and analytical tricks whenever I consulted him, were honored.

I would like to thank Mrs. Gabriele Brunner for her technical advice during the whole period of my lab work and tips for column chromatography.

I am thankful to all my colleagues, who have finished and those who are still pursuing the PhDs at the department of Pharmaceutical Biology - University of Regensburg: Dr. Sebastian Schmidt, Dr. Marcel Flemming, Dr. Daniel Bücherl, Dr. Rosmarie Scherübl, Dr. Petr Jirásek, Dr. Beata Kling, Dr. Tri Hieu Nguyen, Monika Untergehrer, Markus Löhr, Stefan Wiesneth, Eva Lotter, Ilya Volkov, Christian Zeh, Katharina Schiller, Julianna Ziegler, Sebastian Schwindl and Sina Malenke. I appreciate their valuable help, technical discussions and mutual support which made my work in the lab smooth and enjoyable.

My sincere appreciations are extended to the following:

Mr. Fritz Kastner at the NMR department – University of Regensburg, for performing all the NMR measurements.

Mr. Josef Kiermaier at the Mass spectrometry department- University of Regensburg, for carrying out all mass spectra measurements.

PD Dr. Axel Dürkop from the department of Analytical Chemistry – University of Regensburg, for performing measurements of all the CD spectra.

Prof. Dr. Thomas Schmidt from the Institute of Pharmaceutical Biology and Phytochemistry – University of Münster, for carrying out CD calculations.

Mr. Daniel Sitoni from Tanzania National Herbarium, Arusha, and Mr. Canisius Kayombo from Olmotonyi Forestry Institute, Arusha, for a great assistance in plants identification during ethnopharmacological field work.

Mr. Victor Makundi for analyzing the GPS data recorded during ethnopharmacological field work and fixing them in the map.

I am grateful to the Ministry of Education and Vocational Training (MoEVT) - Tanzania and Deutscher Akademischer Austausch Dienst (DAAD) – Germany, for financial support that has enabled me to pursue and successfully complete PhD studies in Germany.

I am indebted to my employer Nelson Mandela African Institute of Science and Technology (NM-AIST), Arusha, for granting me a study leave and for financial support to carry out field work on ethnopharmacological survey.

My special thanks goes to my lovely children Irene Emily, Emmy Claire and Godlisten for having patience on me all the time I was not at home because of my studies. It is my prayer that you live to enjoy the outcomes.

I owe my loving thanks to my husband Mecku for his understanding, positive attitude, support, sacrifices and above all for taking care of the family without complaints all the time I was not at home. Without his great support and encouragements it would have been impossible for me to finish this work.

Lastly, and most importantly, I am indebted to my parents Edward and Felister for their unconditional love, prayers and for raising me to be the person I am today. May GOD bless you abundantly, grant you good health, happiness, peace, prosperity and long life.

Edna Makule

Regensburg - November, 2015

This thesis work is dedicated to:

1. My loving husband Mecku R. Kessy

For all the love, support, patience and words of encouragement. You have made this time a truly wonderful experience in my life. I can't find words to utter but to say, "Thank you for being so kind and loving".

2. My beautiful girls Irene Emily & Emmy Claire

It was such a difficult moment for you being at home without Mama around. You could not clearly explain the feelings you had, but you kept asking this question; Mama when are you coming back home? This question nailed my heart day and night. It also motivated me to work hard so that I can accomplish the goals and be with you again my sweet angels.

List of abbreviations

1D	One-dimensional
2D	Two-dimensional
δ	Chemical shift
J	Coupling constant
brs	Broad singlet
CD	Circular dichroism
COSY	Correlated spectroscopy
COX	Cyclooxygenase
CPC	Centrifugal partition chromatography
d	Doublet
dd	Doublet of doublet
DCM	Dichloromethane
EtOAc	Ethylacetate
EtOH	Ethanol
HCl	Hydrochloric acid
HIV	Human Immunodeficiency Virus
HMBC	Heteronuclear multiple bond correlation
HP	HPLC method
HPLC	High performance liquid chromatography
HRESI-MS	High resolution electron spray ionization-mass spectrometry
HSQC	Heteronuclear single quantum coherence
HTs	Hydrolysable tannins
LC-MS	Liquid chromatography-mass spectrometry
m	Multiplets
MeCN	Acetonitrile
MeOH	Methanol
MHz	Megahertz

MP	Mobile phase
MS	Mass spectrometry
NMR	Nuclear magnetic resonance
NOESY	Nuclear overhauser enhancement spectroscopy
NP-TLC	Normal phase thin layer chromatography
PAs	Proanthocyanidins
PE	Petrol ether extract
ppm	Parts per million
R*f*	Retardation factor
ROESY	Rotating-frame nuclear overhauser effect correlation spectroscopy
rpm	Revolutions per minute
s	Singlet
SMB	Per-*O*-(*S*)-2-methylbutyrate
STDs	Sexual transmitted diseases
TFA	Trifluoroacetic acid
TDDFT	Time dependent density functional theory
TLC	Thin layer chromatography
TMP	Traditional medicinal practitioner
TNH	Tanzania National Herbarium
t_R	Retention time
UV	Ultraviolet

Table of Contents

1 General introduction

1.1 Traditional medicine in Tanzania

Tanzania is a relative large country with a total area of 945,087 square kilometres, which is located in the eastern part of the African continent. Tanzania's population is estimated to be about 45 million people as per national census of 2012[1], whereby about 35 million (69.1%) of the people live in rural areas. Approximately 68% of the population live below the poverty line of $1.25 a day and 90% of the poor population live in the rural areas[2,3]. Despite the existing poverty in the country, Tanzania is endowed with a great abundance of floral diversity which is estimated to constitute about 12,667 plant species of which 1122 are endemic. About 10% of the plant species are reported to be used for traditional medicinal purpose[4,5].

Traditional medicinal practices are a vital component of healthcare in Tanzania. Although the modern health care is increasing, more than 60% of Tanzania's population and actually 80% of the rural people rely on traditional medicine as their primary health care[6,7]. In the year 2000, there were about 80,000 traditional medicinal practitioners (TMPs) and 1,500 doctors in the country, giving a ratio of TMP to patients of 1:400 while the ratio for medical doctors to patients was 1:30,000[4,8,9] . This clearly describes the better access to traditional medicine as compared to the modern healthcare. Additional reasons for the high dependency on traditional medicine are the existing poverty, cultural conservatism, lack of reliable and affordable conventional health care services[4,6,10].

The traditional medicinal system in Tanzania is characterized by two categories of disease aetiology namely natural and supernatural causes[11]. Natural causes of sickness include such as cold, heat, infections and imbalance in the basic body elements. Supernatural causes of illnesses are mainly witchcraft and spiritual causes resulting from penalties incurred for sins and breaking taboos. The most prevalent natural diseases which often cause the reason for seeking medical attention are parasitic diseases such as malaria and intestinal worms; diseases caused by bacterial infections due to inadequate potable water and poor hygienic conditions such as cholera, typhoid, acute respiratory infections, pneumonia, skin and eye infections, diarrhoeal

diseases and others such as anaemia, perinatal conditions and tuberculosis to mention a few[12,13].

TMPs cures the natural caused diseases mostly by using medicinal plants. Medicinal plants are available throughout the year. Furthermore, they are easily accessed by people who have limited contact to modern health services and by low income earners who are equipped with the curative knowledge of the particular plants[14]. In Tanzania, traditional medicinal knowledge and practices have been passed on mainly orally among people as well as TMPs from one generation to another. In some cases the medicinal knowledge remains the secret to the particular TMP until the old age, not till then he/she passes on the knowledge to a selected member of the family. If the TMP encounters sudden death, the knowledge gets lost.

Despite the great abundance of medicinal plants in Tanzania, their curative effectiveness and applicability by a large population, traditional medicine practices are threatened by a lack of reliable documentation which has made its promotion difficult within the country. Furthermore, medicines derived from plants are currently only limited regulated. There is no national pharmacopoeia, no monographs and no safety assessments to demonstrate harmful effects of these medicines[7]. There is also no restriction for selling traditional medicine in the market which as well threatens the biodiversity[7].

Regulatory effort to promote and standardize traditional medicine in Tanzania is underway. In 1974, the government established the Traditional Medicine Research Unit as part of the University of Dar es Salaam and the Muhimbili Medical Centre[15,16]. In 1991, the name of the unit was changed to Institute of Traditional Medicine which is now located in Muhimbili University of Health and Allied Sciences. The Institute is responsible for research on traditional healing systems in Tanzania, to identify useful practices which can be adopted, modernized and developed into drugs for use to improve human health. Furthermore, the Institute is carrying out clinical observations and toxicological studies as a means to promote safe products and identifying and discouraging harmful products. Additionally, it is intending to promote trade in herbal medicines, as a way to contribute to national growth and poverty reduction. The Institute is also planning to promote community based cultivation of medicinal plants and the sale of their extracts and possibly isolated pure compounds within the country and abroad

which in the future will promote commerce in medicinal plants and, therefore, become a source of income for the people.

1.2 Aim of the research work

Tanzania has more than 120 ethnic groups which hold immense knowledge on traditional medicinal practices serving on healing several human ailments. Among Tanzania's ethnic groups the Maasai are renowned for their traditional medicinal practices and they greatly rely on medicinal plants[17,18]. Maasai consume medicinal plants as part of their diet in form of herbal soup, tea, tonic, decoction and infusion[19]. Among the common and frequently utilized medicinal plants in their area are e.g. *Myrica salicifolia, Pappea capensis*, *Flacourtia indica* and *Vangueria apiculata.* Despite the frequent utilization of these plants and its alleged medicinal potent, reliable documentation on their traditional medicinal use, drug preparation, ethnopharmaceutical information, phytochemical composition and pharmacological characterization to prove their medicinal efficacy are scarce.

Therefore the aim of this research work was, to conduct a detailed survey and document information on Maasai traditional medicinal use of these four medicinal plants in Arusha and Manyara regions, north-eastern Tanzania.

In addition to the ethnopharmacological study, plant material should be collected to allow subsequent phytochemical characterization of the plants. Following, phytochemical characterization of *M. salicifolia* bark should be done to identify potential active compounds that could be responsible for documented activity and usage of the drug.

2 Ethnopharmacological survey of four Maasai traditional medicinal plants

Ethnopharmacological survey is a common and crucial method which involves inquiring and gathering information on healing abilities of traditional medicines within one or different ethnic groups. It is a tool for preserving indigenous traditional medicinal knowledge for future generation. Furthermore, ethnopharmacological survey paves a way to scientific investigation, proof and validation of the gathered information through phytochemical and pharmacological characterization, hence complementing to drugs discovery by pharmaceutical industry[20]. In this study ethnopharmacological survey of four Maasai medicinal plants was conducted in Manyara and Arusha regions of the north-eastern Tanzania.

2.1 The Maasai

2.1.1 Culture

Maasai is an ethnic group residing in the north-eastern area of Tanzania extending up to the south area of Kenya. They originate from the Nilotic people indigenous to the Nile valley in the north of Africa who came to southeast Africa through the way of South Sudan. Maasai is a linguistic term, referring to speakers of the Eastern Sudanic language (Maa) of the Nilo-Saharan family[19]. Maasai are a pastoral people, herding cattle, sheep and goats, and sometimes donkeys as their source of income and wealthy symbol[21,22]. Unlike many other ethnic groups in Tanzania, Maasai have managed to maintain most of their traditional life style and by doing so they have become famous touristic attraction. Maasai are semi nomadic people who have no fixed homes and move from one place to another with cattle in searching for pasture. Maasai nomadic life has permitted them to have access to various biological resources, which has contributed to an enormous traditional knowledge on their landscape[21,23].

Generally, Maasai are divided into sixteen tribe sections with differences in customs, appearance, leadership and dialects. These sections are known as the Keekonyokie, Loodokolani, Purko, Wuasinkishu, Matapato, Laitayiok, Loitai, Damat, Dalalekutuk, Kisonko,

Kaputiei, Kankere, Lmoitanik, Loitokitoki, Larusa, and Sikirari. The sections residing in the north-eastern area of Tanzania are the Loitai, Kisonko and Larusa section[19,21,23].

In addition to tribe sections, Maasai are characterized by age groups which is the basic political and social structure is their rigid system. The age set is primarily applied to the men, women become members of the age set through their husbands. Every five to seven years, a new age group of the young generation of about 14 years old is initiated into adult life through circumcision. The group formed is given a name and lasts throughout the life for its members. The oldest groups which were existing in north-eastern Tanzania by the time the survey was conducted were Makaa and Landisi while the youngest groups were Korianga and Nyangulo (Morans - the junior warriors).

The Maasai live in small circular houses which are loosely constructed (Kraals) and fenced with acacia thorns or long strong poles to prevent lions from attacking their cattle[21,22] **(Figure 2.1)**. The houses do not have windows and contain only one small door. Inside the house a skin of an animal (normally a cow skin) is placed on the ground for warmth. Their houses are always smoky and dark due to their habit of cooking inside the house using firewood. In the Maasai community, women are responsible for constructing houses using mud, grass, wood and cow dung, while men are responsible for making the fence. Habitually, Maasai live with extended families in the kraals[21].

Other peculiar characteristics of the Maasai include the application of red ochre to their bodies **(Figure 2.2)**, the long hair worn by the Morans (junior warriors), ear piercing and the stretching of earlobes, the coils of wire worn on the limbs of the women, the loads of beaded jewellery placed around the neck and arms and their colourful tradition sheets (shuka) wrapped around the body. The shuka is worn by both men and women and varies in colour depending on the occasion**.**

Traditionally, Maasai depends on their animals for food such as milk, meat, animal blood, honey, plants barks and leaves. In recent days they have begun to consume other foods like maize meal beans, rice, potatoes and others[19].

Figure 2.1: Maasai houses. **Left:** Fence of long poles. **Right:** Small round houses fenced with acacia thorns.

Figure 2.2: Maasai clothing and decorations. **Left:** Moran worn long hair, stretched earlobes and smeared with red ochre (www. sneezr.ca. 05.10.2015). **Right - up:** Maasai women with shuka and beads decoration (www.gettyimages.com. 06.10.2015). **Right - low:** Morans with shuka and beads decorations (www.reuters.com. 06.10.2015).

2.1.2 Maasai and medicinal plants utilization

Maasai have been utilizing medicinal plants for years and they are deep-rooted in their life. The dependency on medicinal plants is contributed by the immense knowledge they have on nature and also by their life in the isolated remote areas where by modern health care is inaccessible and unavailable, just like other pastoral areas of East Africa. However, this knowledge is declining due to changes towards a more western lifestyle, overgrazing and over exploitation of plant resources have already led to a decline of the plant material available[18].

At their early stage of life children are taught about the medicinal value of herbs[21,24]. Traditionally, it is the duty of Maasai young boys to look after small goats and sheep around their homes. During this process, they also learn about medicinal plants which are used at home. Maasai young boys and the Morans are further trained on medicinal knowledge during their tradition meat eating festival and healing retreat (Orpul). In the Orpul festival, apart from meat eating, meditation, remembrance of ancestor spirits and celebration, young boys and Morans are detailed trained on which medicinal plants are used for the treatments of common ailments so that primary health care is provided at the household level[25]. In another side, young Maasai girls obtained their knowledge of medicinal plants from their mothers and grandmothers, with whom they spend a lot of time[18,23].

Maasai utilize herbs when they are healthy as well as in sickness situation. In a healthy condition, Maasai consume boiled herbal mixtures of bark and roots in soup for improving conditions of the stomach and the blood. Additionally, herbal mixtures are used by Morans preparing for attacks. For example, the *Pappea capensis* Eckl. & Zeyh (Sapindaceae) and *Acacia nilotica* (L.) Willd. ex Del. (Fabaceae) are taken as a digestive, excitant, for prevention of hunger and thirst. They are also known for preventing fatigue and fear in the wilderness[18,26].

During sickness, Maasai use herbal remedies derived from trees and shrubs for curing minor ailments in their home. Some of the diseases treated at home are such as: malaria [18,23], gonorrhea and other sexual transmitted diseases, stomach infections[18,23,27], painful joints, pregnancy disorders, tooth problems, eye infections[19], colds and throat infections[18,28,29] to mention a few. However, for persistent and chronic sicknesses, they seek for professional TMPS

consultations[23]. From the medicinal knowledge they possess, one medicinal plant can be used for the treatment of more than one diseases.

2.2 Surveyed medicinal plants

The survey should include plants which are prevalent in the area and are commonly used for the treatment of diseases by the Maasai. On this basis, four plants were selected, including *Myrica salicifolia, Pappea capensis, Flacourtia indica and Vangueria apiculata.*

Although preparations of the selected medicinal plants are frequently applied, documentation about ethnomedicinal uses, traditional preparation methods, dose administration, contraindications and overdose control methods within the area is scarce. Additionally, there is only little or no scientific data about phytochemistry of these plants nor any reliable scientific investigation about active compounds, bioactivity and healing potential.

2.2.1 *Myrica salicifolia* A. Rich.

2.2.1.1 Botany

Myrica salicifolia A. Rich. is also known as Olkitalaswa (Maasai). It belongs to the family Myricaceae of the order Fagales and the former genus *Myrica.* The genus was divided into two genera: *Myrica* and *Morella* where by *M. salicifolia* is now belonging to the genus *Morella* as detailed described in chapter 3 section **3.1.1**. The former species name of *Myrica salicifolia* will be used in this study.

M. salicifolia may grow like a shrub or a tree of up to a height of 12 m[30,31] **(Figure 2.3 Left)**. The leaves of *M. salicifolia* are shiny, pale green when young and turn to tinged maroon when mature **(Figure 2.3 Right - up)**. They are simple, irregularly serrated and arranged in alternate manner[31]. The bark of *M. salicifolia* is brown-maroon in colour. The flowers are small and very densely, yellow, fragrant and dotted with oil glands, male and female are separate[32]. The fruits of *M. salicifolia* are crowded small (2 - 4 mm) drupes in nature turning to dark blue purple when ripe **(Figure 2.3 Right - down)**. *M. salicifolia* is reported to be spread in many mountainous ranges in Tanzania above 1,200 m high and prefers shallow soil, heath and rocky areas[32]. The

species is distributed mainly in Tanzania, Kenya, Uganda, Rwanda, Burundi, Ethiopia, DR Congo, Yemen and Saudi Arabia[30,32].

Figure 2.3: Left: A small tree of *M. salicifolia* at Ngorongoro conservation area. **Right - up:** *M. salicifolia* leaves. **Right - down:** Fruits of *M. salicifolia* at Miriakamba area, Arusha National Park.

2.2.1.2 Ethnomedicinal uses

Traditional medicinal use of *M. salicifolia* has been previously reported in Tanga – Tanzania. The decoction of the *M. salicifolia* leaves mixed with other plants leaves are used for treatment of swellings on the cheek and face. The powdered, dry stem bark of *M. salicifolia* is mixed with honey and eaten against cough. The bark of *M. salicifolia* is chewed to cure toothache. Decoction of the bark is mixed with milk and given to children as a tonic. Roots are used as a slow acting medicine in stomach troubles and for headaches. Pounded young leaves are mixed with ghee and rubbed on skin diseases[33]. Additionally, in Bukoba, Tanzania, infusion and decoction of *M. salicifolia* bark and/or root are used for the treatment of HIV/AIDS opportunistic diseases such as tuberculosis, chronic diarrhoea, cryptococcal meningitis, and herpes simplex[34].

In Ethiopia, pulverized young leaves of *M. salicifolia* are mixed with butter and used externally to treat skin diseases[35]. In Western Uganda, oral consumption of boiled pounded roots and barks of *M. salicifolia* has been used for the treatment of men sexual impotence and erectile dysfunction[36].

2.2.1.3 Phytochemistry and biological activity

Geyid et al.[37] conducted a phytochemical screening on methanolic extracts of stem bark and leaves of *M. salicifolia* and discovered the presence of polyphenols, unsaturated sterols/triterpenes, saponins, glycosides and carbohydrates. Furthermore, these authors found that a methanolic extract of *M. salicifolia* stem bark at high doses of 2 mg/mL was effective against *Bacillus cereus*, *Neisseria gonorrhoeae*, *Shigella dysenteriae* and *Staphylococcus aureus*. Njung'e et al.[38] carried out an *in-vivo* testing of a methanolic extract of *M. salicifolia* on laboratory mice regarding its analgesic, antipyretic and anti-inflammatory activity. They discovered that *M. salicifolia* methanolic extract exhibited potent analgesic and antipyretic activity at a concentration of 100 mg/kg.

2.2.2 *Pappea capensis* Eckl. & Zeyh.

2.2.2.1 Botany

Pappea capensis Eckl. & Zeyh., also known as Oltimigomi (Maasai), mbamba ngoma (Swahili), jacket plum (English), belongs to the family Sapindaceae in the order Sapindales. It is a long-lived, hardy, evergreen, small to medium tree with a height of 2 - 8 m but occasionally exceeds 12 m, with a dense, rounded crown[32] **(Figure 2.4 Up)**. *P. capensis* grows in open and grassy woodland, rocky outcrops and brackish flat areas, sometimes in the bush close to rivers or dry river vicinities[39]. The leaves of *P. capensis* are alternate, simple, oblong, hard-textured and wavy. They are crowded at the ends of the branches as shown in **Figure 2.4 Left - down**. The leaf margin changes from sharply toothed in young leaves to almost smooth in mature leaves. The leaves are paler green below, wavy, rough and leathery. *P. capensis* has small greenish or pale yellow flowers in spikes to 12 cm, male are located at the end and female at the base of the spike[32] **(Figure 2.4 Middle – down)**. The bark is grey-brown in colour. The fruits of *P.*

capensis are furry green capsules, round and velvety. They have a diameter of over 1 cm. When the fruits ripe they split open to expose a bright red flesh containing a brown seed[32] **(Figure 2.4 Right - down)**. *P. capensis* is drought resistant and adapts to wide temperature variations[32,39]. The species is mainly found in Tanzania Namibia, Botswana, Swaziland Mozambique, Zimbabwe, Zambia, Malawi, Kenya, DR Congo, Ethiopia, Eritrea and South Africa[32].

Figure 2.4: Up: *P. capensis* tree at Ngorongoro conservation area. **Left - down:** *P. capensis* leaves. **Middle - down:** Flowers of *P. capensis* (www.kumbulanursery.za). **Right - down:** *P. capensis* fruits (http://www.wildcard.co.za).

2.2.2.2 Ethnomedicinal uses

Ethnomedicinal use of *P. capensis* has been previously reported from other areas of Tanzania and Africa. In Morogoro region - Tanzania, *P. capensis* is used for treatment of aches and pains[40]. In Bukoba region, decoction of *P. capensis* leaves is used for treating chicken pox and back aches[41].

In Kenya, infusion taken from roots, stem and bark of *P. capensis* is used for the treatment of chronic joints pain in Machakos and Makueni area[27]. It is also documented that bark or leaves decoction is taken with soup to treat stomach problems and diarrhoea[28,29]. Kiringe[18] reported that bark of *P. capensis* boiled in water and then sieved. The mixture is taken for arthritis treatment. Furthermore, roots of *P. capensis* boiled in water and thereafter mixed with soup are used for the treatment of appetite loss and reduced body strength by Morans of Kaijiado[18]. An oral application of *P. capensis* bark decoction for the treatment of post-partum haemorrhage is documented in Machakos district[42]. Further use of *P. capensis* roots decoction is reported in Machakos for the treatment of morning sickness, typhoid, amoebic dysentery and abdominal pains[43]. In South Africa, oil extracted from the seeds, bark, leaves and roots of *P. capensis* are used for the treatment of ringworm and baldness, venereal diseases, chest complaints, sore eyes and constipation[44]. Moreover, leaves of *P. capensis* are used for the treatment of venereal diseases, painful eyes and as aphrodisiac[45].

2.2.2.3 Phytochemistry and biological activity

Phytochemical data and information about the pharmacological activity of *P. capensis* are scarce. A phytochemical screening of *P. capensis* leaves revealed the presence of phenolics, flavonoids, gallotannins and condensed tannins[45].

Dichloromethane (DCM) and petrol ether (PE) extracts of *P. capensis* leaves were found to have good anti-inflammatory activity by inhibition of both cyclooxygenases 1 and 2 (COX-1 and COX-2). In addition, methanolic and water extracts of *P. capensis* leaves exhibited good anti-HIV-1 reverse transcriptase activity. DCM, PE, ethanol and water extracts of *P. capensis* leaves also exhibited moderate to high antimicrobial activities against *Neisseria gonorrhoeae*, *Bacillus subtilis*, *Escherichia coli*, *Klebsiella pneumoniae*, *Staphylococcus aureus* and *Candida albicans.*

Literature data describing the detailed phytochemical composition and pharmacological activity of *P. capensis* barks and roots are not existing to date.

2.2.3 *Flacourtia indica* (Burm. f.) Merr.

2.2.3.1 Botany

Flacourtia indica (Burm. f.) Merr**.** Also known as alaimoronyai (Maasai), mchongoma or mugovigovi (Swahili), governor's plum (English). It belongs to the genus *Flacourtia*, family Salicaceae and the order Malpighiales*. F. indica* is a deciduous tree or a bushy shrub often grows up to 7 m and sometimes up to 15 m maximum[46] **(Figure 2.5 Up)**. It is armed with axillary thorns and with tufts of branched thorns on the stem **(Figure 2.5 Middle - down)**. The bark of *F. indica* is usually pale, grey, powdery, may become brown to dark grey and flaking, revealing pale orange patches. Leaves are red or pink when young, variable in size, oval to round in shape, they are leathery and have toothed edge, contain 4 - 7 pairs of veins clear on both surfaces[32] **(Figure 2.5 Left - down)**. Flowers are small, cream, and fragrant. Male flowers with very many yellow stamens, female flowers with a divided spreading style[32,46]. Fruits are globular, reddish to reddish-black or purple when ripe, fleshy, up to 2.5 cm across, contained up to 10 brown flattened, wrinkled seeds **(Figure 2.5 Right - down)**. *F. indica* grows naturally in dry forest, woodland, bushland, thickets and in the wooded grassland. The species is drought resistant, prefer full sun for best growth but can tolerate light shading. It is found throughout Tanzania[46]. *F. indica* is distributed worldwide in the following countries: Botswana, Burundi, Cameroon, Democratic Republic of Congo, Eritrea, Ethiopia, India, Kenya, Malawi, Namibia, Nigeria, Rwanda, Sierra Leone, Cuba, Dominica, South Africa, Tanzania, Uganda, Zambia, Zanzibar, Zimbabwe, Exotic :Antigua and Barbuda, Barbados, China, Dominican Republic, Grenada, Indonesia, Jamaica, Madagascar, Malaysia, Puerto Rico, Seychelles, Sri Lanka, St Kitts and Nevis, St Lucia, St Vincent and the Grenadines, Trinidad and Tobago, Virgin Islands of United States[32].

Figure 2.5: Up: *F. indica* tree at kikavu area, Kilimanjaro. **Left - down:** *F. indica* leaves. **Middle - down:** Thorns of *F. indica.* **Right - down:** *F. indica* fruits (http://www.especies-seeds).

2.2.3.2 Ethnomedicinal uses

In other areas of Tanzania fruits of *F. indica* are used for treatment of jaundice and enlarged spleens. Decoction of leaves and roots are taken for the treatment of schistosomiasis, malaria, and diarrhoea. Further to this, roots are used for hoarseness, pain reliever, diuretic, pneumonia, intestinal worms and as an astringent [46].

The Lobedu tribe of South Africa takes decoction of root for relief of body pain. Leaves are used as expectorant for asthma, pain relievers, treatment of gynaecological complaints, pneumonia and ring worms[47].

In India and Bangladesh, fruits are used for treatment of jaundice and enlarged spleen, barks are used for the treatment of intermittent fever, roots are applied for treating nephritic colic

and gum is used in cholera treatment[48]. Additionally, bark infusion is suitable as a gargle for hoarseness, and roots are used in treatment of skin diseases, pruritus, nephropathy and scabies. Gum is administered along with other ingredients in cholera. Ground seeds mixed with turmeric and dried ginger is applied in form of a paste on woman body to reduce body pain after delivery[48–50].

In Madagascar, the bark is triturated in oil and used as anti-rheumatic liniment, the root and ash have been used as remedy for kidney complaints[47].

2.2.3.3 Phytochemistry and biological activity

Phytochemical screening of a methanolic and aqueous extracts of *F. indica* revealed the presence of steroids, alkaloids, tannins, saponins, flavonoids, glycosides, phenolic compounds and terpenoids[51]. Individual structures that were isolated and elucidated from *F. indica* include flacourtin - a phenolic glucoside ester[52], pyrocatechol, homaloside D and poliothrysoside[53], mururin A, coumarin, scoparone and aesculetin[54] (**Figure 2.6)**.

Previous literature reports on biological activity of *F. indica* in several *in-vivo* and *in-vitro* testing. *In-vitro* antioxidant activity of a methanolic and aqueous extract of *F. indica* leaves was evaluated by Tyagi et al.[51]. They showed, that the two extracts possess potent free radical scavenging and antioxidant activity at a concentration of 18 µg/mL. The same group investigated the *in-vivo* anti-asthma activity of the same extract on histamine-induced bronchospasm in guinea pigs, and reported that the extract was effective in reducing the symptoms of bronchial asthma and also improved the lung function parameters of asthmatic subjects[55]. Kaou et al.[53] analysed the anti-malaria activity of the compounds isolated from the aerial part of *F. indica*, i.e. pyrocatechol, homaloside D and poliothrysoside, and discovered that poliothrysoside had three times higher activity against the chloroquine-resistant strain of *Plasmodium falciparum* type W2 as compared to pyrocatechol and homaloside D.

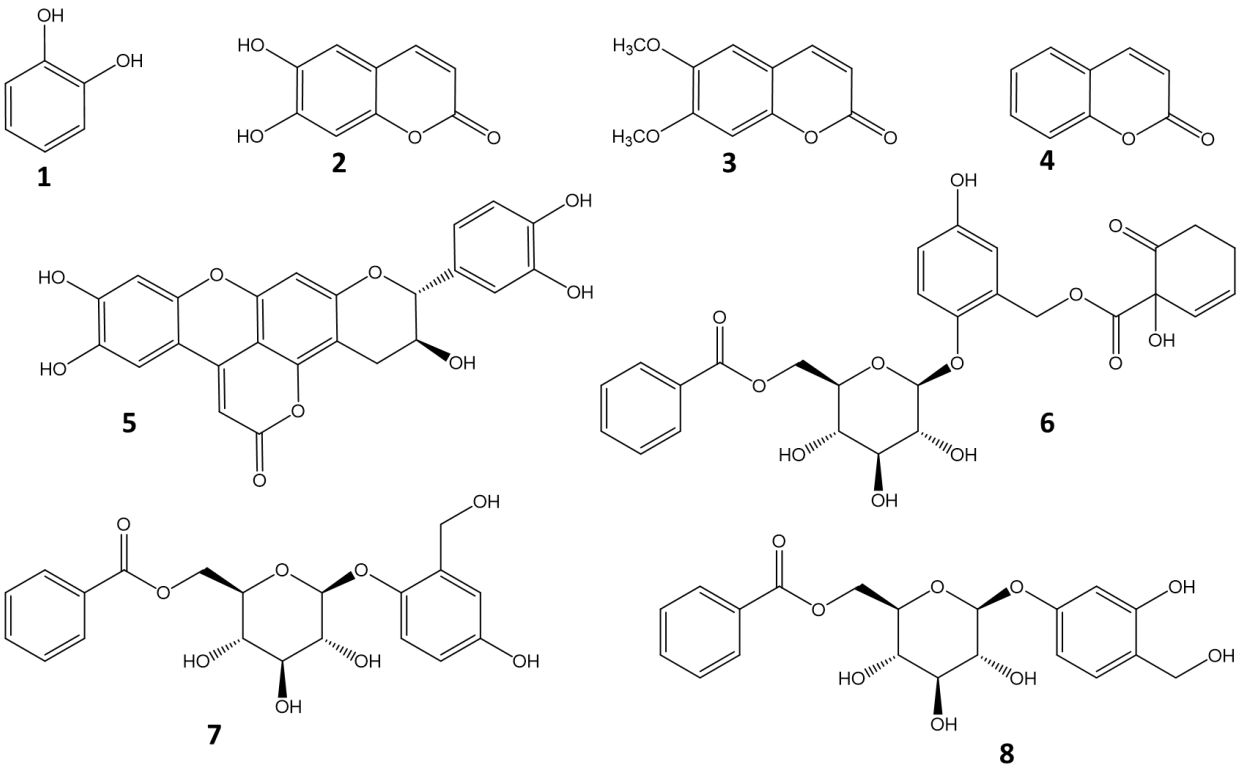

Figure 2.6: Compounds isolated from *F. indica.* **1**: pyrocatechol, **2**: aesculetin, **3**: scoparone, **4**: coumarin, **5**: mururin A, **6**: homaloside D, **7**: poliothrysoside, **8**: flacourtin.

2.2.4 *Vangueria apiculata* K. Schum.

2.2.4.1 Botany

Vangueria apiculata K. Schum., belongs to the family Rubiaceae and the order Gentianales. It is also known as Olgumi (Maasai) and Mviru (Swahili)[56]. *V. apiculata* is a deciduous shrub or small spreading tree 1.8 - 15 m tall[57,58] **(Figure 2.7: Left)**. It has several stems which often branch horizontally. Leaves are opposite, elliptic oblong, ovate to lanceolate, up to 17 cm long, distinctly acuminate at the apex, glossy green, mostly hairless but sometimes finely pubescent beneath. The margin is entire but wavy; petioles are 0.5 - 1.5 cm long **(Figure 2.7: Right - up)**. The bark is greyish-brown to reddish-brown, smooth or finely ridged. Flowers are greenish-white, up to 1 cm in diameter with a conspicuous tuft of fine white hairs in the throat of the corolla. They are found in lax to dense untidy axillary heads. Fruits of *V. apiculata* are subglobose, sometimes asymmetric, 1.5 - 2.5 cm in diameter, green to brown, hairless when ripe **(Figure 2.7: Right - down)**. They grow in a riverine thicket, evergreen forest, open

woodland and montane grassland, often among rocks. The plant is very adaptable, tolerates some drought and a wide range of soils[57–59]. *V. apiculata* is reported to be found in tropical countries of Africa such as Tanzania, Sudan, Ethiopia, Rwanda, eastern DR Congo, Uganda, Kenya, Malawi, Mozambique, Zambia and Zimbabwe[57,59].

Figure 2.7: Left: *V. apiculata* tree at Monduli district. **Right - up:** *V. apiculata* leaves and flowers. **Right - down:** *V. apiculata* unripe fruits.

2.2.4.2 Ethnomedicinal uses

In north-western Tanzania, the Haya tribe use decoction made from *V. apiculata* leaves for the treatment of diabetes[60].

In Uganda, decoction of *V. apiculata* leaves is drunk for the treatment of constipation [61]. Boiled decoction of *V. apiculata* roots is drunk three times a day for the treatment of intestinal worms[62,63]. Oral consumption of *V. apiculata* root juice is used for the induction of labour during child birth[64].

In east Africa, leaves of *V. apiculata* are chewed and juice is swallowed for treatment of stomach ache. Leaf infusion is drunk for the treatment of body swelling and warts. Burned stem ash are licked for the treatment of tuberculosis[62].

2.2.4.3 Phytochemistry and biological activity

Despite their alleged traditional medicinal effectiveness, there is no previous reported study on biological activity and chemical constituents of *V. apiculata*.

2.3 Description of the surveyed area

The ethnopharmacological survey was conducted in Arusha and Manyara regions located at the corner of north-eastern Tanzania between latitudes 2.07235 S and 5.39669 S south of the equator, longitudes 35.48332E and 37.4818E east of prime meridian **(Figure 2.8)**. The area is bordered to Kenya in the north; Kilimanjaro and Tanga region in the east; Dodoma in the south; Singida, Shinyanga and Mara region in the east. The area is estimated to be 82,428.5 km^2 whereby 3,571 km^2 (4.3%) is covered by water bodies and 78,857.5 km^2 is land area. The water bodies in the area include Lake Eyasi, Lake Manyara, Lake Babati and Lake Natron. The population of the area is estimated to be about 3.1 million inhabitants as per Tanzania national census of 2012[1], with about 1.7 million people living in Arusha and about 1.4 million people in Manyara region respectively.

Administratively, the area is divided into eleven districts: Karatu, Arusha, Arumeru Monduli, Longido and Ngorongoro in Arusha region; Babati, Simanjiro, Kiteto, Hanang and Mbulu in Manyara region.

Several ethnic groups are found in the area with the Maasai being the main tribe in Kiteto, Simanjiro, Monduli and Ngorongoro. The Iraqw tribe is mainly found in Mbulu, Babati, Karatu and Hanang districts. The Meru and Arusha tribes are dominating the Arumeru and Arusha Municipality. Furthermore, the small tribes of Barbaig, Sonjo and Hadzabe (Tindiga) form a minority group which depends on hunting for livelihood. They are located in Hanang and Ngorongoro districts[65].

Altitudinal range of the area is estimated to range between 900 and 1,600 m (3,000 - 5,200 ft.) in elevation above sea level. The vast altitudinal ranges have contributed to non-uniformity of climatic conditions. The area experiences temperatures between 25 - 31^oC during the hottest season (November - February) and 13 – 20 ^oC in the coldest season (May - August).

Furthermore, the average annual temperature in the highland areas is estimated to be 21 °C and 24 °C in the lowlands[65].

Concerning the rainfall, the area is classified as a dry and semi-dry area, with a noticeable dry season and a rainy season. Two types of rainfall patterns exist in the area; the monomodal and bimodal rainfalls. Monomodal rainfalls are experienced from November to April with an average annual rainfall range of about 800 - 1000 mm. This occurs in the southern part of the area which includes the districts of Babati, Hanang, Kiteto, Mbulu and Karatu. This type of rainfall is generally reliable and has made these districts to be the major cereal crops producers of the area. The remaining districts of Ngorongoro, Simanjiro, Arusha, Arumeru, Longido and Monduli experience bimodal rainfalls, which are characterized by both a short and a long rain period with an annual average precipitation of 1000 - 1200 mm. The short rains normally occur from October to December, while the long rains last from February to June. The whole area experiences a dry season between July and October[65].

The vegetation of the area is characterized by savannah with high floral diversity. It can be divided into four natural vegetation zones, namely wooded bushlands, wooded grasslands, bushed grasslands and open grasslands. The latter is estimated to cover 80% of the area.

Figure 2.8: Map of Tanzania showing the location of the surveyed area (www.mapsofworld.com - 28.09.2015).

2.4 Methods

2.4.1 Informant selection

Informant selection was achieved through purposive sampling based on knowledge and practices on traditional medicine. Village Executive Officers were involved in obtaining a list of highly experienced traditional medicinal practitioners (TMPs) in a particular village and also identifying those who use medicinal plants for treatment without witchcrafts. Thereafter, identified TMPs were well informed about the study and requested for their participation consent. Then appointments for the interviews were planned prior the interview session. In this study, 65 TMPs (36 male, 29 female) aged between 50 - 75 years were selected and interviewed. Selected TMPs acquired the knowledge from their forefathers and mothers. The interviewed TMPS were residing in different villages of the four districts of Arusha (Monduli and Ngorongoro) and Manyara (Simanjiro and Kiteto) regions.

2.4.2 Interviews and data collection

Interviews with TMPs and ethnopharmacological data collection about the four medicinal plants *Myrica salicifolia, Pappea capensis, Flacourtia indica* and *Vangueria apiculata* was carried out from January to March, 2013. The interviews were built on the trust to conserve the knowledge of medicinal plants utilization and to improve health care situation not only in Maasai area but also in other parts of the country. The interviews were conducted in informal meetings with individual TMP and in group discussions as shown in **Figure 2.9**. Groups of TMPs were formed in the area where more than one TMP was willing to participate in the interview. The formed groups consisted of either men only or women only. The information to be documented from the group of TPMs was taken after consensus was reached between the TMPs and was regarded as single information. Interviews were conducted in Maasai language and translated to Swahili language with exception of few cases where TMPs understood and could speak Swahili. Translation of Maasai to Swahili was done by a person who understood both languages Maasai and Swahili.

The interviews were guided with a prior prepared semi-structured open ended questionnaire **(Figure 2.10)**. TMPs were asked about tradition medicinal use of the selected plants, part(s) used, preparations methods, drug administration, diseases treated, side effects and overdose control. In addition, TMPs were requested to show the medicinal plants after the interview for control as depicted in **Figure 2.11**. In cases where these plants were found only very far from their home, TMPs were asked to collect them for identification by a botanist.

A global positioning systems (GPS) was used to record the sites where interviewed TMP were located and also where plants samples for later phytochemical investigation were collected.

All collected data were summarized in a Microsoft Excel 2013 sheet.

Figure 2.9: Pictorial presentation of how interviews were conducted. **Up - left**: A group of female TMPs at Enduleni village, Ngorongoro district. **Up - right**: A group of male TMPs at Emairete village, Monduli district. **Down - left**: Individual male TMP (right) and his son (translator), at Esilalei village, Monduli Arusha. **Down - right**: Individual female TMP at Sepeko village Monduli, Arusha.

Questionnaire

Informant details

Name: .....
Gender: .....
Age: .....
Education: .....
Occupation: .....
Type of healer: .....
Ethnical group: .....
District: .....
Village name: .....
GPS: .....

Taxonomic information

Popular local name(s): .....
Scientific name(s): .....
Synonym(s): .....
Plant family: .....
Short description of the plant: .....
Illustration /Picture: .....

Pharmaceutical information

Medicated diseases/Diseases treated: .....
Explanation of the diseases: .....
Plant parts used: .....
Method of collection and storage: .....
Preparation: .....
Application form: .....
Application time: .....
Dosage: .....
Contraindication(s): .....
Observation: .....
Side effect(s): .....
Overdose control: .....
Other uses: .....

Figure 2.10: Questionnaire used for the interviews of TMPs during the ethnopharmacological survey.

Figure 2.11: TMP showing *V. apiculata*, for control at Emairete village, Monduli district- Arusha.

2.4.3 Plant identification and preparation of herbarium specimens

All described and collected plants were identified by the skilled botanists Mr Daniel Sitoni from National Herbarium of Tanzania and Mr Canisius J. Kayombo from Olmotonyi Forestry Institute, both situated in Arusha, Tanzania. Additionally, plant specimens were collected **(Figure 2.12)**, pressed, dried, mounted on a sheet, labelled and kept at National Herbarium of Tanzania and Olmotonyi Forestry Institute, Arusha, Tanzania **(Figure 2.13, 1 – 4)**. The voucher number for the collected plant specimen are: *M. salicifolia* (CK 7792), *P. capensis* (CK 7789), *F. indica* (CK 7790) and *V. apiculata* (CK 7791).

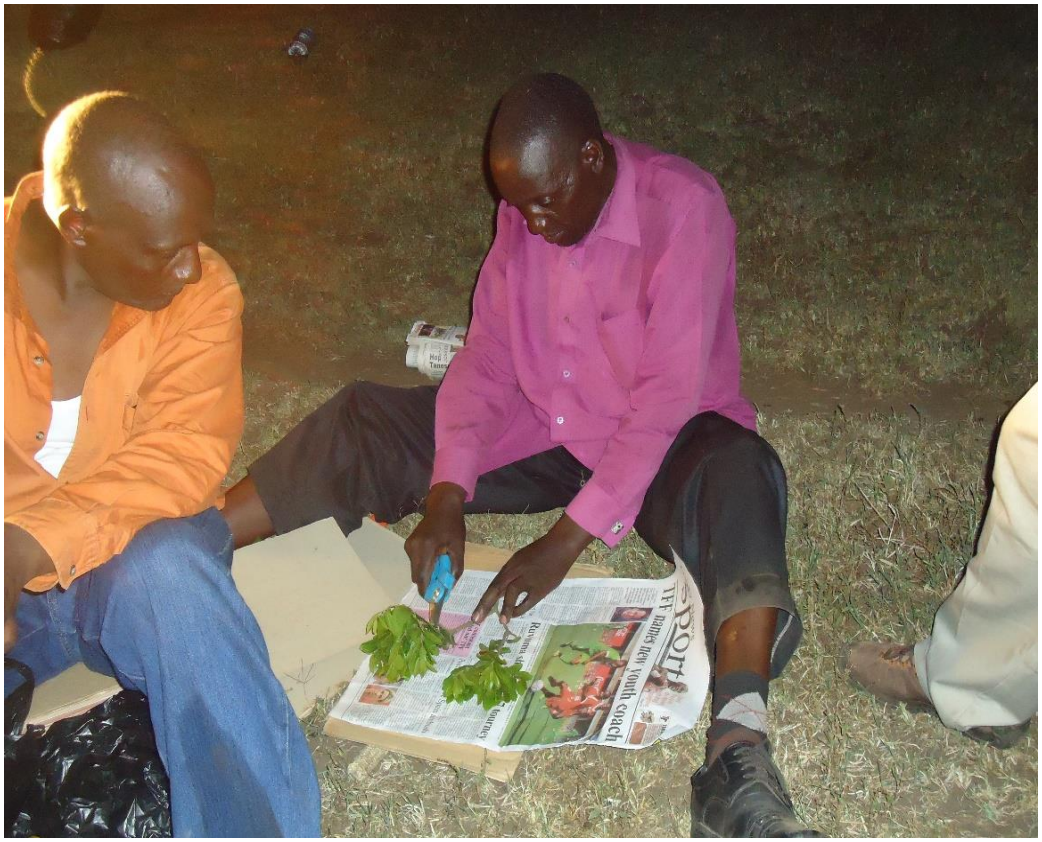

Figure 2.12: Botanist (Mr. Daniel Sitoni) preparing a herbarium specimen of *M. salicifolia* during field work.

Figure 2.13: Herbarium specimens of the four surveyed medicinal plants. **1:** *M. salicifolia*. **2:** *P. capensis*. **3:** *F. indica* and **4:** *V. apiculata*.

2.5 Results

2.5.1 TMPs location and plants samples collection sites

In this survey, a total of 65 TMPs from 50 villages of the four districts of Arusha and Manyara regions were interviewed.

16 TMPs from 11 villages of Monduli district: Emairete (3), Mti mmoja (3), Mswakini juu (2), Esilalei (1), Lemoyoni (1), Makuyuni (1), Lokisale (1), Moita bwawani (1), Engaruka chini (1), Engaruka juu (1) and Selela village (1).

19 TMPs from 14 villages of Ngorongoro district: Osinoni (1), Enduleni (1), Olerobi (2), Nainokanoka (2), Erkepus (2), Nakurro (1), Alailalei (1), Ngoile (1), Oloipiri (1), Sakala (1), Masurumunyi (1), Samunge (1), Digodigo (1) and Engarasero village (3).

21 TMPs from 17 villages of Simanjiro district: Narakauo (2), Njiro (2), Laangai (1), Narosoito (1), Namalulu (1), Sukuro (2), Terrat (2), Loswaki (1), Ngage (1), Loiborsot B (1), Landanai (1), Naberera (1), Rotiana (1), Kitwai A (1), Loibosiret (1), Emboreet (1) and Loibosit A village (1).

9 TMPs from 8 villages of Kiteto district; Ndedo (1), Ndaleta (1), Mbigiri (1), Kibaya (1), Loolera (2), Lembapuli (1), Namelok (1) and Irkiushbor village (1).

The percentage of TMPs interviewed from each district is summarized in the pie chart below **(Figure 2.14)**. All interviewed TMPs were from Maasai ethnic group with exception of 4 TMPs. 2 of those TMPs were from Sonjo and 2 from Arusha ethnic group, but they all also practiced Maasai traditional medicine.

A GPS was used to determine and record all locations where interviews were conducted as well as the plant collection sides **(Figure 2.15**, **Appendix 6.1** and **6.2)**.

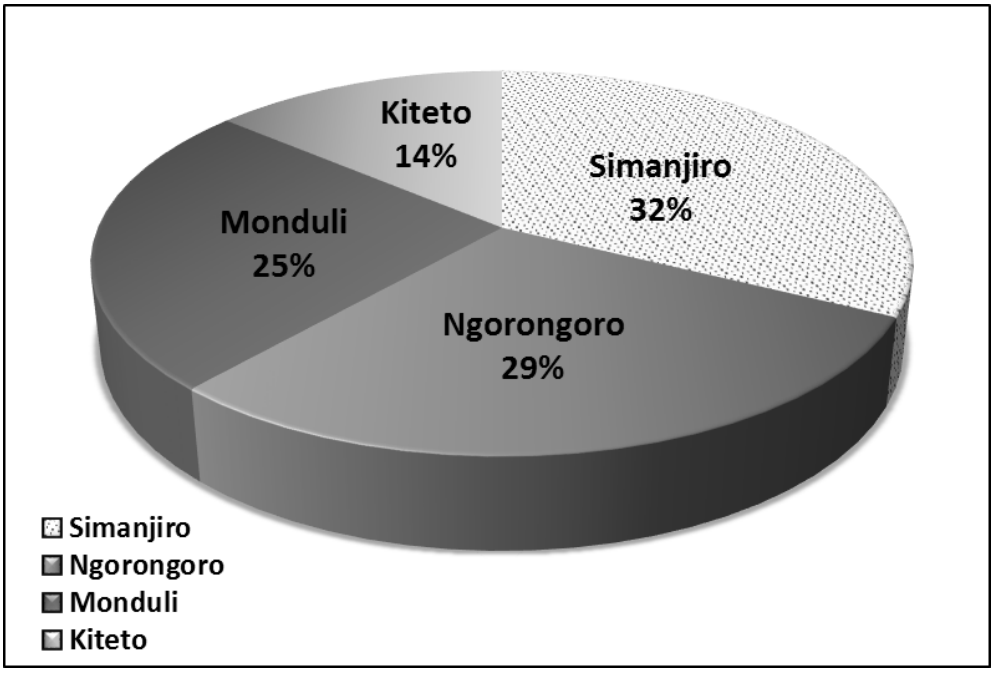

Figure 2.14: Percentage of TMPs interviewed in every surveyed district (n = 65).

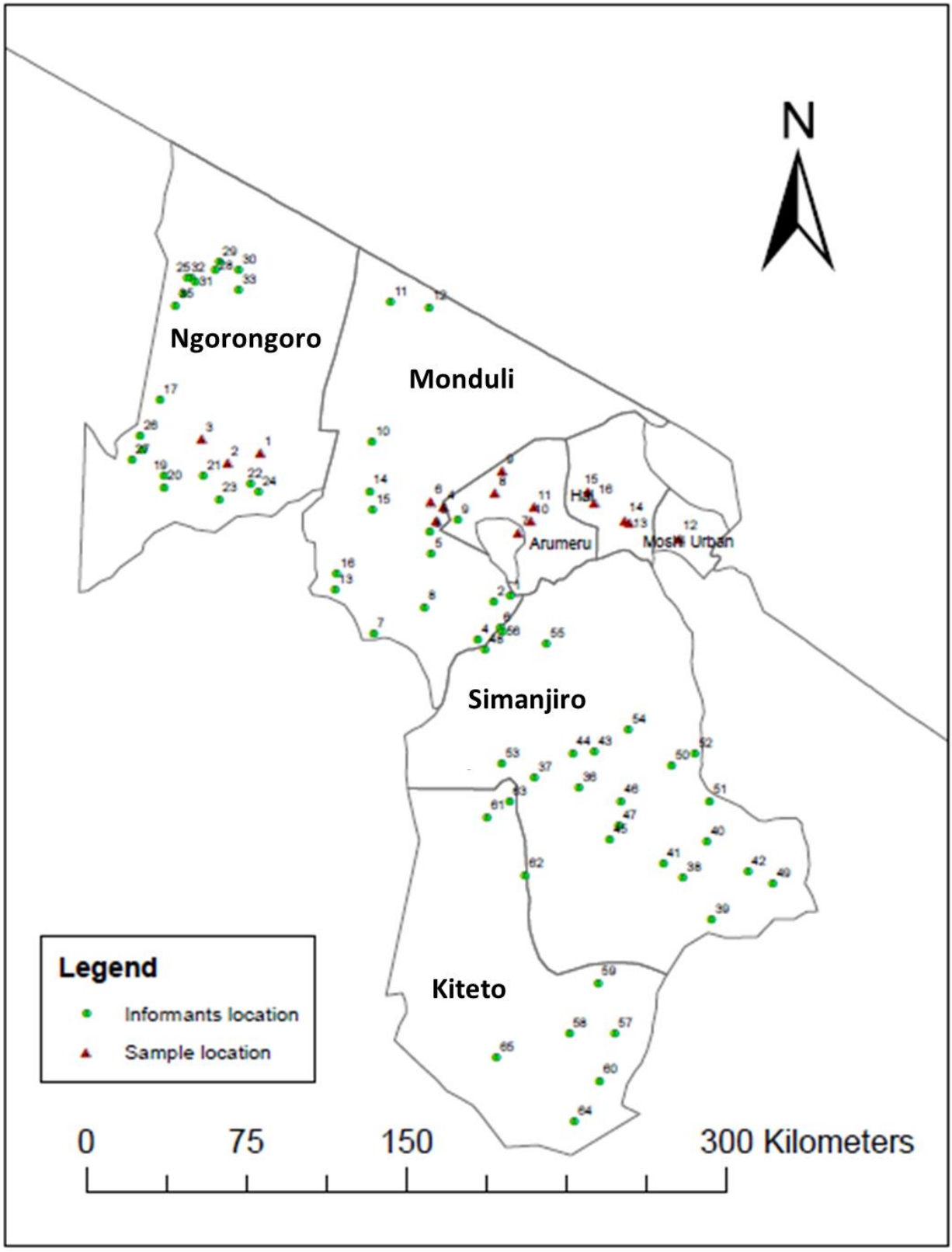

Figure 2.15: A map showing TMPs location **(green)** and plant sample collection sites **(red).**

2.5.2 Traditional description of the documented diseases

A number of different diseases were documented to be cured by the four medicinal plants. During the survey, TMPs were asked to describe each disease they mentioned and the way they diagnose the disease from the patient. TMPs reported, that they mainly diagnose diseases by taking a history of the patient in combination with physical diagnosis such as body temperature (measured by touching the body), face condition (swollen, pale and/or shine), stomach inflammation, hand palm colour, colour of the eyes, colour of the urine and other visible signs of inflammation. It was observed, that TMPs have similar description of diseases commonly affected their community as summarized in **Table 2.1**.

Table 2.1: TMPs description of the mentioned diseases.

Name of a disease	Swahili name	Description given by TMPs
Asthma	Pumu	Painful and difficult breathing.
Back pain	Maumivu ya mgongo	Pain at the back bone.
Bile oversecretion	Nyongo kujaa	Feeling nausea in the morning (morning sickness) and sometimes associated with high body temperature.
Blood loss	Kupungukiwa damu	Low blood volume after sickness, poor diet and after delivery. This is detected by paleness of eyes and hand palm.
Breast inflammation during lactation (Mastitis)	Matiti kujaa maziwa na kuuma	Breast diseases appear especially during the first twelve weeks postpartum. Diagnosed by painful inflamed breasts.
Colic	Chango	Abdominal cramps and pains.
Diarrhoea	Kuharisha	Condition of having frequent liquid bowel movement.
Dizziness	Kizunguzungu	A feeling of faint and unsteady.
Enlarged spleen	Kuvimba bandama	Inflamed spleen (diagnosed by inflamed stomach).
Eye infection/sticky eyes	Ugonjwa wa macho	Yellow/creamy discharge from the eye, increased redness of the eye/eyelids.
Fever	Homa	High body temperature, shivering and headache.
Gonorrhoea / STDs	Kisonono/ Magonjwa ya zinaa	Painful and burning sensation during urination followed by pus discharge both in women and men.

Table 2.1 continued

Name of a disease	Swahili name	Description given by TMPs
Gouts	Gauti	Painful inflamed knee joint.
Jaundice	Homa ya nyongo ya manjano	Yellowish pigmentation of the skin, the whites of the eyes and other mucous membranes.
Joint pain	Maumivu ya viungo	Painful inflamed joint and sometimes associated with joint stiffness.
Libido/Erectile dysfunction	Kupungukiwa na nguvu za kiume	Inability to develop or maintain an erection for men during sexual performance.
Malaria	Malaria	Body weakness, headache, appetite loss, cold sensation, high body temperature, headache and nausea.
Pneumonia	Nimonia	Severe and painful coughing, chest pain, high body temperature, and difficulty breathing.
Phlegmon	Jipu la tambazi	A painful inflammation (a boil like) which spreads on skin, and release pus after some days.
Stomach upset	Tumbo kujaa	Stomach pain, cramps and a sense of fullness.
Urination problems	Matatizo ya mkojo	Painful and difficulty urination.
Running nose/ flue	Mafua	Continuous light mucus flow from nose.
Sinus / Tension headache	Kipanda uso	Severe pains on the forehead at the upper part of the eyes.
Severe prolonged cough / Tuberculosis	Kikohozi kisichopona/ Kifua kikuu	Persistent coughing associated with chest pain and sputum.
Tonsillitis	Ugonjwa wa mafindofindo	Red, swollen tonsils, sore throat, experiencing pain during swallowing, high body temperature.
Liver problems	Ugonjwa wa ini	The liver problem is detected by inflamed abdomen and legs (Oedema). In some cases the body colour turns to yellowish.

2.5.3 Medicinal uses of the selected plants

It should be noted that for all four surveyed plants the percentage of respondents on every mentioned disease was calculated based on the total number of interviewed TMPs (n = 65). The reason for the percentage of respondents not to be 100% is due to TMPs do not using the particular plant for the treatment of a particular disease.

2.5.3.1 *Myrica salicifolia*

M. salicifolia was mainly reported to treat gonorrhoea (81%), running nose (73%), back pains (66%), sinus headache (61%), severe cough (55%), joint pains (47%) and immunity boosting (46%). Other diseases alleged to be treated by *M. salicifolia* were reported to be abdominal pains, pneumonia, gouts, urination problems, fever, tonsillitis, colic, liver problems, diarrhoea, tuberculosis and malaria. Reported diseases which are treated by *M. salicifolia* are summarized in **Figure 2.16** and **Appendix 6.3**.

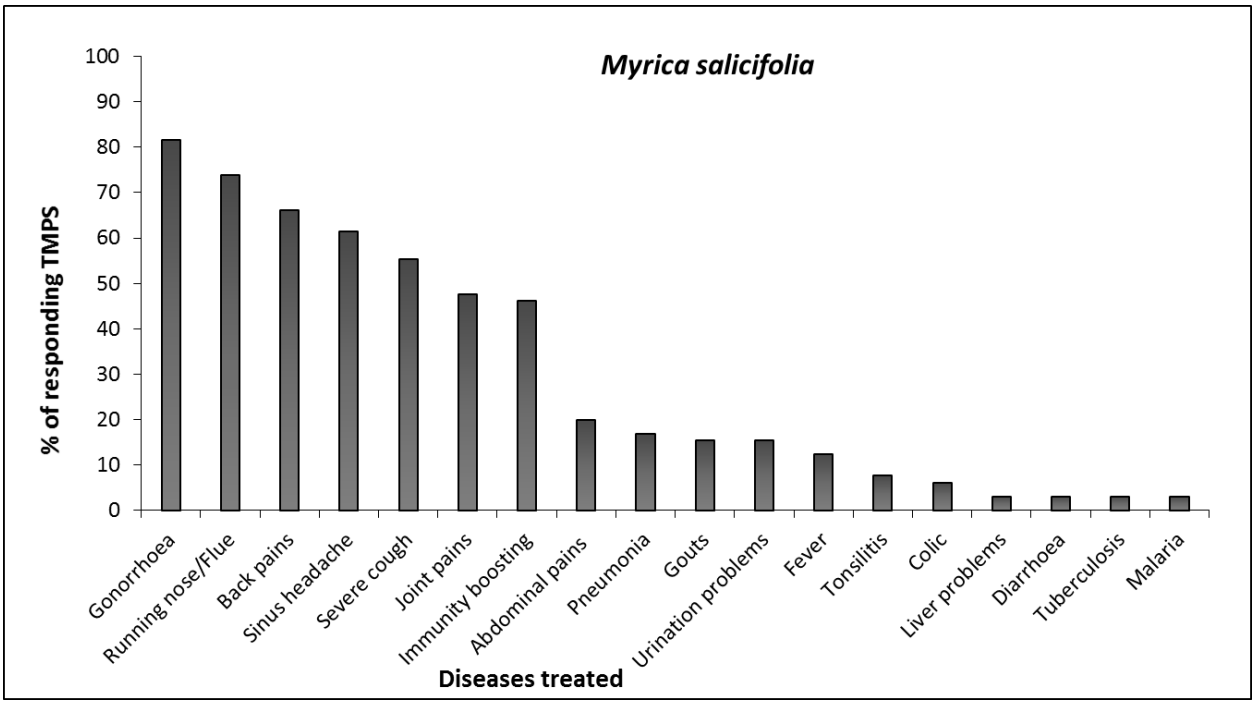

Figure 2.16: Reported diseases treated by *M. salicifolia*. The chart shows the percentage of responding TMPs that use the plant for the treatment of a specific disease.

2.5.3.2 *Pappea capensis*

The most mentioned diseases to be treated by *P. capensis* was mainly: enhancement of libido (89%), blood loss (72%), joint pains (69%), back pains (58%), general body strength (50%), abdominal pains (32%) and malaria (30%). Other diseases reported by TMPs were such as: bile over secretion, stomach upset, diarrhoea, gouts, sexual transmitted diseases (STDs), appetizer, urination problems, fever and colic. A summary of the reported diseases treated by *P. capensis* is shown in **Figure 2.17** and **Appendix 6.3**.

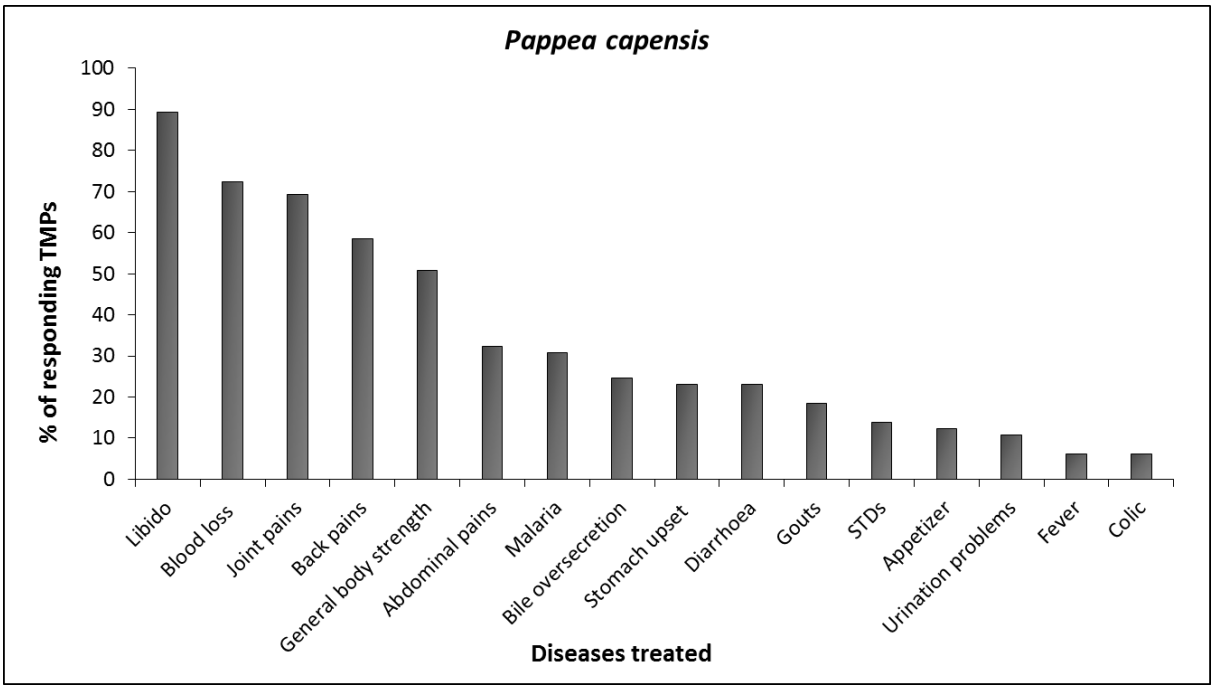

Figure 2.17: Reported diseases treated by *P. capensis*. The chart shows the percentage of responding TMPs that use the plant for the treatment of a specific disease. STDs = Sexual transmitted diseases.

2.5.3.3 *Flacourtia indica*

Among others, *F. indica* was commonly applied to treat fever (92%), malaria (90%), jaundice (87%), enlarged spleen (86%), joint pains (75%), pneumonia (73%), stomach upset (69%), difficulty breathing (69%) and back pains (66%). Other diseases mentioned to be treated by *F. indica* were; gouts, mastitis breasts, asthma, dizziness, body strength, urination problems, diarrhoea, STDs, bile over secretion, phlegmon and burn wounds. In **Figure 2.18** and **Appendix 6.3** the diseases which were reported to be treated by *F. indica* are summarized.

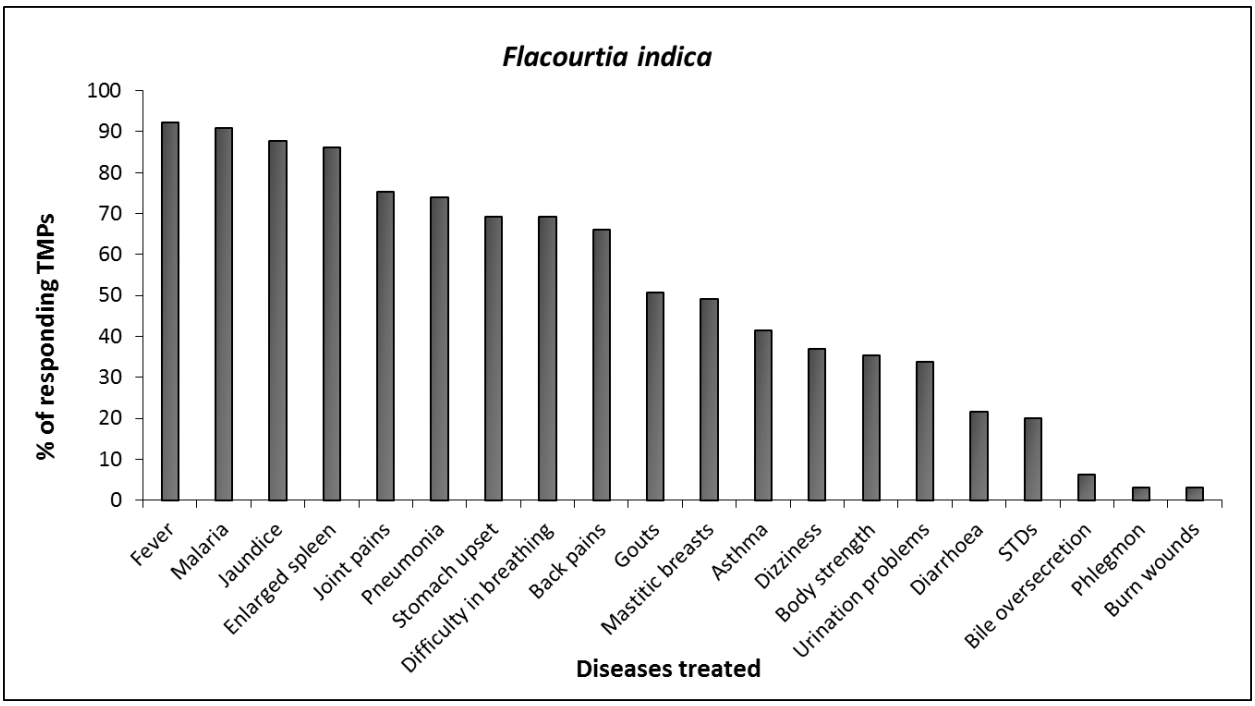

Figure 2.18: Reported diseases treated by *F. indica*. The chart shows the percentage of responding TMPs that use the plant for the treatment of a specific disease. STDs = Sexual transmitted diseases.

2.5.3.4 *Vangueria apiculata*

The most mentioned applications for *V. apiculata* were eye infection (73%), diarrhoea (66%), stomach upset (64%), reduced milk secretion (50%), general body strength (46%) and joint pains (36%). Further mentioned diseases were such as back pain, gouts, malaria and lungs pain. **Figure 2.19** and **Appendix 6.3** shows an overview of the diseases reported to be treated by *V. apiculata*.

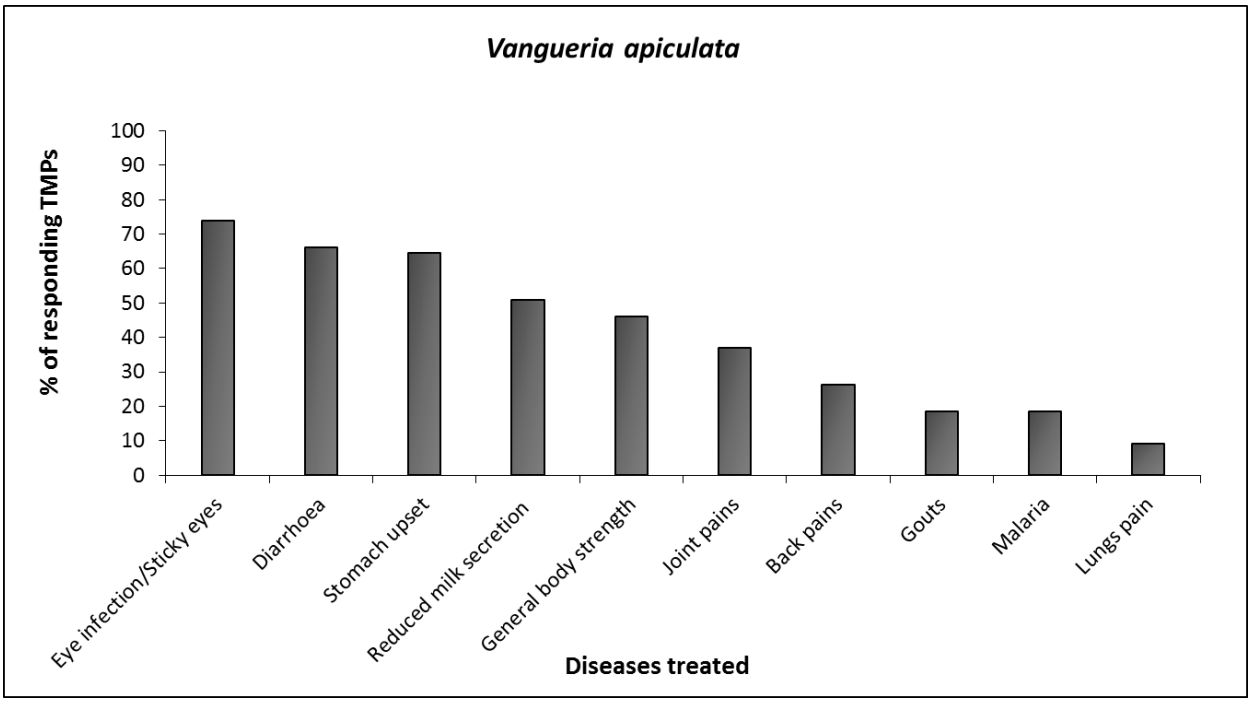

Figure 2.19: Reported diseases treated by *V. apiculata*. The chart shows the percentage of responding TMPs that use the plant for the treatment of a specific disease.

2.5.3.5 Diseases reported to be treated by all four plants

Some diseases were reported to be treated by each of the surveyed plants, including joint pain, back pain, gouts, diarrhoea, malaria and stomach upset. Also all the four plants were used to increase body strength or boost immunity. **Figure 2.20** summarizes the diseases treated by all four plants and also allows a direct comparison of the frequency of usage a distinct plant. Noteworthy is the prominent role of *F. indica* for treatment of malaria (90.7%) and gouts (50.7%), *V. apiculata* for the treatment of diarrhoea (66.1%) and treatment of stomach upset or abdominal problems by *F. indica* (69.2%) and *V. apiculata* (64.6%).

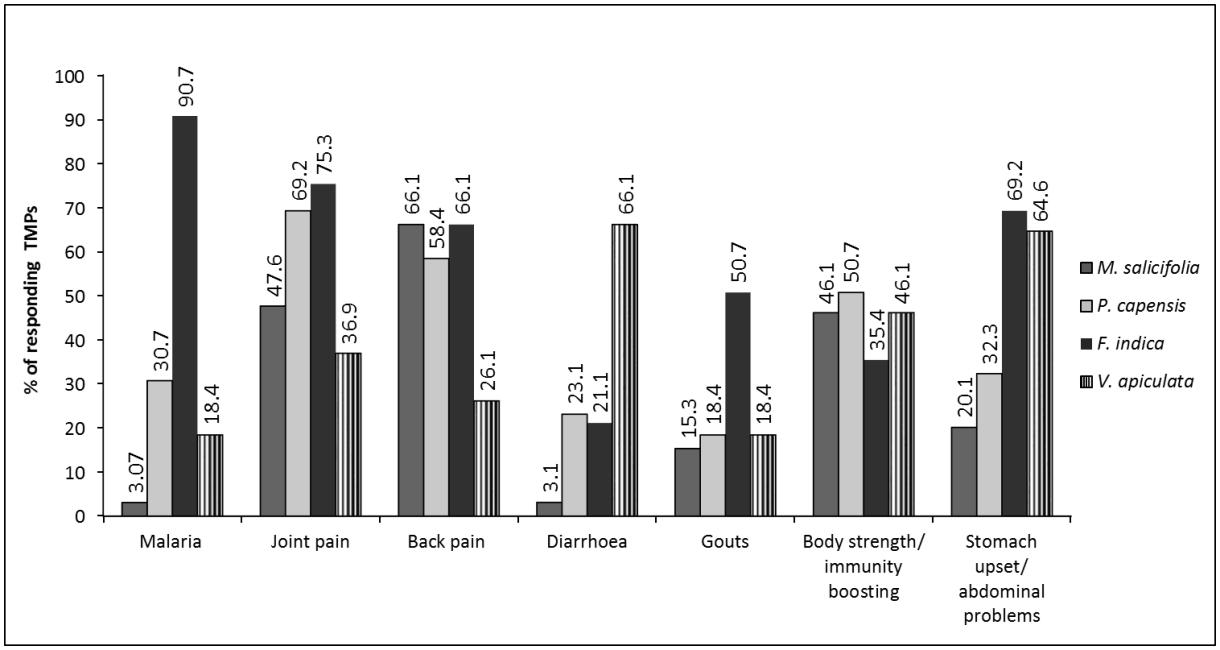

Figure 2.20: The percentage of responding TMPs that use a specific plant for a specific disease is indicated for each plant.

2.5.4 Plant parts used and medicinal preparation

Bark and roots of *M. salicifolia* were frequently mentioned by TMPs to be utilized for remedy preparation. Stems were also mentioned to be used but less often as compared to roots and bark. Leaves of *M. salicifolia* were not reported to be applied in the area for medicinal purposes.

From the survey it was further discovered, that, bark and roots of *P. capensis* are the most utilized plant parts for medicinal purposes. Again, stems are less utilized and leaves were not mentioned at all to be used for medicinal purposes.

Likewise, roots and bark of *F. indica* are the most frequent utilized parts of the plant followed by stems. Leaves were not reported to be used for medicinal purposes.

V. apiculata turned out to be the only plant among the four surveyed plants whose leaves are used for medicinal purposes. Utilization of *V. apiculata* leaves was mentioned for the treatment of eye infection. In addition to that bark, stems and roots were also mentioned to be used for remedy preparations.

The roots and bark which are the most utilized plant parts of all the four plants are believed to have stronger medicinal effect as compared to stems. It was further mentioned by TMPs that

utilization of stems is opted for, when they do not have possibility of getting bark and roots out of the plant. **Figure 2.21** and **Appendix 6.4** shows the percentage summary of the frequency the plant parts of the particular plant were mentioned to be used by interviewed TMPs in treatment of different diseases.

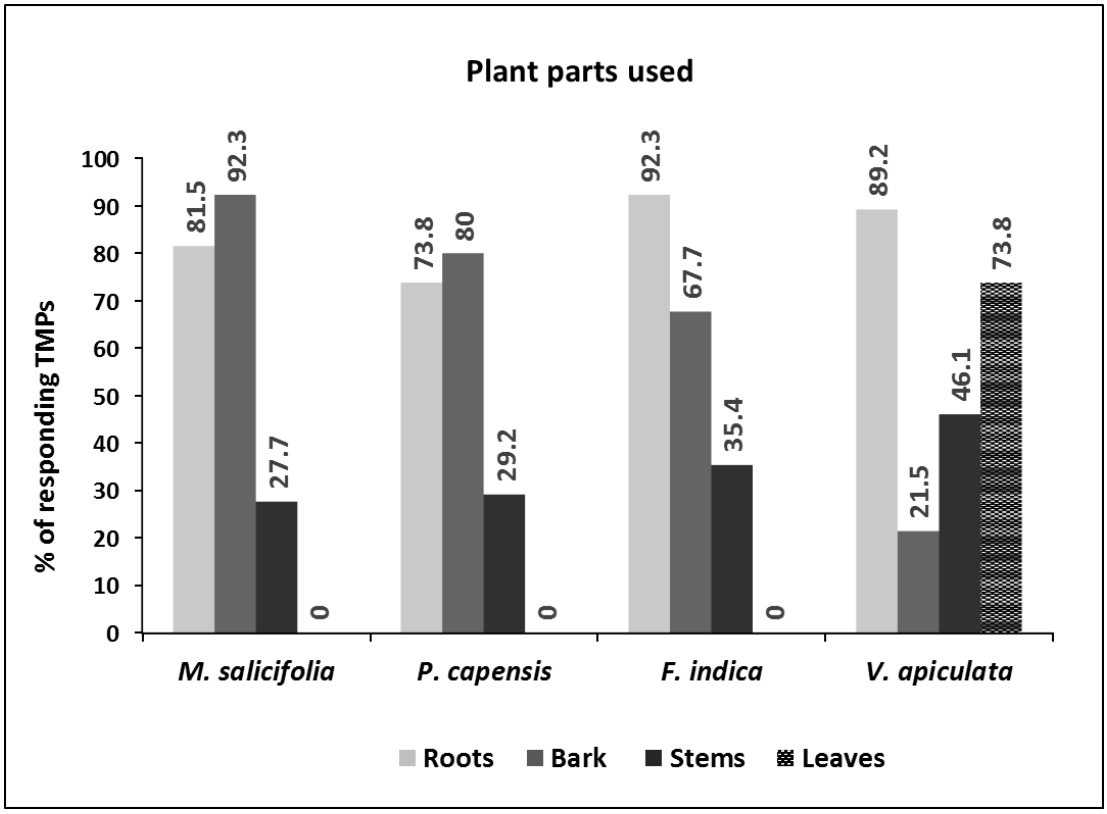

Figure 2.21: Plant parts used for medicinal purposes of the four plants.

Similar remedy preparation methods of the four medicinal plants were reported during the interviews **(Appendix 6.5)**. The preparation procedure starts by crushing the respective (dried/fresh) plant part. The remedy obtained from crushed plant part is prepared by decoction, infusion, maceration, mixing drug in a boiling black tea or boiling drugs with a mixture of water and ghee. Furthermore, infusions, decoctions, fresh pounded plant parts or powder mixed into boiling fatty beef or goat or lamb soup was further reported to be an effective preparation method of Maasai drugs. Thereafter, an herbal soup is warm consumed.

The mentioned methods of herbal remedy preparations are commonly practiced in the area not only for the four surveyed medicinal plants but also for other medicinal plants. Decision to use

which method was reported to depend on the convenience of the TMPs and the available resources. For example, the presence or absence of milk, ghee, and fatty meat for soup can determine which remedy preparation method is used.

Preparation of herbal remedies by infusion method is achieved through mixing crushed plant parts in warm water, thoroughly stirring and leaving to stand for few hours before utilization. Likewise, decoction is achieved by boiling crushed plant parts with water for some time and leaving to cool before utilization.

A medicinal tea was reported to be prepared by adding one teaspoon of dried powdered herb in a boiling tea with milk, leaving to boil for few minutes. Then the tea is filtered and consumed.

2.5.5 Drug administration and ethnopharmaceutical information

Oral consumption of drug remedies was the main reported administration method. Exceptions were the inhalation of *M. salicifolia* bark powder for the treatment of sinus headache and eye washing using *V. apiculata* leaves as remedy for the treatment of eye infection **(Appendix 6.5)**.

One pinch of fine powder of *M. salicifolia* bark is placed on the hand of a patient suffering from sinus headache, then a patient is required to close one nostril by pressing against the side of the nose with a finger and inhale with one hole and the same is done for the other nostril. The administration is usually once followed by multiple sneezes and mucus discharge.

For the treatment of eye infection, a filtered decoction or infusion of *V. apiculata* leaves (preferably from fresh pounded leaves) is used to wash the infected eyes two to three times a day until total recovery is experienced.

Drug administration by the different interviewed TMPs was not uniform in terms of concentration, dosage and application time. There exist no established ratios concerning the amount of crushed medicinal plant to that of water used for remedy preparation.

It was further noted, that children and pregnant women are given less amount of prepared drug remedy compared to adult men and women. For example, a child or pregnant woman would take about 250 mL as compared to adult men and women who would take about 500 - 1000 mL of the prepared drug remedy at one time depending on body weight and regardless of the concentration.

Time for drug remedy administration was also observed not to be uniform. Some TMPs reported a certain unit of prepared drug remedy is taken three times a day prior/after food consumption and others reported that prepared drug remedy (no amount specified) is taken in replacement of water every time a patient is thirsty. Furthermore, duration of prepared drug remedy administration was reported by many respondent TMPs to be three to seven days or longer until relief or total recovery is experienced.

Ethnopharmaceutical information such as general accompanying symptoms observed after drug remedy administration, severe side effects and contraindications of the four medicinal plants were also documented in this survey and summarized in the **Table 2.2**.

General accompanying symptoms are those symptoms which are expected by TMPs to happen after drug administration to a patient as a result of drug reaction. However, severe drugs side effect were not clearly known except for *M. salicifolia,* which was reported to cause gastric ulcers when the patient does not eat well during medication.

Table 2.2: Observed accompanying symptoms following drug administration, severe side effects and reported contraindications.

Plant name	Observed accompanying symptoms	Severe side effects	Reported contraindication
M. salicifolia	Sweating, increased heart beat rate is observed following oral consumption. Multiple sneezes and nasal mucus discharge is observed immediately after inhalation of drug powder for a patient with sinus/tension headache. Thick pus, thread like discharge followed after urination is observed on patient with gonorrhoea after 3 days of treatment and that is the marker of recovery from the diseases.	Gastric ulcers may develop if a patient does not eat well.	Not to be taken during pregnancy, by children under 10 years and when on prescription of other medication.
P. capensis	Nausea, sweating, frequent urination and fatigue may be observed as a result of medicinal reaction of a patient, liquid bowel movement may also be observed.	None reported	Not to be taken when using other medications.
F. indica	Sweating, dizziness and fatigue are observed. Relief and total recovery is observed after 2 - 7 days of treatment.	None reported	None reported
V. apiculata	Fatigue and drowsiness are observed. Relief of the mentioned diseases is observed after 2 - 3 days of treatment.	None reported	None reported

2.5.6 Traditional management of overdose symptoms

From the survey, overdose signs following herbal remedy consumption were reported, although not occurring very often. However, all interviewed TMPs reported to have experienced overdose symptoms from some of their patients. Reported overdose symptoms were rise in body temperature, high heart beat rate, body trembling, worsened of patient condition few hours following remedy consumption and in some cases unconsciousness and even death may occur if the situation is not quickly controlled.

It was further mentioned that the common methods used by Maasai for management of overdose symptoms are cold bath, consumption of cold milk, fatty beef/goat/lamb soup and consumption of soup prepared from goat or lambs entrails mixed with fresh animal blood. Additionally, it was reported that most overdose cases are experienced when the consumed herbal remedies are prepared by decoction or infusion (very strong remedies). Less overdose symptoms are experienced when the consumed herbal remedy was prior mixed with fatty soup or in tea containing milk. The mechanism on how the overdose symptoms are controlled was not reported.

2.5.7 Other uses of the surveyed plants

In addition to the medicinal uses, also some other, non-medicinal uses of the plants were documented in this survey.

Decoctions or infusion remedies from *M. salicifolia* bark or roots are used as appetizer during Maasai meat festival when huge amounts of meat are consumed. Further to this, is has been reported by TMPs, that prolonged intake of the remedies rises anger and aggressiveness and lowers sexual desire of Morans as well as elder men. Hence, they use it to get a sense of courage and fearlessness towards dangerous wild animals when they are out in the wilderness with their cattle.

The infusion of *P. capensis* was reported to be used as appetizer, tonic and for thirsty prevention especially for Morans (Maasai young men) when they are exposed to the sun for a long time in the wilderness feeding cattle. The same infusion remedy is taken by Maasai during

dry seasons and in the villages where access to portable water is limited. Fruits of *P. capensis* are edible and leaves are used for ruminant fodder.

The fruits of *F. indica* are edible and reported to be very delicious. The thorns of the plant are used for traditional ear piercing and the leaves serve as ruminant fodder.

The fruits of *V. apiculata* are also edible. The dried stems of the plant are used as fire wood and the leaves often serve as ruminant fodder. *V apiculata* is highly used in the area for making walking supporting sticks for elder men as well as Morans.

2.6 Discussion

2.6.1 General observations from the survey

Maasai ethnic group is well known to have sound knowledge of traditional medicine which is among others mainly practiced with the aid of medicinal plants utilization [21,23]. The sound knowledge concerning traditional medicine was also demonstrated in this study where by 34 different diseases were reported to be cured by the four surveyed medicinal plants **(Appendix 6.3)**. 18 diseases were reported to be treated by *M. salicifolia* **(Figure 2.16,)**, *P. capensis* was reported to cure 16 diseases **(Figure 2.17)**, 20 diseases were indicated to be cured by *F. indica* **(Figure 2.18)**, and *V. apiculata* is used to treat 10 diseases **(Figure 2.19)**. Some of the diseases were mentioned to be treated by more than one of the surveyed medicinal plants as indicated in **Figure 2.20**. The commonly mentioned diseases treated by all surveyed plants in this study were malaria, sexually transmitted diseases, reduced body strength/lower immunity, joint pain, back pain, diarrhoea and stomach upset and/or abdominal pain. These diseases often affect the Maasai community and are caused by hard physical work, long walking distances, cultural life style and hygiene problems to mention a few.

The hard physical work and frequent long walking distance have often resulted to back and joint pain complaints in the Maasai community. Polygamy cultural life style practiced in the Maasai culture has been the cause of prevalence of STDs within their community. Further to this, frequent consumption of red meat i.e. goat, lamb and beef has contributed to gout problems. Lack of portable water and general hygiene problems have also contributed to frequent sound diarrhoea, stomach upset and abdominal complaints.

The majority of the Maasai do not rely on modern medication in the first place to treat these common mentioned diseases as well as other diseases affecting them due to their conversancy in traditional medicine. Moreover, remoteness of their living premises has caused limited accessibility to modern health care facilities. Addition to that, poverty prevalence in many Maasai families has prevented them to afford modern medications. Apart from that, even those who are in position to pay for the modern health care facilities do often seek for the traditional medicine help until when the condition is persistent or worsened. Then this is the time they attend to the nearest hospitals to seek for western based consultation and medication.

The survey results also showed the inconsistency regarding the amount of remedy administered and dosage. Unlike to modern medication where chemical constituents, concentration and dosage are uniform and well described to the patient, the active substances and their concentration in the traditional remedies are not known by the TMPs, all what they know is that the remedy cures. According to the interviewed TMPs, the overdose risk of Maasai medicinal remedies exists and sometimes leads to death. However, this survey revealed the traditional ways to control overdose symptoms as described in section **2.5.6**. Additionally, TMPs have knowledge on poisonous plants hence they are not involved in their remedies. They also have different methods for remedies preparation which reduce the drug strength, e.g. mixing a decoctions or infusions with milk tea or with fatty soup.

The medicinal potential of the four surveyed medicinal plants was witnessed from the reported diversity of the diseases treated by their remedies. Additionally, acquired information exhibited that all interviewed TMPs either use two plants or all of the four plants in their remedies and at least all TMPs knows about the four plants.

2.6.2 Preservation and transfer of traditional medicinal knowledge in the area

The current study revealed the threat of disappearance of Maasai medicinal knowledge within the area in the future. All interviewed skilled TMPs were in the senior age, majority being in the age group between 50 - 75 years and even older. These skilled TMPs are the most consulted in case of chronic diseases situation and when home treatments fails.

The formal western education and religious issues are seen to have an impact on the young generation practicing traditional medicinal practices in the Maasai community. The majority of the young generation who acquire formal education and have converted to Christianity were observed to have only basic knowledge of traditional medicine. Additionally, they do not have much time to further acquire the medicinal knowledge from the elders because of their engagement in acquiring formal education and most of their time is spent at schools away from their homes. Majority of the TMPs interviewed during the survey had the feeling that there is a lack of respect and interest among the young generation, especially regarding to those who have formal education and/or have converted to Christianity.

Moreover, it was observed that medicinal knowledge transfer to the young generation is only done by word of mouth from elder men to young men and the same applies from elder women to young women. No documentation is done during the knowledge sharing. The continuous decrease of the senior population and the seeking of formal education for the young generation may contribute to a significant loss of Maasai traditional medicinal knowledge. Therefore, detailed knowledge documentation is highly needed for preservation purposes.

2.6.3 Medicinal plants conservation in the area

It was discovered from the survey that roots and bark are the most utilized plant parts for preparation of medicinal remedies of the four investigated plants. It was further revealed that, most of the medicinal plants are harvested in the wild area. Only very few families have planted some of the medicinal plants in their home surroundings for conservation purposes as well as getting them easily without going to the wilderness whenever they need them. Additionally, the medicinal plant parts are largely sold in the local markets. The dependency on medicinal plants for treatment of diseases and the overuse of the medicinal plants by selling them in the market for economic reasons threaten the environment as well as biodiversity.

The concern of medicinal plants protection is understood to a certain extent in the surveyed area. The interviewed TMPs are aware of the need of protecting the medicinal plants. Whenever they harvest plant parts they make sure that they leave most of the tree or bush behind so that it can survive. They also believe that cutting the whole plant can lead to curse generation on a particular person. Addition to that, a group of Maasai youth (Morans) responsible for the environment protection were found in villages of Monduli and Ngorongoro districts. Their duties were to direct TMPs and other plants harvesters on where to harvest at that particular time and make sure that the harvesters do it safely without leaving the harvested plant in a dying condition.

Besides the little conservation efforts by Maasai, several big problems are obvious. Over-grazing, deforestation, and prolonged drought, which was observed in some village areas of Simanjiro and Ngorongoro districts due to climate change, has increased the threat of disappearance of some plants in this area. Hence, this calls a need of addressing some

intervention strategies before the situation is worsened and Maasai loose the basis for their traditional medicinal plant medicine.

2.7 Conclusion

The ethnopharmacological survey of four commonly used medicinal plants (*M. salicifolia, P. capensis, F. indica and V. apiculata*) in the Maasai community of north-eastern Tanzania has resulted to documentation of 34 different diseases alleged to be treated by these plants. However, the response rate of TMPs on the usage of particular plant against particular diseases reflects, that each plant has a strong effect or is highly reliable in treatment of some diseases and less in other diseases. The reasons why certain plants are highly used against particular diseases and less in treating others could be belief, location and the knowledge transfer from one TMP to another.

It was further observed, that traditional medicine is a preferred form of primary medical care as compared to modern health care which is consulted after the traditional medicine fails. This is contributed to cultural conservatism, life in the wilderness and poverty. Traditional medicinal practices constitute and will remain a key role in Maasai community, including the use of medicinal plants for the treatment of various health problems.

Additionally, threat of disappearance of the bold traditional medicinal skills was evident to the young generation of the surveyed area. This is a clear alert signal, that a proper documentation to preserve and promote the Maasai ethnomedicinal practices knowledge has to be done. There is also the need of thorough phytochemical and pharmacological investigations. This will provide scientific medicinal support for the usage of the four surveyed medicinal plants as well as improve preparation methods and safe administration of drug remedies in terms of dosage.

The high dependency on medicinal plants in Maasai area also calls for strategies to protect the plants and for measures to promote their sustainable utilization. It was observed that a few of the TMPs already have started domesticating some medicinal plant in their homestead and care during harvesting of medicinal plants is taken. But the conservation measures which are taken at the moment will not suffice in the long term as the demand for medicinal plants is growing. Hence, strong conservation strategies are highly recommended, considering that the main reported plant parts used for medicinal purposes are roots and bark.

3 Phytochemical investigation of *Myrica salicifolia* A. Rich bark

3.1 Introduction and background

3.1.1 The genus *Myrica*

The genus *Myrica* is native to warm temperate and subtropical regions in the world such as Africa, Asia, Macaronesian islands, and warm temperate and subtropical North, Central, and South America. It belongs to the family Myricaceae and is characterized by shrubs (up to 1 m) and small trees (up to 20 m), minority being deciduous and majority being evergreen. The species of the genus *Myrica* grow in nitrogen depleted soil such as gravelly sites and sandy soil due to their ability of nitrogen fixation by their root nodules which is induced by the *Frankia* soil actinomycetes[66,67].

In former times the genus *Myrica* was comprised of about 55 species distributed worldwide[67]. Recently, the genus *Myrica* is divided into two genera, the *Myrica* and *Morella* genus based on identified differences in their morphological characteristics as indicated in **Table 3.1**. Therefore, some of the species which belonged to the genus *Myrica* are now belonging to the genus *Morella*, *Myrica salicifolia* being among them. Following *Myrica* genus splitting, the *Morella* genus is now the biggest genus comprising of approximately 50 species distributed in Africa, Europe, Asia and America **(Figure 3.1)**. The genus *Myrica* comprises of the remaining species such as *M. gale, M. nagi* and *M. esculenta*[68]. Distribution is shown in **Figure 3.2**. The *Myrica* genus reclassification has posed some challenges in natural product research, as most of the authors are still using the species former scientific names and some using the current scientific names, which is confusing when searching for literature data. In this work the former species name *M. salicifolia* will be used.

Table 3.1: Morphological characteristic distinguishing the genera *Myrica* and *Morella*[69].

Character	*Myrica*	*Morella*
Leaves	Thin, deciduous, entire or feebly dentate. Stomata sunken.	Leathery, evergreen, entire or dentate. Stomata not sunken.
Flowering	Catkins inserted on the deciduous branches. Usually 4 stamens.	Catkins inserted on the growing branches. From 4 - 8 (-20) stamens.
Fruit	Subtended by 2 spongiose bracteoles. Bracteoles strongly adnate with fruit wall. Fruits are in a dense sub cylindric spike. Dry and lacking wax.	Bracteoles absent. Bracteoles not adnate with fruit wall. Fruits are mainly in a loose cluster. Fleshy and mostly waxy.

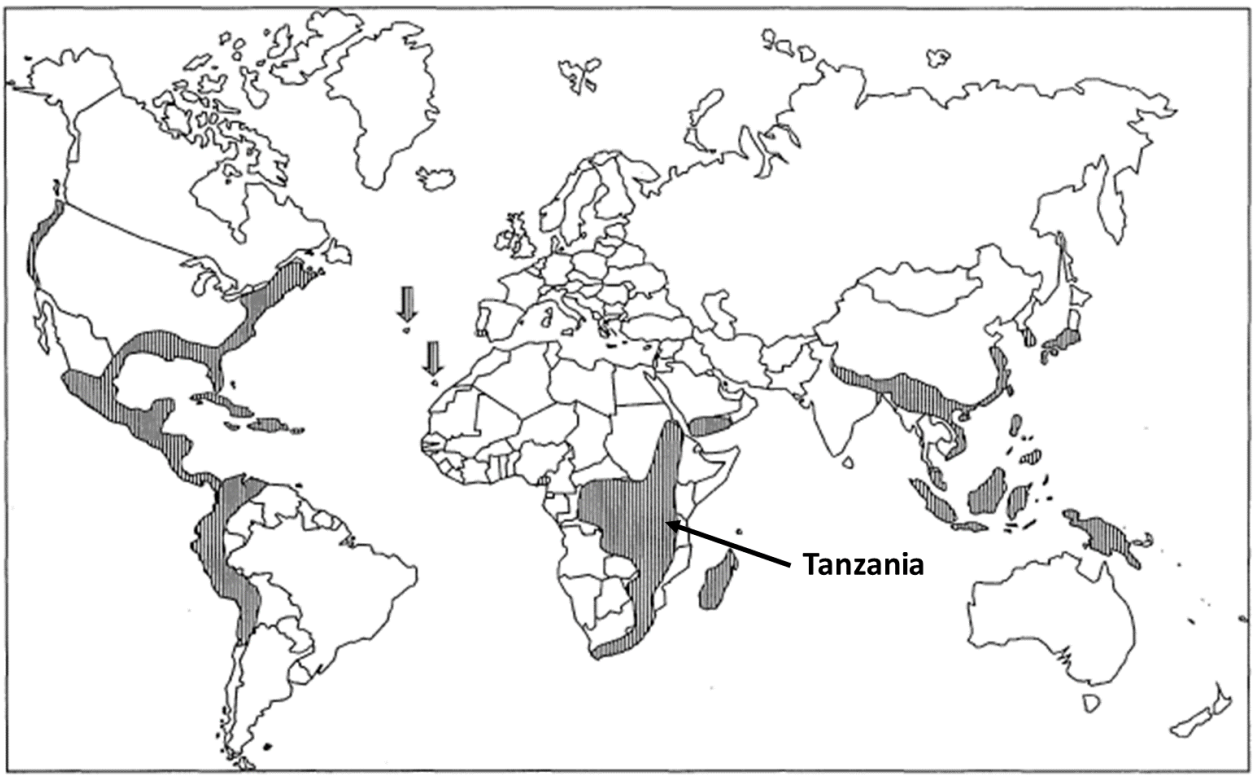

Figure 3.1: World map showing distribution of the new genus *Morella* in shaded areas[69].

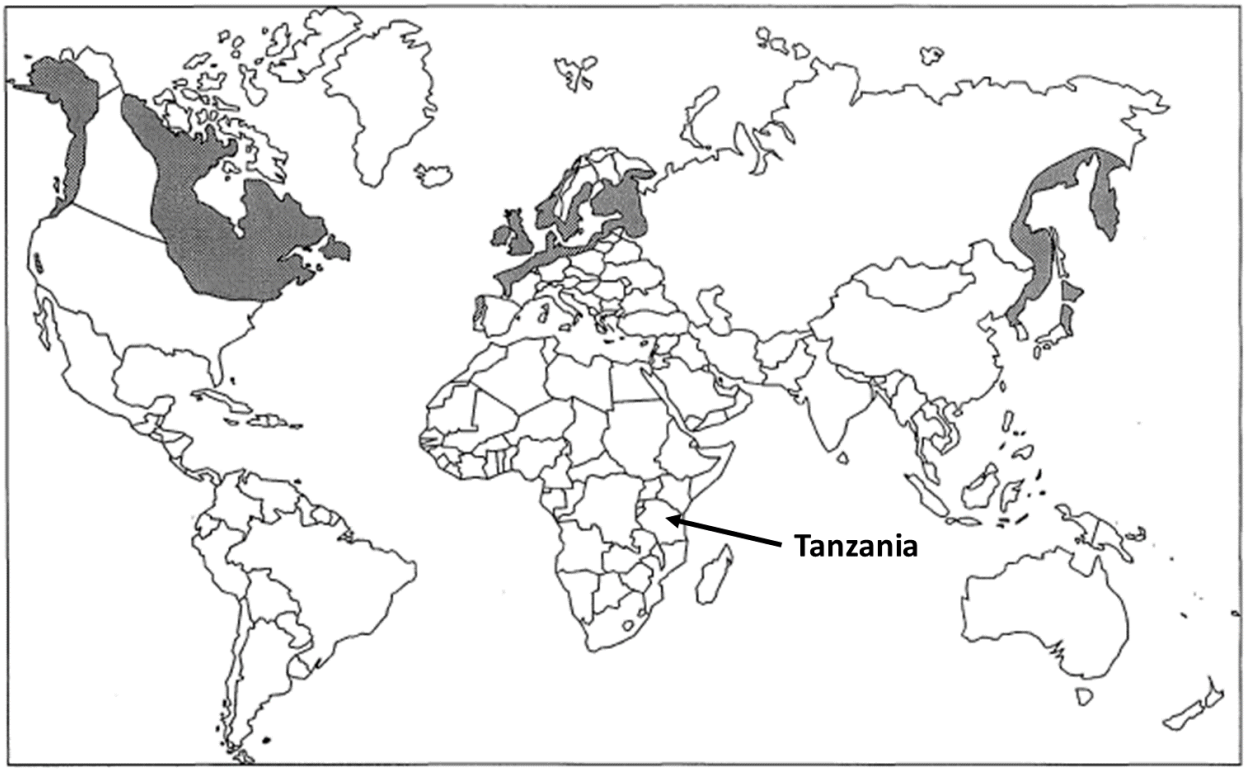

Figure 3.2: World map showing distribution of the current *Myrica* genus in shaded areas[69].

3.1.2 Phytochemical composition of the former genus *Myrica*

The *Myrica* species, not all but quite a number of them, are used for medicinal purposes in the countries where they are found. In Japan and China, remedies from different parts of *Myrica rubra* are taken for treatment of gastrointestinal disorders, headaches, burns, skin diseases and inflammatory diseases[70]. Bark, leaves and fruit juices of *Myrica esculenta* are used in India for the treatment of asthma, bronchitis, fever, lung infection, dysentery, toothache, worms, jaundice and wounds[71–74]. *Myrica nagi* is employed in China, India, Nepal and Pakistan for the treatment of cardiovascular diseases, bronchitis, gonorrhoea, diuresis, dysentery, epilepsy, gargle, haemoptysis, hypothermia, catarrh, headache, menorrhagia, putrid sores, typhoid and wounds[75,76]. *Myrica cerifera* is applicable in North America for treating irritable bowel syndrome, ulcerative colitis, digestive system disorders, diarrhoea, dysentery, leucorrhoea, mucous colitis, colds, stomatitis, sore throat, measles and scarlet fever, convulsions, nasal catarrh and jaundice[71,77]. In southern African countries, *Myrica serrata* is used for treatment of asthma, shortness of breath, painful menstruation, cold, coughs, headaches, enhancement of

male sexual performance, management of sugar related disorder and as laxative to treat constipation[78,79]. The leaf extract of *M. gale* is used as antiviral agent[80], addition to that *M. gale* is appropriate for the treatment of ulcers, intestinal worms, cardiovascular disorders and aching muscles[71,81].

Owing to its medicinal benefits and other economic importance (not described in this thesis) of the *Myrica* species, studies to investigate *Myrica* phytochemical constituents are continuously conducted for years mainly in Asian countries such as Japan, China, India and few studies from Europe. Phytochemical investigation on barks, fruits, leaves and roots of some *Myrica* species revealed the presence of tannins, cyclic diarylheptanoids, flavonoids, triterpenes and others.

3.1.2.1 Tannins

Tannins constitute a major wide class of plant secondary metabolites normally found in leaves, bark, wood, fruits and roots. They form a complex group of water soluble polyphenols characterized by higher molecular weight ranging between ≥500 to ≥3000 Dalton and their ability to bind to proteins and form tannin protein complexes. Chemically, tannins are classified into three main structural groups: hydrolysable tannins (HTs), condensed tannins/ proanthocyanidins (PAs) and complex tannins. However, only the two groups of tannins, HTs and PAs are reported in *Myrica* to date.

HTs are derived from esterification of hydroxyl groups of β-D-glucose with gallic acid **(Figure 3.3)**. HTs containing mostly a core polyol moiety of β-D-glucose and are further classified as ellagitannins and gallotannins based on their structural variations[82,83].

Gallotannins are simple HTs resulting from further attachment of galloyl groups on pentagalloylglucose through a characteristic meta-depside bonds **(Figure 3.4 A)**. Unlike gallotannins, ellagitannins are esters of hexahydroxydiphenic acid (HHDP) formed after oxidative C-C coupling between adjacent neighbouring galloyl moieties of pentagalloylglucose molecule **(Figure 3.3 and Figure 3.4 B)**[82,84]. The most common linkages occur between galloyl groups attached to position C2 and C3 and/or position C4 and C6 of the glucose moiety, but it is also possible for the combination of different linkages to occur at other positions[84]. Apart from

ellagitannins containing a glucopyranose ring there are some which contain a unique feature of open chain glucose and they have been identified to contain a 2,3- linked HHDP unit[84,85].

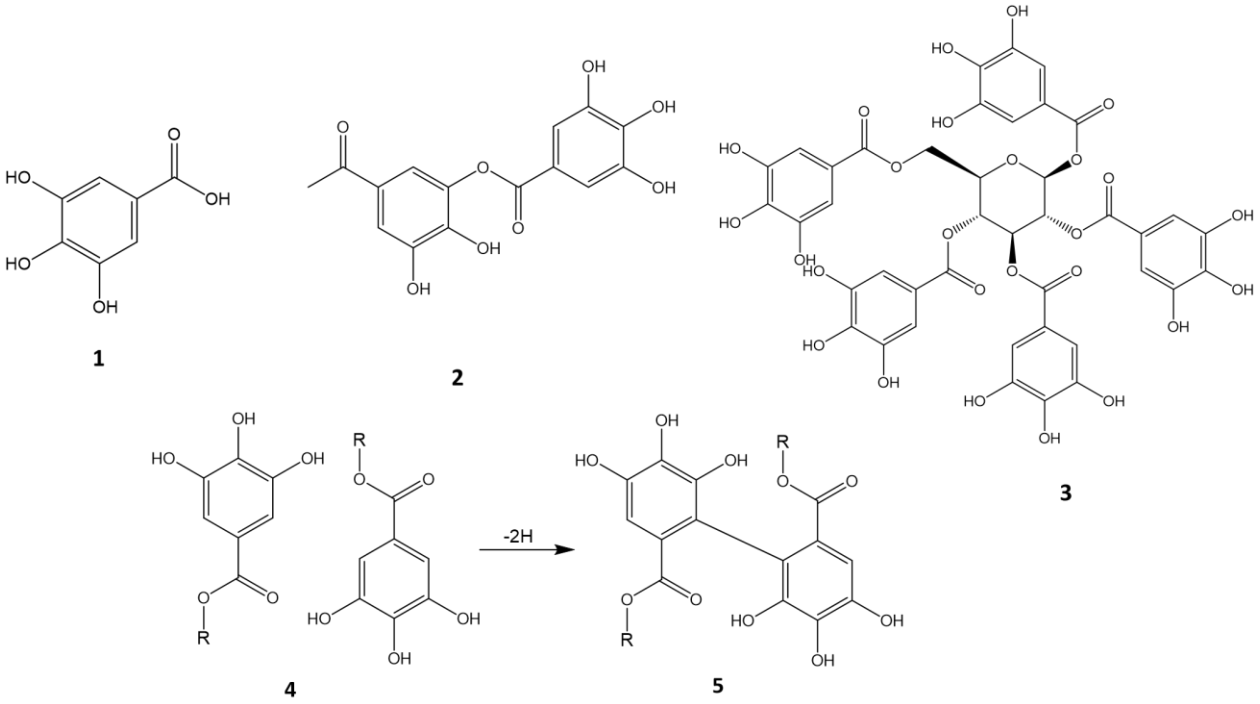

Figure 3.3: 1: gallic acid. **2:** *meta*-depside bond digalloyl ester. **3:** pentagalloylglucose. **5:** hexahydroxydiphenoyl (HHDP) ester formed through oxidative coupling between C-C linkages of the two adjacent galloyl residues **(4)**.

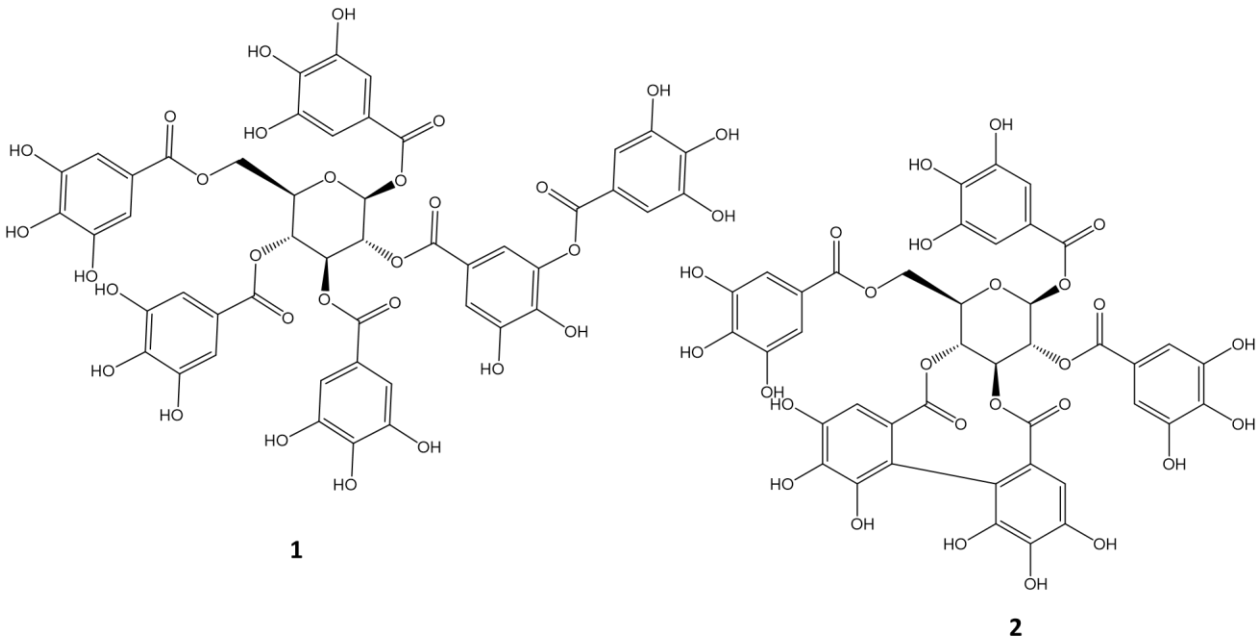

Figure 3.4: 1: Gallotannin; 2-*O*-digalloyl-1,3,4,6-tetra-*O*-galloyl-β-D-glucopyranose. **2:** Ellagitannin; nupharin A.

Condensed tannins (*syn*. proanthocyanidins (PAs)) are polyphenolic secondary metabolites of the flavan-3-ols. They are oligomers and polymers built by flavan-3-ol units. PAs are classified on the basis of hydroxylation patterns on the B ring of monomeric flavan-3-ol and the linkages between flavan-3-ol units. Based on hydroxylation patterns of their constitutive units PAs are divided into three groups, namely propelargonidins ((epi-/ent-) afzelechin), procyanidins ((epi-/ent-) catechin) and prodelphinidins ((epi-/ent-) gallocatechin) as it is indicated in **Figure 3.5**. Further to the hydroxylation pattern, the nomenclature of the monomeric units depends on the configuration at position C2 and C3[86] **(Figure 3.6)**. The configuration determines prefixes to be used such as epi- for epimer and ent- for enantiomer.

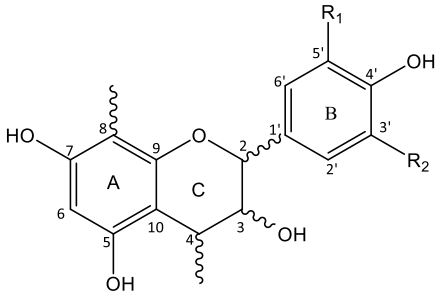

Figure 3.5: Flavan-3-ol monomeric unit of PAs. R_1, R_2 = H, propelargonidins; R_1 = H, R_2 = OH, procyanidins; R_1, R_2 = OH, prodelphinidins.

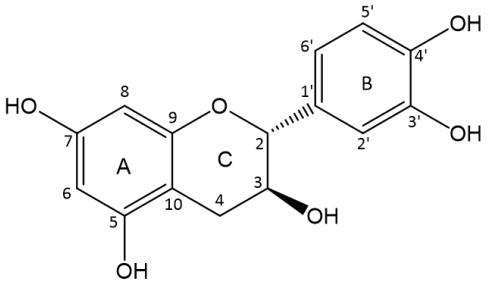

catechin (*2R,3S*)

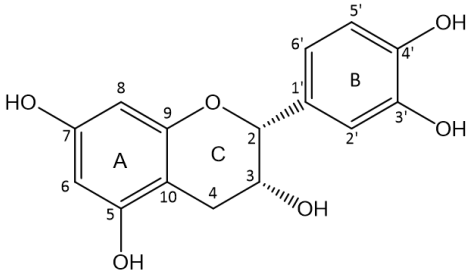

epicatechin (*2R,3R*)

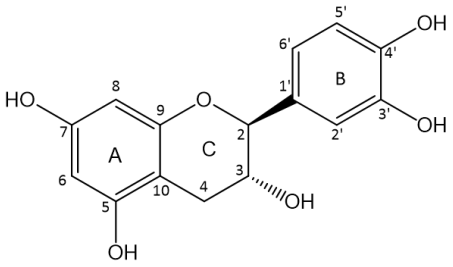

ent-catechin (*2S,3R*)

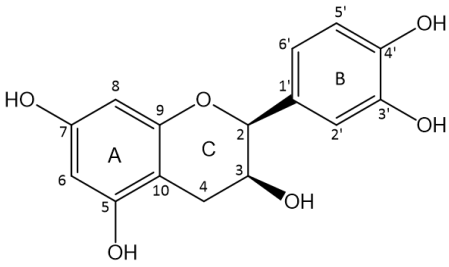

ent-epicatechin (*2S,3S*)

Figure 3.6: Possible configurations of common naturally occurring flavan 3-ol. Example of dihydroxylated flavan-3-ol.

PAs are further classified either as A-type, B-type or C-type PAs depending on their interflavan linkages in the PAs chain. The monomeric units of oligomeric and polymeric PAs of the B- and C-type are single linked by either C4 of an upper unit to C6 or C8 of the lower unit **(Figure 3.7**, **1** and **3)**. The A-type PAs are double linked through additional ether linkage between C2 of the upper unit and C5 or C7 of hydroxyl function of an A- ring of the lower unit **(Figure 3.7**, **2)**. The complete name assignment and absolute configuration of PAs dimers, oligomers and polymer is achieved when the position and stereochemistry of the interflavan bond is specified. Additionally, PAs can be esterified, glycosydated or methylated with other molecules at position C3 or C5. The most common esters of PAs are the 3-*O*-gallates formed with gallic acid and PAs[84,86].

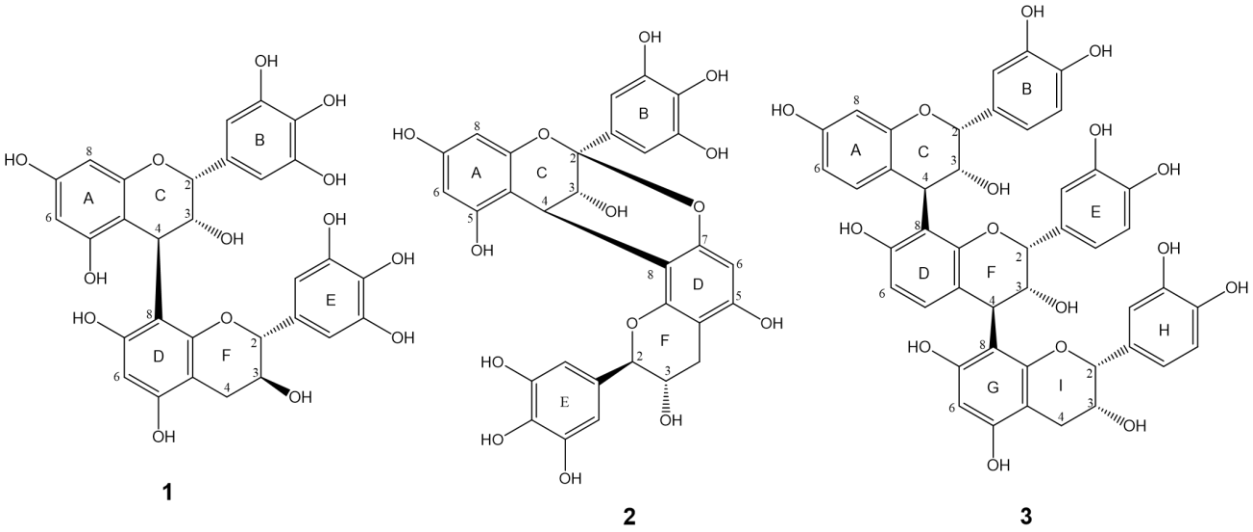

Figure 3.7: A-, B- and C-type PAs. **1:** B-type, prodelphinidin B1 (epigallocatechin-(4β→8)-gallocatechin). **2:** A-type, ephedrannin D5 (epigallocatechin-(2β→7,4β→8)-ent-gallocatechin). **3:** C-type, procyanidins C1 (epicatechin-(4β→8)-epicatechin-(4β→8)-epicatechin).

3.1.2.1.1 Tannins from *Myrica sp.* and their biological activities

Phytochemical and biological studies on *Myrica* tannins are limited. However, previous phytochemical investigations on different plant parts of few *Myrica* species revealed the presence of both, hydrolysable and condensed tannins. Castalagin, an ellagitannin isolated from *M. esculenta*[87] is the only reported hydrolysable tannin from the genus *Myrica* to date. Furthermore, the reported PAs belong to the class of prodelphinidins and a few are

procyanidins. The individual monomeric, dimeric and even trimeric PAs of B-type and A-type isolated from *Myrica* are summarized in **Table 3.2** and their respective structures in **Figure 3.8**.

Tannins are known for their numerous biological activities through conducted *in-vitro* and/or *in-vivo* studies using either a single tannin compound, fractions containing tannin polymers/oligomers or extracts rich in tannins. Biological activity investigations on tannins isolated from *Myrica* species are limited. However, some of the tannins isolated from *Myrica sp*. have also been found in other plant species and biological activities of these compounds have been reported.

In-vitro biological activity studies on ellagitannin (castalagin) revealed its antioxidant[88], antibacterial[89], antiviral[90] and leishmanicidal activity[91]. Additionally, PAs were shown to have diverse bioactivities such as antioxidant potential and beneficial effect in preventing diseases caused by oxidative stress and free radicals[71,92–94]. They also possess anti-inflammatory[95], antimicrobial[96], anti-adhesive[97], antimelanogenic[95], wound healing[98,99], anticarcinogenic[100], antidiabetic[101], anti-angiogenic[102], immunomodulatory[103] activities and show cytotoxic activity against cancer cell lines[94,103–105].

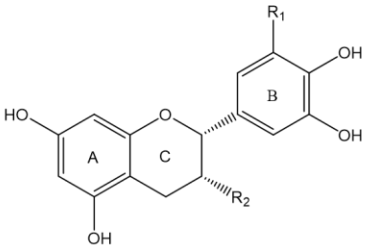

1: R1, R2 = OH
2: R1 = OH, R2 = O-gall.
5: R1 = H, R2 = O-gall.
7: R1 = H, R2 = OH

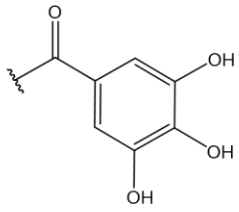

galloyl (gall.)

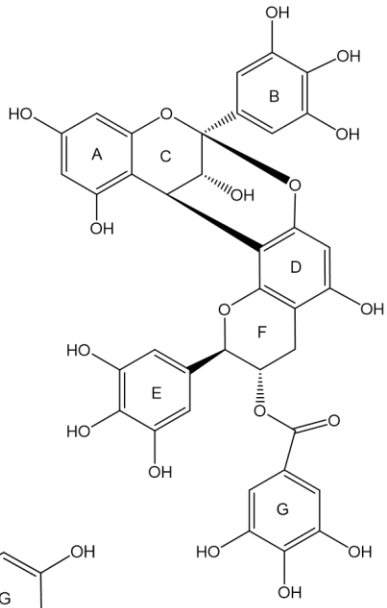

11

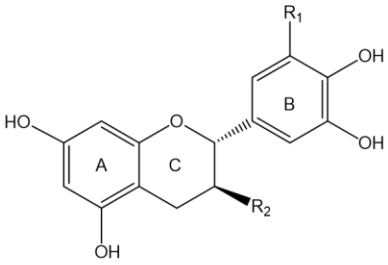

3: R1, R2 = OH
4: R1 = OH, R2 = O-gall.
6: R1 = H, R2 = OH

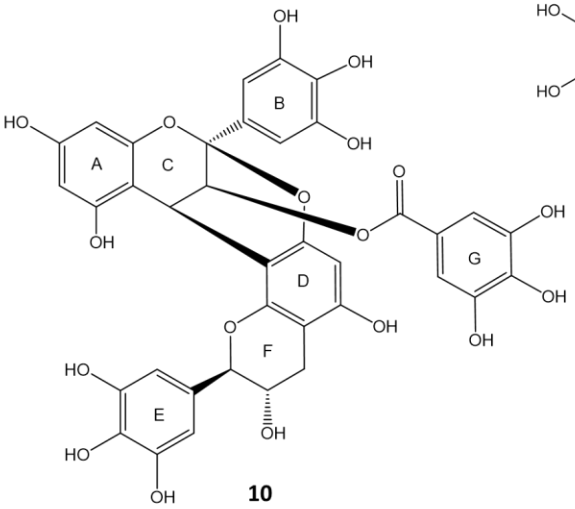

10

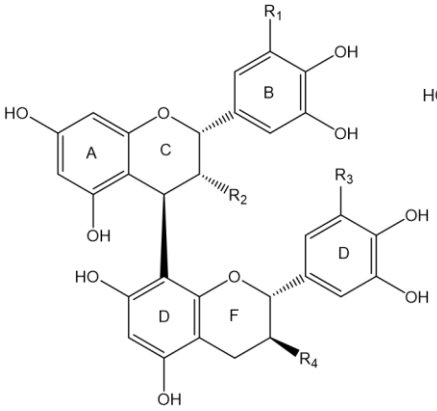

14: R1 = R2 = O-gall.

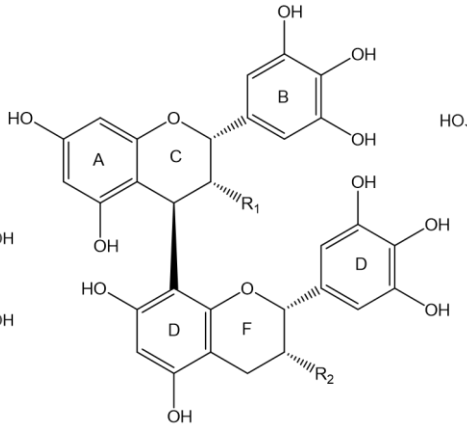

12: R1 =R2 = O-gall.
13: R1 = OH, R2 = O-gall.

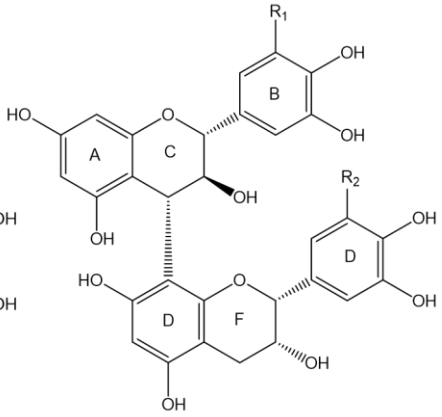

8: R1 = OH, R2 =H
9: R1 = OH, R2 = OH

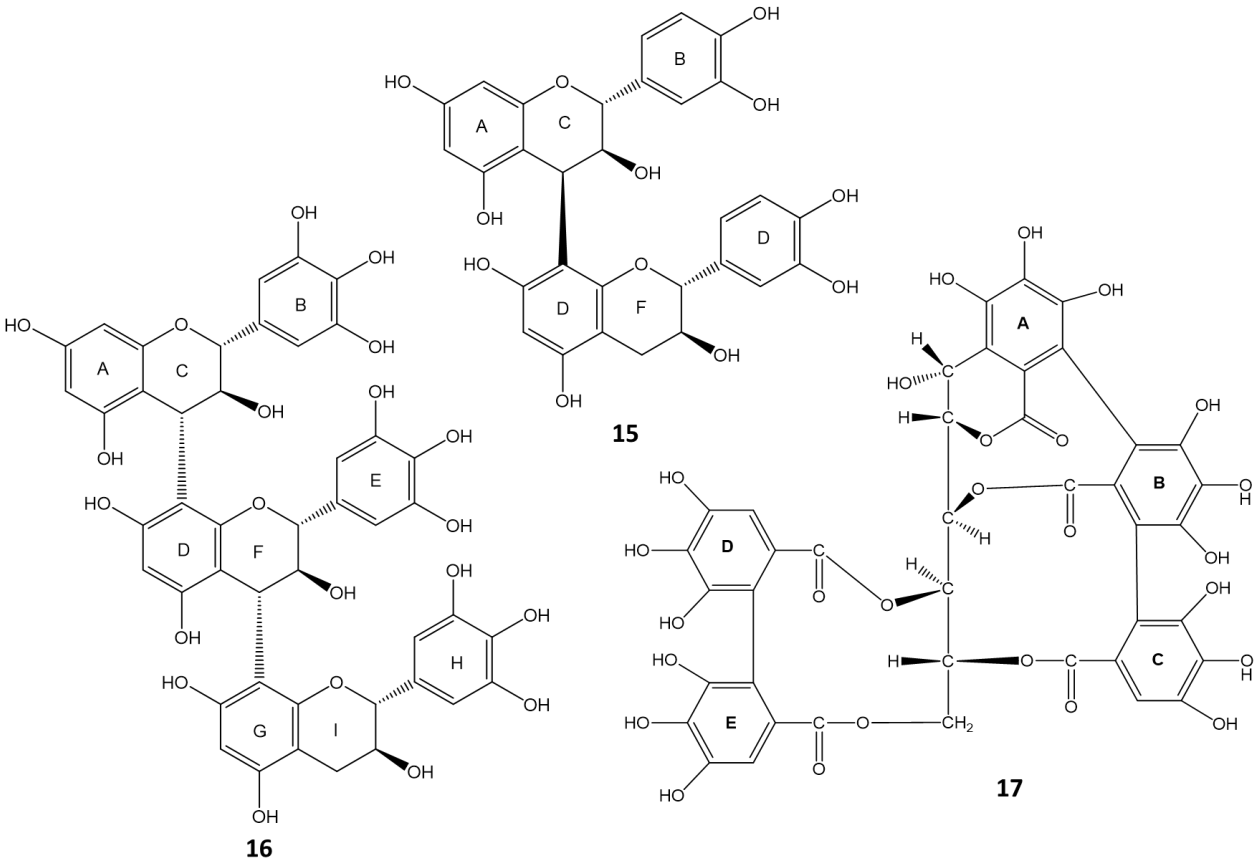

Figure 3.8: Structures of reported *Myrica* tannins. The names of the compounds are indicated in **Table 3.2**.

Table 3.2: Reported *Myrica* PAs and their occurrence within genus. Compounds numbers refers to **Figure 3.8**.

	Compound name	***Myrica* species**
	Monomeric PAs	
1	epigallocatechin	*M. rubra*[106], *M. gale*[107]
2	epigallocatechin-3-*O*-gallate	*M. rubra* var. *acuminata*[108], *M. rubra*[92,106], *M. esculenta*[87], *M. gale*[107]
3	gallocatechin	*M. rubra*[92], *M. gale*[107]
4	gallocatechin-3-*O*-gallate	*M. rubra*[92]
5	epicatechin-3-*O*-gallate	*M. rubra*[71,93], *M. gale*[107]
6	catechin-3-*O*-gallate	*M. gale*[107]
7	epicatechin	*M. rubra*[92,106]
	Dimeric PAs	
8	gallocatechin-(4α→8)-epicatechin	*M. gale*[107]
9	gallocatechin-(4α→8)-epigallocatechin,	*M. gale*[107]
10	adenodimerin C	*M. adenophora*[109]
11	prodelphinidin A-2,3'-O-gallate	*M. rubra* var. *acuminata*[108]
12	prodelphinidin B-2 3,3'-di-O-gallate	*M. rubra*[106,110], *M. esculenta*[87]
13	prodelphinidin B-2 3'-O-gallate	*M. rubra*[106], *M. esculenta*[87]
14	prodelphinidin B-1 3,3'-di-O-gallate	*M. rubra*[106]
15	procyanidin B2	*M. rubra*[71,93]
	Trimeric PAs	
16	gallocatechin-(4α→8)-gallocatechin-(4α→8)-gallocatechin	*M. gale*[107]
	Ellagitannin (HTs)	
17	castalagin	*M. esculenta*[87]

3.1.2.2 Diarylheptanoids

Diarylheptanoids are a group of plants secondary metabolites which occur in root bark, bark, inner stem, leaves and twigs[111]. They have a common structural feature with two aromatic rings linked by a linear seven-carbon chain (heptane). Diarylheptanoids are classified into two groups as linear and cyclic diarylheptanoids. Linear diarylheptanoids are further divided into acyclic diarylheptanoids which contains no oxygenic ring in the chain and epoxy diarylheptanoids which contain an oxygenic ring in the chain **(Figure 3.9**, **1** and **2)**. Cyclic diarylheptanoids in which the two phenyl groups are linked either directly or as a diaryl ether are also divided further into two groups depending on the position of the two phenyl groups join with each other and with the heptane chain, metametacyclophanes (*meta,meta*-bridged biphenyl) and metaparacyclophanes (*meta,para*-bridged diphenyl ether) as shown in **Figure 3.9**, **3** and **4**.

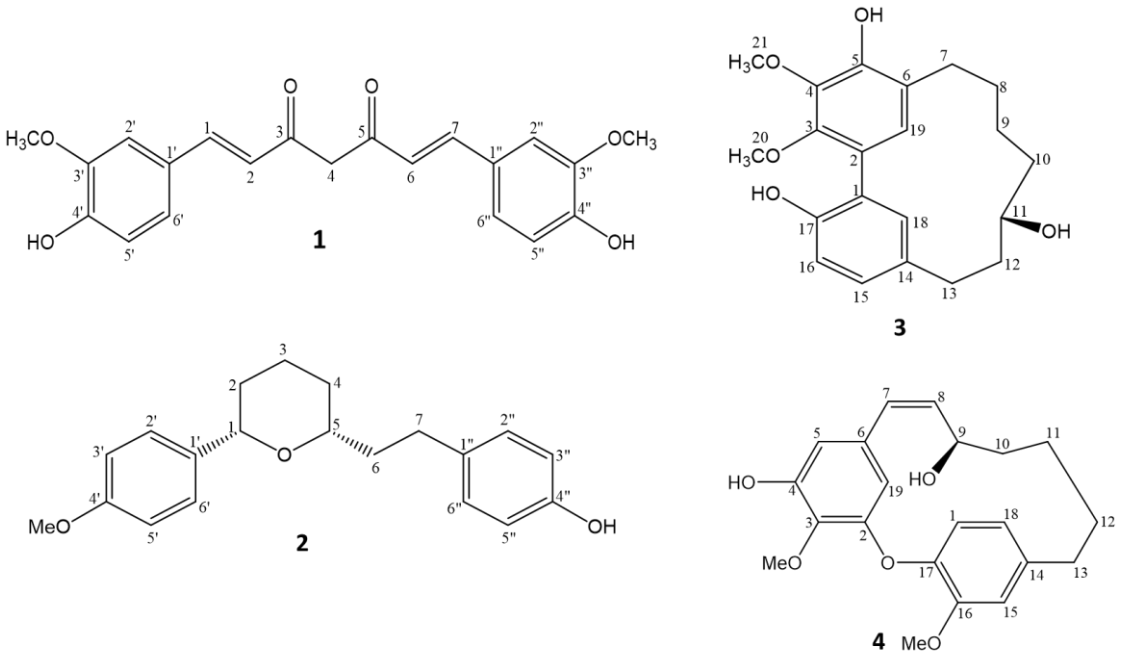

Figure 3.9: Compound examples for different groups of diarylheptanoids. **1:** curcumin: acyclic diarylheptanoid. **2:** centrolobine: epoxy diarylheptanoid. **3:** myricanol: metametacyclophane. **4:** platycarynols: metaparacyclophane.

3.1.2.2.1 Diarylheptanoids from *Myrica* sp. and their biological activities

Cyclic diarylheptanoids are among the groups of compounds isolated over the years from the genus *Myrica*. Phytochemical data reporting the isolation of linear diarylheptanoids from *Myrica* are scarce. However, *Myrica* species are well known to contain biphenyl cyclic diarylheptanoids. The isolated biphenyl cyclic diarylheptanoids from *Myrica* have structural features variations due to the presence of carbonyl group, hydroxylation, methoxylation, and glycosydation patterns of the two aromatic rings and the aliphatic chain. Additionally, isolation of biphenyl cyclic diarylheptanoids containing galloyl and sulphate groups from *M. rubra* were reported[110,112]. Apart from the occurrence of biphenyl cyclic diarylheptanoids in *Myrica*, isolation of few diphenyl ethers like galleon, myrica tomentoside, myrica tomentogenin[113], hydroxygaleon, myricananadiol[114,115] and 16-methoxyacerogenin B 9-*O*-β-D-apianofuranosyl-6)-β-D-glucopyranoside[116] were reported **(Figure 3.10)**. Structures and names of isolated biphenyl cyclic diarylheptanoids from *Myrica* species are shown in **Table 3.3** and **Figure 3.11**.

The *in-vitro* or *in-vivo* biological activity investigations performed on the cyclic diarylheptanoids isolated from *Myrica* species revealed anti-oxidative[71,109,110], anti-inflammatory [71,109,110,112,117,118], neuroprotective[119], antitumor-promoting[120], melanogenesis inhibitory[116], hepatoprotective[116,121] and antiandrogenic activity[122].

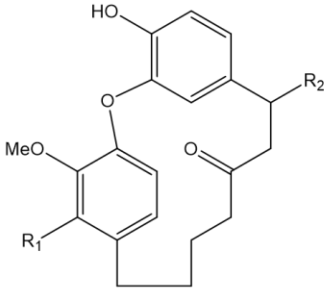

		R1	R2
1.	galeon	H	H
2.	myricatomentogenin	OH	H
3.	myricatomentoside	O-β-D-glc.	H
4.	hydroxygaleon	H	H

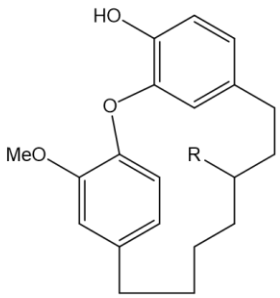

		R
5.	16-methoxyacerogenin B 9-*O*-β-D-apianofuranosyl-6)-β-D-glucopyranoside	O-glc-api
6.	myricananadiol	OH

Figure 3.10: Diarylheptanoids from *Myrica* belong to the class diphenyl ethers.

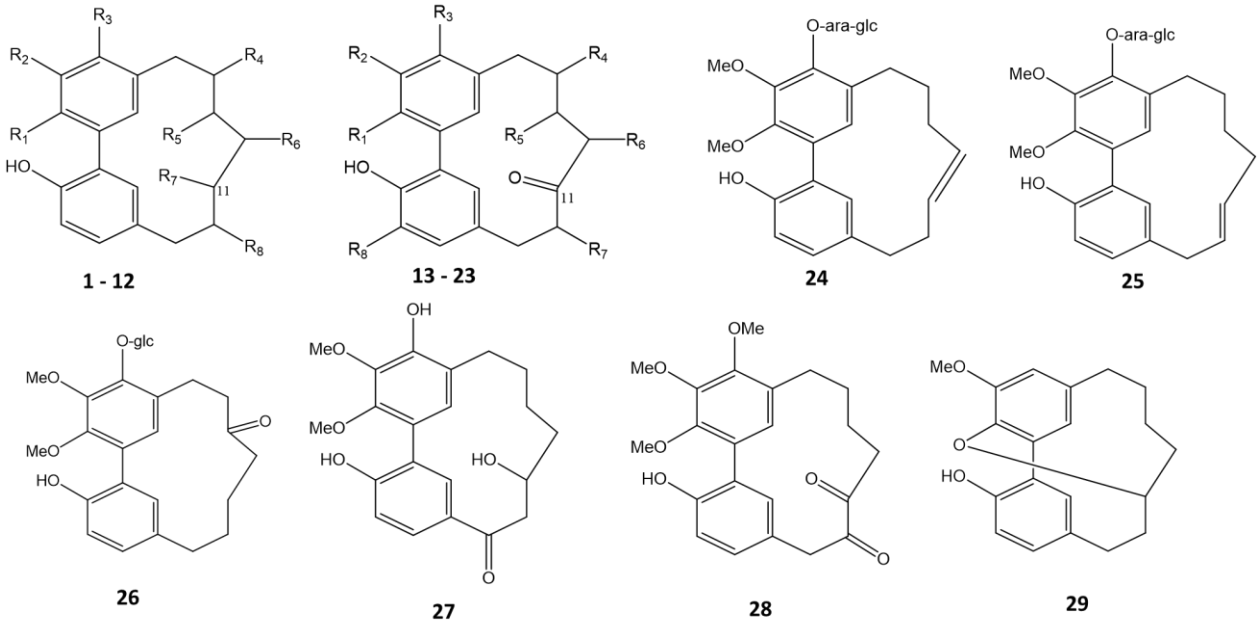

Figure 3.11: Some of the isolated biphenyl diarylheptanoids from *Myrica*. Compound **1-12** and **13-23** are listed in **Table 3.3**. **24:** myricanene A 5-*O*-α-L-arabinofuranosyl (1-6)-β-D-glucopyranoside[117,123]. **25:** myricanene A 5-*O*-α-L-arabinofuranosyl (1-6)-β-D-glucopyranoside[117,123]. **26:** neomyricanone-5-O-β-D-glucopyranoside[117]. **27**: 13-oxomyricanol[124]. **28**: 12-dehydroporson[125]. **29:** myricaborin[126].

Table 3.3: Compound **1-12** and **13-23**. Compounds numbers refers **Figure 3.11**.

	Compound 1-12 (contain no carbonyl substitution at C11)							
		R1	**R2**	**R3**	**R4**	**R5**	**R6**	**R7**	**R8**
1	myricanol[123]	OMe	OMe	OH	H	H	H	OH	H
2	myricananin F[127]	OH	OMe	H	H	H	OH	H	H
3	myricananin A[118]	OH	OMe	H	H	H	H	OH	OH
4	myricananin H[127]	OH	OMe	OMe	H	H	H	OH	OH
5	myricananin G[127]	OMe	OMe	OH	H	H	H	OH	OH
6	myricanol-11-*O*-β-D-glucopyranoside[117,127]	OMe	OMe	OH	H	H	H	O-glc.	H
7	myricanol-5-*O*-β-D-glucopyranoside [117,127]	OMe	OMe	O-glc.	H	H	H	OH	H
8	11-*O*-β-D-xylopyranosylmyricanol[126]	OMe	OMe	OH	H	H	H	O-xyl.	H

		R1	R2	R3	R4	R5	R6	R7	R8
9	myricanol galloylglucoside[110,116]	OMe	OMe	O-glc-gall.	H	H	H	OH	H
10	myricanol gentiobioside[128]	OMe	OMe	O-glc-(6-1)-glc	H	H	H	OH	H
11	myricanol-5-*O*-β-D-glucopyranosyl-(1-3)- β-D-glucopyranoside[129]	OMe	OMe	O-glc-(1-3)-glc	H	H	H	OH	H
12	myricanol 5-*O*-α-L-arabinofuranosyl (1-6)-β-D-glucopyranoside[129]	OMe	OMe	O-ara-(1-6)-glc	H	H	H	OH	H
	Compound 13-23 (contain carbonyl substitution at C11)								
13	myricanone[117]	OMe	OMe	OH	H	H	H	H	H
14	myricananin C[118]	OH	OMe	H	H	H	H	H	H
15	myricananone[118,130]	OMe	OMe	OH	OH	H	H	H	H
16	myricananin E[118]	OMe	OMe	OH	H	H	H	OMe	H
17	12-hydroxymyricanone[118,125]	OMe	OMe	OH	H	H	H	OH	H
18	porson[125,130,131]	OMe	OMe	OMe	H	H	H	OH	H
19	myricatomentoside II[131]	OMe	OMe	O-glc.	H	H	H	OH	H
20	myricanone-5-*O*-β-D-glucopyranoside[117]	OMe	OMe	O-glc.	H	H	H	H	H
21	5- deoxymyricanone[131]	OMe	OMe	H	H	H	H	H	H
22	myricanone 5-*O*-α-L-arabinofuranosyl (1-6)-β-D-glucopyranoside[129]	OMe	OMe	O-ara-(1-6)-glc	H	H	H	H	H
23	myricanone galloylglucoside[110]	OMe	OMe	O-glc-gall.	H	H	H	H	H

3.1.2.3 Other groups of compounds from *Myrica* sp.

Flavonoids are another group of compounds isolated from *Myrica* and there are several ones isolated from this genus. However, among others, the most frequent reported flavonoids from *Myrica* species are myricetin, kaempferol, myricitrin, quercetin, quercitrin, and myricetin 3-*O*-(6″-*O*-galloyl)-β-D-galactopyranoside[71,109,117,128,132,133]. The structures of *Myrica* flavonoids are shown in **Figure 3.12**.

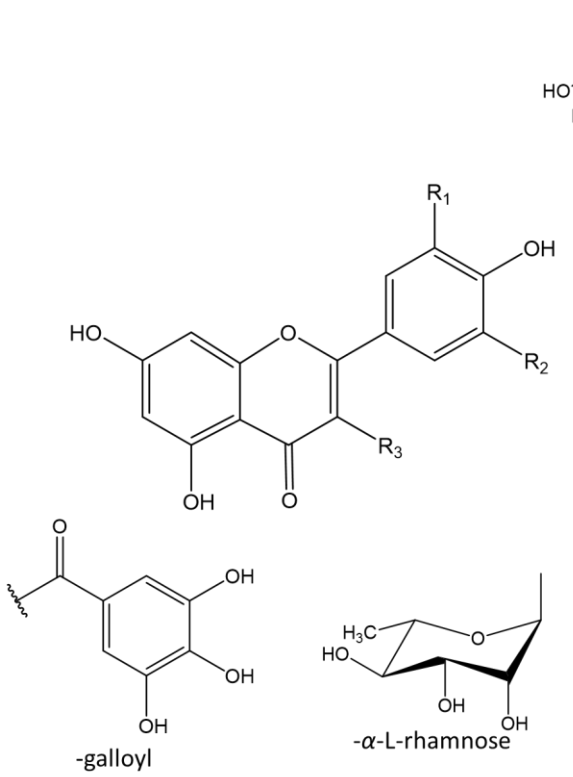

	R1	R2	R3
myricetin	OH	OH	OH
myricitrin	OH	OH	*O*-rham.
myricetin 3-*O*-(6-O-galloyl)-β-D-galactopyranoside	OH	OH	*O*-galact-galloyl
myricetin 3-*O*-(2-*O*-galloyl)-β-D-galactopyranoside	OH	OH	*O*-galact-galloyl.
myricetin 3-*O*-(2-*O*-galloyl)-α-L-rhamnopyranoside	OH	OH	*O*-rham-galloyl.
quercetin	OH	H	OH
quercitrin	OH	H	*O*-rham.
quercetin 3-*O*-(2-*O*-galloyl)-β-D-galactopyranoside	OH	OH	*O*-galact-galloyl.
kaempferol	H	H	OH

Figure 3.12: Structures of flavonoids isolated from *Myrica.*

Furthermore, identification and isolation of triterpenes from *Myrica* was reported. Some of the reported triterpenes **(Figure 3.13)** are teraxerol, myricadiol, myricalactone, myricolal, rhoiptelenol, ursonic acid, ursolic acid, acetylursolic acid oleanolic acid, oleanolic acid acetate, arjulonic acid, alphitolic acid, and maslinic acid[117,125,128,134,135].

Besides flavonoids and triterpenes, sterols, phenolic acids and dihydrochalcones were isolated from the genus *Myrica*.

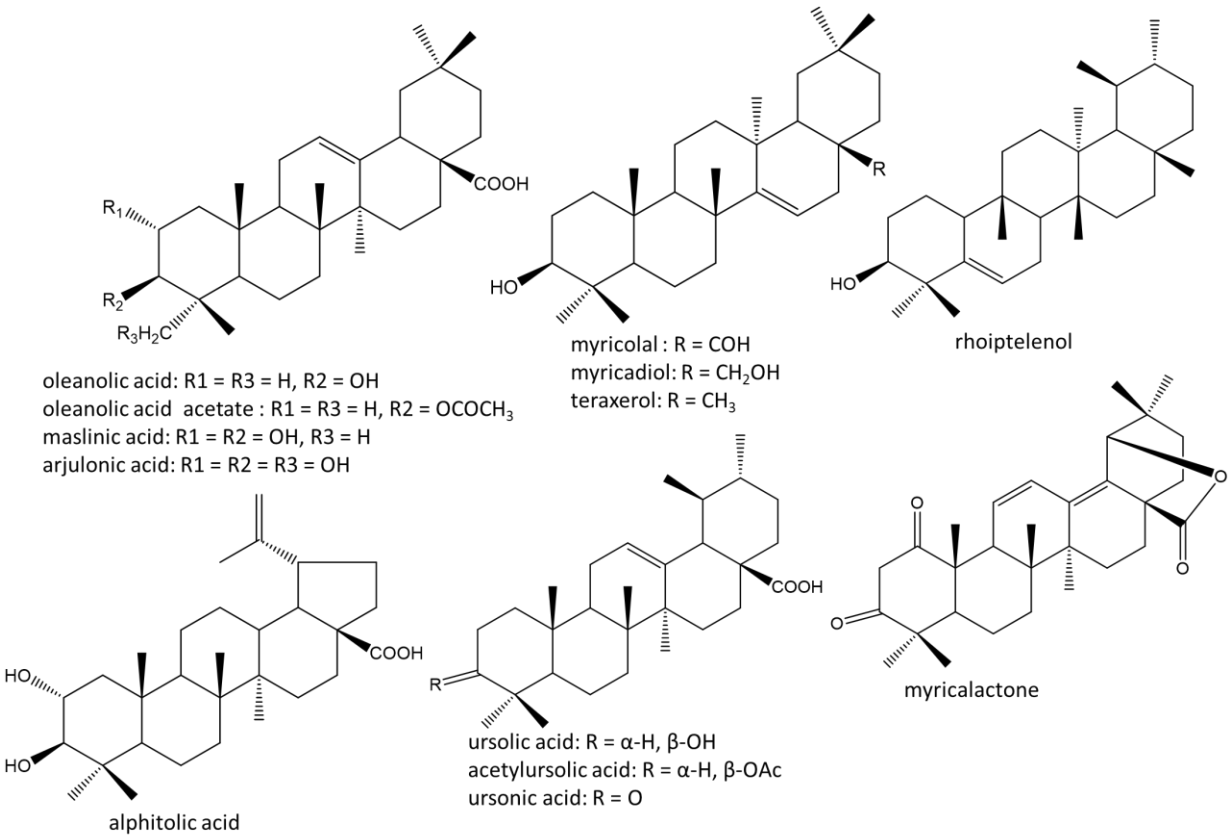

Figure 3.13: Structures of triterpenes isolated from *Myrica.*

3.1.2.4 Phytochemical investigation and biological activities of *Myrica salicifolia*

Myrica salicifolia is a common traditional medicinal plant used for treatment of many ailments in Tanzania[136] (see also **chapter 2**) like headache, pain inflammation and respiratory disorders in Ethiopia[137,138]. Despite of many traditional uses of *M. salicifolia*, literature describing its phytochemical characterization and bioactivity tests is scarce.

Performed phytochemical screening on the extracts of *M. salicifolia* showed the presence of polyphenols, triterpenes, saponins and glycosides[37]. To date, no literature reports isolation of individual compounds from *M. salicifolia.*

In-vivo bioactivity investigation on laboratory mice using a methanolic extract of *M. salicifolia* roots revealed potent antipyretic and analgesic activity in this experimental arragements[38]. Moreover, antimicrobial activity against *Bacillus cereus*, *Neisseria gonorrhoea*, *Shigella dysenteriae* and *Staphylococcus aureus* was observed for a methanolic extract of *M. salicifolia* stem bark[37].

3.2 Materials and Methods

3.2.1 Chemicals, solvents, reference sugars and enzyme

Name	Manufacturer
Acetic acid 98 - 100%, for analysis	Merck, Darmstadt
Acetone, for analysis	Merck, Darmstadt
Acetonitrile, HPLC grade	Merck, Darmstadt
Chloroform, for analysis	Merck, Darmstadt
Deuterated acetone - d_6, 99.8%	Deutero, Kastellaun
Deuterated chloroform - d_1, 99.8%	Deutero, Kastellaun
Deuterated methanol - d_4, 99,8%	Sigma-Aldrich, Taufkirchen
Deuterated pyridine-d_5, 99,5%	Deutero, Kastellaun
Dichloromethane, for analysis	Acros Organics, USA
Ethanol, absolute	Sigma-Aldrich, Steinheim
Ethylacetate, for analysis	Acros Organics, USA
Formic acid 99%, for analysis	Merck, Darmstadt
Methanol, for analysis	Merck, Darmstadt
Methanol, HPLC grade	Merck, Darmstadt
Methanol, for spectroscopy (Uvasol)	Merck, Darmstadt
(*S*)-(+)-2-Methylbutyric anhydride, 95%	Sigma-Aldrich
4-Methoxybenzaldehyde, for analysis	Merck, Darmstadt
Diphenylboryloxyethylamine, 95% (Natural product reagent)	Fluka/Sigma-Aldrich, USA
2-Propanol, for analysis	Merck, Darmstadt
Pyridine, for analysis	Merck, Darmstadt
Sodium acetate, 99%	Merck, Darmstadt
Sodium carbonate, 99.5%	Sigma-Aldrich, Taufkirchen
Sulphuric acid, 95-97%, for analysis	Merck, Darmstadt
Toluene, for analysis	VWR Chemicals, France
Trifluoroacetic acid (TFA), 99%	Sigma-Aldrich, Taufkirchen
D-Arabinose	Sigma-Aldrich, Taufkirchen
L-Arabinose	Merck Darmstadt
D-Galactose	Sigma-Aldrich, Taufkirchen
L-Galactose	Sigma-Aldrich, Taufkirchen

Name	Manufacturer
D-Glucose	Sigma-Aldrich, Taufkirchen
L-Glucose	Roth, Karlsruhe
D-Mannose	Merck, Darmstadt
D-Xylose	Merck, Darmstadt
β-Glucosidase (Almond)	Roth, Karlsruhe

3.2.2 Laboratory equipment

Equipment	Model	Manufacturer
Analytical HPLC	Elite LaChrom HPLC Auto sampler: L-2200 Pump: L-2130 DAD: L-2455 Column oven: L-2350 Software: EZChrom Elite 3.1.7	VWR, Darmstadt
CD spectrometer	J-710	JASCO, Groß-Umstadt
Centrifuge	Hermle Z 365	Kontron & Hermle KG, Switzerland
CPC	SPOT centrifugal partition chromatography Pump: 515 HPLC pump	Armen Instrument, Saint-Avé, France Waters, USA
Flash chromatography	Spot Liquid Chromatography Flash Software: Armen Glider Flash V2.3	Armen Instrument, Saint-Avée,
Fraction collector	2111 Superrac	LKB Bromma, Sweden
Freeze dryer	Ilmvac 100 with pump 302061 PK8D	ILMVAC GmbH, Ilmenau
Heating plate	Thermoplate S	Desaga, Nümbrecht
Mass spectrometer	ESI-MS: Finnigan MAT SSQ 710 A LC-MS: Thermo Quest Finnigan TSQ 7000	Thermo Quest, Egelsbach
Milling machine	UZM ZM1 Yellow line A10	Retsch, Haan IKA-Werke, Staufen
NMR spectrometer	AVANCE 300 AVANCE 600 Software: Top spin 3.2	Bruker, Ettlingen

Equipment	**Model**	**Manufacturer**
Oven	Memmert	Memmert, Schwabach
Polarimeter	UniPol L 1000	Schmidt and Haensch, Berlin
Rotary vacuum evaporator	Laborota 4003-control	Heidolph, Schwabach
Scales	Analytical scale Research 160 P Extend ED 2245	Sartorius, Göttingen
Semi preparative HPLC	ProStar HPLC Autosampler: 410 Two pumps system: 210 DAD: 335 Fraction collector: 701 Software: Galaxie 1.9.302.952	Varian, Darmstadt
Semi preparative HPLC	1260 Infinity HPLC Binary pump cluster: 2x G1361A DAD: G1315D Fraction collector: G1364B Software: Open LAB CDS Chemstation Edition C.01XX	Agilent Technologies, Waldbronn
TLC	Sample application : Linomat 5 Linomat syringe (100 µl) Photo documentation: Reprostar 3 Software: WinCats 1.4.2	CAMAG - Muttenz, Switzerland
TLC developing chamber	Twin Trough Chamber 20 x 20 cm Twin Trough Chamber 10 x 10 cm	CAMAG - Muttenz, Switzerland
Ultrasonic bath	VWR Ultrasonic cleaner	VWR, Darmstadt
UV spectrometer	Cary 50 Scan Software: Cary WinUV 3.00(182)	Varian, Darmstadt
Water purifier	MembraPure	PMA Purification Membranes Analytics, Hennigsdorf

3.2.3 Other laboratory materials

Material	Manufacturer
Micropipette / capillary tube (5, 10, 20 µL)	BRAND, Wertheim
NMR tubes 507-HP-8	Norell, Landisville (USA)
Preparative HPLC syringe (manual injection - 5 mL)	VWR, Darmstadt
Quartz cuvettes (1 mm, 10 mm)	Hellma, Müllheim
Silica gel 60 F_{254} aluminium sheets, 20 × 20 cm	Merck, Darmstadt
Syringe filter (pore size = 0.25 microns)	Wicom, Heppenheim

3.2.4 Columns used for chromatography

	Stationary phase	Particle size	Amount loaded	Dimension/ volume	Manual/pre-packed	Manufacturer
C1	Sephadex® LH-20	25 – 100 µm	265 g	L = 90 cm, Ø = 4.76 cm	Open column chromatography. Manual packed.	GE Healthcare GmbH, München
C2	RP-18	25 - 40 µm	30 g	44 mL	Column for flash chromatography. Manual packed.	Merck, Darmstadt
C3	RP-18 (SVP D40-RP18)	25 - 40 µm	90 g	131 mL	Column for flash chromatography. Pre-packed.	Merck Chimie SAS, France
C4	MCI- Gel® CHP20P	75 - 150 µm	170 g	L = 60 cm, Ø = 2.5 cm	Column for flash chromatography. Manual packed.	Mitsubishi Chemical Europe GmbH, Düsseldorf
C5	Silica gel (Reveleris Flash Cartridges)	20 µm	12 g		Column for flash chromatography. Pre-packed.	Grace, Deerfield-Illinois, USA
C6	RP-18 (Purospher STAR, RP18)	5 µm		L = 250 mm, Ø = 4 mm	HPLC column. Pre-packed.	Merck, Darmstadt

	Stationary phase	**Particle size**	**Amount loaded**	**Dimension/ volume**	**Manual/pre-packed**	**Manufacturer**
C7	RP-18 (Eclipse XDB-C18)	5 µm		Ø = 9.4 mm, L = 250 mm	HPLC column. Pre-packed.	Agilent Technologies, USA
C8	RP-18 (Eclipse XDB-C18)	5 µm		Ø = 21.2 mm, L = 250 mm	HPLC column. Pre-packed.	Agilent Technologies, USA

3.2.5 Plant material

The bark of *M. salicifolia* was collected in February 2013 at Monduli mountain ranges Arusha region, Tanzania. Identification of the plant was done by Mr. Daniel Sitoni, senior botanist from Tanzania National Herbarium (TNH) and later the specimen was stored at TNH with voucher number CK 7792. The collected bark material was spread on a clean cotton cloth under direct sunlight with a temperature between 30 – 35 ^{o}C until it was completely dried. The dried bark material was reduced in size **(Figure 3.14)** packed and sent to Regensburg, Germany for phytochemical investigation.

Figure 3.14: A: Collection of *M. salicifolia* bark. **B**: Drying. **C:** The dried *M. salicifolia* bark. **D:** The process of size reduction. **E:** *M. salicifolia* bark after size reduction, before packaging and transport to Regensburg-Germany for phytochemical characterization.

3.2.6 Extraction of plant material

Prior to extraction, the dried *M. salicifolia* bark (390.1 g) was further reduced in size by cutting it into small pieces and which were then pulverized using a milling machine. The obtained powder was mixed with 400 g of sea sand, packed in a column and macerated overnight with 1 L of dichloromethane. After maceration, bulk extraction of *M. salicifolia* bark was performed using four different solvents with increasing polarity. The solvents used for the extraction were dichloromethane, ethylacetate, methanol 100% and methanol 50%. Approximately 4 litre of each extraction solvent was used during extraction.

At the end of extraction, four crude extracts were obtained **(Figure 3.15)** and were evaporated to complete dryness using a rotary vacuum evaporator at 40 ^{o}C. To achieve crude extracts homogeneity, the residues recovered after evaporation were mixed in water, completely frozen at -20 ^{o}C and lyophilized. The dried powder crude extracts were stored at 4 ^{o}C in the refrigerator.

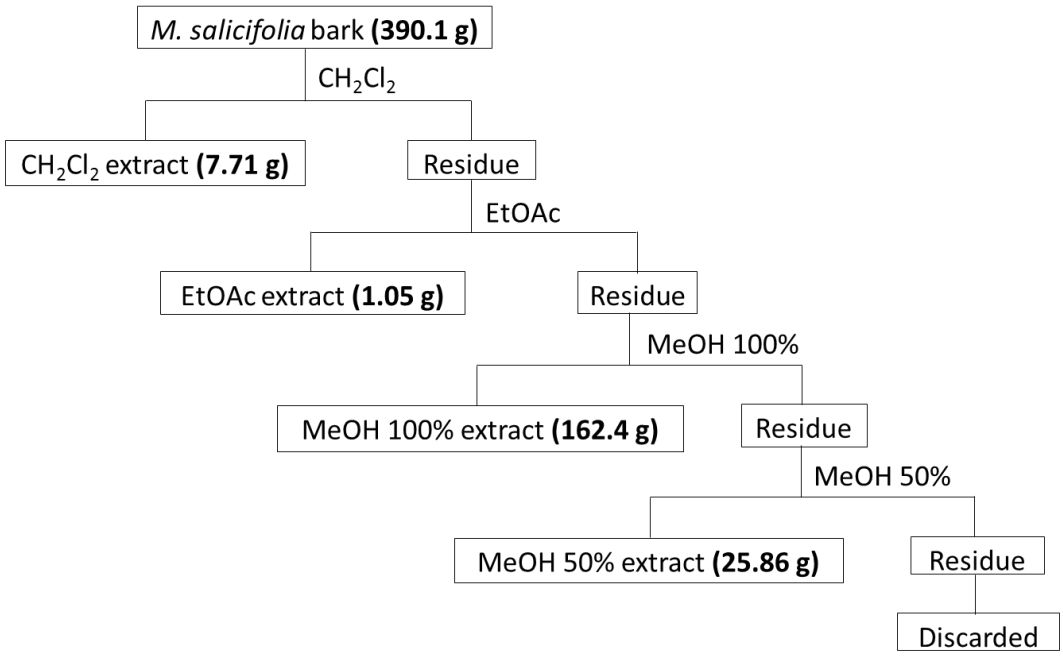

Figure 3.15: Extraction protocol of *M. salicifolia* bark.

3.2.7 Fractionation and isolation

3.2.7.1 Thin layer chromatography (TLC)

TLC was performed for control check during the extraction and fractionation steps. In the course of extraction, TLC was used to determine the time to change from one extraction solvent to another. The solvent change was done following no further detection of spots on a TLC sheet when visualized under UV 254 nm. Furthermore, TLC methods utilizing different spray reagents were used for preliminary confirmation on the groups of compounds present in the extracts.

Besides, throughout chromatography TLC method was done for determination of identical fractions to be combined during and/or after chromatographic run. It was further used for open column chromatography where UV detector was not applicable for control check on the time to stop chromatography. Lastly, selection and optimization of chromatographic solvent system was achieved through TLC. The solvent system was considered optimal for the chromatography after migrating the substances of interest between retardation factor (R_f) value of 0.3 – 0.8. Retardation factor is defined as the ratio of the distance the compound spot migrated to the distance migrated by the solvent front (**Formula 1**).

Unless stated otherwise in the text, the analytical TLC parameters and method used in this study is described in **Table 3.4** below.

Formula 1: Calculation of Retardation factor (R_f).

$$Rf = \frac{\text{Distance migrated by the compound}}{\text{Distance migrated by the solvent font}}$$

Table 3.4: The analytical TLC method and parameters.

Stationary phase	Silica gel 60 F_{254} aluminium sheets, 20 × 20 cm.
Mobile phases (MP)	**MP_1:** Ethylacetate : water : acetic acid : formic acid (100:26:11:11) **MP_2:** Toluene : ethylacetate : formic acid (70:30:1)
Application tools	TLC spotting capillaries and Linomat 5
Sample volume	5 – 40 µL depending on sample concentration
Application method	Either as a narrow band 1 cm wide or as a spot. Distance between two bands/spots was set to be 0.5 - 1 cm. TLC sheets were allowed to air dry before inserted in a development chamber.
TLC development	In a covered twin trough TLC chamber 20 x 20 cm containing mobile phase. After development (migration distance 10 cm) TLC sheets were left to air dry before detection with spray reagent.
Spray reagents (SR)	**SR_1:** Anisaldehyde-sulphuric acid reagent (0.5 mL anisaldehyde, 10 mL acetic acid, 85 mL methanol, 5 mL concentrated sulphuric acid). **SR_2: A:** Vanillin 1% in methanol. **B:** Conc. HCl. **SR_3:** Iron (III) chloride ($FeCl_3$) - (2 g $FeCl_3$ in 10 mL water, diluted to 200 mL by ethanol). **SR_4:** Natural product reagent (1% diphenylboryloxyethylamine in methanol solution). **SR_5:** Dragendorff reagent (0.85 g basic bismuth (III) nitrate in 40 mL water and 10 mL of acetic acid mixed with a 20 mL solution of potassium iodide (400 g/L).
Detection	TLC detection was done using Reprostar 3 under VIS and/or UV 366 nm. Detection and photo documentation was done after heating a sprayed TLC sheet at 105 ^{o}C for 3 – 10 min until maximum visualization of spots was observed. TLC plates derivatized with vanillin/HCl were not heated.

3.2.7.2 Sephadex® LH-20 fractionation

In the first step, the methanolic extract was subjected to Sephadex® LH-20 column chromatography using column (C1) equilibrated with 70% EtOH (v/v). The aim was to separate tannins from non-tannin compounds. In the course of fractionation by Sephadex® LH-20, non-tannins and oligomeric PAs are eluted first with EtOH 70% (v/v). The polymeric PAs adsorb to the stationary phase in alcohol and are released in the 70% acetone fraction[139].

In this study, 119 g of crude methanolic extract of *M. salicifolia* bark was fractionated in several runs. In each run, about 12 g of extract was dissolved in 14 mL of 70% EtOH (v/v) and carefully applied using pasteur pipettes on the surface of a Sephadex® LH-20 column. Subsequently, 70% EtOH (v/v) was added without disturbing the surface level and elution proceeded with a flow of 0.98 mL/min. Fraction collection was achieved by using a superrac fraction collector. The collection time and volume in each test tube was 18 min and 17.6 mL respectively. Fraction control was performed on normal phase TLC (NP-TLC) after every 3rd glass until no visible spot was observed on the TLC sheet under UV 254 nm.

Eluent was changed to acetone 70% (v/v) for elution of polymeric tannins which were adsorbed on the stationary phase. Prior to solvent change, the length of Sephadex® LH-20 in the column was marked due to shrinking and swelling behavior of the Sephadex® LH-20 material with use of different solvents. Elution of polymeric tannins from the column was completed following observation of a clear Sephadex column and colourless eluent for 1 h.

Commencement of the subsequent run was done after equilibration of the column with 70% EtOH (v/v), swelling of Sephadex® LH-20 material in the column to its original mark before elution with acetone 70% (v/v) was achieved and no further acetone was eluted from the eluent.

Fractions separation was done by means of TLC. Test tubes which appeared to have alike fingerprints were pooled together to form a fraction. The formed fractions were evaporated using a rotary vacuum evaporator at 40 ^{o}C until all organic solvent was evaporated. Remained aqueous fraction was frozen at -20 ^{o}C, lyophilized to complete dryness and then stored at 4 ^{o}C in the refrigerator.

3.2.7.3 Flash chromatography

Some of the obtained Sephadex® LH-20 fractions and their sub-fractions were further fractionated by flash chromatography. Chromatography was preceded by column equilibration with starting gradient conditions. The time taken for column equilibration was 10 – 20 min.

Preparation of fractions to be fractionated using RP-18 columns was done by dissolving the sample in MeOH, mixing with RP-18 material in the ratio of 1:2 (m/m) and the solvent was carefully evaporated to complete dryness using a rotary vacuum evaporator. The dried sample/RP-18 mixture was loaded on the surface of a pre-column packed with stationary phase, then chromatography was started.

In the case of using MCI-Gel® CHP-20P column and silica gel cartridges for chromatography, sample was clearly dissolved in solvent (initial condition). The concentrations were varying due to solubility but care was taken to achieve a thin starting zone at the column bed. The concentrated sample solution was loaded directly to the equilibrated main column. Pre-column was not used for this case.

Different flash columns and methods used in this study are described in the **Table 3.5** below. Factions were collected with the aid of inbuilt automatic fraction collector, TLC control was performed on every test tube. Similar fractions were pooled together, evaporated to complete dryness, weighed and stored at 4 ^{o}C in the refrigerator.

Table 3.5: Flash chromatography methods used. **M:** method, **C:** column, **MP:** mobile phase, **G:** gradient, **t:** time (min.), **F:** flow (mL/min), **V:** volume collected per test tube (mL), **D:** UV detector (nm).

M	C	MP A	MP B	G	t	F	V	D
FL-1	C2	water	MeOH	20 - 100% B	60	5	10	280
				100% B	15			
FL-2	C4	water	MeOH	20% B	40	7.5	15	280
				30% B	40			
				40% B	40			
				50% B	40			
				60% B	40			
				100% B	60			
FL-3	C3	water	MeOH	20 - 40% B	10	40	23	220
				40 - 100% B	20			
				100% B	30			
FL-4	C5	$CHCl_3$	MeOH	30 - 20% B	35	7	5	250
				20 -100% B	1			
				100% B	25			
FL-5	C5	$CHCl_3$	MeOH	5 - 12% B	30	15	10	220
				12 - 60% B	1			
				60 - 100% B	9			
				100% B	10			
FL-6	C5	$CHCl_3$	MeOH	5% B	40	15	10	220
				5 - 100% B	25			
				100% B	15			

3.2.7.4 Semi preparative HPLC

Semi preparative HPLC was the final isolation step used to obtain the majority of the isolated pure compounds. Prior to every HPLC purification run, numerous trials to find optimal eluents were performed on RP-18 TLC aluminium sheets.

The sample to be purified was applied on several RP-18 TLC sheets, thereafter TLC sheets were developed using different mobile phase compositions. The mobile phase which could migrate the compounds of interest between R_f value of 0.3 – 0.8 was considered to be optimal for the preparative HPLC run.

After the optimal mobile phase was found, samples were dissolved in the initial conditions of solvent system for the chromatography. The sample solution was filtered using syringe filter and manually injected to the HPLC sample loop at room temperature.

Eluted peaks were manually collected in test tube and completely dried under nitrogen stream. Their yield were determined and then stored at 4 ^{o}C. **Table 3.6** describes HPLC preparative methods used in this study.

Table 3.6: Preparative HPLC methods. **M:** method, **C:** column, **MP:** mobile phase, **SC:** sample concentration (mg/mL), **IV:** injection volume (µL), **G:** gradient, **t:** time (min.), **F:** flow (mL/min), **D**: UV detector (nm). **TFA:** trifluoroacetic acid.

M	C	MP A	MP B	SC	IV	G	t	F	D
HP-1	C7	Water+ 0.05% TFA	MeCN + 0.05% TFA	10	250	25 – 40% B 40 – 100% B 100% B	30 5 3	2	280
HP-2	C7	Water+ 0.02% TFA	MeCN + 0.02% TFA	10	250	20 – 30% B 30% B 30 - 70% B 70% B	15 1 2 6	2	280
HP-3	C6	Water+ 0.02% TFA	MeCN + 0.02% TFA	10	10	15 – 19% B 19 – 23% B 23 – 60% B 60% B	5 15 2 3	1	280
HP-4	C8	Water	MeOH	100	500	50 – 70% B 70 – 100% B 100% B	20 0.1 2	20	290
HP-5	C7	Water	MeOH	10	250	50 – 70% B 70 – 100% B 100% B	20 0.1 2	3	290
HP-6	C7	Water + 0.02% TFA	MeCN + 0.02% TFA	10	250	25 - 35% B 35 – 65% B 65% B	30 1 4	2	256
HP-7	C7	Water	MeOH	13	300	50 – 60% B 60 – 100% B 100% B	15 1 4	3	250

M	C	MP A	MP B	SC	IV	G	t	F	D
HP-8	C7	Water	MeOH	10	200	50 – 60% B	20	2	240
						60 – 100% B	1		
						100% B	4		
HP-9	C7	Water	MeOH	10	200	75 – 80% B	15	2	250
						80 – 100%	1		
						100% B	3		
HP-10	C7	Water	MeOH	10	200	70% B	15	2	220
						70 – 100% B	1		
						100% B	4		
HP-11	C7	Water	MeOH	10	100	60% B	10	2	270
						60 – 100% B	1		
						100% B	4		
HP-12	C7	Water	MeOH	10	100	75 – 78% B	10	2	250
						78 – 100% B	1		
						100% B	4		

3.2.7.5 Centrifugal partition chromatography (CPC)

Preparative liquid/liquid partitioning chromatography was used as a pre-purification step to some of the fractions following Sephadex® LH-20 and flash chromatography. A bi-phasic solvent system was used during chromatography, one phase as the mobile phase and the other phase as stationary phase.

A bi-phasic solvent system optimal for chromatography was prepared by mixing and shaking two immiscible solvents in a separatory funnel. The mixture was left to stand for few seconds thereafter separation of the upper phase from lower phase was done.

The stationary phase (the lower phase) was pumped in the rotor (column). Then the mobile phase was pumped into the rotor through the stationary phase while CPC rotation speed was 800 rpm. This continued until the equilibrium between the two phases was attained. The equilibrium between the two phases was observed when the volume of the eluted stationary phase remained constant.

After equilibrium was reached, the sample was prepared by completely dissolving in the biphasic system (1:1) at the concentration of 0.25 g/mL. The sample solution was manually injected in the CPC sample loop by using a syringe, immediately the chromatography was

started. The eluted fractions were collected in test tubes by use of an automatic multrac fraction collector. TLC control was performed on every third test tube.

Elution mode was changed or stopped, when no more spots were detected on a TLC sheet. Two elution modes were used for chromatography, i.e. ascending mode when the upper (lighter) phase was the mobile phase and descending mode when the lower (heavier) was the mobile phase. Fraction cuts were performed in the same way as described in the sections **3.2.7.2** and **3.2.7.3**. The CPC conditions are illustrated hereunder:

Solvent system: Ethylacetate/water.

Ascending mode: Ethylacetate-mobile phase.

Descending mode: Water-mobile phase.

Rotation: 800 rpm.

Flow (mL/min): 5 mL/min.

Volume collected: 10 mL/ test tube.

3.2.8 Structure elucidation

3.2.8.1 NMR spectroscopy

Isolated pure compounds were dissolved in 600 µL of deuterated solvent, filled in the NMR tubes (507-HP-8) prior to NMR spectra measurement. Deuterated NMR solvents such as methanol, acetone, chloroform and pyridine were used in this study (quality of solvents: chapter 3.2.1).

Two NMR spectrometers of the Central Analytics, Department of NMR spectroscopy, Faculty of Chemistry and Pharmacy, University of Regensburg were used for recording of one dimensional (1D) and two dimensional (2D) NMR spectra.

The NMR spectra for compounds with low yields < 5 mg were recorded using Bruker Avance 600 (600.25 MHz for ^{1}H and 150.93 MHz for ^{13}C, 298.0 K) and for compounds with higher amount > 5 mg, Bruker Avance 300 (300.13 MHz for ^{1}H and 75.47 MHz for ^{13}C, 296.1 K) was used. The NMR spectra were referenced to tetramethylsilane (TMS).

Recorded NMR data were: ^{1}H and ^{13}C for 1D-NMR spectra, Heteronuclear Single Quantum Coherence (HSQC), Heteronuclear Multiple Bond Correlation (HMBC), ^{1}H-^{1}H Correlation Spectroscopy (COSY), Nuclear Overhauser Enhancement Spectroscopy (NOESY)/Rotational Overhauser Enhancement Spectroscopy (ROESY) for the 2D-NMR spectra respectively.

Analysis of NMR spectra data for the determination of structure was performed using Topspin 3.2 (Bruker, Ettlingen) software.

3.2.8.2 Mass spectrometry

Molecular mass and molecular formula of isolated compounds were confirmed by mass spectrometry. Samples were submitted to the Department of Mass Spectrometry, Faculty of Chemistry and Pharmacy, University of Regensburg for measurement. Liquid chromatography LC-MS and low resolution ESI-MS were measured on TSQ 7000 (Thermo Quest, Finnigan). High resolution ESI-MS were measured on a MAT SSQ 710 A (Finnigan).

3.2.8.3 UV-VIS spectroscopy

A concentration of 0.06 mg/mL in methanol (for spectroscopy) of each compound was prepared. Sample solution was filled in a quartz cuvette with 1 cm path length. The cuvette containing the sample solution was placed in the spectrophotometer. An absorption spectrum was recorded as a plot of the light absorbed by that compound (A) against wavelength (nm) following measurement of pure methanol as blank. All UV measurements were performed at room temperature with a wave length range from 200 – 500 nm.

Absorbance and its corresponding UV-maximum were recorded for calculation of molar extinction coefficient (ε) using Lambert beer's equation as described below:

Formula 2: Calculation of absorbance.

$$A = \varepsilon \times c \times l$$

Formula 3: Calculation of molar extinction coefficient.

$$\varepsilon = \frac{A}{c \times l}$$

ε: Molar extinction coefficient [L/(mol × cm]
A: Absorbance
c: Concentration [mol/L]
l: Length of the quartz cuvette [l = 1 cm]

3.2.8.4 Polarimetry

Isolated compounds were subjected to optical rotation measurement. 1 mg of each substance was dissolved in 1 mL of methanol (for spectroscopy, Uvasol). The sample solution was carefully filled in the polarimetry cell (l = 5 cm) and placed in the polarimeter for measurement. Observed optical rotation (α) was recorded six times and the average was calculated. In all cases measurement conditions were: temperature range was from 22 – 26 °C, wave length = 589 nm (D-line of the sodium lamp). The average optical rotation was used for calculations of specific rotation as described in the formula below:

Formula 4: Calculation of optical rotation.

$$[\propto]_D^T = \frac{\propto}{c \times l}$$

$\propto$: Observed optical rotation [°]
T: Temperature [°C]
l: Length of the tube [dm]
c: Concentration [g/mL]

3.2.8.5 Circular dichroism (CD) spectroscopy

CD spectra measurements were performed at the Department of Analytical Chemistry-University of Regensburg. Each isolated compound (0.6 mg) was dissolved in 10 mL of methanol (for analysis), filled in the quartz cuvette with 0.1 cm path length and placed in the CD

spectrometer for measurement at room temperature. All CD spectra were recorded after subtraction of the instrument base line which was recorded using only solvent (methanol) prior to sample measurement.

Data recording was done using a Microsoft Excel sheet and graphically presented in terms of molar ellipticity (degrees·cm^2·decimole^{-1}) as a function of wave length (nm). On the other hand, molar ellipticity could be calculated using the following formula:

Formula 5: Calculation of optical rotation.

$$[\theta]_M = \frac{\theta \times M}{100 \times c \times l}$$

$[\theta]_M$: Molar ellipticity, expressed in degrees·cm^2·decimole^{-1}
θ: Ellipticity value [^{0}]
M: Molar mass [g/mol]
c: Concentration [g/mL]
l: Optical path of the cell [dm]

3.2.8.6 Determination of type and absolute configuration of glycosides

Determination of the glycoside type and their respective absolute configuration was achieved by recording the ^{1}H NMR spectra of their per-*O*-(S)-2-methylbutyrate (SMB) derivatives[140].

1 mg of each compound containing a sugar moiety was hydrolyzed using 200 µL of 2 N trifluoroacetic acid (TFA) at 121 °C for 90 min in a Wheaton vials sealed with teflon lined screw cap. After hydrolysis, the solvent was evaporated to complete dryness under nitrogen stream.

100 µL of (*S*)-(+)-2-methylbutyric anhydride and 100 µL of pyridine were added to the mixture and incubated at 121 °C for 4 h. The mixture was dried under nitrogen stream for about 8 h and 300 µL of toluene was added to the residue and evaporated. The residue was dissolved in 1 mL of dichloromethane and extracted three times with a 2 mL of 2 M Na_2CO_3 solution and one time with 2 mL of water. The dichloromethane phase containing the SMB derivatives was concentrated using nitrogen stream, then completely dried by addition of 300 µL of 2-propanol and evaporation.

Preparation of samples for NMR measurement was done by dissolving each of the obtained SMB derivative in 0.6 mL of deuterated acetone. The mixture was transferred to the NMR tube and their ^{1}H NMR spectra were recorded at 300 MHz, 298 K.

The same procedure was applied to reference monosaccharides with the exception of hydrolysis reaction. Absolute configuration and the type of glycoside was confirmed by comparing chemical shifts and coupling constants of anomeric proton resonances of the SMB derivative to that of reference monosaccharides SMB derivative. For compounds with two sugar substitutions, ^{1}H NMR of SMB derivatives were compared to a ^{1}H NMR of the SMB derivative of a mixture of the two concerning reference sugars.

3.2.8.7 Enzymatic deglycosydation of cyclic diarylheptanoid glycoside

Enzymatic hydrolysis was done using β-glucosidase (almond) to obtain the aglycone by deglycosidation of cyclic diarylheptanoid glycosides[123]. The enzyme hydrolysis was conducted as follows:

21.0 mg (0.040 mmol) of a compound was dissolved in 3.0 mL of 0.2 M acetate buffer (0.2 M acetic acid + 0.2 M sodium acetate, pH 4.4). The solution was treated with 40 mg of β-glucosidase and stirred. The mixture was incubated while stirring in the ultrasonic water bath at 38 °C for 2 days. After incubation, the reaction mixture was mixed with 10 mL of absolute EtOH and evaporated to dryness by using a vacuum rotary evaporator. The residue was dissolved in chloroform/water (1:1), thoroughly mixed, left to settle and finally the two phases were separated. The obtained upper and lower phase were dried and separately purified by (semi) preparative HPLC method HP-11 **(Table 3.6)**.

The peaks obtained from HPLC purification of the upper and lower phase were subjected to ^{1}H NMR measurement. Prior to ^{1}H NMR measurement, the samples were dissolved in 0.6 mL deuterated methanol, filled in the NMR tubes followed by measurement at 300 MHz. The recorded ^{1}H NMR spectra data of the obtained peaks were compared with the existing data to identify which peak stands particularly for the aglycone.

3.2.8.8 CD spectra simulation

0.6 mg of the obtained myricanol aglycone from enzymatic deglycosydation was dissolved in 10 mL methanol and submitted for CD spectra measurement to the Department of Analytical Chemistry, University of Regensburg. The recorded CD data of the aglycone were submitted to Prof. Dr. Thomas Schmidt - Institute of Pharmaceutical Biology and Phytochemistry, University of Münster, for performing electronic CD spectra simulation using time-dependent density functional theory (TDDFT) quantum mechanics.

At the University of Münster, molecular models of the *R*-enantiomer of myricanol were generated with the software package MOE (CCG, Montral, Canada). After a low-mode-dynamics conformational search (default settings), three conformations were obtained within an energy window of 3 kcal/mol of which conformer 1 corresponded to the 11*R,Ra* and conformers 2 and 3 to two slightly different 11*R*,*Sa* forms. The 3D structures were exported to the software Gaussian 03W and completely energy minimized using the B3LYP Density Functional and the 6-31D (d,p) basis set. According to these calculations, conformer 3 was the energetically most favourable form, conformer 1 being 2.01 and conformer 2 even 3.31 kcal/mol higher in energy. These energy differences would indicate that conformer 3 would strongly dominate (>97%) in a conformational equilibrium. Indeed, the geometry of conformer 3 is in very good agreement with the crystal structure of myricanol as published by Begley et al.[141].

Electronic CD spectra were simulated by performing a time-dependent DFT (TDDFT) calculation for the first 30 electronic transitions of each of the three conformers using the same basis set as mentioned above. The resulting transition vectors (R, length) were used to simulate the CD spectra for each form by multiplying them with Gaussian functions of width of 0.1 eV and summing the resulting curves up over the whole energy/wavelength scale. Furthermore, an averaged spectrum was generated for the theoretical equilibrium mixture corresponding to 97% *R,Sa* and 3% *R,Ra*-myricanol. The resulting spectra were compared with the experimental CD spectrum of myricanol and the obtained results were used to confirm the absolute configuration of the aglycone myricanol and other isolated diarylheptanoids.

3.3 Results

3.3.1 Extraction and preliminary investigation of *M. salifolia* bark

The bark of *M. salicifolia* is the most reported plant part used for medicinal purposes by Maasai. In the course of investigating its phytochemical composition, four crude extracts were obtained by increasing polarity of extraction solvents: dichloromethane, ethylacetate, methanol 100% and methanol 50% extract.

Control TLCs of the four crude extracts provided a preliminary reflection of the compounds and their distribution within the extracts **(Figure 3.16)**. It was also detected that the methanolic extract of *M. salifolia* bark seemed to contain more interesting compounds than the methanol 50%, dichloromethane and ethylacetate extracts. This was further supported by extraction yields of the crude extracts **(Table 3.7)**. The high content of compounds in the methanolic extract demonstrated that the majority of *M. salicifolia* bark compounds are polar compounds. This is in agreement with the decoction and infusion methods being used as the major traditional medicinal preparations of this plant part, which leads to the extraction of most of its ingredients (**Chapter 2**).

Additionally, to get an idea about compound groups present in crude extracts TLC sheet were sprayed with different spray reagents. Visualization of red spots (VIS) after spraying with Vanillin/HCl reagent, black spots after spraying with $FeCl_3$ and orange spots after spraying with anisaldehyde-sulphuric acid reagent, were a hint for the presence of condensed tannins in methanol and methanol 50% crude extracts. They were the dominant group of compounds in these two extracts **(Figure 3.17)**.

Alkaloids were below detection limits due to the lack of orange colored spots when TLC was visualized under visible light following TLC spraying with Dragendorff reagent as described in the method section **3.2.7.1**. Few blue fluorescent spots were detected under UV 366 nm after spraying the TLC sheet containing four crude extracts with natural product reagent. The blue fluorescent spots observed could be phenolic acids, coumarins and/or plant acids present in all four extracts.

In this study, the methanolic extract was selected for further fractionation and phytochemical characterization based on the obtained preliminary phytochemical investigation results of *M. salicifolia* bark.

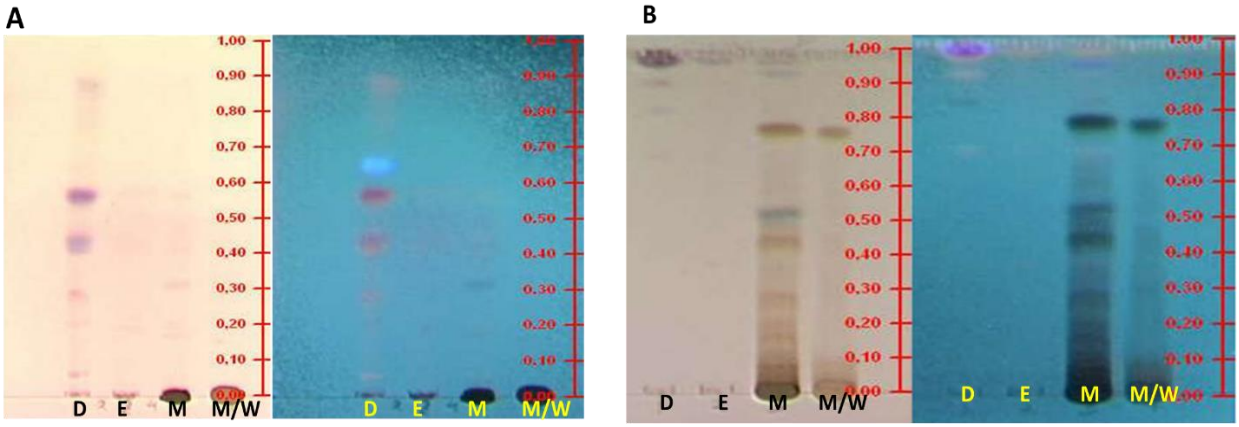

Figure 3.16: TLCs displaying compounds distribution within *M. salicifolia* bark extracts. **A:** NP-TLC developed with TLC mobile phase MP_2. **B:** TLC developed with mobile phase MP_1. D: $CHCl_2$ extract. E: EtOAc extract. M: MeOH extract. M/W: MeOH/H_2O extract. All TLCs were derivatized with anisaldehyde-sulphuric acid reagent. Detection VIS **(left)** and UV 366 nm **(right)**.

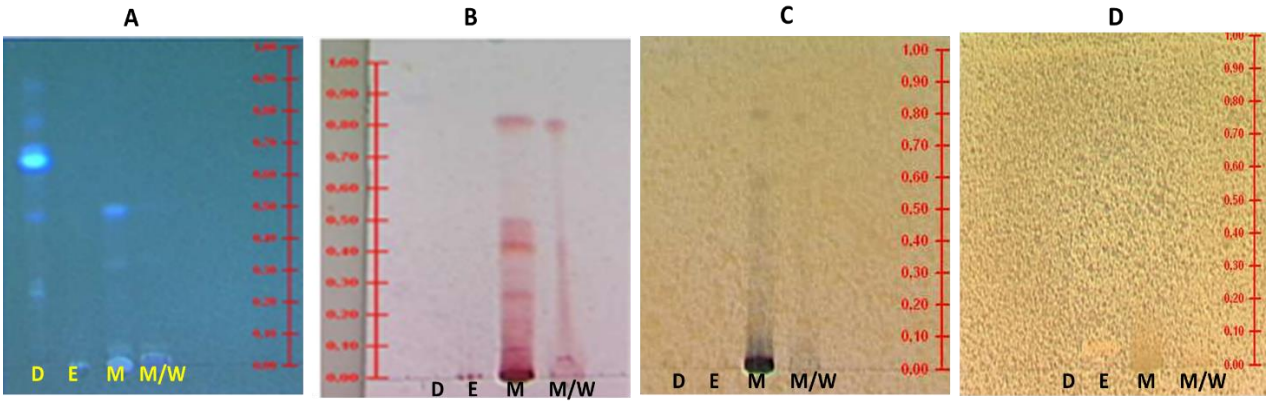

Figure 3.17: Preliminary confirmation of compound groups' composition of *M. salicifolia* bark extracts. NP-TLC derivatized with **A:** Natural products reagent (UV 366 nm), **B:** Vanillin/HCl (VIS), **C:** Ferric (III) chloride (VIS), **D:** Dragendorff reagent (VIS).

Table 3.7: Extraction yields of *M. salicifolia* bark (390.1 g).

Extract	Empty glass (g)	Glass + Extract (g)	Extract wt. (g)	Yield (%)
Dichloromethane	134.87	142.58	7.71	1.90
Ethylacetate	129.52	130.57	1.05	0.27
Methanol	328.85	491.31	162.46	41.64
Methanol/water	292.83	318.69	25.86	6.62

3.3.2 Fractionation and chromatography of *M. salicifolia* bark crude methanolic extract

M. salicifolia bark crude methanolic extract was subjected to further fractionation. In a first step, Sephadex® LH-20 open column chromatography was used to separate tannins from non-tannin phenolics. Two eluents were used, ethanol 70% and acetone 70% as described in materials and methods **3.2.7.2**. Seven fractions (S1-S7) were obtained. Fractions S1-S6 were eluted with ethanol 70%. Fraction S7, which comprised of PAs polymers, retained in the column and could not be eluted with ethanol 70%. Its elution was achieved by acetone 70%.

All seven fractions (S1-S7) obtained from Sephadex® LH-20 open column chromatography were made up by several compounds **(Figure 3.18)**. Therefore, fractions separation was achieved by selection of marker compound spots for each fraction. A deep blue spot having R_f value between 0.5 – 0.6 was selected as a marker for fraction S2. All compounds eluted before this compound were combined in fraction S1, and those fractions containing this compound were grouped in S2. Furthermore, all compounds eluted after the deep blue compound and before elution of a deep orange compound with R_f value of 0.8 were combined in fraction S3 and all those containing the deep orange compound in fraction S4. The marker spot for fraction S5 was the deep orange compound with R_f value of 0.4 and those eluted afterwards with ethanol 70% until no compound was detected on the TLC sheet were combined in fraction S6.

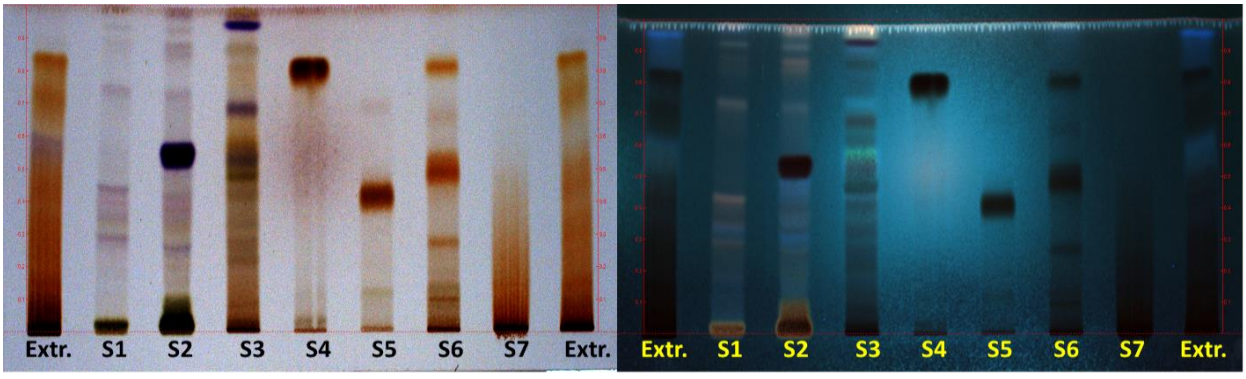

Figure 3.18: Control TLC of Sephadex® LH-20 chromatography of *M. salicifolia* bark methanolic extract. NP-TLC developed with mobile phase MP_1 and sprayed with anisaldehyde-sulphuric acid reagent. Detection VIS **(left)** and UV 366 nm **(right)**.

3.3.3 Fractionation and preparative isolation of tannins

PAs presence in the obtained Sephadex® LH-20 fractions was confirmed by TLC method. A TLC silica sheet spotted with the seven fractions S1-S7, was developed with TLC mobile phase MP_1. The developed TLC sheet was sprayed with vanillin/HCl without heating **(Figure 3.19)**. Subsequently, deep red spots on TLC fingerprints of fractions S4-S7 and colourless on fraction S1-S2 fingerprints were detected under VIS, hence a confirmation of PAs presence in these fractions. Traces of red colour were detected in fraction S3 concluding that PAs are present in low concentrations. Additionally, catechin was below detection limits due to none of the compound spots appeared to have the same R_f value as that of catechin when it was used as a reference substance.

Isolation of tannins was achieved by further fractionation or purification of the PAs containing fractions as summarizes in the fractionation scheme **(Figure 3.25)**.

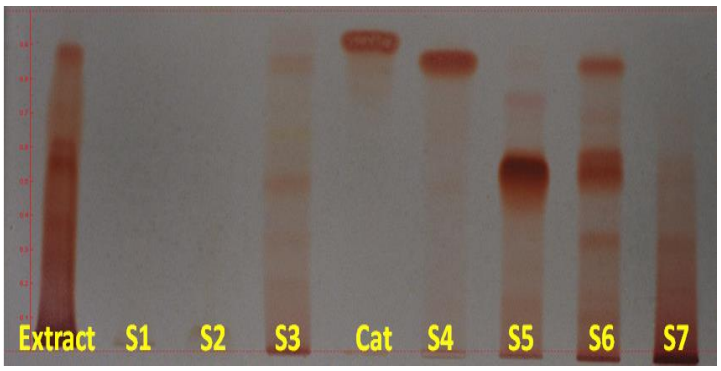

Figure 3.19: NP-TLC overview of fractions S1-S7 after spraying with Vanillin/HCl, a confirmation of fractions containing PAs. Cat = catechin (reference substance). Detection VIS.

3.3.3.1 Fraction S4

Fractionation of S4 (0.4 g) was performed by RP-18 flash chromatography using method FL-1. Five fractions S4.1-S4.5 **(Figure 3.20)** were obtained and subjected to ^{1}H NMR (300 MHz, methanol - d_4). S4.1 was observed to be impure and discarded due to its very low yield (26.0 mg). S4.5 was identified as plasticizer and was also discarded. Fractions S4.2-S4.4 were pure and possessed the same proton spectra, hence resulted in isolation of compound **1** (0.2 g).

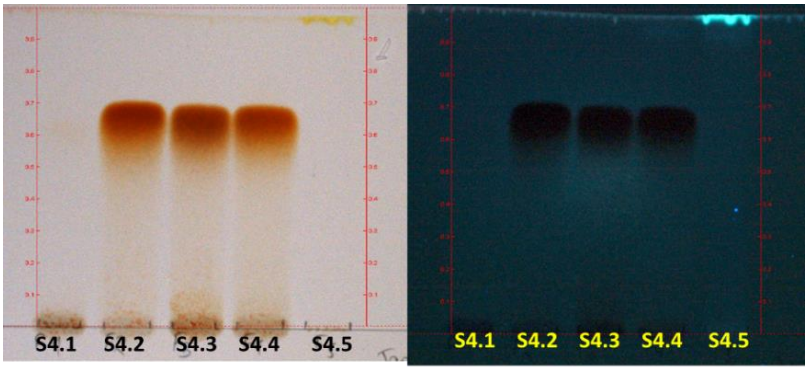

Figure 3.20: TLC overview of S4.1 – S4.5 fractions (NP-TLC). TLC mobile phase: MP_1. Detection VIS **(left)** and UV 366 nm **(right).**

3.3.3.2 Fraction S5

Fraction S5 (0.32 g) was fractionated by means of MCI-Gel® CHP-20P flash chromatography method FL-2. A step gradient with increasing methanol concentration in 10% steps was performed. Good separation was achieved resulting in twelve fractions S5.M1-S5.M12 **(Figure 3.21)**. Fractions were obtained with the aid of TLC control performed on every second glass and selection of a marker compound for each fraction.

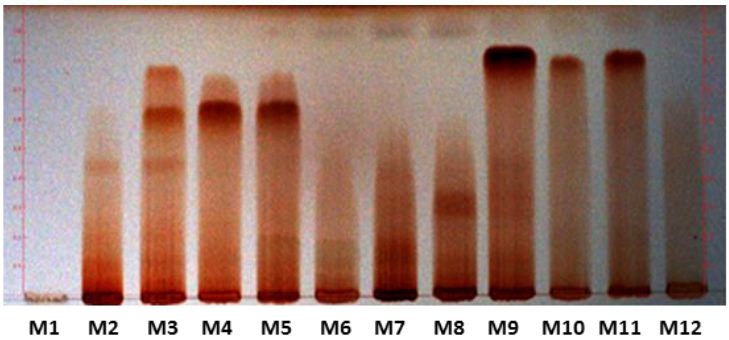

Figure 3.21: TLC overview of S5 MCI-Gel® CHP-20P fractions. NP-TLC developed with mobile phase MP_1 and sprayed with anisaldehyde-sulphuric acid reagent. Detection VIS.

The four fractions containing tannins, S5.M4 (9.0 mg), S5.M6 (9.4 mg), S5.M9 (17.0 mg) and S5.M11 (2.6 mg) were subjected to a purification step on preparative RP-18 HPLC using method HP-1.

In the process of separation and purification of S5.M4 two peaks were collected **(Figure 3.22 A)**. The collected peaks were subjected to ^{1}H NMR (300 MHz, methanol-d_4) for purity control. The first peak with t_R = ~ 5 min was pure, hence resulted in isolation of compound **3** (2.3 mg). The

second peak eluted at 7.5 min was impure and due to small yield no further purification step was possible. The hip observed from 15.8 - 23 min was considered as impurities and discarded.

Purification process of S5.M6 **(Figure 3.22 B)** lead to collection of three eluted peaks. ^{1}H NMR (300 MHz, methanol-d_4) of the collected peaks were recorded and it was observed that the peak eluted at 6.5 min was pure (compound **9**, 1.6 mg). The peak which eluted at 19 min in all cases was identified as plasticizer, therefore discarded.

Similarly, RP-18 preparative HPLC purification of fractions S5.M9 **(Figure 3.22 C)** and S5.M11 **(Figure 3.22 D)** resulted in isolation of pure compound **6** (6.0 mg) with t_R = 7 min and compound **7** (0.7 mg) with t_R = 8 min respectively. In both cases no further purification steps were performed on the impure collected peaks due to their low yields.

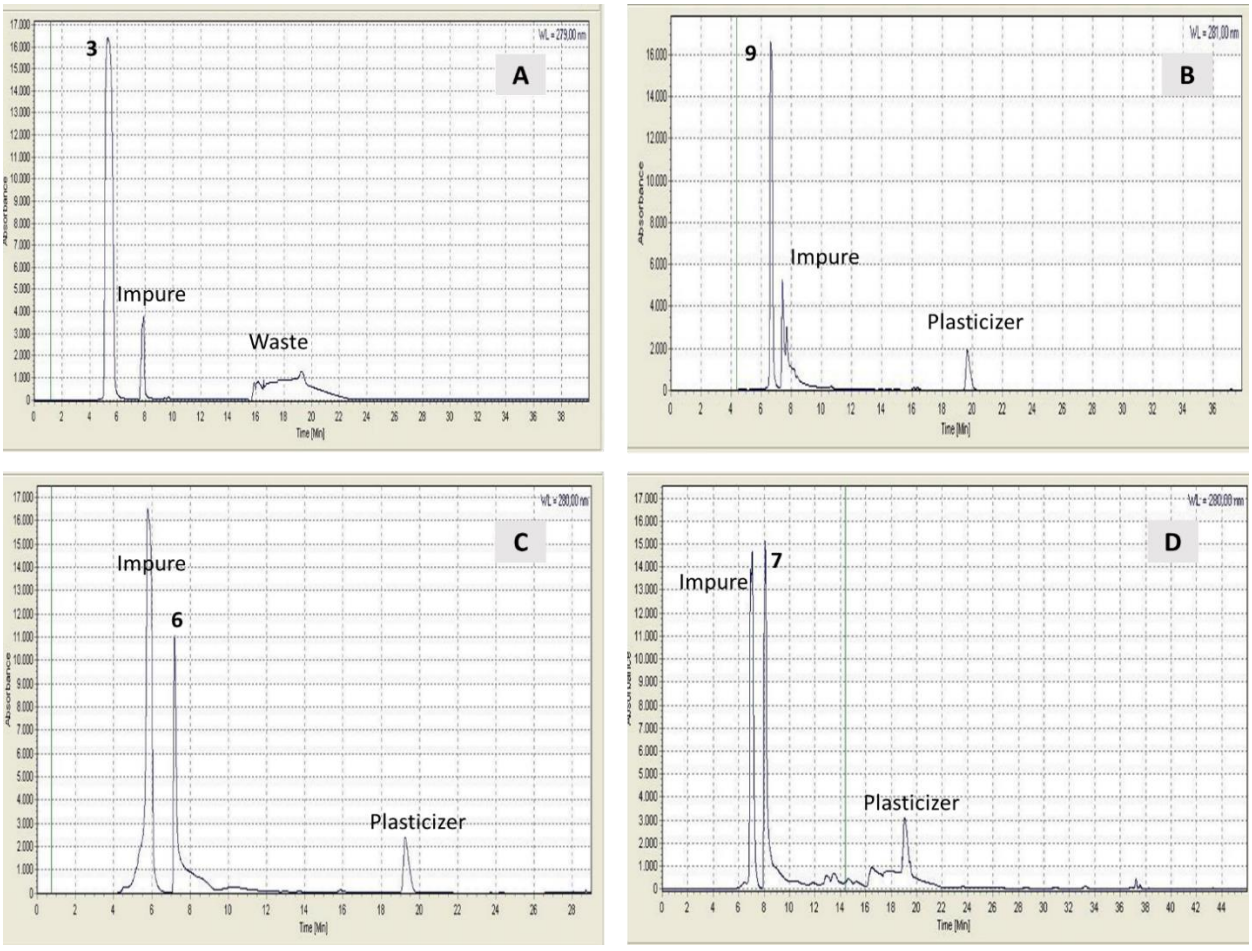

Figure 3.22: Preparative RP-18 HPLC chromatograms (method HP-1) monitored by UV detection at 280 nm. **A:** Fraction S5, **B:** Fraction S5.M6, **C:** Fraction S5.M9, **D:** Fraction S5.M11.

3.3.3.3 Fraction S6

S6 was subjected to MCI-Gel® CHP-20P flash chromatography using the same chromatographic conditions as for fraction S5 (FL-2). At the end of chromatography thirteen fractions S6.M1-S6.M13 were obtained as depicted in **Figure 3.23**.

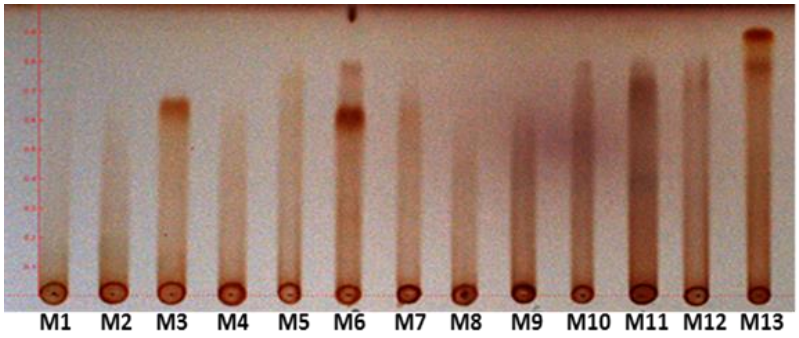

Figure 3.23: TLC overview of S6 MCI-Gel® CHP-20P fractions. NP-TLC developed with mobile phase MP_1 and sprayed with anisaldehyde-sulphuric acid reagent. Detection VIS.

Two fractions, S6.M6 (32.0 mg) and S6.M13 (16.0 mg), out of thirteen obtained fractions were subjected to the purification steps by RP-18 preparative HPLC using method HP-2. HPLC separation and purification of S6.M6 resulted in collection of three eluted peaks at 6.5, 7.5 and 10.7 min **(Figure 3.24 A)**, hence isolation of compound **4** (12.5 mg), compound **5** (9.1 mg) and compound **8** (2.56 mg) respectively.

Separation and purification of compounds from fraction S6.M13 **(Figure 3.24 B)** was not accomplished by RP-18 preparative HPLC method HP-2. Further purification of the collected double peak with t_R = ~ 10 min was attempted using HP-3 method on analytical HPLC operated in a semi preparative way. Two clear sharp peaks with t_R = ~ 8 and 9 min were collected **(Figure 3.24 C)**, which led to isolation of compound **2** (1.8 mg) and re isolation of compound **8** (0.7 mg) respectively.

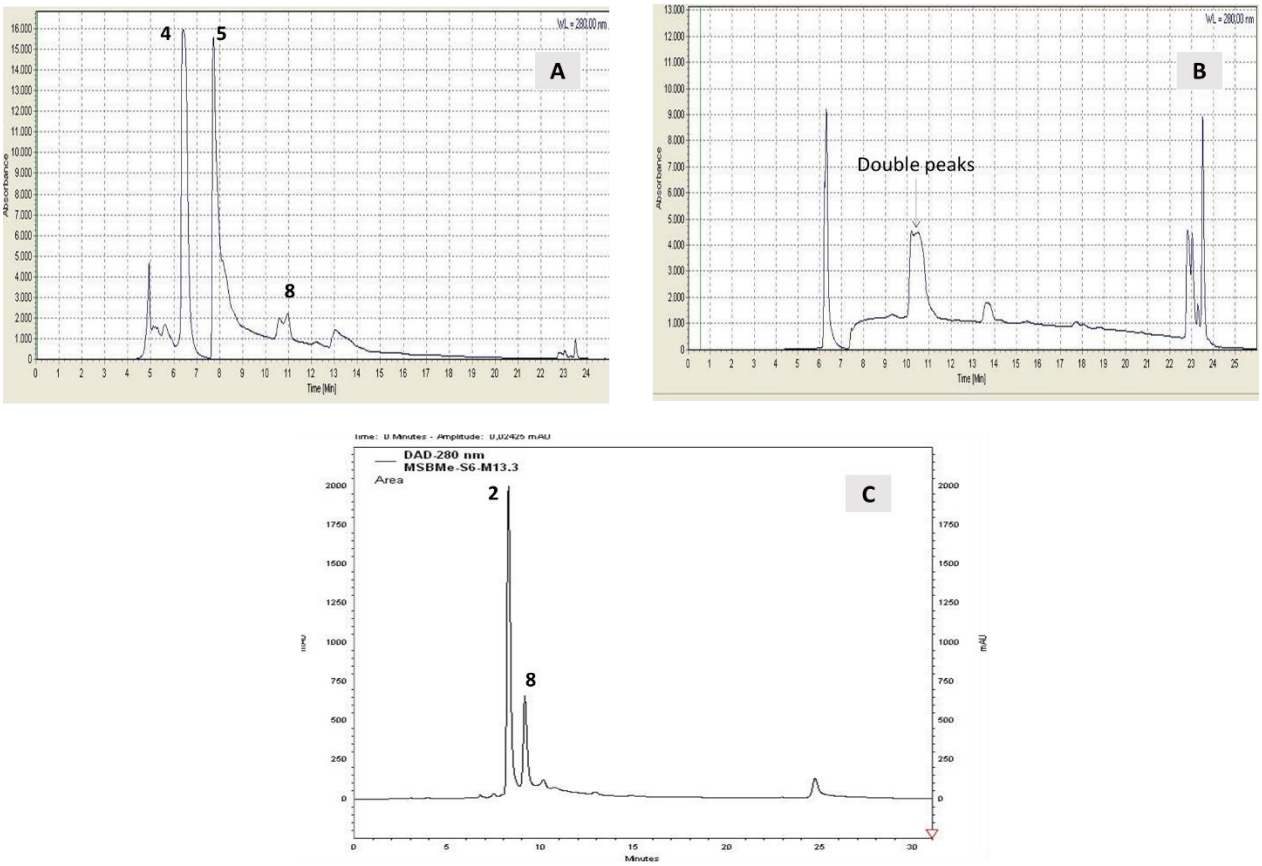

Figure 3.24: Preparative RP-18 HPLC chromatograms monitored by UV detection at 280 nm. **A**: Fraction S6.M6 (method HP-2), **B:** Fraction S6.M13 (method HP-2), **C:** Fraction S6.M13-separation and purification by analytical HPLC (method HP-3).

3.3.3.4 Fraction S7

Fraction S7 contained polymeric proanthocyanidins. Therefore, long ^{13}C NMR spectrum (2048 scans) of this fraction was recorded to get fundamental information on the composition.

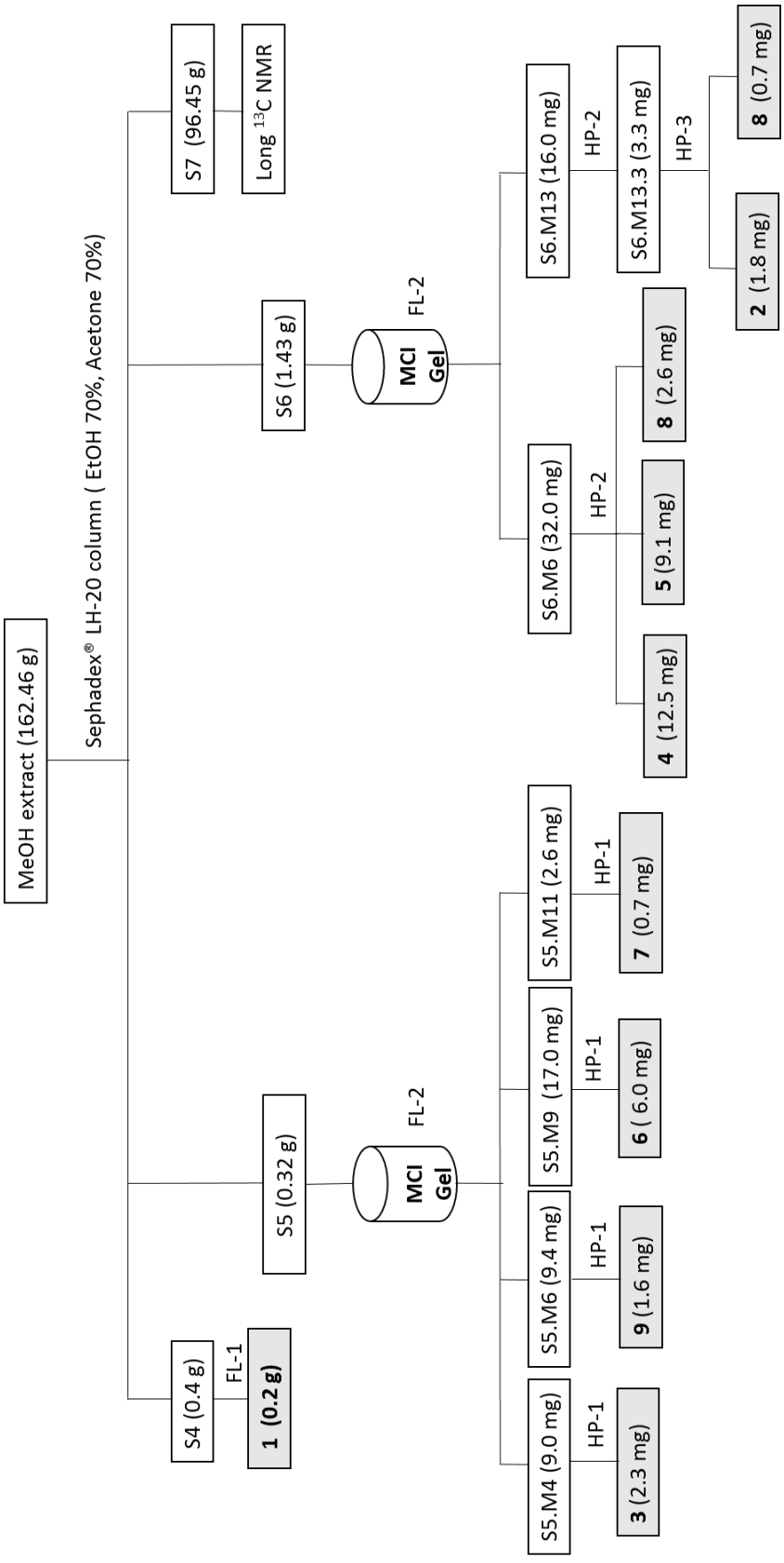

Figure 3.25: Fractionation and isolation scheme of tannins from crude methanolic extract of *M. salicifolia* bark.

3.3.4 Fractionation and preparative isolation of non-tannin compounds

Sephadex® LH-20 fractions S1 and S2 **(Figure 3.18 and 3.19)** contain non-tannin compounds. S3 contained non-tannins and traces of tannins **(Figure 3.19)**. Therefore, fractionation and isolation was performed on fraction S2 as summarized in the fractionation scheme **Figure 3.34**. Fractions S1, S3 which also contain non-tannin compounds were not investigated in this study due to time limitations.

Additionally, it was observed from Sephadex® LH-20 TLC control that fraction S2 contained sugars. Therefore, in the first step fraction S2 (15.7 g) was fractionated by means of RP-18 flash chromatography method FL-3 aiming to separate sugars from other compounds. Seven fractions F1–F7 were obtained at the end of chromatography. The gradient starting at polar conditions resulted in elution of most of the sugars at the beginning of the chromatography (fraction F1), hence their separation from other compounds. Fractions F4–F6 **(Figure 3.26)** which contained several compounds were further purified to isolate individual compounds.

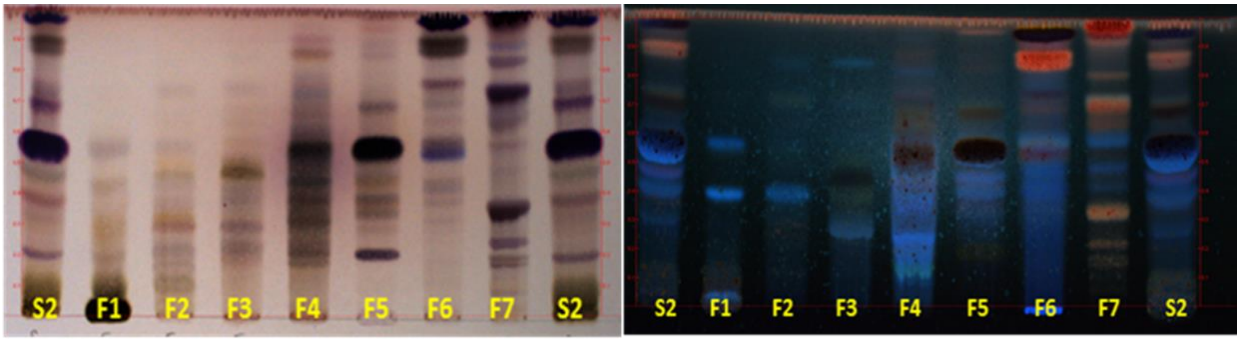

Figure 3.26: NP-TLC control of fraction S2 RP-18 flash chromatography. Mobile phase MP_1, sprayed with anisaldehyde-sulphuric acid reagent. Detection VIS **(left)** and UV 366 nm **(right)**.

3.3.4.1 Fraction S2.F4

S2.F4 (0.76 g) was fractionated by centrifugal partition chromatography (CPC) as described in the material and method section **3.2.7.5**. The CPC separation of S2.F4 resulted in six fractions F4.C1-F4.C6 **(Figure 3.27)**. The obtained CPC fractions F4.C2 (49.8 mg), F4.C3 (53.9 mg) and F4.C6 (288.0 mg) were separated and purified on preparative RP-18 HPLC. No further separation was done on fractions F4.C1, F4.C4 and F4.C5 due to time limitation.

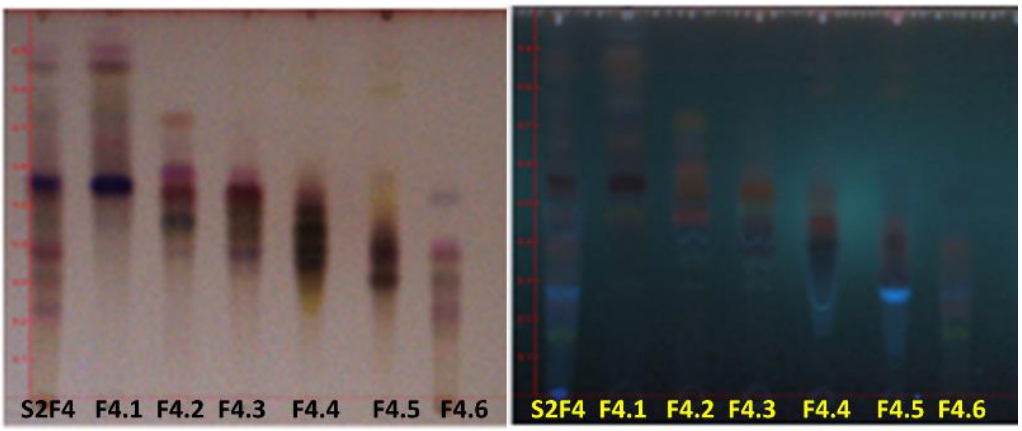

Figure 3.27: Control NP-TLC of S2F4 CPC fractionation. Mobile phase MP_1, sprayed with anisaldehyde-sulphuric acid reagent. Detection VIS **(left)** and UV 366 nm **(right)**.

Separation and purification of fraction F4.C2 with method HP-8 **(Figure 3.28 A)**, lead to isolation of compounds **29** (8.0 mg, t_R = ~ 12.2 min), **30** (1.4 mg, t_R = ~ 9.6 min), and **31** (0.6 mg, t_R = ~ 16 min). F4.C3 **(Figure 3.28 B)** was also separated by the same method and resulted in compound **32** (8.1 mg, at t_R = ~ 8 min), **33** (3.7 mg at t_R = ~ 9 min), **34** (2.4 mg at t_R = ~ 10.4 min) and reisolation of compound **29** (10.6 mg, at t_R = ~ 12.2 min). The peak eluted at t_R = ~ 19.6 min in both fractions F4.C2 and F4.C3 could not be identified due to solubility problems. Following evaporation of the eluent, several attempts to dilute it with different solvents were done without success.

Likewise, separation of F4.C6 **(Figure 3.28 C)** on preparative HPLC (HP-8) resulted in isolation of compound **28** (6.0 mg, t_R = ~ 15.8 min) and reisolation of compounds **26** (2.1 mg) and **22** (4.1 mg).

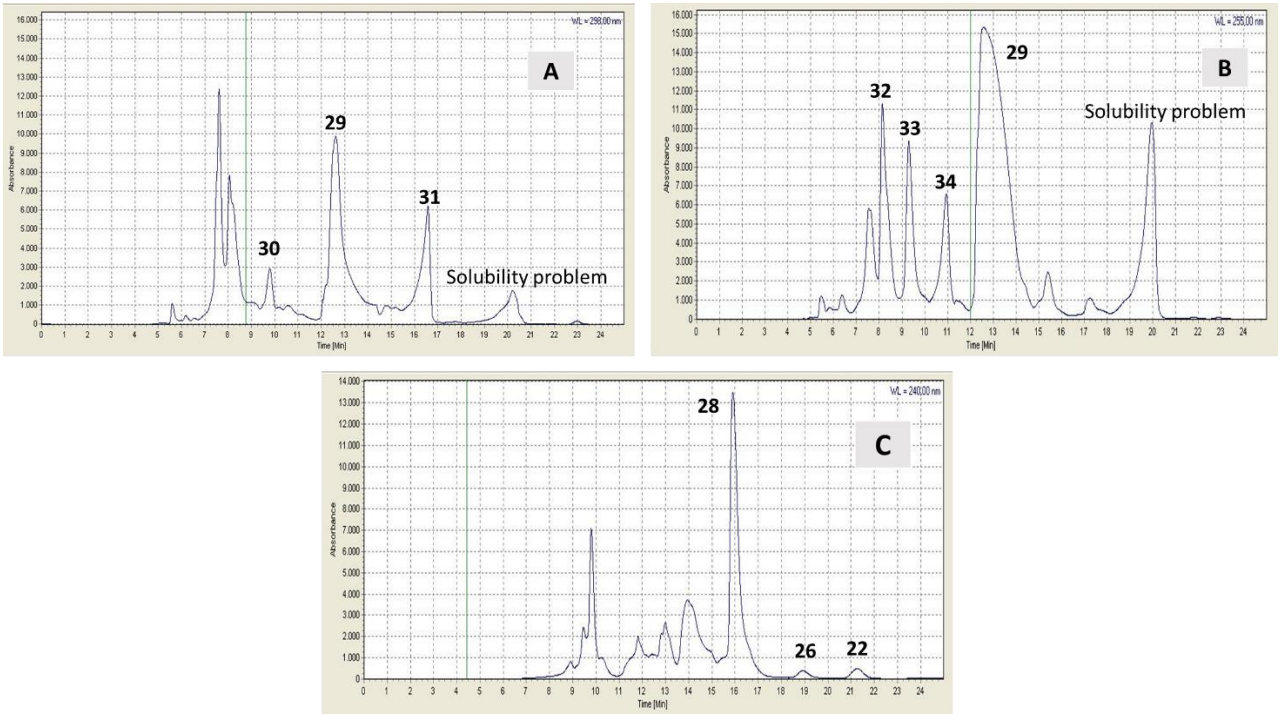

Figure 3.28: Preparative RP-18 HPLC chromatograms. **A**: Fraction F4.C2 (HP-8), UV 298 nm. **B**: Fraction F4.C3 (HP-8), UV 255 nm. **C:** Fraction F4.C6 (HP-8), UV 240 nm**.**

3.3.4.2 Fraction S2.F5

TLC control **(Figure 3.26)** depicted the presence of several compounds on fraction S2.F5. Optimal separation method of this fraction was achieved after several attempts with different stationary phases and mobile phases. Among other methods, CPC was found to be the best method, the same parameters and conditions were used as for the separation of S2.F4. Therefore, CPC fractionation of S2.F5 resulted to nine fractions F5C1-F5C9 **(Figure 3.29)**.

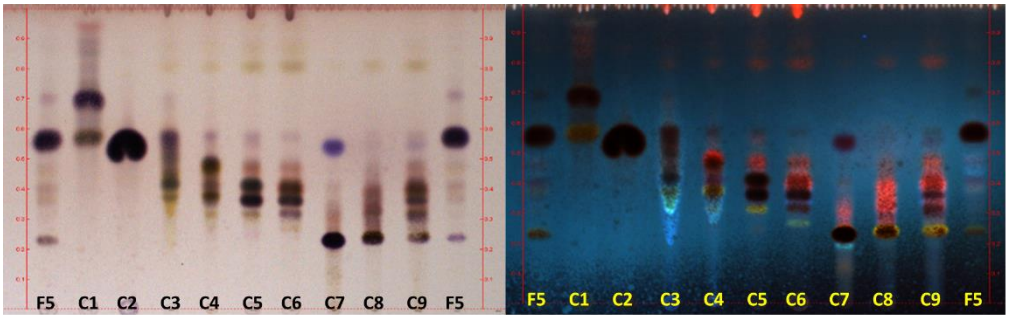

Figure 3.29: Control NP-TLC of S2.F5 CPC fractionation. Mobile phase MP_1, sprayed with anisaldehyde-sulphuric acid reagent. Detection VIS **(left)** and UV 366 nm **(right)**.

Fractions F5.C1-F5.C5 and F5.C7-F5.C8 were further separated and isolation of individual compounds was achieved. The small yields obtained and the presence of several compounds in the fractions F5.C6 (9.8 mg) and F5.C9 (8.5 mg) made them impossible for further fractionation steps.

F5.C1 (79.5 mg) was subjected to preparative HPLC using method HP-5 **(Figure 3.30 A)**. Four peaks eluted, however two peaks resulted to isolation of compounds **21** (3.1 mg, t_R = ~ 12 min), and **13** (6.5 mg, t_R = ~ 13.3 min). The third peak at t_R = ~ 11 min (2.0 mg) and the fourth peak at t_R = ~ 14 min (42.9 mg) were not pure, hence required a subsequent purification step which was not possible to the third peak due to its low yield.

The fourth peak was further detected by TLC **(Figure 3.30 B)** to contain several compounds. Thereafter, an optimal separation method for these compounds was investigated and found to be silica gel flash chromatography method FL-6. Successful separation and purification of the fourth peak (42.9 mg) was achieved and resulted to isolation of compounds **14** (10.2 mg, R_f = 0.60), **19** (13.3 mg, R_f = 0.81) and **20** (5.8 mg, R_f = 0.60) as depicted in **Figure 3.30 C**.

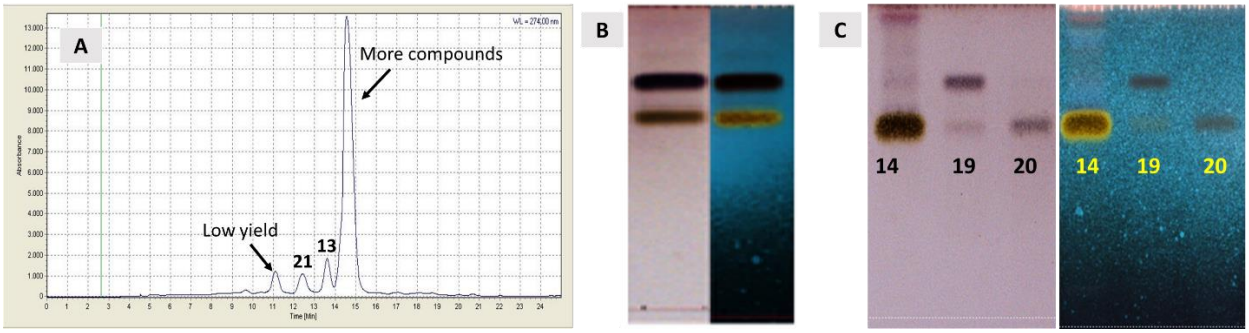

Figure 3.30: A: Preparative RP-18 HPLC chromatogram of fraction F5.C1 monitored by UV detector at 274 nm (HP-5). **B:** TLC control of the fourth peak (from **A**) at t_R = ~ 14 min depicting the presence of more than one compound. **C:** Control TLC of flash chromatography of the fourth peak t_R = ~ 14 min. NP-TLCs were developed using mobile phase MP_1 and sprayed with anisaldehyde-sulphuric acid reagent. Detection VIS **(left)** and UV 366 nm **(right)**.

F5.C2 (1.13 g) was purified using HPLC method HP-4 and resulted in reisolation of compound **13** (77.0 mg). Similarly, separation and purification of F5.C3 (21.8 mg) using HPLC method HP-5 lead to isolation of compounds **18** (0.7 mg, t_R = ~ 7.5 min), **17** (0.6 mg, t_R = ~ 5.8 min) and reisolation of **13** (1.81 mg) as depicted in **Figure 3.31 A**. Separation of F5.C4 (22.7 mg) by preparative HPLC method HP-6 resulted in compound **27** (0.6 mg, t_R = ~ 16 min) and **24** (0.9 mg,

t_R = ~ 24.2 min) as depicted in **Figure 3.31 B**. Separation of F5.C5, (15.5 mg) by method HP-7 **(Figure 3.31 C)** led to isolation of compound **16** (2.5 mg, t_R = ~ 10.5 min) and **25** (2.2 mg, t_R = ~ 14 min). F5.C7 (39.5 mg) and F5.C8 (11.0 mg) were separated using method HP-7 and resulted in compounds **10** (1.0 mg, t_R = ~ 6.3 min), **26** (2.6 mg, t_R = ~ 11.9 min) and **22** (1.0 mg, t_R = ~ 10.5 min) for F5.C7 **(Figure 3.31 D)**. F5.C8 resulted in reisolation of **18** (1.8 mg, t_R = ~ 12 min) and **22** (4.2 mg, t_R = ~ 10.5 min) and compound **23** (0.9 mg, t_R = ~ 17.1 min) **(Figure 3.31 E)**.

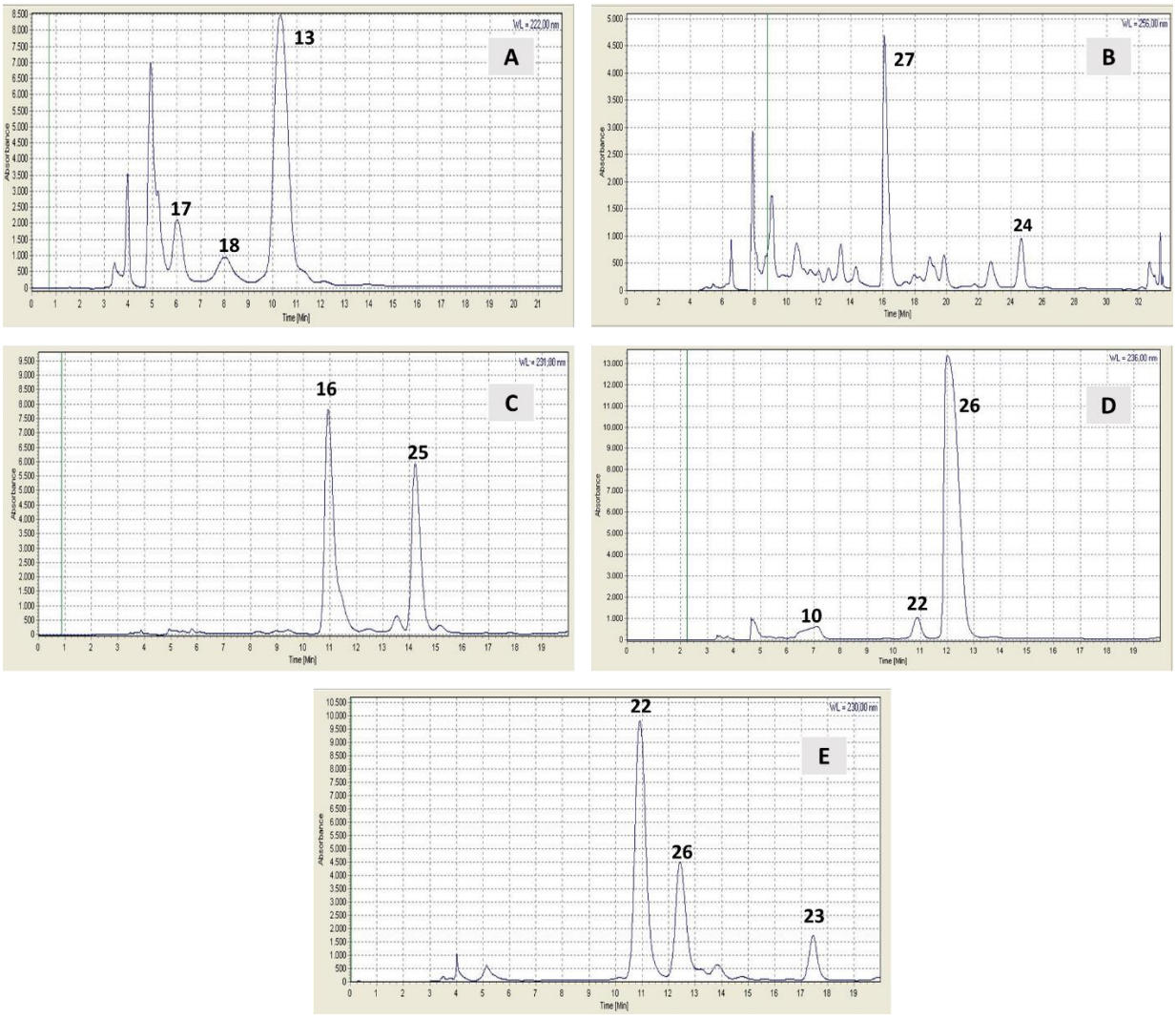

Figure 3.31: Preparative RP-18 HPLC chromatograms. **A:** Fraction F5.C3 (method HP-5), UV detection at 222 nm. **B:** Fraction F5.C4 (method HP-6), UV detection at 255 nm **C:** Fraction F5.C5 (method HP-7), UV detection at 291 nm. **D:** Fraction F5.C7 (method HP-7), UV detection at 236 nm**. E:** Fraction F5.C8 (method HP-7), UV detection at 230 nm.

3.3.4.3 Fraction S2.F6

S2.F6 was fractionated on silica gel flash chromatography using method FL-5 which resulted to ten subfractions F6.1–F6.10 **(Figure 3.32)**.

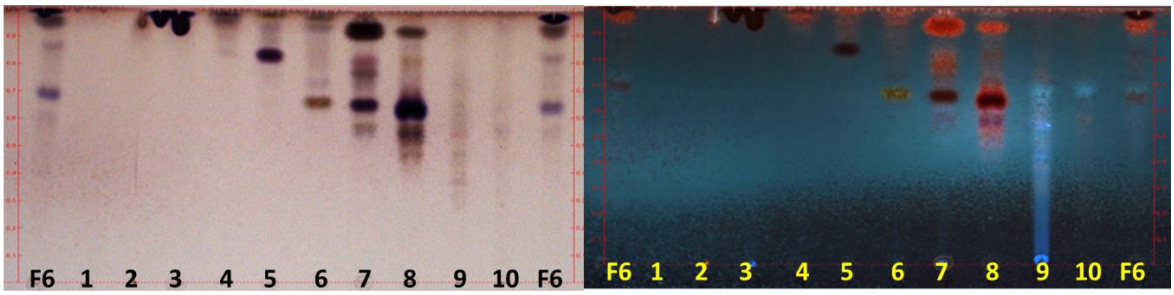

Figure 3.32: Control NP-TLC of S2.F6 silica gel flash chromatography. Mobile phase MP_1, sprayed with anisaldehyde-sulphuric acid reagent. Detection VIS **(left)** and UV 366 nm **(right)**.

Subfractions F6.3 (43.4 mg), F6.5 (1.8 mg) and F6.10 (8.2 mg) were subjected to preparative RP-18 HPLC using method HP-9, HP-10 and HP-11 respectively. After chromatography, compounds **11** (30.5 mg, t_R = ~ 10.5 min) and **12** (6.6 mg, t_R = ~ 11.8 min) were obtained from F6.3 **(Figure 3.33 A)**, compound **15** (0.7 mg, t_R = ~ 11 min) from F6.5 **(Figure 3.33 B)** and compound **27** (0.9 mg, t_R = ~ 5.9 min) from F6.10 **(Figure 3.33 C)** respectively.

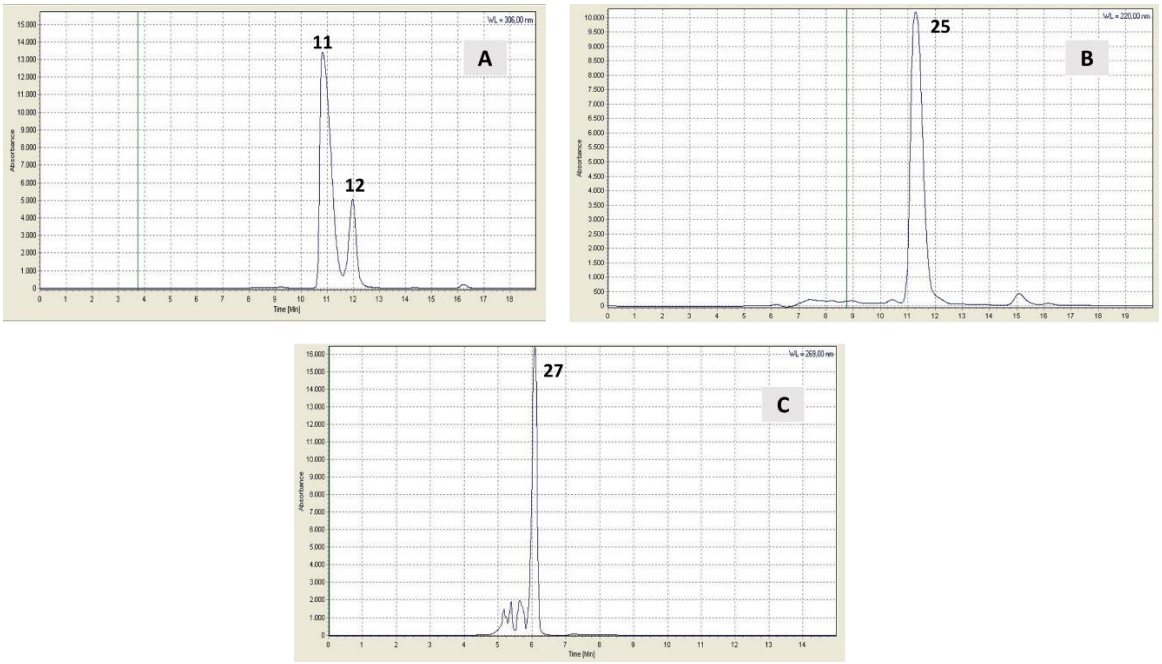

Figure 3.33: Preparative RP-18 HPLC chromatograms. **A**: Fraction F6.3, UV 306 nm (method HP-9)**. B:** Fraction F6.5 (method HP-10), UV 220 nm. **C:** Fraction F6.10 (method HP-11), UV 269 nm.

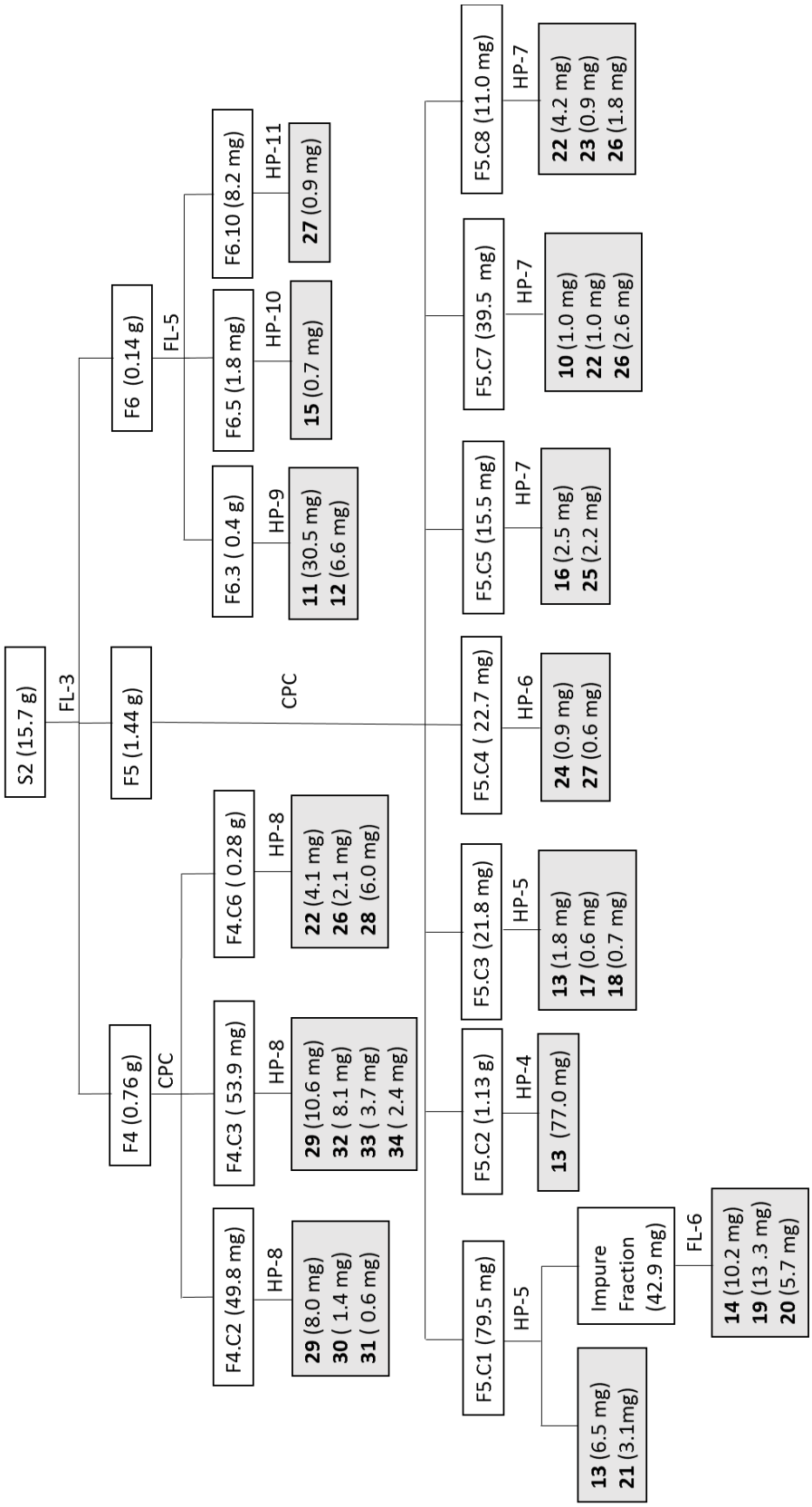

Figure 3.34: Fractionation and isolation scheme of non-tannin compounds obtained from Sephadex® LH-20 fraction S2 from crude methanolic extract of *M. salicifolia* bark.

3.3.5 Structure elucidation of the isolated compounds

Structure elucidation of the isolated compounds was accomplished in two steps. In the first step, the relative stereochemistry of the isolated compounds was attained. Thereafter, determination of the absolute configuration was done.

Determination of relative configuration of the isolated compounds

The relative configuration of the isolated compound was achieved by the aid of 1D NMR (^{1}H and ^{13}C) and 2D NMR (HSQC, HMBC, COSY, and NOESY/ROESY). Molecular mass and molecular formula of the structure were achieved by mass spectroscopy (LC-MS, HRESI-MS). Additionally, UV measurements to determine the absorption maxima were performed.

^{1}H NMR spectrum is the starting point for many structure determinations. The spectrum provides important information on chemical shifts which gives a hint to the kind of hydrogens, for example alkane, alkene, benzene or aldehyde. It also provides the relative number of (not exchangeable) protons which are obtained by integral of a peak/peaks signals generated by different hydrogens in a compound. In addition to that, the number of hydrogens on the neighbouring carbon atom are obtained through observation of signal splitting/multiplicity caused by interactions with neighbouring hydrogens.

^{13}C spectra measurement gives information on the number of carbons by observing the number of signals generated, and chemical shift values (ppm) are telling something about the type of carbons that are present in the compound of interest.

The HSQC spectrum shows heteronuclear correlation between a proton and its direct attached carbon. The spectrum gives information on single bond linkages ($^{1}J_{H,C}$) within the molecule. It also provides information about the group of protons attached to the particular carbon. The HSQC experiment relies on magnetization transfer from the proton to its attached carbon and back to the proton, therefore signals for non-protonated carbons, e.g. carbonyl group and signal of H attached to another heteroatom other than carbon e.g. OH, are not displayed.

The HMBC experiment provides heteronuclear correlation information on long-range couplings between ^{1}H-^{13}C connectivity, i.e. proton and its neighbouring carbons that are separated from

each other by two, three, and sometimes four bonds ($^2J_{H,C}$ and $^3J_{H,C}$ or $^4J_{H,C}$). Additionally, HMBC is often used in structure elucidation for assignment of the quaternary and carbonyl carbons, as well as assignment of the linkage position between two substructures in a compound, e.g. position assignment of glycosidic linkages between aglycone and its sugar moiety.

COSY is a homonuclear 2D NMR experiment which provides information on which protons are coupled with each other (H-H coupling). COSY determines the protons coupling through the bonding electrons hence provides effective way of assigning connectivity when a numerous coupling networks need to be identified. The H-H coupling can either be vicinal H-H or germinal H-H coupling. In vicinal H-H coupling, protons coupled with each other are separated by three bonds ($^3J_{H-H}$) proton resonances located on the adjacent carbon nuclei and in geminal coupling, protons coupled with each other through two bonds ($^2J_{H-H}$) or they are defined as proton resonances located on the same carbon nuclei. Signals of protons that are more than three bonds away cannot be detected in this case because coupling to their neighbours is too small to affect their spin.

NOESY and ROESY experiments give information on interaction between protons that are close to each other through the space. In the NOESY experiment, the observed nuclear overhauser cross relaxation between nuclear spins in the mixing period is used to create the correlations. The NOESY spectrum is comparable to COSY in terms of diagonal peaks and cross peaks. Although, in NOESY the cross peaks connect resonances from nuclei that are spatially close rather than those nuclei which are coupled to each other through bond.

The ROESY is similar to NOESY experiment. However, ROESY measures the homonuclear NOE effects under spin-locked conditions by an external magnetic field so that it is not rotating. In ROESY the mixing time is the spin-lock period where by spin exchange occurs among spin-locked magnetization components of different nuclei. ROESY is suitable for those molecules whose rotational correlation time falls in a range where the nuclear overhauser effect is too weak to be detected.

Molecular mass and molecular formula of the isolated compounds were measured by LC-MS and/or HRESI-MS. The LC-MS is a HPLC system coupled with a mass detector. Consequently, the compounds are separated through the column that is packed with a suitable stationary phase.

As the compounds eluted from the column to the mass detector, the solvent is completely removed, the residues are ionized to generate charged molecules. Thereafter, mass detector scans every molecule ion in the vacuum by mass to charge ratio (*m/z*) and produces a spectrum depicting all ions with different masses. In this study, the LC-MS was used to confirm the molecular mass of isolated compound for easier structure elucidation and also to detect the existence of isomers, which could have same molecular weight but having slight differences in retention time.

Molecular formula of the new isolated compounds and the compounds whose mass did not fit to the prior elucidated structure (by using NMR data) were confirmed by HRESI-MS. HRESI-MS gives information of the elemental composition of a compound by providing *m/z* values with four decimal numbers which match with only one molecular formula.

Absolute stereochemistry of the isolated compounds

The absolute stereochemistry of the isolated compounds was determined based on the elucidated relative configuration. Absolute stereochemistry of the isolated tannins was achieved mainly through optical rotation, CD spectra measurement and comparison with literature values.

The absolute stereochemistry and the type of the sugar moieties attached to the compounds was attained by recording the ^{1}H NMR of the SMB derivatives of glycosides and comparing their chemical shifts and coupling constants of the anomeric proton to that of reference sugars (materials and methods 3.2.7.5). Likewise, the absolute configuration of the aglycone (cyclic diarylheptanoids) was obtained following detachment of the linked sugar by enzyme hydrolysis recording CD spectra data and comparing the experimental data versus CD spectra simulated by TDDFT (materials and methods **3.2.8.6** and **3.2.8.8**).

Detailed structure elucidation of individual compounds is described and discussed in the following paragraphs.

3.3.5.1 Tannins

Nine compounds belonging to the group of tannins (PAs and HTs) were isolated and their structures elucidated. Among the isolated tannins, two compounds were flavan-3-ol monomers with a trihydroxylated B-ring, three dimeric B-type prodelphinidins, three dimeric-A-type prodelphinidins and one ellagitannin. The isolated tannin compounds were obtained from further fractionation of the fractions S4, S5 and S6 as indicated in the fractionation scheme **(Figure 3.25)**. The overview of the isolated tannin compounds are depicted in the control TLC **(Figure 3.35)**. All isolated PAs changed to deep orange colour after sprayed with anisaldehyde-sulphuric acid reagent which is characteristic for the PAs[142]. This was not the case with the isolated ellagitannin under the same conditions.

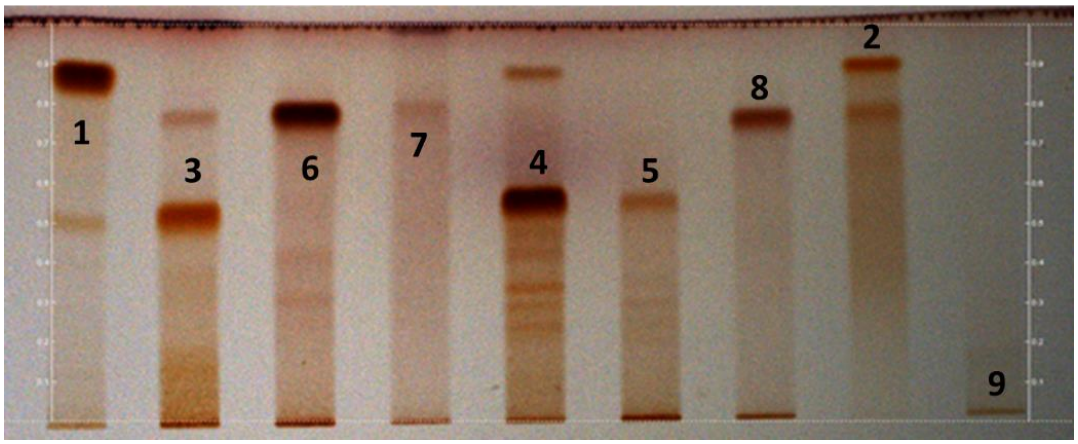

Figure 3.35: NP-TLC overview of the isolated tannins compounds **1** -**9**. Mobile phase MP_1. Detection: VIS. Spraying reagent: anisaldehyde-sulphuric acid reagent.

3.3.5.1.1 Proanthocyanidins

Monomeric flavan-3-ols

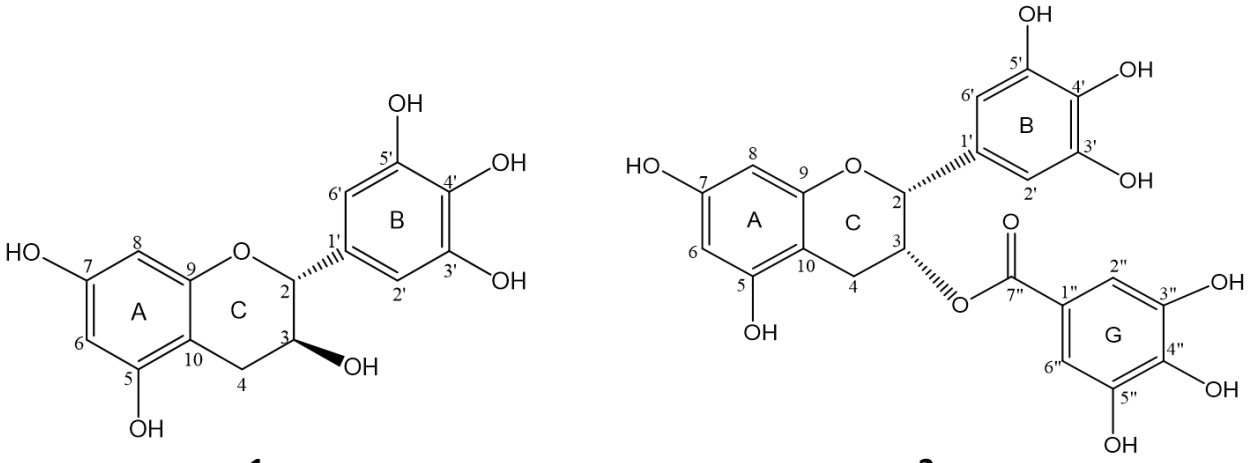

Figure 3.36: Structures of (+)-gallocatechin **(1)** and (-)-epigallocatechin-3-*O*-gallate **(2)**.

Compound **1**((+)-gallocatechin) and **2** ((-)-epigallocatechin-3-*O*-gallate) **(Figure 3.36)** were isolated as light orange amorphous powders from fractions S4 and S6.M13.3 as illustrated in the fractionation scheme **(Figure 3.25)**. The two compounds were identified by their NMR data **(Table 3.8)** and confirmed by comparing with the published data for compound **1**[92,143,144] and compound **2**[92,108,143,145].

The observed singlet signals on the aromatic region of ^{1}H NMR of the compound **1** (δ_H 6.39 ppm) and **2** (δ_H 6.47 ppm) integrating for two protons indicated the trihydroxylated B-ring.

Compound **2** had an extra singlet observed on ^{1}H NMR spectrum at δ_H 6.95 ppm, integrating for two protons. The observed HMBC long range correlation between this proton and carbonyl carbon at δ_C 167.6 ppm indicated that compound **2** possibly contain a gallate moiety. The gallate moiety was assigned to position 3C based on HMBC long range correlation between H-3C (δ_H 5.50 ppm) and the carbonyl carbon C-7" at δ_C 167.6 ppm.

Additionally, the *2,3 cis* orientation of compound **2** was concluded by H-2C signal on ^{1}H NMR spectrum of **2** at δ_H 4.95 ppm (s) and H-3C (δ_H 5.50 ppm, brs) together with their respective carbons at δ_C 78.6 and 69.9 ppm which is characteristic in case of a *cis* orientation[99,146]. The optical rotation of compound **2** was $[\alpha]_D^{25}$ = -96.8 (c 0.1, MeOH) and UV maximum emerged at 275 nm. The ESI-MS exhibited ions at *m/z* 459.092 $[M+H]^+$ in the positive mode and *m/z*

457.076 $[M-H]^-$ in the negative mode calculated for mass of 458 Da which fits with the molecular formula of epigallocatechin-3-*O*-gallate ($C_{22}H_{18}O_{11}$). Overall, compound **2** was confirmed to be (-)-epigallocatechin-3-*O*-gallate (*2S,3S*).

The *2,3 trans* orientation of **1** was deduced from the chemical shifts of H-2C (δ_H 4.52, d) and H-3C (δ_H 3.96, td) with $J_{2,3} > 7$ Hz which is characteristic of *trans* orientation. ESI-MS exhibited ions at *m/z* 307.08 $[M+H]^+$ in the positive mode and *m/z* 305.07 $[M-H]^-$ in the negative mode calculated for mass of 306.27 Da and molecular formula of $C_{15}H_{14}O_7$. The optical rotation for compound **1** was $[\alpha]_D^{22.4}$ = +25.06 (c 0.1, MeOH) and UV maximum was at 270 nm. Hence, the absolute configuration of compound **1** was deduced to be (+)-gallocatechin compared to literature data.

Table 3.8: NMR data for compound **1:** ^{1}H NMR (300 MHz), ^{13}C NMR (75 MHz), MeOH-d_4, 294 K and **2:** ^{1}H NMR (600 MHz), ^{13}C NMR (150 MHz), MeOH-d_4, 278 K.

Position	**1**		**2**	
	δ_C (ppm)	**δ_H (ppm), m, *J* (Hz)**	**δ_C (ppm)**	**δ_H (ppm), m, *J* (Hz)**
2C	82.5	4.52, (1H, d, *J* = 7.1)	78.6	4.95, (1H, s)
3C	68.3	3.96, (1H, td, *J* = 5.3, 7.4)	69.9	5.50, (1H, brs)
4C	28.0	2.80, (1H, dd, *J* = 5.3, 16.1)	26.8	2.96, (1H, dd, *J* = 4.6, 17.2)
		2.49, (1H, dd, *J* = 7.8, 16.1)		2.81, (1H, dd, *J* = 2.3, 17.3)
5A	156.5		157.2	
6A	96.9	5.91, (1H, d, *J*= 2.3)	96.1	5.93, (1H, d, *J* = 2.2)
7A	157.1		157.6	
8A	96.1	5.85, (1H, d, *J* = 2.3)	95.7	5.92, (1H, d, *J* = 2.2)
9A	157.0		157.3	
10A	101.4		99.1	
1’B	131.5		130.6	
2’B	107.9	6.39, (1H, s)	106.6	6.47, (1H, s)
3’B	146.7		146.4	
4’B	134.0		133.9	
5’B	146.7		146.4	
6’B	107.9	6.39, (1H, s)	106.6	6.47, (1H, s)
1”G			121.2	
2”G/6” G			110.1	6.92, (1H, s)
3”G/5”G			147.1	
4”			140.4	
7”			167.6	

Dimeric B-type prodelphinidins

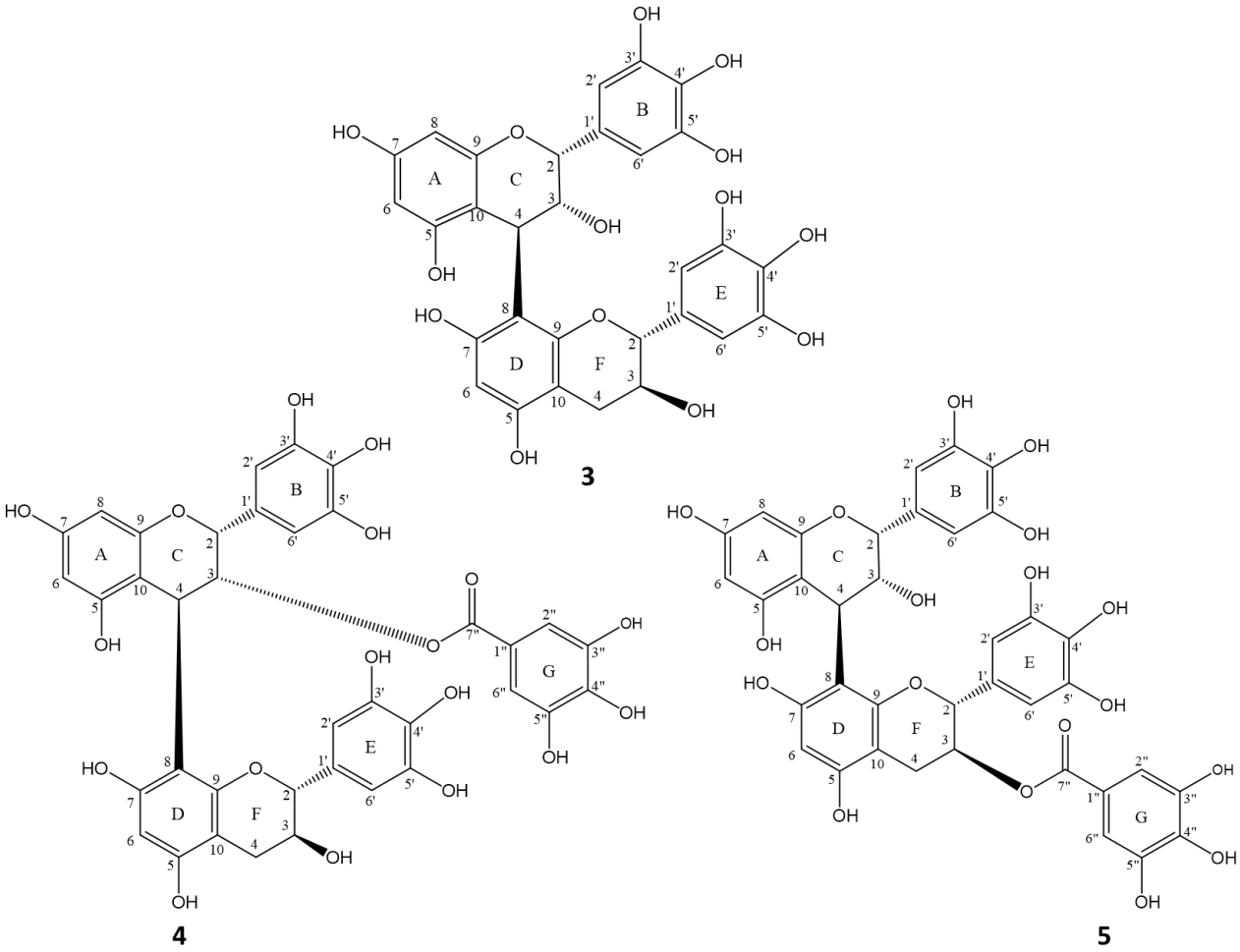

Figure 3.37: Structures of epigallocatechin-(4β→8)-gallocatechin **(3)**, epigallocatechin-3-*O*-gallate-(4β→8)-gallocatechin **(4)** and epigallocatechin-(4β→8)-gallocatechin-3-*O*-gallate **(5)**.

Dimeric B-type prodelphinidins with and without gallate moiety were also isolated from the Sephadex® LH-20 fractions S5 and S6 of the methanolic extract of *M. salicifolia* bark. These compounds were identified as prodelphinidin B1 (epigallocatechin-(4β→8)-gallocatechin **(3)**, epigallocatechin-3-*O*-gallate-(4β→8)-gallocatechin **(4)** and epigallocatechin-(4β→8)-gallocatechin-3-*O*-gallate **(5) (Figure 3.37)**. The ^{1}H and ^{13}C NMR data of the three compounds are summarized in the **Table 3.9**.

The NMR measurement of these compounds were performed at low temperature (233 K) because of the broadening of ^{1}H NMR signals due to rotational isomerism caused by steric

interactions in the vicinity of the interflavanoid bond of freely rotating flavan-3-ol units when measurements are performed at room temperature[86,147].

Table 3.9: ^{1}H and ^{13}C NMR of compounds **3**, **4** and **5**. ^{1}H NMR (600 MHz), ^{13}C NMR (150 MHz), MeOH-d_4, 233 K.

Pos.	**3**		**4**		**5**	
	δ_C (ppm)	**δ_H (ppm), m, *J* (Hz)**	**δ_C (ppm)**	**δ_H (ppm), m, *J* (Hz)**	**δ_C (ppm)**	**δ_H (ppm), m, *J* (Hz)**
2C	76.8	4.96, (1H, brs)	74.8	5.26**,** (1H, brs)	75.7	5.25, (1H, brs)
3C	72.8	3.88, (1H, brs)	74.3	5.37, (1H, brs)	75.5	5.31, (1H, brs)
4C	36.7	4.58, (1H, brs)	34.3	4.60, (1H, brs)	34.6	4.59, (1H, brs)
5A	156.1		155.7		155.4	
6A	95.8	5.95, (1H, dd, *J* = 9.4, 2.3)	106.1	6.27, (1H, s)	105.7	6.26, (1H, s)
7A	154.3		153.9		154.2	
8A	95.8	5.95, (1H, dd, *J* = 9.4, 2.3)	106.2	6.31, (1H, s)	105.7	6.26, (1H, s)
9A	157.9		156.2		157.9	
10A	101.4		102.4		102.7	
1’B	131.8		131.8		137.8	
2’B	106.4	6.38,(1H, s)	109.8	6.36, (1H, s)	106.0	6.36, (1H, s)
3’B	146.4		146.5		146.6	
4’B	133.6		133.4		132.8	
5’B	146.4		146.5		146.6	
6’B	106.4	6.38, (1H, s)	109.8	6.36, (1H, s)	106.0	6.36, (1H, s)
Lower						
2F	82.3	4.71, (1H, d, *J* = 6.2)	81.9	4.83, (1H, d, *J* = 5.4)	81.9	4.83, (1H, d, *J* = 5.4)
3F	68.2	4.05, (1H, m)	68.4	4.04, (1H, m)	68.9	4.04, (1H, m)
4F	27.3	2.76, (1H, m) 2.57, (1H, m)	26.7	2.96, (1H, m) 2.70, (1H, dd, *J* = 5.3, 16.1)	27.3	2.94, (1H, dd, *J* = 5.6, 16.6) 2.78, (1H, dd, *J* = 5.3, 16.1)
5D	152.9		152.0		151.2	
6D	96.7	5.82,(1H, s)	107.4	6.12, (1H, s)	106.9	6.12, (1H, s)
7D	156.3		157.6		156.6	
8D	107.4		107.8		107.6	
9D	150.2		156.2		156.1	
10D	100.9		102.4		102.0	
1’E	124.0		131.8		130.9	
2’E	106.6	6.49, (1H, s)	106.3	6.75, (1H, s)	106.0	6.75, (1H, s)
3’E	146.8		146.5		146.3	
4’E	133.6		133.7		132.8	
5’E	146.8		146.5		146.3	
6’E	106.6	6.49, (1H, s)	106.3	6.75, (1H, s)	106.2	6.75, (1H, s)

Pos.	3		4		5	
	δ_C (ppm)	δ_H (ppm), m, *J* (Hz)	δ_C (ppm)	δ_H (ppm), m, *J* (Hz)	δ_C (ppm)	δ_H (ppm), m, *J* (Hz)
1"G			121.1		121.0	
2"G			109.9	6.85, (1H, s)	109.3	6.85, (1H, s)
3"G			146.2		145.0	
4"G			139.4		139.7	
5"G			146.2		145.0	
6"G			109.9	6.85, (1H, s)	109.3	6.85, (1H, s)
7"			166.2		166.0	

Compound **3**, prodelphinidin B1 (epigallocatechin-(4β→8)-gallocatechin) was isolated as amorphous light orange powder, with $[\alpha]_D^{25}$ = -15.33 (c 0.1, MeOH) and UV maximum at 270 nm. The ESI-MS exhibited ions at *m/z* 611.14 $[M+H]^+$ in the positive mode and *m/z* 609.12 $[M-H]^-$ in the negative mode calculated for 610 Da which fits to the molecular formula of $C_{30}H_{26}O_{14}$. The compound exhibited positive cotton effect in the region 213-243 nm of CD spectrum. This confirms a 4β-interflavanol linkage with 4R configuration of the upper unit[148–151]. The ^1H and ^{13}C NMR data are summarized in **Table 3.9**.

Prodelphinidin B1 is a known compound, however the complete published ^1H and ^{13}C NMR literature data are of the peracetylated derivative[152–155] and the data of free phenolic compound are not complete, hence they could not fit exactly with the obtained data of **3**. The NMR data for **3** were almost comparable to the published data of non-acetylated but methylated prodelphinidin B1[99]. The observed difference between both compounds are the carbon shifts of the lower unit E-ring where the hydroxyl group at C-4' is replaced by a methoxy group. The carbon shift values of the E-ring containing methoxy group which are different from the isolated prodelphinidin B1 are δ_C 137.1 ppm (C-1') and 151.6 ppm (C-3' /C-5') while those of prodelphinidin B1 are δ_C 124.0 ppm (C-1') and 146.8 ppm (C-3' /C-5').

Compound **4** (epigallocatechin-3-*O*-gallate-(4β→8)-gallocatechin) was isolated as amorphous orange powder with $[\alpha]_D^{25.4}$ = +168 (c 0.1, MeOH) and UV maximum at 275 nm. The upper unit was identified as epigallocatechin, because of the observed chemical shift of H-2C (δ_H 5.26 ppm), and H-3C (δ_H 5.37), both broad singlets which is characteristic for *2,3 cis* orientation. The lower unit was identified as gallocatechin by the chemical shifts of H-2F (δ_H 4.83, d) and H-3F (4.04, d) with $J_{2,3}$ = 5.4 Hz and also by their carbon signals 2F (δ_C 81.9) and 3F (δ_C 68.4) which is

characteristic of the *2,3 trans* orientation[156]. Assignment of the galloyl moiety to upper unit was based on HMBC long correlation between H-3C (δ_H 5.37) to carbon C-7" (δ_C 166.2). The ESI-MS exhibited ions at *m/z* 761.1533 $[M-H]^-$ in the negative mode, calculated for 762 Da and the molecular formula $C_{37}H_{30}O_{18}$.

Positive cotton effects were observed in the region 225 - 250 nm of the CD spectrum which confirms a 4β-flavanol linkage with 4R configuration. From the obtained data of **4**, it was concluded that it is epigallocatechin-3-*O*-gallate-(4β→8)-gallocatechin. Compound **4** is a known compound, previously reported by, Danne et al.[154], Hartisch and Kolodziej[157]. The published data reported on the acetylated derivative and could not exactly match with free phenolic compound **4**. No literature is available to this free phenolic prodelphinidin derivative.

Compound **5** (epigallocatechin-(4β→8)-gallocatechin-3-*O*-gallate) was isolated as amorphous orange powder with $[\alpha]_D^{25}$ = +220 (c 0.1, MeOH) and UV maximum at 275 nm. The obtained mass spectrometry data were the same as for the compound **4**, exhibiting ions *m/z* 761.1487 $[M-H]^-$ in the negative mode and calculating for the molecular formula $C_{37}H_{30}O_{18}$.

The NMR data of the two compounds **4** and **5** were similar, but a difference was noted in their retention time **(Figure 3.24 A)**. Thus, the structural difference is likely the position of the galloyl moiety. Assignment of galloyl moiety of compound **5** was not clear due to broad ^{1}H NMR signal even after measurement at -40 ^{o}C. The recorded broad ^{1}H NMR signals caused overlapping of some cross peaks in the lower field of the HMBC experiment. Additionally, there was no HMBC correlation observed between H-3C (δ_H 5.31 ppm) and the carbonyl carbon at δ_C 166.0 ppm (C-7") which could prove that the galloyl moiety is not attached to the upper unit, and gave a clue that attachment of the galloyl moiety could be linked to the lower unit of compound **5** as shown in **Figure 3.38**.

A positive cotton effect in the region 210 -254 nm was observed in the CD spectrum of **5** which confirmed a 4β-interflavanol linkage with 4R configuration. From the obtained data, compound **5** was identified as epigallocatechin-(4β→8)-gallocatechin-3-*O*-gallate. The isolation of **5** was hitherto not reported, however further investigations have to be done to provide a proof of the galloyl position.

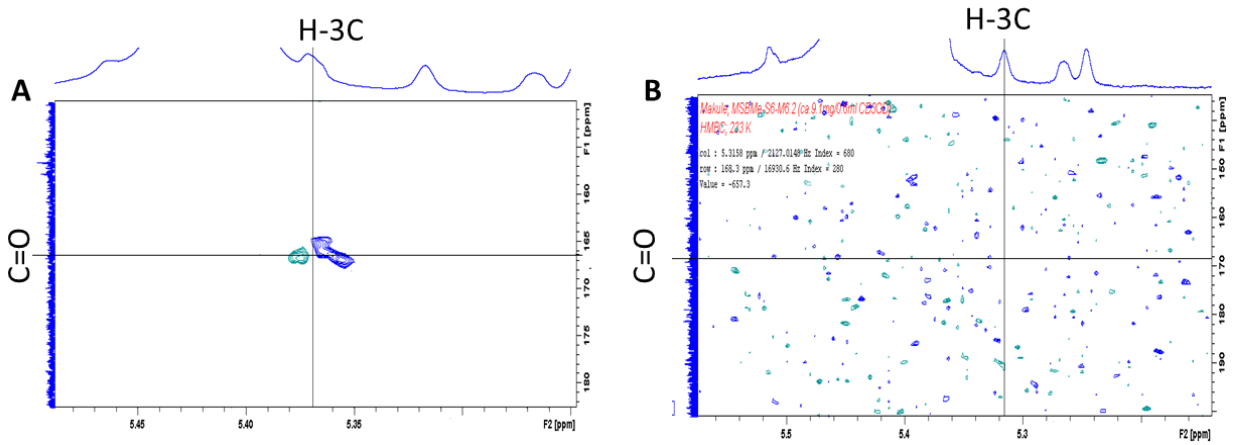

Figure 3.38: Part of the HMBC spectrum, **A**: Showing correlation between H-3C and the carbonyl carbon of the gallate moiety for compound **4** and **B**: No correlation was observed to proof the attachment of gallate moiety for compound **5.**

Dimeric A-type prodelphinidins

The compounds **6** - **8** were isolated and identified as A-type prodelphinidins. The identification of these compounds was mainly based on obtained NMR data **(Tables 3.10** and **3.11)** in comparison to literature data on the A-type PAs. The characteristics of the A-type PAs which were observed from recorded NMR spectra data are: the characteristic of C ring protons (H-3C, H-4C) which possess small coupling constants between 3-4 Hz[158]. The NOESY/ROESY correlation between H-3C and H-6D is an indicative feature for assigning the configuration of position 3C. The presence of a NOESY correlation between H-3C and H-6D confirms the *3,4 trans* relative configuration and the lack of a NOESY correlations confirms the *3,4 cis* relative configuration[158,159]. The double linkages of either (2β,4β) or (2α,4α) of these compounds were confirmed by CD spectra measurements, as the high amplitude of positive cotton effect at 200-240 nm confirms (2β,4β) orientation and the negative cotton effect at 240 nm confirms (2α,4α)[148,149,151].

Myricedin (7)

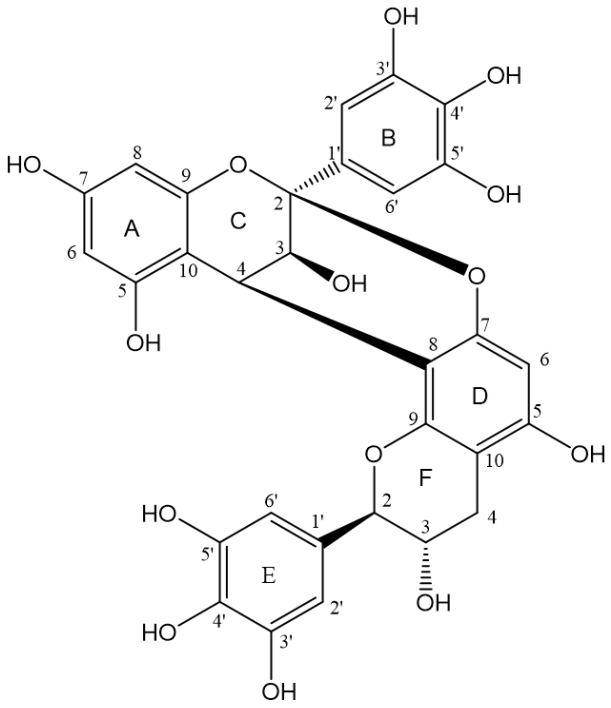

7

Figure 3.39: Structure of myricedin: (+)-gallocatechin-(2β→*O*→7,4β→8)–gallocatechin **(7)**.

Compound **7**, myricedin ((+)-gallocatechin-(2β→*O*→7,4β→8)–gallocatechin) **(Figure 3.39)**, was isolated as amorphous light orange powder. It displays an orange spot on the TLC sheet after spraying with anisaldehyde-sulfuric acid reagent **(Figure 3.35)**, an R_f value of ~ 0.8 and optical rotation $[\alpha]_D^{25}$ = -22.6 (c 0.1, MeOH). The HRESI-MS exhibited ions at *m/z* 607.1099 $[M\text{-}H]^-$ in the negative mode correlating with molecular formula of $C_{30}H_{23}O_{14}$. The UV spectrum of **7** display a maximum at wavelength 279 nm corresponding to those of PAs.

Two singlets δ_H 6.33 and 6.71 were observed in the aromatic region of the ^{1}H NMR spectrum, all integrating for two protons indicating the presence of two trihydroxylated flavan-3-ol units. The AB coupling system was detected at δ_H 4.0 - 4.5 with $J_{3,4}$= 3.5 Hz, characteristic for the C-ring protons of A-type PAs[151,158,159]. The doubly linked dimeric structure was demonstrated by one acetal carbon at δ_C 100.3 ppm which was detected from the long range HMBC correlation between δ_H 4.06 (H-3C), δ_H 4.23 (H-4C) and δ_C 100.3 ppm (C-2). In addition to this, the *meta*-

coupled doublets of the A ring were observed at δ_H 5.99 ppm (H-6A) and 6.05 ppm (H-8A), each doublets, integrated for one proton with *J* = 2.2 Hz and 2.1 Hz respectively.

The absolute configurations at position 2C and 4C were established by CD spectra measurements. The detected positive cotton effects in the wavelength region of 226 - 255 nm indicated the (2β, 4β) configuration. The absence of ROESY correlation between H-3C (δ_H 4.06 ppm) and H-6D (δ_H 6.07 ppm) indicates the *3,4 cis* configuration of ring C. Hence the upper unit was identified to be (+)-gallocatechin.

The lower unit was identified as gallocatechin from the chemical shifts δ_H 4.62, d (H-2F) and δ_H 4.01, dd (H-3F) with $J_{2,3} > 6$ together with their corresponding carbon signals at δ_C 84.7 and δ_C 68.1 ppm which is characteristic of *2,3 trans* orientation[99,146]. Together with the 2D NMR data compound **7** was therefore deduced to be (+)-gallocatechin-(2β→*O*→7,4β→8)-gallocatechin. It is not yet described in literature and was named myricedin.

Table 3.10: ^{1}H NMR, ^{13}C NMR and HMBC correlation of compound **7**. ^{1}H NMR (600 MHz), ^{13}C NMR (150 MHz), MeOH-d_4, 278 K.

Position	δ_C (ppm)	δ_H (ppm), m, *J* (Hz)	HMBC
Upper			
2C	100.2		
3C	68.3	4.06, (1H, d, *J* = 3.5)	2C, 10A, 8D, 4B, 9A
4C	29.3	4.23, (1H, d, *J* = 3.5)	3C, 2C, 10A, 8D, 5A, 10D
5A	153.5		
6A	96.8	5.99, (1H, d, *J* = 2.2)	A8/A6, 10A, 7A
7A	157.9		
8A	96.4	6.05, (1H, d, *J* = 2.1)	3C, 6A, 2C, A10, 5A, 7A
9A	152.7		
10A	103.5		
1’B	131.4		
2’B	107.8	6.71, (1H, s)	2C, 2’B/6’B, 1’B, 4’B, 3’B/5’B
3’B	145.8		
4’B	135.3		
5’B	145.8		
6’B	107.8	6.71, (1H, s)	2C, 2’B/6’B, 1’B, 4’B, 3’B/5’B
Lower			
2F	82.5	4.62, (1H, d, *J* = 6.1)	4F, 3F, 2’E/6’E, 1’E, 7D
3F	68.6	4.01, (1H, dd, *J* = 6.3, 11.5)	10D, 9D
4F	27.6	2.74, (1H, dd, *J* = 4.9, 16.5) 2.61, (1H, dd, *J* = 6.5, 16.4)	3F, 2F, 9D.
5D	155.2		

Position	δ_C (ppm)	δ_H (ppm), m, *J* (Hz)	HMBC
6D	96.6	6.07, (1H, s)	10D, 8D, 9D, 5D
7D	154.2		
8D	107.2		
9D	151.3		
10D	103.9		
1'E	131.7		
2'E	106.6	6.33, (1H, s)	2F, 2'E/6'E, 4'E, 3'E/5'E
3'E	147.1		
4'E	133.1		
5'E	147.1		
6'E	106.6	6.33, (1H, s)	2F, 2'E/6'E, 4'E, 3'E/5'E.

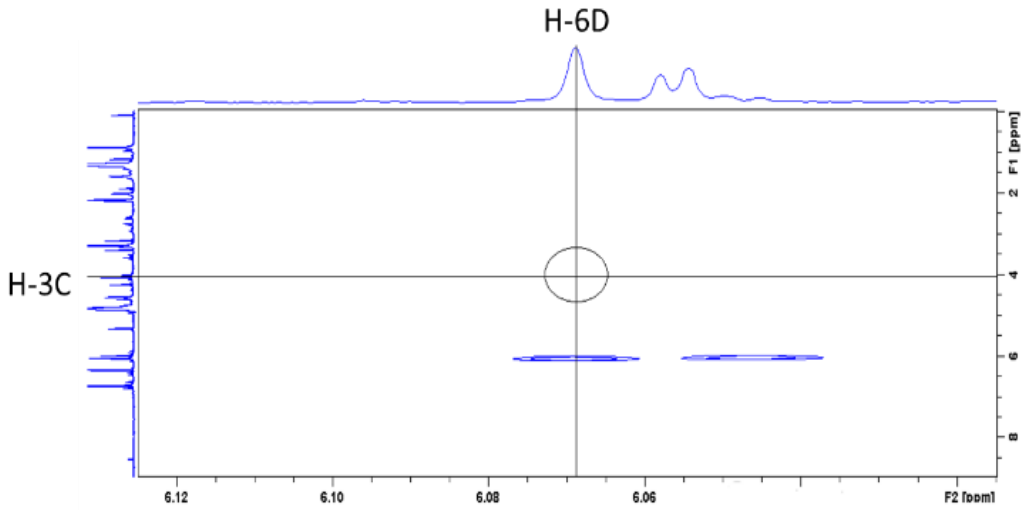

Figure 3.40: Absence of ROESY correlation of H-3 of ring C to H-6 of ring D, an important indication for the *3,4 cis* configuration of ring C for compound **7**[158,159].

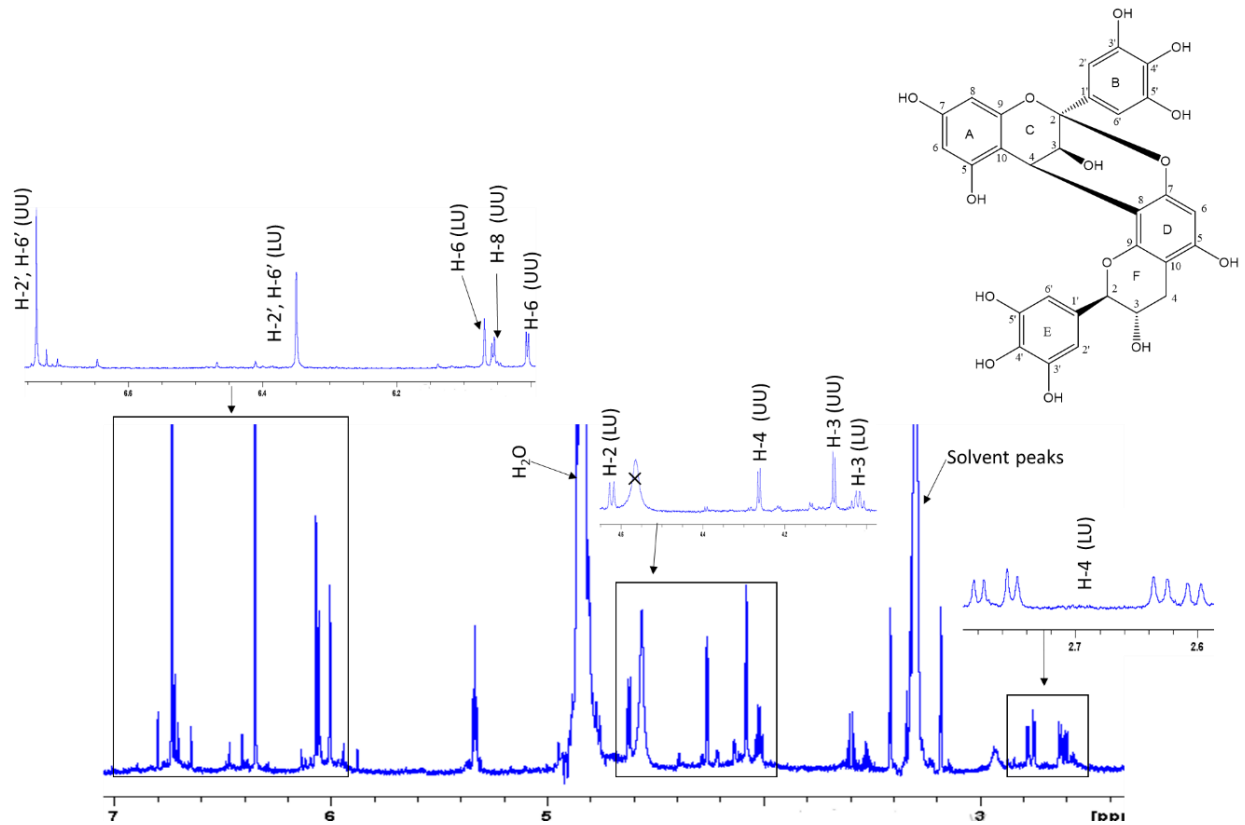

Figure 3.41: ^{1}H NMR spectrum of compound **7**. MeOH-d_4, 600 MHz, 298 K. LU = lower unit, UU = upper unit.

Ephedrannin D5 (6) and adenodimerin C (8)

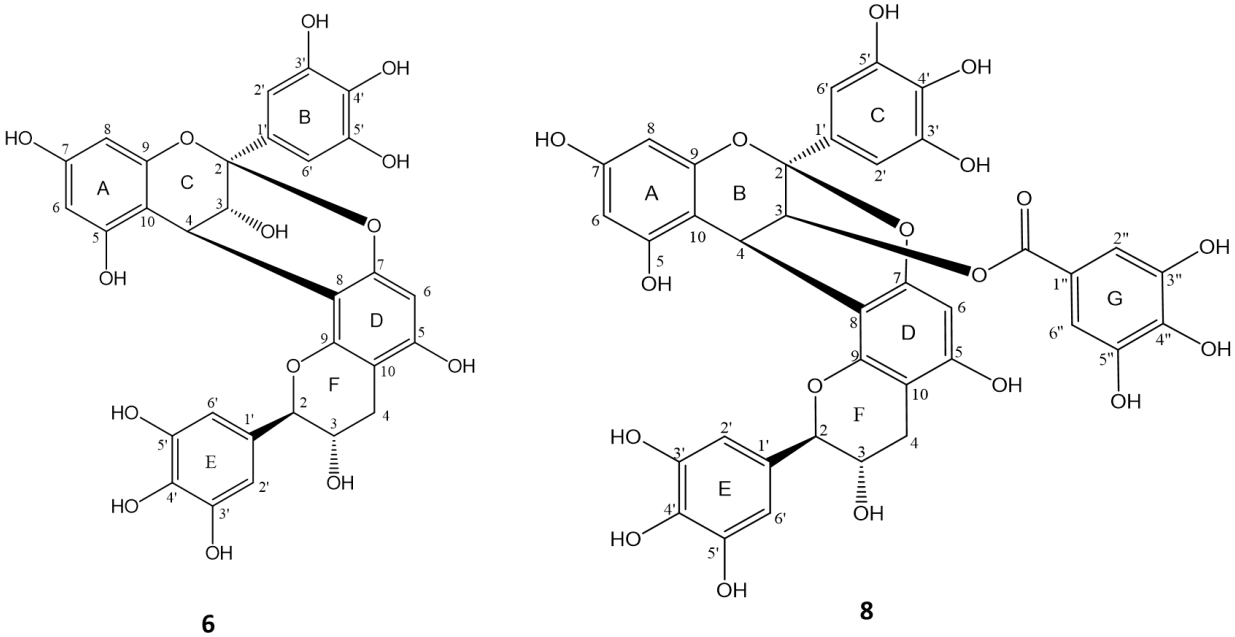

6 **8**

Figure 3.42: Structures of ephedrannin D5 **(6)** and adenodimerin C **(8)**.

Compound **6** (epigallocatechin-(2β→*O*→7,4β→8)-gallocatechin) **(Figure 3.42)**, was isolated as amorphous light orange powder with optical rotation value $[\alpha]_D^{25}$ = -82.4 (c 0.1, MeOH). It appeared as deep orange spot on the TLC sheet with the same R_f value as that of compound **7** **(Figure 3.35)**. Compound **6** exhibited a UV maximum at 270 nm. The ESI-MS exhibited ions at *m/z* 609.1246 $[M+H]^+$ in the positive mode and *m/z* 607.1085 $[M-H]^-$ in the negative mode, calculating for molecular mass of 608 Da which corresponds to molecular formula of $C_{30}H_{24}O_{14}$, which is the same like that of **7**.

The NMR data of compound **6** were comparable to those of **7** in terms of coupling constants and chemical shifts of carbons **(Table 3.11)**. The difference between the two compounds was clearly observed on their ^{1}H NMR spectrum on the arrangement of the signals of H-3C, H-4C and H-3F as it is depicted in **Figure 3.46**. For compound **6**, the multiplet for H-3F (lower unit (LU)) was in the middle of H-4C and H-3C, both doublets (upper unit (UU)), while for compound **7**, the H-3C doublet (UU) was in the middle of the multplet of H-3F (LU) and H-4C doublet (UU). The difference was further observed in the ROESY experiment as there was a ROESY correlation between H-3C (δ_H 4.04) and H-6D (δ_H 6.07), an indication for the *3,4 trans* configuration of the C ring **(Figure 3.43)**.

The absolute configurations at C-2 and C-4 in the upper unit were established from the detected positive cotton effects of the CD spectrum in the wavelength region 209 - 251 nm, indicating the 2β,4β-configuration[148–150]. Therefore, the upper unit was concluded to be epigallocatechin unlike gallocatechin for the compound **7**.

The lower unit was identified as gallocatechin *(2,3 trans)* from the detected chemical shifts and coupling constants of H-2F (δ_H 4.67, d, J = 7.6 Hz) and H-3F (4.11, m) and their corresponding carbon signals at δ_C 84.7 and 68.1 respectively. The obtained data of **6** are in agreement with the published data of ephedrannin D5 isolated from *Ephedra sinica*[160]. Hence, it was concluded that **6** is also epigallocatechin-(2β→*O*→7,4β→8)-gallocatechin (ephedrannin D5).

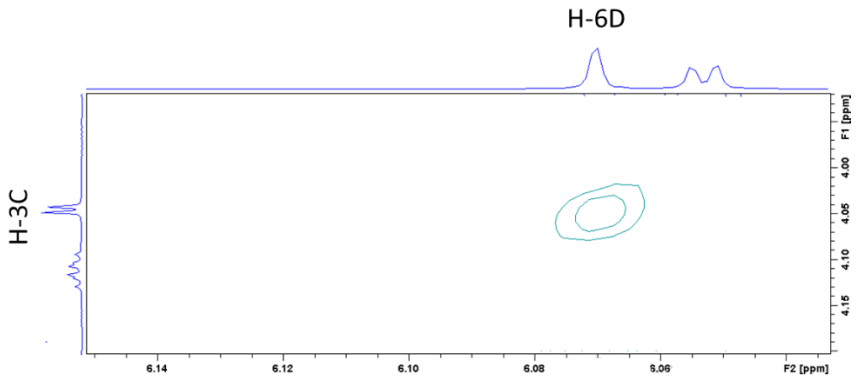

Figure 3.43: Presence of a ROESY correlation between H-3C and H-6D of the compound **6,** indicating the *3,4 trans* configuration of ring C.

Compound **8 (Figure 3.42)** was isolated as an amorphous orange powder, showing optical rotation $[\alpha]_D^{25}$ = +20.5 (c 0.1, MeOH), orange spot on TLC sheet with R_f value ~ 0.8 **(Figure 3.35)** and UV maximum (MeOH) at 275 nm. The recorded NMR data were almost similar to that of compounds **6** and **7** with exception of an extra singlet proton signal at δ_H 6.71 signal integrating for two protons. This signal has a long range HMBC correlation with a carbonyl carbon at δ_C 166.2 indicating that there was a galloyl moiety attached to this compound. In addition to this, HMBC experiments showed a correlation between H-3C (δ_H 5.58 ppm) and the carbonyl carbon at δ_C 166.2 ppm **(Figure 3.44)** providing a proof of galloyl moiety's attachment to the upper unit. The absolute configurations at C-2 and C-4 of ring C of the upper unit were deduced from CD spectrum showing the strong positive cotton effects in the wavelength region between 219 - 258 nm indicating the (2β,4β)-configuration[148–150]. Moreover, there was no ROESY correlation between H-3C (δ_H 5.38 ppm) and H-6D (δ_H 5.94 ppm) of compound **8 (Figure 3.45)**, a diagnostic feature of the *3,4 cis* configuration in the C-ring. From the obtained NMR data of **8 (Table 3.11)** and the CD data, the upper unit was identified as gallocatechin-3-*O*-gallate and the lower unit as gallocatechin. Hence, compound **8** was also based on 2D NMR data identified as gallocatechin-3-*O*-gallate (2β→*O*→7,4β→8)–gallocatechin **(Figure 3.42)**. This was further verified by mass spectrometry data due to exhibited ions at *m/z* 761.1343 $[M+H]^+$ in the positive mode and *m/z* 759.1206 $[M-H]^-$ in the negative mode, calculating for molecular formula of $C_{37}H_{28}O_{18}$. The obtained data of compound **8**, were in agreement with the existing literature of adenodimerin C isolated from *Myrica adenophora*[109].

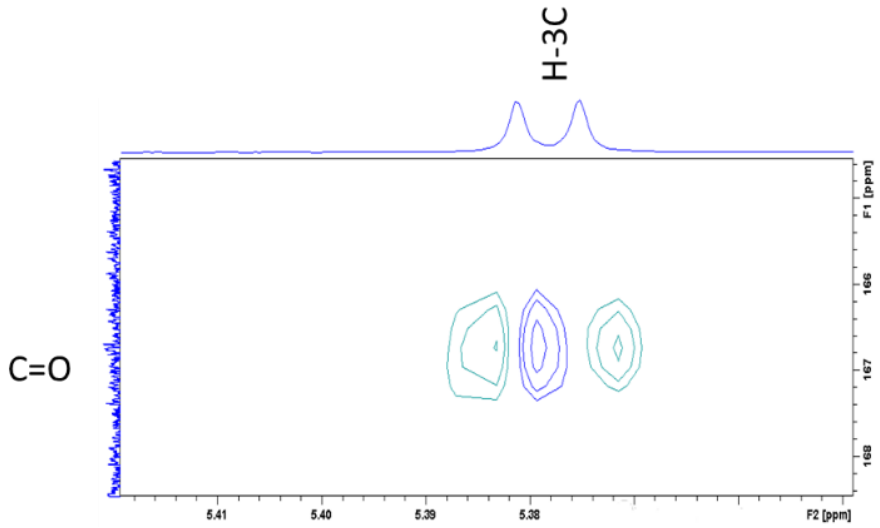

Figure 3.44: Part of HMBC spectrum of compound **8** showing a long range coupling between H-3C (δ_H 5.58) and the carbonyl carbon (δ_C 166.2), a proof of the attachment of the galloyl moiety to the upper unit.

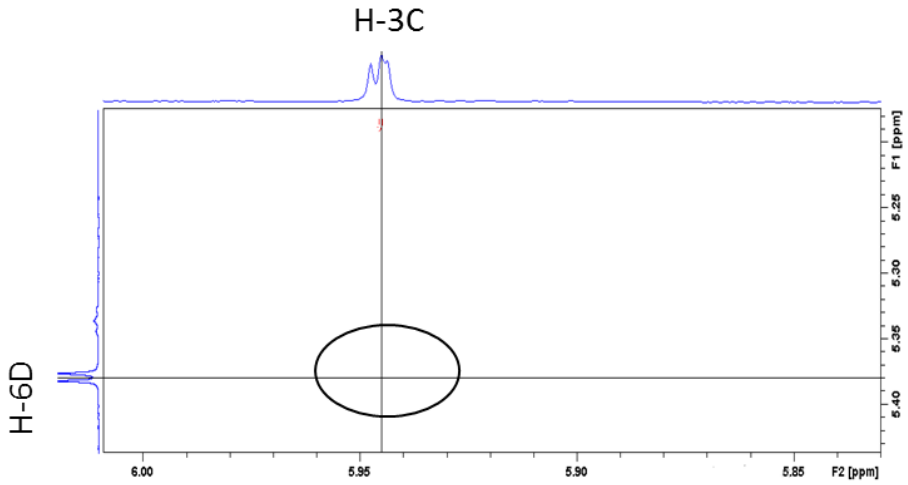

Figure 3.45: Lack of a ROESY correlation between H-3C (δ_H 5.38) and H-6D (δ_H 5.94) of compound **8,** a diagnostic feature of the *3,4 cis* configuration of ring C.

Table 3.11: ^{1}H NMR and ^{13}C NMR of compounds **6** and **8**. ^{1}H NMR (600 MHz), ^{13}C NMR (150 MHz), MeOH-d_4, 278 K.

	6		**8**	
Position	**δ_C (ppm)**	**δ_H (ppm), m, *J* (Hz)**	**δ_C (ppm)**	**δ_H (ppm), m, *J* (Hz)**
Upper				
2C	100.3		99.0	
3C	67.8	4.04, (1H, d, *J* = 3.6)	69.0	5.38, (1H, d, *J* = 3.6)
4C	29.2	4.21, (1H, d, *J* = 3.6)	27.2	4.48, (1H, d, *J* = 3.5)
5A	156.6		154.3	
6A	98.2	5.95, (1H, d, *J* = 2.3)	96.3	6.11, (1H, s)
7A	158.2		158.1	
8A	96.5	6.05, (1H, d, *J* = 2.3)	96.3	6.11, (1H, s)
9A	151.8		152.0	
10A	104.1		104.0	
1’B	131.5		130.4	
2’B	107.5	6.71, (1H, s)	107.2	6.69, (1H, s)
3’B	146.4		146.6	
4’B	134.7		134.8	
5’B	146.4		146.6	
6’B	107.5	6.71, (1H, s)	107.2	6.69, (1H, s)
Lower				
2F	84.7	4.67, (1H, d, *J* = 7.6)	84.4	4.72, (1H, d, *J* = 7.2)
3F	68.1	4.11, (1H, m)	68.2	4.10, (1H, td, *J* = 7.4, 5.5)
4F	28.7	2.91, (1H, dd, *J* = 16.4, 5.5)	28.3	2.88, (1H, dd, *J* = 5.3, 16.4)
		2.56, (1H, dd, *J* = 16.4, 8.1)		2.58, (1H, dd, *J* = 7.8, 16.3)
5D	156.0		156.6	
6D	96.5	6.07, (1H, s)	98.0	5.94, (1H, s)
7D	156.8		158.6	
8D	106.9		105.8	
9D	151.4		151.6	
10D	103.0		103.4	
1’E	130.0		129.3	
2’E	107.8	6.48, (1H, s)	107.6	6.45, (1H, s)
3’E	147.0		146.9	
4’E	134.6		134.4	
5’E	147.0		147.7	
6’E	107.8	6.48, (1H, s)	107.6	6.45, (1H, s)
Galloyl				
1”G			120.8	
2”G			110.3	6.71, (1H, s)
3”G			146.0	
4”G			140.5	
5”G			146.0	
6”G			110.3	6.71, (1H, s)
C=O			166.2	

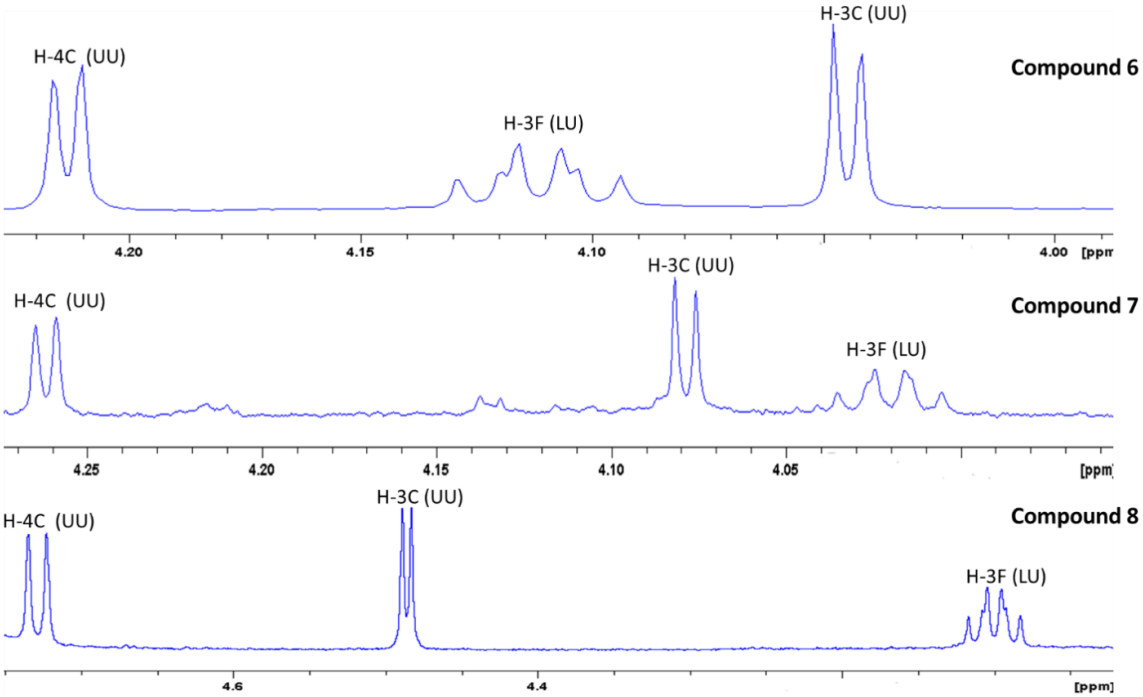

Figure 3.46: Part of the ^{1}H NMR spectra of compounds **6 - 8** showing the positions H-3C, H-4C of the upper unit and H-3F of the lower unit. A preliminary observation of either *3,4 trans* or *3,4 cis* configuration of a ring C of the upper unit. UU = upper unit and LU = lower unit.

3.3.5.1.2 ^{13}C NMR analysis of polymeric PA fraction of *M. salicifolia*

Oligomeric PAs containing more than four flavan-3-ol units are very difficult to isolate and to elucidate. Based on isolation difficulties of the individual oligomeric PA compounds, fractions containing oligomeric and even polymeric PAs were processed by chromatography using Sephadex® LH-20[139,161]. The ^{13}C NMR spectrum of the isolated polymeric fraction was measured and extensively analyzed to determine their composition and to get more structure information. Based on ^{13}C NMR spectra, structural elucidation of oligomeric or polymeric fraction of the PAs can be achieved in dependence of three criteria: the ratio of procyanidin to proanthocyanidin units, the stereochemistry of the heterocyclic ring (*2,3 cis/trans*) of the monomeric units, and the middle length chain weight[139].

The polymeric fraction of *M. salicifolia* bark methanolic extract was analyzed by measuring a long ^{13}C NMR spectrum (2048 scans). The ^{13}C NMR spectrum resonance assignment **(Figure 3.47)** was based on the available literature for isolated PAs polymer fractions[87,139,162–165]. From the ^{13}C NMR spectrum it was observed that the dominant polymeric proanthocyanidins of *M. salicifolia* bark are of the prodelphinidin type due to observed unsubstituted B ring carbon at δ_C

106.7 ppm (C-2', C-6'). There were no detectable signals assigned for procyanidins at the region of 116 - 117 ppm (C-2', C-5'), demonstrating their concentration below detection limit.

The relative amount of *2,3 cis* or *trans* isomer was found to be 36:1 indicating the dominance of *2,3-cis* configuration. The said ratio was attained by integrating the signals of the upper units for the C-2 of *2,3 cis* units observed in the region of 76.8 ppm and very weak signal for C-2 of *2,3 trans* units in the region of δ_C 82.3 ppm.

The estimated average degree of polymerization was obtained to be 16 flavan-3-ols units obtained from the ratio of 15:1 following integration of the C-3 resonances of the extender units at δ_C 73.3 ppm and the resonances of C-3 of terminal units at δ_C 68.3 ppm. Likewise, the same ratio of 15:1 was obtained by integrating C-4 signals of the upper units (δ_C 35.2 – 37.4 ppm) and that of terminal unit (δ_C 29.6 ppm).

Occurrence of the signals at δ_C 110.6, 121.8, 139.7, 146.5 ppm and the carbonyl carbon at δ_C 166.3 ppm was indication of the presence of 3-O-gallate units [87,165] in the polymeric fraction of *M. salicifolia* bark. This was further evidenced by the presence of upfield C-4 (δ_C 35.1 ppm) in addition to the normal C-4 (δ_C 37.4 ppm) of the extender units[165].

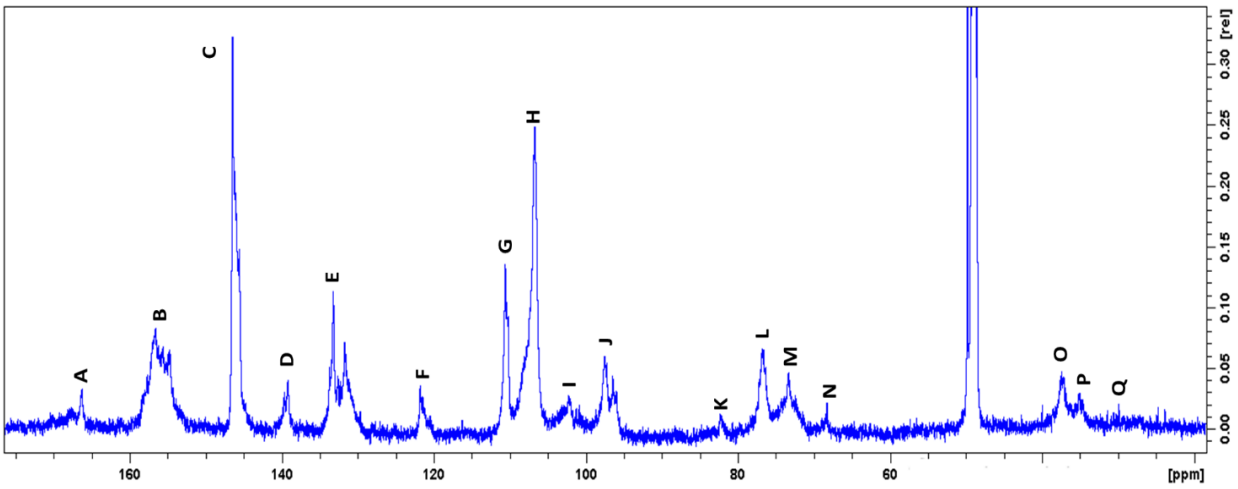

Figure 3.47: ^{13}C NMR spectrum of general features of *Myrica salicifolia* polymeric flavan-3-ol fraction measured at 273 K, 150 MHz, MeOH-d4. **A**: Carbonyl carbon, C=O (166.32 ppm), **B**: Oxygenated A ring carbons, C-5, C-7, C-9 (154.8 – 156.6 ppm), **C**: C-3 and C-5 of the B ring (145.6 – 146.5 ppm), **D**: C-4 of the galloyl ring (139.2 - 139.7 ppm), **E**: C-1 and C-4 of B ring (131.7 – 133.7 ppm), **F**: C-1 of the galloyl ring (121.8 ppm), **G**: Unsubstituted gallate carbons (110.6 ppm), **H**: Unsubstituted B-ring carbon (106.7 ppm), **I**: C-2 of the C ring for A type prodelphinidins (100.9 ppm), **J**: Unsubstituted A-ring carbons (96.5 -97.5 ppm), **K**: C-2 of prodelphinidin units, 2,3- trans configured units (82.3 ppm), **L**: C-2 of 2,3-cis configured units (76.8 ppm), **M**: C-3 of all extender units (73.4 ppm), **N**: C-3 of terminal units (68.3 ppm), **O** and **P:** C-4 of the extender units with and without gallate substituent (35.1 -37.4 ppm), **Q:** C-4 of terminal units (29.6 ppm).

3.3.5.1.3 Ellagitannin

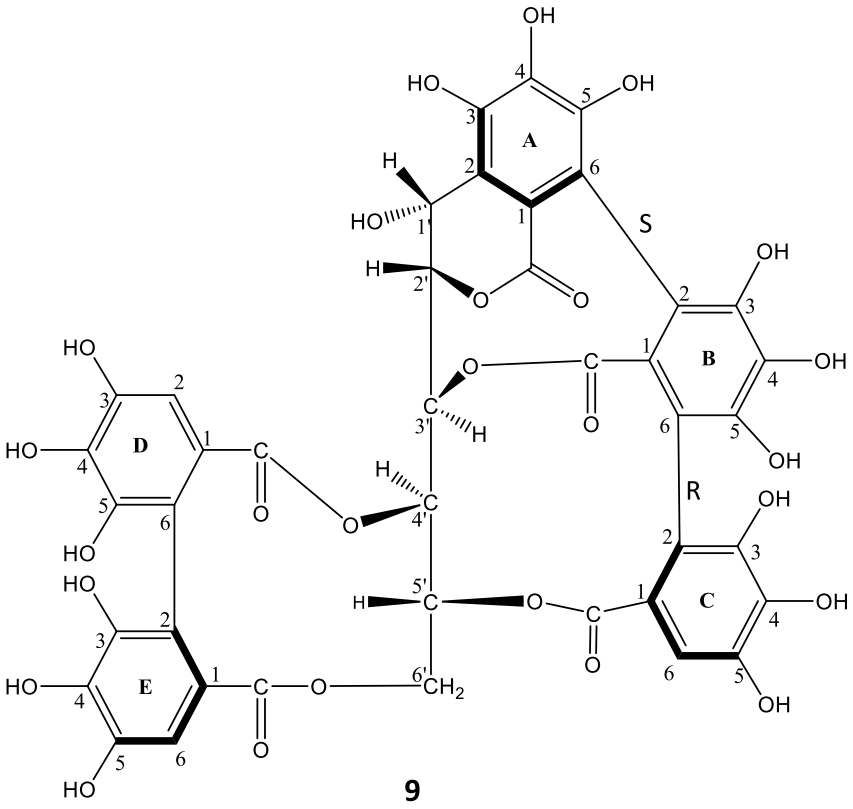

Figure 3.48: Structure of castalagin **(9)**.

Compound **9** was isolated from fraction S5 **(Figure 3.25)** as an off-white amorphous powder with the optical rotation value $[\alpha]_D^{25}$ = +15.6 (0.1, MeOH), thereafter identified as castalagin (an ellagitannin) by comparing obtained 1 and 2D NMR spectral data with existing literature data[87,166,167].

From the ^{1}H NMR spectrum, three singlets signals at δ_H 7.13, 6.78 and 6.60 ppm in aromatic region were observed, each integrating for one proton. These protons were assigned as two protons (δ_H 7.13 and 6.60 ppm) for biphenyl group and one proton (δ_H 6.78 ppm) for triphenoyl group. The carbonyl carbon signals at δ_C 163.2, 166.5, 166.3, 166.5 and 165.9 ppm observed in the long range heteronuclear correlation HMBC between the three aromatic and the glucose protons evidently show the presence of five ester linkages.

The cross signal was observed in the heteronuclear experiment HSQC between the anomeric proton at δ_H 5.70 ppm and carbon at δ_C 67.0 ppm and not in the downfield at δ_C ~ 100 ppm. The presence of the hemiacetal carbon at δ_C 67.0 ppm signifies that the glucose moiety is present in

an open chain. Furthermore, the open chain glucose moiety was deduced with aid of the proton coupling networks from COSY experiment. The obtained coupling constant of $^{3}J_{1,2}$ = 4.6 Hz is the characteristic which led to confirmation of castalagin in comparison to its epimer which has $^{3}J_{1,2} < 2$[166].

Attachment of one ring of the nonahydroxytriphenoyl group to C-1' of the glucose moiety through a C-C bond was observed in the long range correlation HMBC spectrum between H-1' at δ_H 5.70 ppm and and four aromatic carbons at δ_C 115.0 ppm (C-1A), 104.1 ppm (C-2A/6A), 133.2 ppm (C-4A) and 142.6 ppm (C-3A). The ^{1}H and ^{13}C NMR data of this compound are summarized in the **Table 3.12**.

Further confirmation of castalagin was deduced by mass spectrometry data. The molecular mass of **9** was exhibited by ESI-MS ions at *m/z* 933.08 $[M-H]^-$ in the negative mode, calculated for 934 Da which adheres to the molecular formula of $C_{41}H_{26}O_{26}$.

The CD spectrum exhibited positive cotton effects in the wavelength 233 and 289 nm and negative cotton effects at 213 and 260 nm. The obtained CD data are in accordance with the literature data by Matsuo et al.[168], which reports positive cotton effects in the wavelengths 240 and 295 nm and negative cotton effects at 218 and 263 nm, confirming the *S,R*-configuration of the triphenoyl moiety **(Figure 3.48)**.

Table 3.12: ^{1}H and ^{13}C NMR data for compound **9** ^{1}H NMR (600 MHz), ^{13}C NMR (150 MHz), acetone-d_6, 278 K.

Position	**δ_C (ppm)**	**δ_H (ppm), m, *J* (Hz)**
1E	114.2	
2E	107.3	
3E	144.4	
4E	135.8	
5E	144.4	
6E	107.3	6.60, (1H, s)
E (C=0)	165.9	
1D	114.3	
2D	108.2	7.13, (1H, s)
3D	145.1	
4D	136.0	
5D	145.1	
6D	108.2	
D(C=0)	166.5	
1C	114.2	
2C	108.6	
3C	144.5	
4C	136.0	
5C	144.5	
6C	108.6	6.78, (1H, s)
C (C=0)	166.3	
1B	110.5	
2B	108.6	
3B	144.5	
4B	136.0	
5B	144.5	
6B	108.6	
B (C=0)	166.5	
1A	115.0	
2A	104.1	
3A	142.6	
4A	133.2	
5A	142.6	
6A	104.1	
A (C=0)	163.2	
Sugar		
1’	67.0	5.70, (1H, d, *J* = 4.6)
2’	74.0	4.96, (1H, dd, *J* = 1.4, 4.6)
3‘	66.2	4.99, (1H, dd, *J* = 1.1, 7.0)
4‘	69.3	5.25, (1H, t, *J* = 7.1)
5‘	70.9	5.61, (1H, brd)
6’a	65.0	5.12, (1H, dd, *J* = 2.6, 12.9)
6’b	65.0	3.99, (1H, d, *J* = 12.8)

3.3.5.2 Cyclic diarylheptanoids

Cyclic diarylheptanoids were isolated following further fractionation of S2 subfractions as indicated in **Figure 3.34**. A total of 17 cyclic diarylheptanoids belonging to the subgroup of meta-meta cyclophanes were isolated and their structures elucidated to complete stereochemistry. Among the isolated diarylheptanoids, 3 compounds were aglycones, 6 were monoglycosides, 3 were galloyl-glycosides and 5 were diglycosides.

The TLC overview of the isolated diarylheptanoids is given in **Figure 3.49**. From the TLC it was discovered that all isolated cyclic diarylheptanoids which contain carbonyl group (C=O) at position C-11 changed to yellow-brownish colour after derivatization with anisaldehyde-sulphuric acid reagent followed by plate heating at 100 ^{o}C for 3 min. The yellow-brownish colour was visualized at day light. Additionally, a fluorescent yellow-brownish colour was observed under UV 366 nm. No detection was possible prior to derivatization with anisaldehyde-sulphuric acid reagent at 366 nm and daylight. In addition to that, blue to deep purple blue colour was detected for the isolated diarylheptanoids which contain either an OH group or a sugar moiety at position C-11.

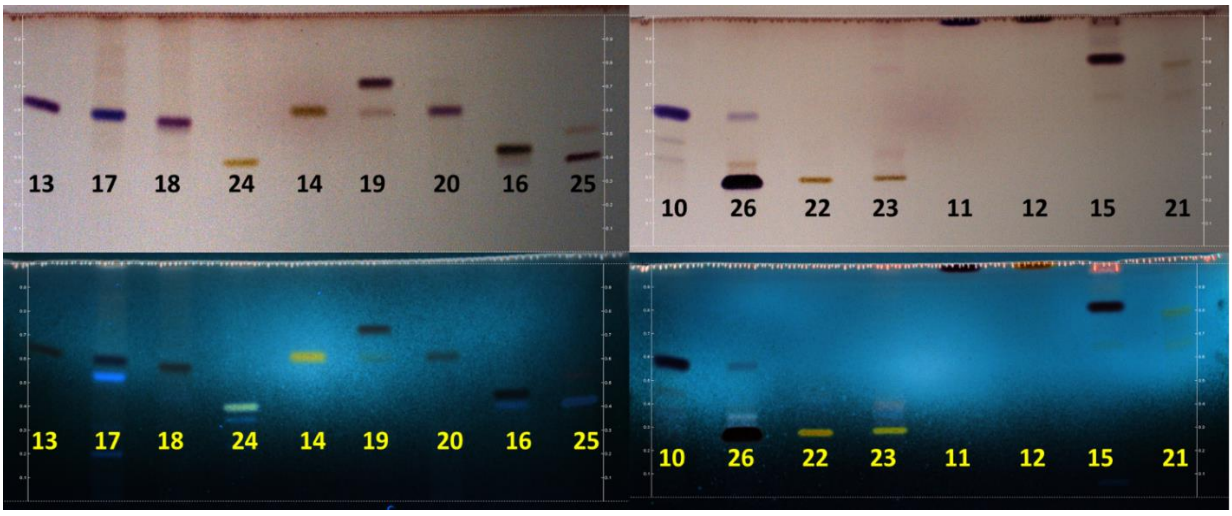

Figure 3.49: TLC overview (NP-TLC) of the isolated cyclic diarylheptanoid compounds **10 - 26.** Mobile phase MP_1. Detection: VIS **(upper**) and UV 366 nm (**lower**). Spray reagent: anisaldehyde-sulphuric acid.

3.3.5.2.1 Determination of absolute configuration of isolated cyclic diarylheptanoids

The isolated cyclic diarylheptanoids were categorized in two groups: those without sugar substitution, such as compound **10**, **11** and **12**, and those with sugar substitution (mono- and di-glycosides), which comprised the rest of the isolated cyclic diarylheptanoids. Therefore, determination of the absolute configuration of the two identified groups was done for complete provision of their full stereochemistry.

Confirmation of the glycoside type and its absolute configuration

Compounds identified to contain glycoside substitution were subjected to confirmation and determination of the absolute configuration of the particular glycoside by recording ^{1}H NMR spectra of their per-*O*-(*S*)-2-methylbutyrate derivative (SMB) in comparison to ^{1}H NMR of the SMB derivatives of reference sugars as described in the material and methods section **3.2.8.6**[140]. The reference sugars used in this study were: D- and L-glucose, D- and L-arabinose and D- and L-xylose. The recorded ^{1}H NMR spectra of the SMB references (D and L) were overlaid to observe their differences as indicated in **Figure 3.50**. The overlaid spectra of the D- and L SMB derivatives of sugars provide a clear significant difference between the two through their small chemical shift differences. Therefore, this technique proved that the diastereomeric SMB derivatives of D- and L-monosaccharides can be distinguished and the spectra of the SMB derivatives of their mixture can be clearly analysed [140].

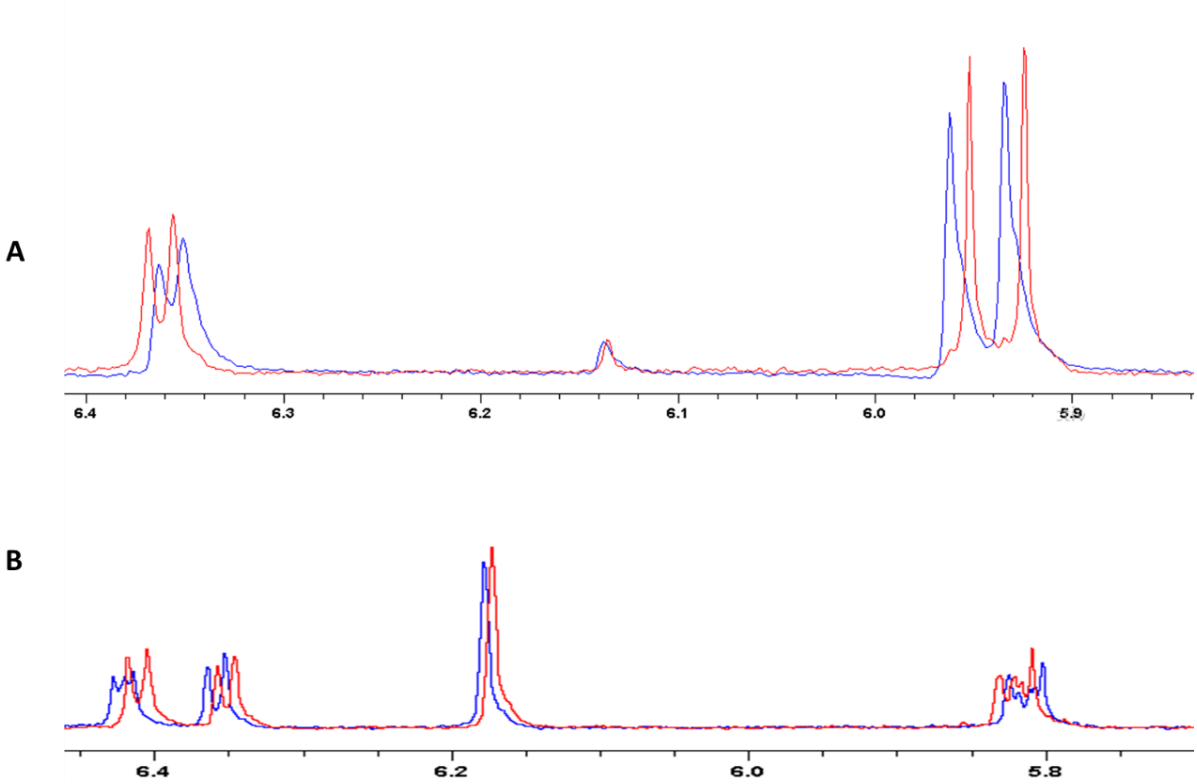

Figure 3.50: Part of overlaid ^{1}H NMR spectra (300 MHz, acetone-d_6, 298 K) of the D- and L-SMB derivatives of reference sugars showing a clear significant difference between the two through their small chemical shift differences. **A:** D- and L-glucose**. B:** D- and L-arabinose esters**.**

In the first step, absolute configuration of the glycoside moiety of the particular compound was confirmed by overlaying ^{1}H NMR spectra of SMB derivatives of particular compound to that of reference monosaccharides **(Figure 3.51 – 3.53)**. When the two spectra were superimposable then the second step was comparison of their chemical shifts (ppm) and coupling constants (*J* (Hz)) of anomeric proton resonances **(Table 3.13)**. Anomeric proton resonances of the SMB derivatives were identified by their characteristic downfield shifts and coupling patterns[140].

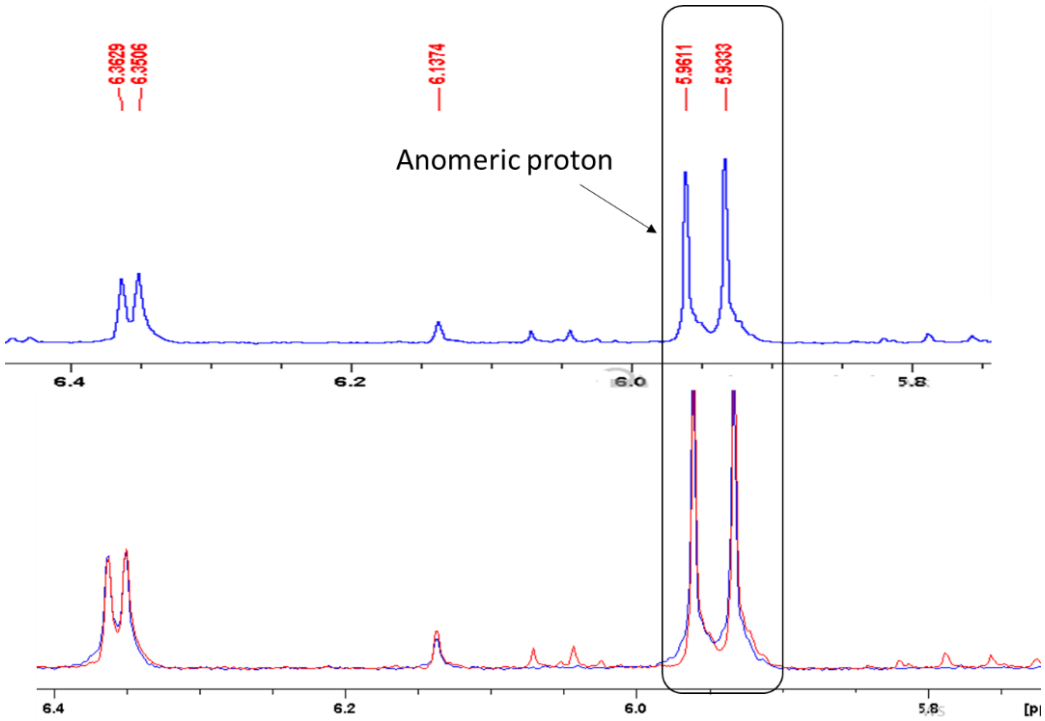

Figure 3.51: Part of ^{1}H NMR spectrum (300 MHz, acetone-d_6, 298 K) of the SMB derivative of compound **13 (top)** and overlaid spectra of SMB derivatives of **13 (blue - down)** and SMB derivative of D-glucose **(red - down)**. Representative example of how absolute configuration of D-glucose substitution was attained in all isolated compounds containing D-glucose i.e. mono- and di-glucoside substitution.

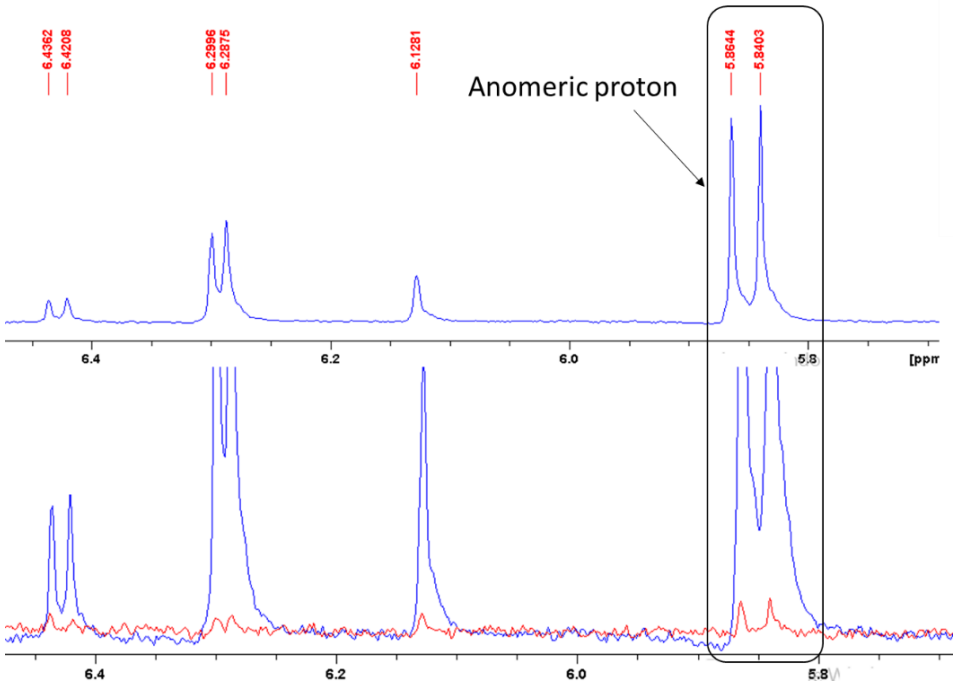

Figure 3.52: Part of ^{1}H NMR spectrum (300 MHz, acetone-d_6, 298 K) of the SMB derivative of compound **15 (top)** and overlaid spectra of SMB derivative of **15 (red - down)** and SMB derivative of D-xylose **(blue - down).** Representative example of how absolute configuration of D-xylose substitution was attained in all isolated compounds containing D-xylose.

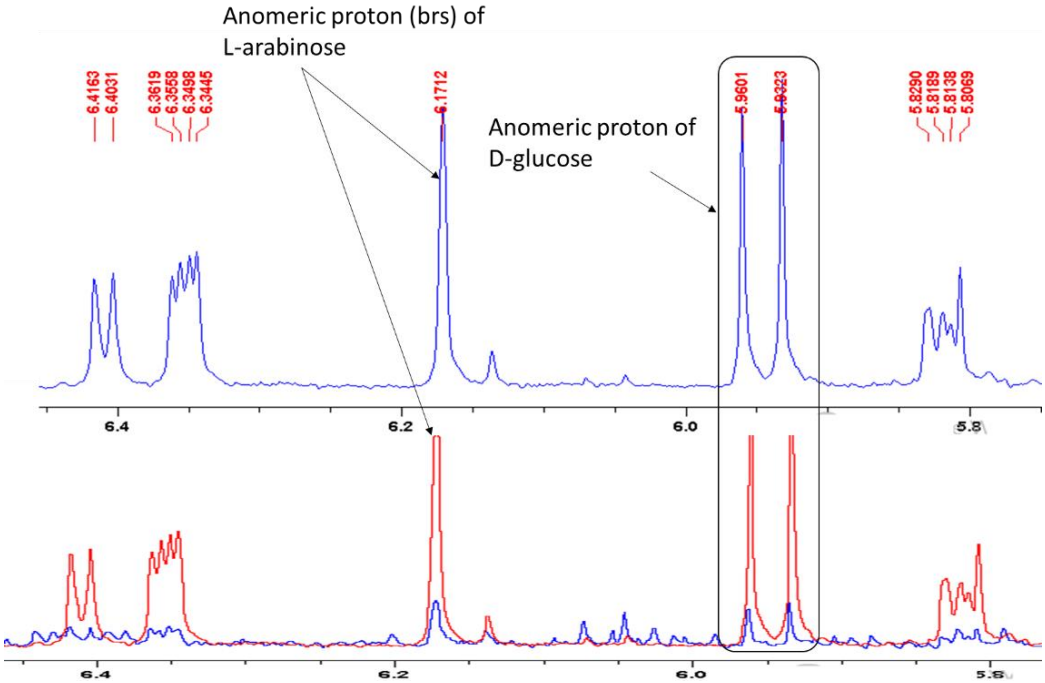

Figure 3.53: Part of ^{1}H NMR spectrum (330 MHz, acetone-d_6, 298 K) of the SMB derivative of compound **25 (top)** and overlaid spectra of SMB derivative of **25 (blue - down)** and SMB derivative of the mixture of D-glucose and L-arabinose **(red - down)**. Demonstration of how the absolute configuration of sugar substitution was accomplished in compounds **25** and **24.**

Table 3.13: Representative data showing comparison of anomeric SMB derivative proton resonances of isolated compounds and the reference monosaccharides.

Representative compounds	**Sugar geometry**	**Configuration at position 1 and 2**	**Compound - SMB derivative**		**Reference sugar - SMB derivative**	
			δ_H (ppm)	**$^3J_{1,2}$ (Hz)**	**δ_H (ppm)**	**$^3J_{1,2}$ (Hz)**
14, **19**, **22**, **17**, **18**, **30** and **31**	β-D-glucose (*pyranose)*	1*S*, 2*R*	5.94	8.3	5.94	8.3
15, **27** and **29**	β-D-xylose (*pyranose*)	1*S*, 2*R*	5.85	7.2	5.85	7.2
24 and **25**	α-L-arabinose (*furanose*)	1*S*, 2*R*	6.17	brs	6.17	brs

Absolute configuration of myricanol and other isolated diarylheptanoids

The absolute configuration of isolated cyclic diarylheptanoids was achieved through electronic CD spectra simulation as described in the materials and method section **3.2.8.8**. Recorded experimental CD spectra of the isolated diarylheptanoids and the aglycone obtained from enzyme hydrolysis of myricanol 5-*O*-β-D glucose **(13)** are shown in **Figure 3.54**. Similarity of the CD spectra graph was observed on graph **1-12**, hence concluding that the attached sugar and sulphate moieties had no influence on the conformation of the aglycone and its chromophore.

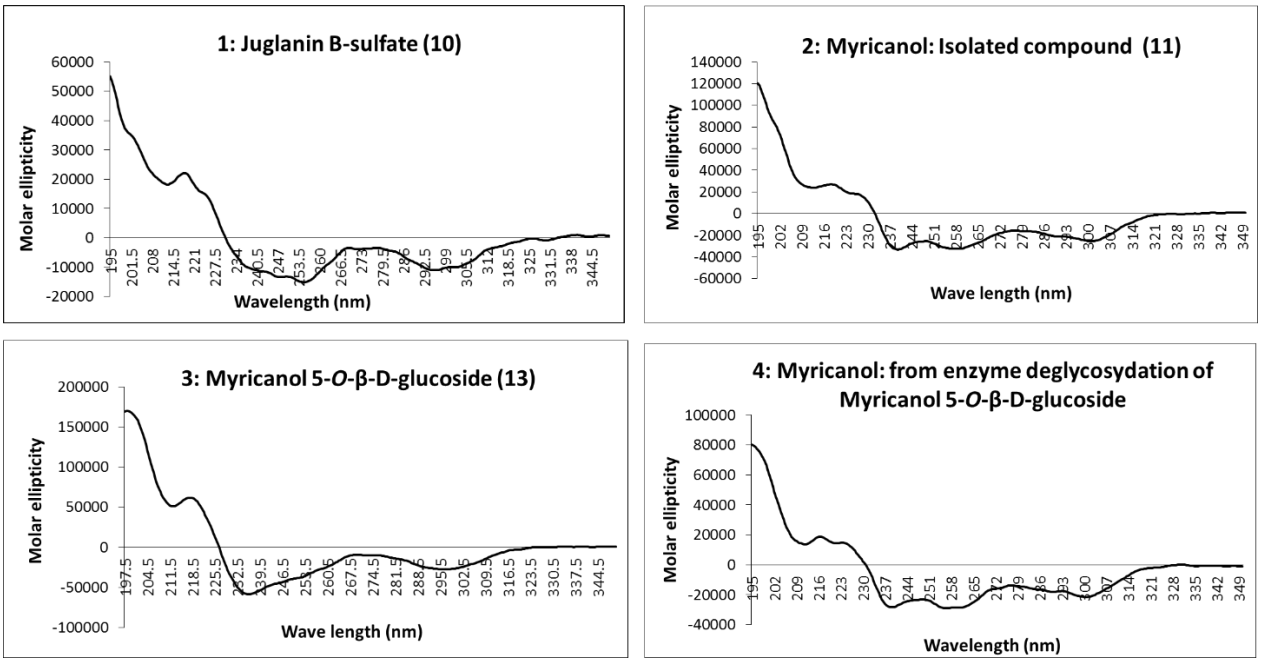

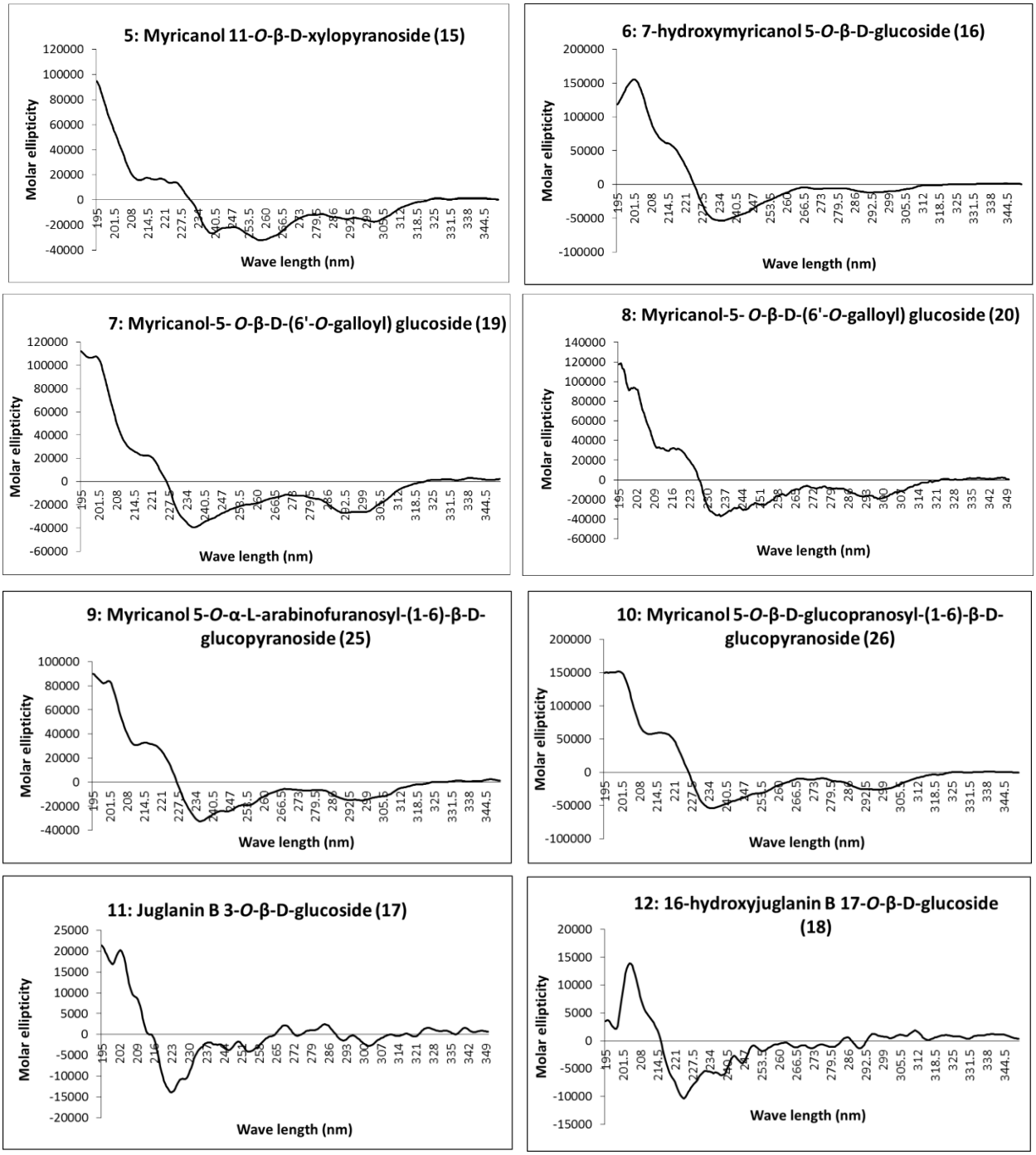

Figure 3.54: Recorded experimental CD spectra of isolated diarylheptanoids (molar ellipticity vs. wavelength (nm).

Myricanol structure contains one chiral centre at position 11 which is axially dissymmetric due to the twisted biphenyl. Therefore, the structure of myricanol can occur as two pairs of enantiomers i.e. (*R,Ra*), (*S,Sa*) and (*R,Sa*), (*S,Ra*), where "a" stands for the chirality of the axially dissymmetric biphenylic-system[169,170]. Generated molecular models of the *R*-enantiomer

of myricanol resulted in three conformations corresponding to the 11*R,Ra* and the 11*R,Sa* (a) and 11*R,Sa* (b) forms as described in the material and methods section **3.2.8.8 (Figure 3.55 A-C)**. The 11*R,Sa* (b) conformation corresponds to the X-ray structure determined by Begley et al.[141].

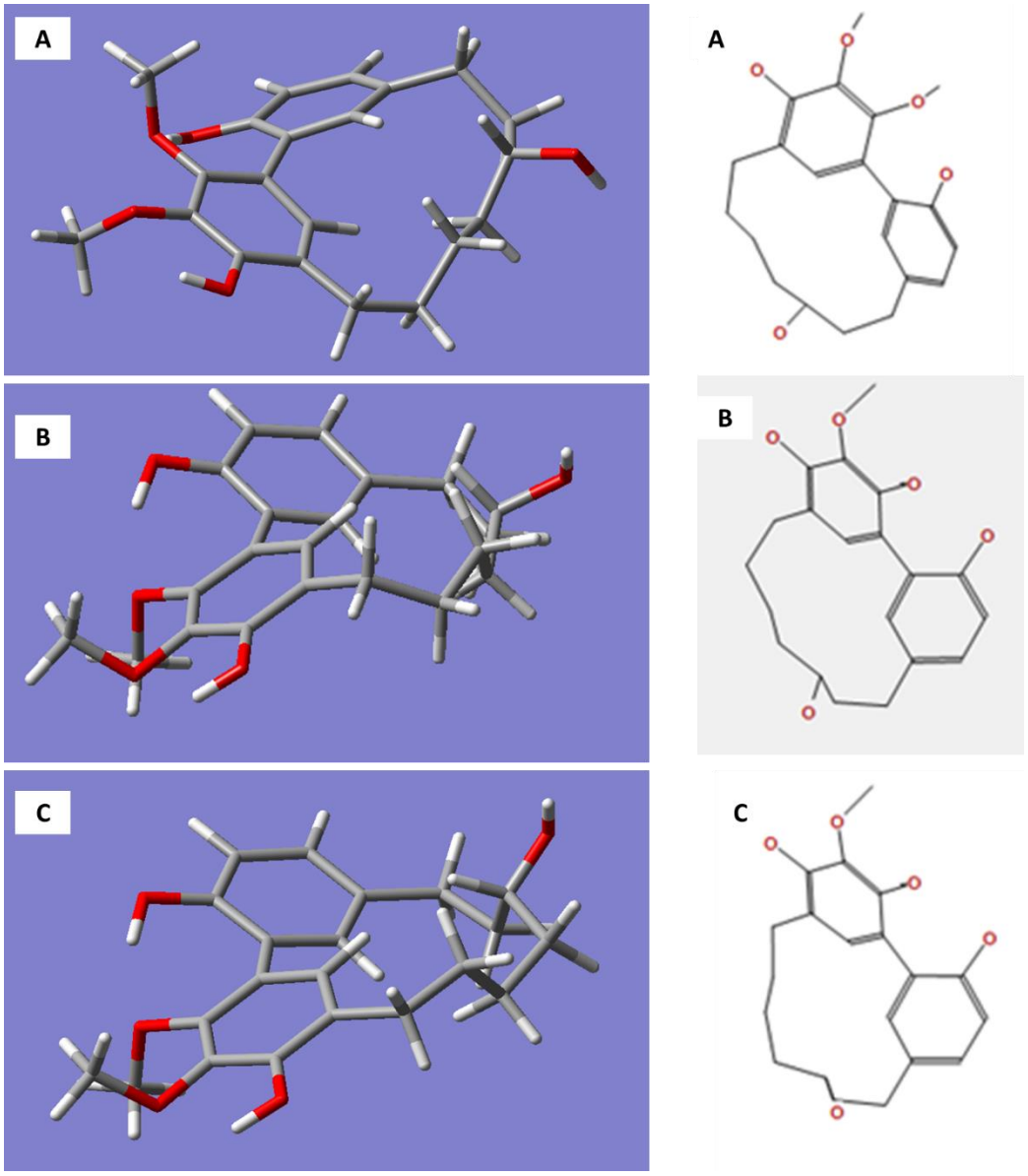

Figure 3.55: 3D-structures of the conformations of *R*-myricanol. **A:** 11*R,Ra* myricanol. RB3LYP/6-31G(d,p) Energy: -1192.01521911 a.u. Energy difference from lowest conformer: 2.01 kcal/mol. **B:** 11*R,Sa* myricanol **(a)**. RB3LYP/6-31G(d,p) Energy: -1192.01342066 a.u. Energy difference from lowest conformer: 3.31 kcal/mol. **C:** 11*R,Sa* myricanol **(b)**. Conformation corresponds to the X-ray cystal structure[141]. RB3LYP/6-31G(d,p) Energy: -1192.01842217 a.u.Energy difference from lowest conformer: 0.000 kcal/mol. With kind permission from Prof. T. Schmidt (Universität Münster).

The simulated CD spectrum of the energetically most favourable 11*R,Sa*-myricanol (conformer C, **Figure 3.55 C**) was found to be similar to the experimentally determined spectrum **(Figure 3.56 C)**. The major cotton effects are of equal sign indicating that the compound has indeed the 11*R*,*Sa*-configuration, as would also be expected based on its reported crystal structure. The spectrum would appear exactly opposite if the 11*S*,*Ra*-enantiomer were present.

The spectrum for the less favourable 11*R*,*Ra*-atropisomer (conformer 1, **Figure 3.55 A**) shows almost entirely opposite sign **(Figure 3.56 A)**. Since its internal energy is predicted to be more than 2 kcal/mol, it was neglected. The two conformers (2 and 3, **Figure 3.55 B and C**) show similar signs with experimental spectrum **(Figure 3.56 B** and **C)** which gives a hint to confirmation of 11*R,Sa*-configuration. Additionally, an averaged spectrum generated for the theoretical equilibrium mixture corresponding to 97% *R,Sa* and 3% *R,Ra*-myricanol was compared with the experimental CD spectrum of myricanol **(Figure 3.56 D)**. The results presenting a very good match with the experimental spectrum. According to these calculations, natural myricanol was concluded to be 11*R* and very predominantly *Sa*-configured. This corresponds to the X-ray structure and matches the CD data of myricanol reported in literature[131,141]. It is possible that a very small amount of the *Ra*-atropisomer is present in the conformational equilibrium.

In another case, the experimental CD spectrum showed a good match with the calculated CD spectrum of the *S,Sa*- enantiomer (averaged CD spectrum of *S,Sa* (87%) and *S,Ra* form (13%)) as shown in **Figure 3.56 E**. This was not concluded to be the absolute configuration of the natural myricanol due to its much higher energy content which is identical to that of conformer 1.

A slight inconsistency which was observed in the 230 nm range **(Figure 3.56, B - D)**, can be explained by an exchange of two electronic transitions very close to each other, at 217 and 223 nm. However, this does not change the general picture of the main bands at long and short wavelength being of the same sign.

Finally, a confirmation of the 11*R*-configuration to the isolated diarylheptanoids demonstrated the same experimental CD spectra **(Figure 3.54, 1 – 12)** as to that of myricanol was established**.**

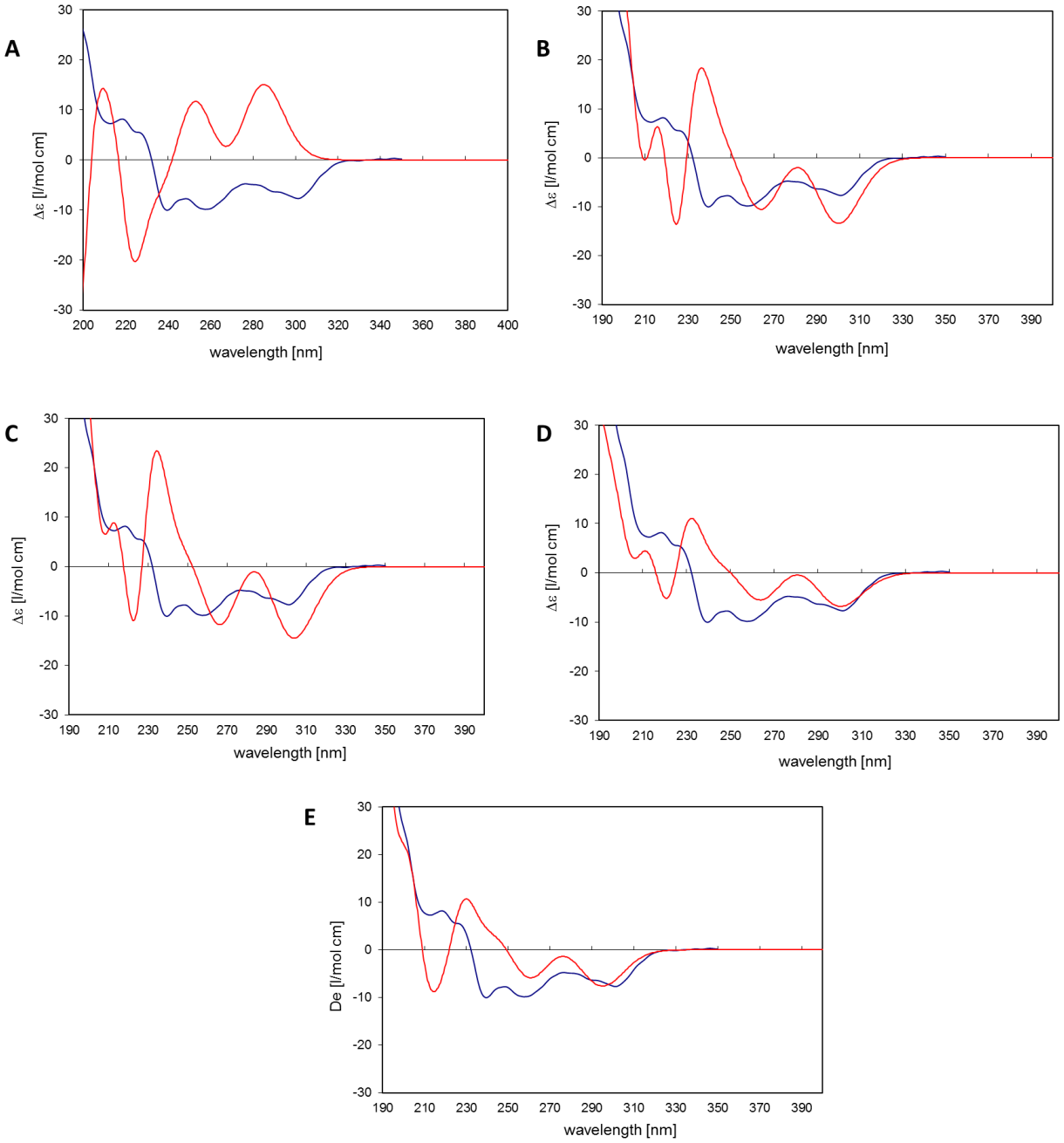

Figure 3.56: A: Conformer 1: 11*R,Ra* myricanol. Blue: Experimental CD spectrum of myricanol. **Red:** CD spectrum simulated for conformer 1 by TDDFT: RB3LYP/6-31G(d,p), nstates=30. No shift, no scaling of calculated spectrum. **B: Conformer 2: 11*R,Sa*-myricanol (a). Blue:** Experimental CD spectrum of myricanol. **Red:** CD spectrum simulated for conformer 2 by TDDFT: RB3LYP/6-31G(d,p), nstates=30 No shift, no scaling of calculated spectrum. **C: Conformer 3: 11*R,Sa*-myricanol (b),** conformation corresponds to the X-ray structure**. Blue:** Experimental CD spectrum of myricanol. **Red:** CD spectrum simulated for conformer 3 by TDDFT: RB3LYP/6-31G(d,p), nstates=30 No shift, no scaling of calculated spectrum. **D: Blue:** Experimental CD spectrum of myricanol. **Red**: Averaged CD spectrum for the ***R,Sa* (97%)** and ***R,Ra* form (3%).** TDDFT: RB3LYP/6-31G(d,p), nstates=30. Calculated spectrum was red-shifted by -0.15 eV and scaled by factor 0.5. **E: Blue:** Experimental CD spectrum of myricanol. **Red:** Averaged CD spectrum for the *S,Sa* (87%) and *S,Ra* form (13%). TDDFT: RB3LYP/6-31G(d,p), nstates=30. Calculated spectrum was red-shifted by -0.15 eV and scaled by factor 0.67. With kind permission from Prof. T. Schmidt (Universität Münster).

3.3.5.2.2 Cyclic diarylheptanoids without glycoside moiety

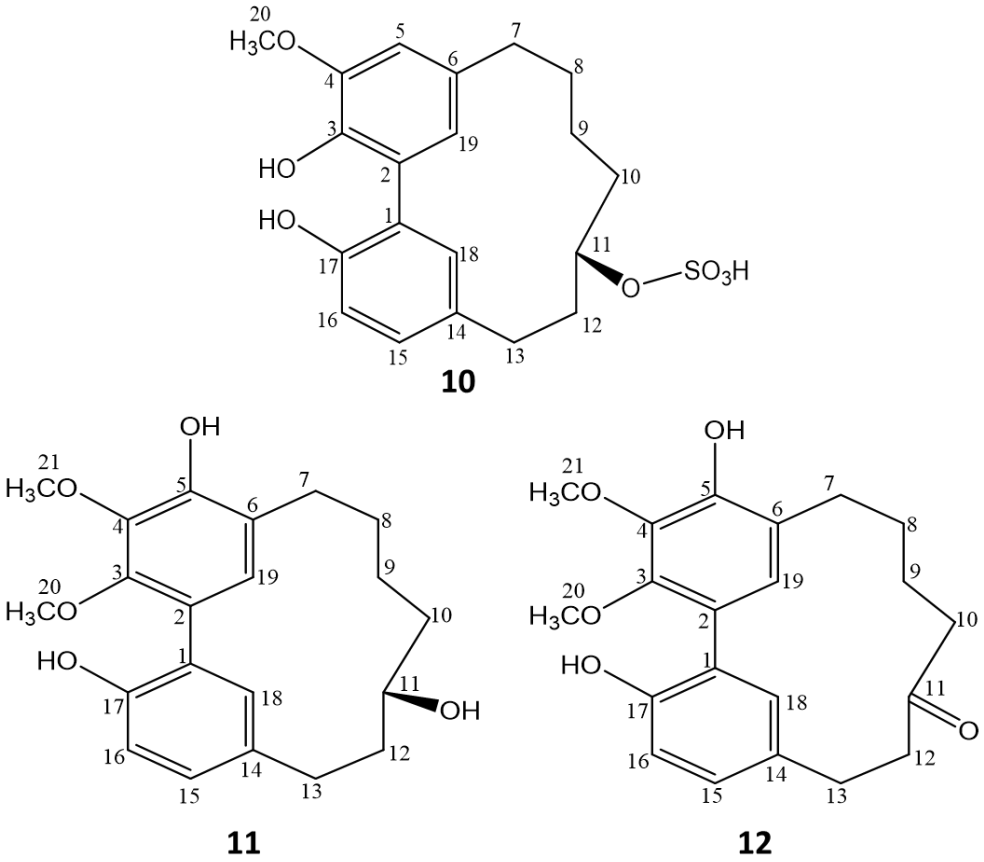

Figure 3.59: Structures of juglanin B-sulphate **(10),** myricanol **(11)** and myricanone **(12)**.

Compounds **10**, **11** and **12 (Figure 3.59)** were isolated from S2 subfractions F5C7 and F6.3 as illustrated in **Figure 3.34.** Compounds **10** and **12** were isolated as off-white amorphous powder while **11** was a white amorphous powder. The optical rotations values of **10** and **11** were $[\alpha]_D^{25}$ = -12.5 (c 0.1, MeOH) and $[\alpha]_D^{25}$ = -76.5 (c 0.1, MeOH) respectively. They exhibit UV maxima (MeOH) at 254 and 300 nm (**10**), 260 and 298 nm (**11**) and 260 and 300 nm (**12**). The three compounds were identified following comparison of obtained 1D and 2D NMR data with the available literature data of these compounds, as juglanin B-sulphate (**10**)[110,112], myricanol (**11**)[87,119,141,169] and myricanone (**12**)[87,141]. The ^{1}H and ^{13}C NMR data of these compounds are summarized in **Table 3.14**.

It was observed from ^{13}C NMR spectrum that compounds **11** and **12** possess similar carbon chemical shifts in the aromatic region and both contain two methoxy groups assigned to

position 20 and 21. The difference was observed in their six methylenes carbons shifts at position 7, 8, 9, 10, 12 and 13 which could be attributed by the change of attachment of oxygen bearing methine (δ_H 3.96 ppm) at position 11 of compound **10** to carbonyl carbon (δ_C 212.9 ppm) of compound **12**.

The chemical shifts and coupling patterns observed in NMR spectra of **10** were comparable to that of **11**. The difference between the two compounds was one extra proton singlet observed at δ_H 6.71 ppm which was assigned to position 5 and only one methoxy proton assigned to position 20 was observed at δ_H 3.86 ppm. A downfield shift of $+\delta_H$ 0.85 ppm for the proton and $+\delta_C$ 10.8 ppm for the carbon at position 11 compared to compound **11** was observed. The changes in chemical shifts gave an alert that the group attached to position 11 is a substituent which could not be detected from the NMR spectra. HRESI-MS concluded the presence of sulphate group by exhibiting ions at *m/z* 407.1174 $[M-H]^-$ in the negative mode calculated for molecular formula of $C_{20}H_{24}O_7S$. Likewise, the molecular masses for compound **11** and **12** were calculated to be 358 Da and 356 Da following the ESI-MS ions exhibited at *m/z* 357.17 $[M-H]^-$ and at *m/z* 355.15 $[M-H]^-$ in the negative mode respectively. Their molecular formula were deduced to be $C_{21}H_{26}O_5$ (**11**) and $C_{21}H_{24}O_5$ (**12**) respectively. For determination of absolute configuration of **10** and **11** see section **3.3.5.2.1**.

Table 3.14: ^{1}H and ^{13}C NMR data for compounds **10 –12**. ^{1}H NMR (600 MHz), ^{13}C NMR (150 MHz), MeOH-d_4, 298 K.

Pos.	10		11		12	
	δ_C (ppm)	δ_H (ppm), m, *J* (Hz)	δ_C (ppm)	δ_H (ppm), m, *J* (Hz)	δ_C (ppm)	δ_H (ppm), m, *J* (Hz)
1	129.0		125.8		126.4	
2	127.5		123.5		123.3	
3	143.6		147.6		147.8	
4	149.9		140.3		140.4	
5	112.1	6.71, (1H, brs)	149.7		149.9	
6	130.8		123.9		124.2	
7	31.6	2.95-2.92, (1H, m) 2.51-2.46, (1H, m)	26.3	2.76–2.72, (1H, m) 2.53–2.48, (1H, m)	27.5	2.67, (2H, m)
8	27.1	2.29-2.19, (1H, m) 1.80-1.77, (1H, m)	26.5	1.94–1.85, (2H, m)	25.2	1.92, (2H, m)
9	24.2	1.80-1.77, (1H, m) 1.51-1.47, (1H, m)	23.8	1.68–1.61, (1H, m) 1.51–1.44, (1H, m)	22.8	1.77, (2H, m)
10	34.6	2.29-2.19, (1H, m). 1.92–1.87, (1H, m)	40.4	1.83–1.78, (1H, m) 1.57–1.53, (1H, m)	45.7	2.74, (2H, m)
11	78.9	4.81, (1H, m)	68.1	3.96, (1H, t, *J* = 9.8)	212.9	
12	37.6	2.14-2.10, (1H, m) 1.86-1.82, (1H, m)	35.4	2.29–2.24, (1H, m) 1.68–1.61, (1H, m)	42.6	2.82, (2H, m)
13	27.8	3.08-3.03, (1H, m 2.78–2.75, (1H, m)	27.6	2.94–2.88, (1H, m) 2.83–2.79, (1H, m)	28.9	2.93, (2H, m)
14	132.3		131.6		133.1	
15	130.3	6.99, (1H, brd, *J* = 7.3)	130.3	7.02, (1H, dd, *J* = 2.3, 8.2)	129.4	7.02, (1H, dd, *J* = 8.1, 2.4)
16	117.3	6.74, (1H, d, *J* = 8.1)	117.2	6.78, (1H, d, *J* = 8.2)	117.2	6.76, (1H, d, *J* = 8.1)
17	152.9		152.3		152.7	
18	134.1	7.21, (1H, s).	134.1	7.19, (1H, brs)	133.3	6.74, (1H, d, *J* = 2.2)
19	126.9	6.89, (1H, brs)	129.9	6.88, (1H, s)	129.4	6.58, (1H, s)
20	56.7	3.86, (3H, s)	61.6	3.86, (3H, s)	61.6	3.81, (3H, s)
21			61.4	3.89, (3H, s)	61.4	3.88, (3H, s)

3.3.5.2.3 Cyclic diarylheptanoid monoglycosides

Compounds 13, 14 and 15

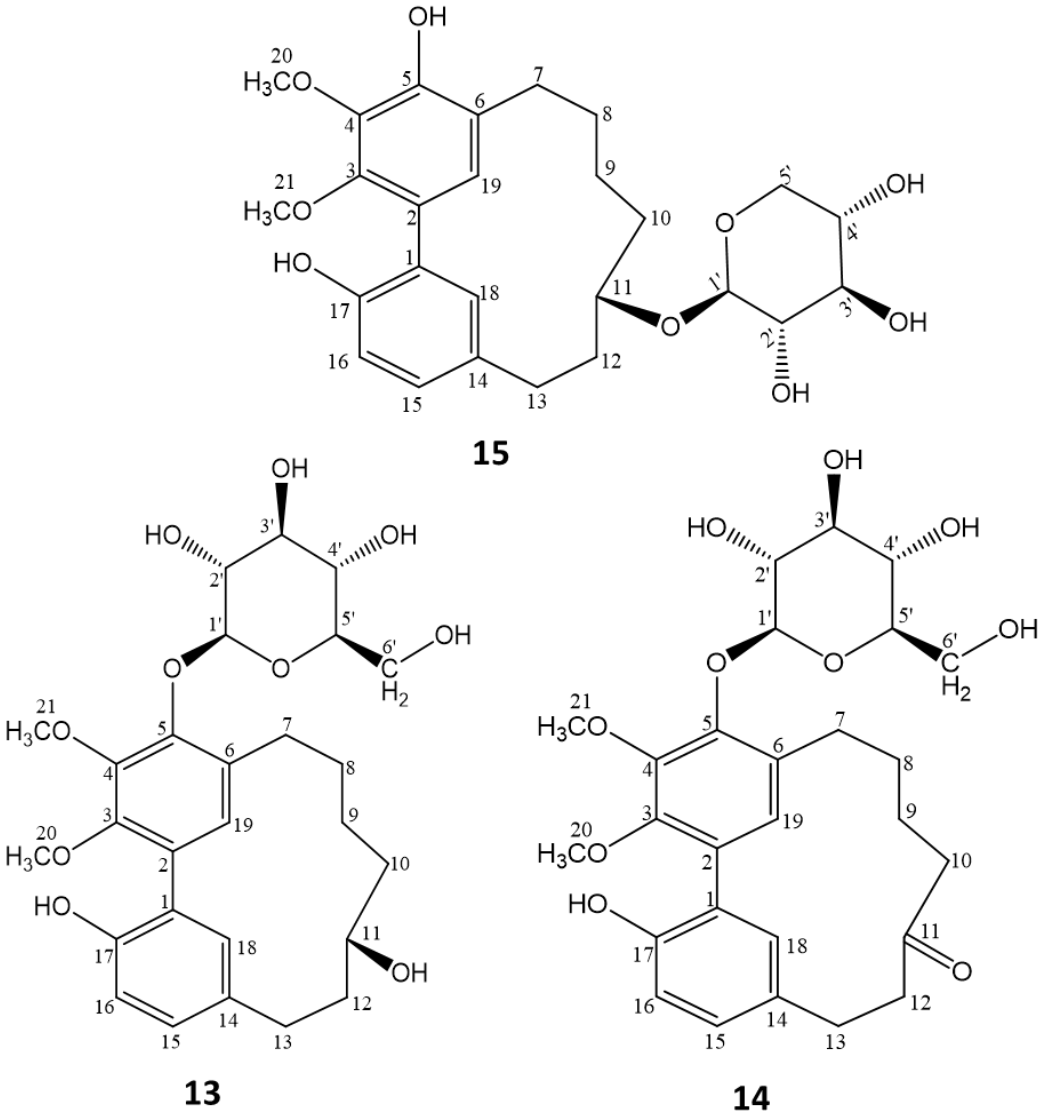

Figure 3.60: Structures of myricanol 5-*O*-β-D-glucoside **(13)**, myricanone 5-*O*-β-D-glucoside **(14)** and myricanol 11-*O*-β-D-xylopyranoside **(15)**.

Compounds **13** and **15 (Figure 3.60)** were isolated as white amorphous powders and **14** as off-white amorphous powder. On NP-TLC, compound **13** (R_f ~ 0.68) and **15** *(*R_f ~ 0.85) were detected as deep purple blue spots while compound **14** (R_f ~ 0.67) was detected as a yellow-brownish spot **(Figure 3.49)** under day light after derivatization with anisaldehyde-sulphuric acid reagent and mobile phase MP_1.

The three diarylheptanoids monoglycosides were confirmed to be myricanol 5-*O*-β-D-glucoside **(13)**, myricanone 5-*O*-β-D-glucoside **(14)**, and myricanol 11-*O*-β-D-xylopyranoside **(15)** by comparing their NMR and MS data with the available literature data of Matsuda et al.[123], Tene et al.[126] for **13**, Tao et al.[117] for **14** and Tene et al.[126] for **15**. ^{1}H and ^{13}C NMR data for these compounds are summarized in **Table 3.15**. The absolute configuration of these compounds were determined as described in section **3.3.5.2.1**.

Table 3.15: NMR data for compounds **13**–**15**. ^{1}H NMR (600 MHz), ^{13}C NMR (150 MHz), MeOH-d_4, 298 K).

Pos.	**13**		**14**		**15**	
	δ_C (ppm)	**δ_H (ppm), m, *J* (Hz)**	**δ_C (ppm)**	**δ_H (ppm), m, *J* (Hz)**	**δ_C (ppm)**	**δ_H (ppm), m, *J* (Hz)**
1	126.6		126.5		126.7	
2	129.8		129.3		123.5	
3	149.3		149.3		148.3	
4	146.5		146.3		140.6	
5	149.8		149.8		150.5	
6	131.1		131.7		131.5	
7	27.5	2.95–2.90, (1H, m) 2.71–2.66, (1H, m)	28.2	2.76, (2H, m)	26.6	3.01–2.98, (1H, m) 2.93–2.86, (1H, m)
8	27.1	1.93–1.83, (2H, m)	22.8	1.72, (2H, m)	25.9	2.16–2.12, (1H, m) 1.82–1.75, (1H, m)
9	24.0	1.58–1.51, (2H, m)	25.5	1.89, (2H, m)	23.2	1.82–1.75, (1H, m) 1.41–1.37, (1H, m)
10	40.4	1.93–1.83, (2H, m)	45.9	2.64, (2H, m)	36.5	2.10–2.04, (1H, m) 1.90–1.85, (1H, m)
11	69.3	3.90, (1H, m)	215.8		76.3	4.43, (1H, t, *J* = 9.3)
12	35.8	2.28–2.23, (1H, m) 1.67–1.62,(1H, m)	42.8	2.86, (2H, m)	34.0	2.36–2.32, (1H, m) 2.10–2.04, (1H. m)
13	28.2	2.87–2.81, (2H, m)	28.9	2.94, (2H, m)	27.6	3.42–3.37, (1H, m) 2.93–2.86, (1H, m)
14	132.0		132.8		131.4	
15	131.0	7.03, (1H, dd, *J* = 2.1, 8.2)	129.6	7.03, (1H, brd, *J* = 8.2)	130.1	7.19, (1H, m)
16	117.3	6.77, (1H, d, *J* = 8.2)	117.2	6.77, (1H, d, *J* = 8.22)	117.5	7.19, (1H, m)
17	153.0		152.9		152.8	
18	135.0	7.09, (1H, brs)	133.9	6.65, (1H, brs)	134.2	7.47, (1H, brs)
19	130.5	6.83, (1H, s)	129.9	6.58, (1H, s)	130.5	7.15,(1H, s)
20	61.6	3.88, (3H, s)	61.4	3.81, (3H,s)	61.0	3.94, (3H, s)
21	62.0	3.96, (3H, s)	61.7	3.93, (3H, s)	60.7	3.74, (3H, s)

	13		14		15	
	δ_C (ppm)	**δ_H (ppm), m, *J* (Hz)**	**δ_C (ppm)**	**δ_H (ppm), m, *J* (Hz)**	**δ_C (ppm)**	**δ_H (ppm), m, *J* (Hz)**
Gl.						
1’	105.4	5.00, (1H, d, *J* = 7.3)	105.0	5.00, (1H, d, *J* = 7.2)	103.2	4.79, (1H, d, *J* = 7.3)
2’	75.8	3.45–3.43,(1H, m)	75.5	3.45, (1H, m)	75.0	3.98, (1H, td, *J* = 11.8, 4.36)
3’	78.3	3.25–3.22, (1H, m)	78.3	3.22, (1H, m)	71.1	4.16–4.11, (1H, m)
4’	71.5	3.40–3.37, (1H, m)	71.3	3.39, (1H, m)	78.4	4.16–4.11,(1H, m)
5’	78.0	3.45–3.43, (1H, m)	78.0	3.46, (1H, m)	67.1	4.59, (1H, dd, *J* = 11.5, 4.6) 3.47, (1H, dd *J* = 9.6, 11.3)
6’	62.7	3.79, (1H, dd, *J* = 2.3, 11.9) 3.66, (1H, dd, *J* = 5.3, 11.9)	62.4	3.78, (1H, d, *J* = 2.4) 3.67, (1H, dd, *J* = 11.7, 5.4)		

Compound 16

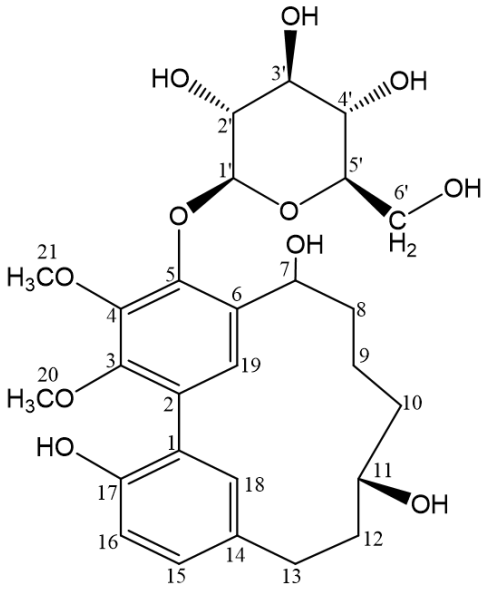

16

Figure 3.61: Structure of salicimeckol: 7-hydroxymyricanol 5-*O*-β-D-glucoside **(16)**.

Compound **16 (Figure 3.61)** was identified as new cyclic diarylheptanoid glycoside and was named salicimeckol (7-hydroxymyricanol 5-*O*-β-D-glucoside). The compound was isolated as

white amorphous powder with $[\alpha]_D^{25}$= -56 (c 0.1, MeOH). It was detected as deep purple blue spot on TLC with R_f value ~ 0.45 **(Figure 3.49)** after derivatization with anisaldehyde-sulphuric acid reagent (mobile phase MP_1). In the negative mode HRESI-MS exhibited ions at *m/z* 581.2257 [M+HCOO$^-$] and 1071.4445 [2M–H]$^-$ are consistent with the molecular formula of $C_{27}H_{36}O_{11}$. The UV spectrum (MeOH) of compound **16** showed absorption maxima at 213, 250 and 295 nm which are typically for biphenyl type diarylheptanoids[117,171].

The ^{1}H NMR spectrum of compound **16** showed four aromatic protons at δ_H 7.02, 6.77, 6.88 (2H) ppm assigned to position 15, 16, 18, and 19. Two methoxy groups resonating at δ_H 3.95 ppm, integrated for 6H, can be assigned to positions 20 and 21. Five methylenes were observed in the highfield ^{1}H NMR region between δ_H 1.12 -2.88 ppm and assigned to position 8, 9, 10, 12 and 13 of the aglycone determined by COSY experiments. Two methine bearing a hydroxyl group at δ_H 3.84 and 4.92 ppm assigned to position 7 and 11 following proton coupling network from COSY experiment and HMBC long range correlation.

Anomeric proton for glucose moiety was observed at δ_H 5.04 ppm with coupling constant of 7.4 suggestive for the β-configuration of a sugar moiety. The position of the glycosidic linkage was elucidated from HMBC long-range correlation between the anomeric proton at δ_H 5.05 and the C-5 carbon of the aglycone moiety δ_C 150.0 ppm **(Figure 3.59)**. Other sugar protons at position 2', 3', 4', 5' and 6' were assigned based on homonuclear COSY experiments. Their respective carbons were determined by HSQC through direct correlation of the particular proton to its respective carbon. The NMR data of **16** are summarized in **Table 3.16** and its proton spectrum in **Figure 3.58**. Absolute configuration of **16** was completed as described in section **3.3.5.2.1**. From the obtained data compound **16** was concluded to be 7-hydroxymyricanol 5-*O*-β-D-glucose (salicimeckol).

Table 3.16: NMR data summary for compound **16**. ^{1}H NMR (600 MHz), ^{13}C NMR (150 MHz), MeOH-d_4, 298 K.

Pos.	δ_C (ppm)	δ_H (ppm), m, *J* (Hz)	HMBC	COSY	NOESY
1	126.8				
2	120.2				
3	147.0				
4	152.2				
5	150.0				
6	131.0				
7	66.7	4.92, (1H, dd, *J* = 3.6, 11.4)	9, 8, 6, 5	8	9, 8, 18, 19
8	35.6	2.19–2.07, (1H, m) 2.01–1.94, (1H, m)	9, 10, 7	9, 7	9, 12, 13, 11, 18, 19
9	21.8	1.55–1.48, (1H, m) 1.18-1.12, (1H, m)	8, 10, 7, 11	8, 10	8, 11, 7, 18.19
10	40.0	1.82–1.77, (1H, m) 1.55–1.48, (1H, m)	9, 12, 11	9, 11	9, 8, 11, 18, 19
11	68.9	3.84, (1H, m)	29, 13, 12, 10	12, 10	9, 12, 10, 8, 13, 18, 19
12	35.5	2.19–2.07, (1H, m) 1.65–1.60, (1H, m)	13, 11, 14	13, 11	9, 13, 11, 18, 19
13	27.7	2.88-2.79, (2H, m)	12, 11, 14, 18	12	12, 11
14	131.3				
15	131.0	7.02, (1H, dd, *J* = 2.2, 8.2)	13, 16, 1, 18, 17	16	13, 16
16	117.1	6.77, (1H, d, *J* = 8.2)	1, 14, 17	15	10, 13, 15
17	153.1				
18	135.8	6.87, (1H, brs)	13, 1, 17		9, 10, 12, 13, 11, 15
19	130.8	6.87, (1H, s)	7, 2, 1, 6, 3, 5, 4, 17		9, 10, 12, 13, 11, 15
20	61.1	3.95, (3H, s)	3		
21	61.9	3.95, (3H, s)	4		
Glu.					
1’	104.8	5.05, (1H, d, *J* = 7.4)	4‘, 5	2‘	8, 5‘, 6‘, 7
2‘	75.5	3.52-3.49, (1H, m)	4‘, 1‘	1‘, 3‘	1‘
3’	71.4	3.39, (1H, m)	6‘, 4‘	4‘, 2‘	
4’	77.7	3.47, (1H, m)	3‘, 2‘	3‘, 5‘	1‘
5‘	78.5	3.32, (1H, m)	3’, 1’		6’, 1’
6‘	62.1	3.80, (1H, dd, *J* = 2.4, 11.8) 3.64, (1H, dd, *J* = 5.7, 11.8)	3‘, 5‘	5’	5’

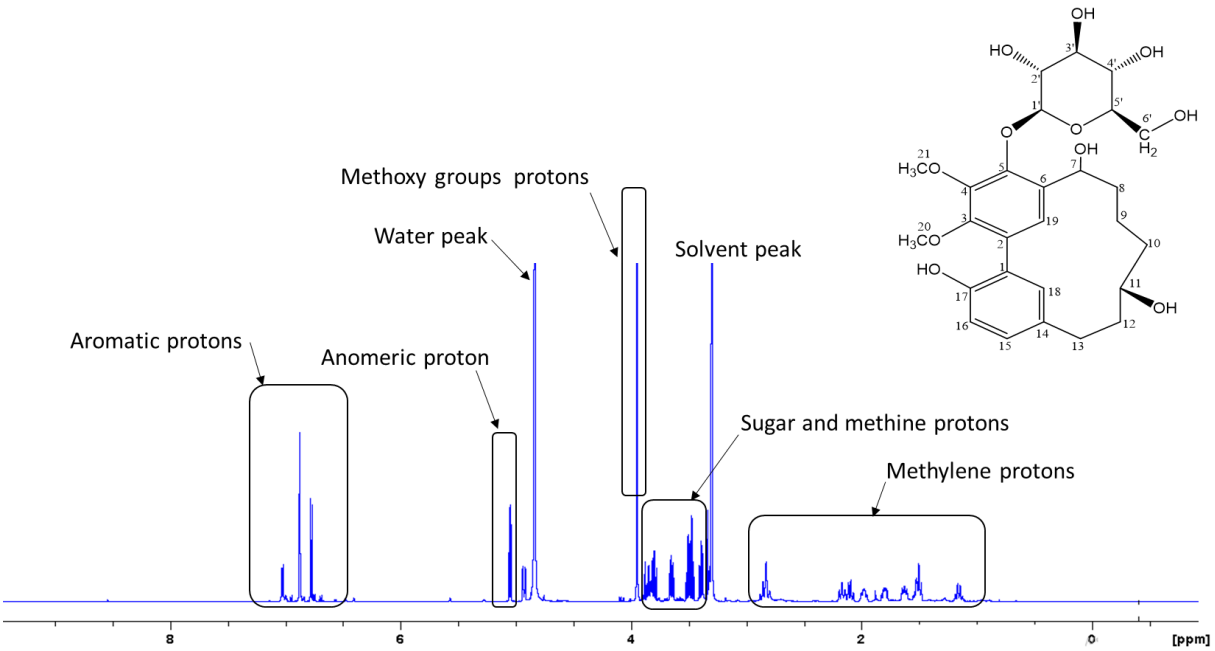

Figure 3.62: ^{1}H NMR spectrum of compound **16**. ^{1}H NMR (600 MHz), ^{13}C NMR (150 MHz), MeOH-d_4, 298 K.

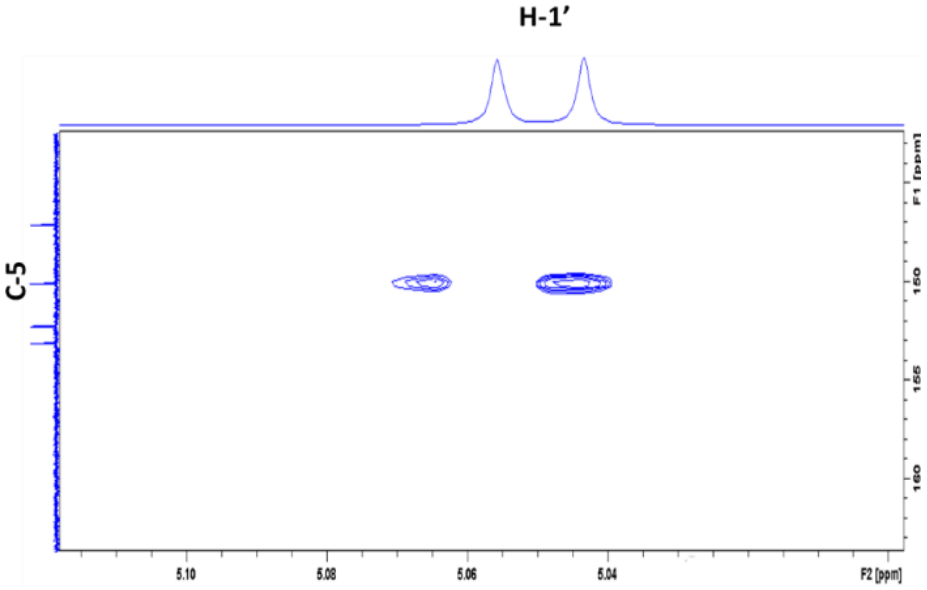

Figure 3.63: Part of the HMBC spectrum depicting a long correlation between anomeric proton H-1' (δ_H 5.05 ppm) and C-5 (δ_C 150 ppm), a proof of assignment of glycosidic bond to position 5 of compound **16**.

Compound 17

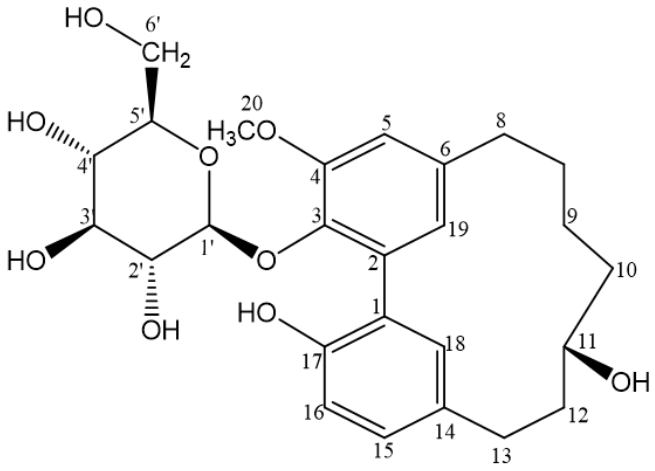

17

Figure 3.64: Structure of salicireneol A: juglanin B 3-*O*-β-D-glucoside **(17)**.

Compound **17 (Figure 3.64)**, a new cyclic diarylheptanoid monoglycoside was identified as juglanin B 3-*O*-β-D-glucoside and given the name salicireneol A. It was isolated as white amorphous powder with an optical rotation value $[\alpha]_D^{25}$= -49 (c 0.1, MeOH) and gave a blue spot on a TLC after derivatization with anisaldehyde-sulphuric acid reagent with R_f value ~ 0.6, mobile phase MP_1 **(Figure 3.49)**. HRESI-MS exhibited ions at *m/z* 489.2137 $[M-H]^-$ and *m/z* 979.4324 $[2M- H]^-$ corresponding to molecular formula of $C_{26}H_{33}O_9$. The UV spectrum (MeOH) showed absorption maxima at 214, 254 and 285 nm, indicative of biphenyl cyclic diarylheptanoids.

The ^{1}H NMR spectrum of **17** showed five aromatic protons at $\delta_{H\text{-}5}$ 6.85, brs, $\delta_{H\text{-}15}$ 7.04, dd, $\delta_{H\text{-}16}$ 6.78, d, $\delta_{H\text{-}18}$ 7.07, brs and $\delta_{H\text{-}19}$ 6.76, brs. The spectrum also included signals attributable to six aliphatic methylenes at δ_H 1.41 – 2.99 ppm assigned to position 7, 8, 9, 10, 12 and 13. One methoxy group at δ_H 3.88 ppm, s, integrated for 3H, assigned to position 20 and one methine bearing a hydroxyl group δ_H 3.91 ppm, m, integrated for 1H, assigned to position 11. Anomeric carbon for sugar moiety was observed at δ_H 4.99 ppm, d, *J* = 7.3 Hz and other five sugar protons between δ_H 3.07 - 3.45 ppm. The position of the glycosidic linkage was elucidated to be at position 3 of the aglycone from long-range correlation HMBC experiment between the anomeric proton δ_H 4.99 ppm, d, *J* = 7.3 (H-1'), and the δ_C 140.9 ppm (C-3) of the aglycone

moiety. The confirmation of sugar and its absolute configuration was achieved as described in section **3.3.5.2.1**.

The 1D and 2D NMR data for **17** are summarized in the **Table 3.17**. The carbon data of **17** are in agreement with the published data of juglanin B [172,173], with the exception that compound **17** has the sugar substitution at position 3 of the aglycone. Therefore, compound **17** was concluded to be juglanin B 3-*O*-β-D-glucoside (salicireneol A).

Table 3.17: NMR data for compound **17**. ^{1}H NMR (600 MHz), ^{13}C NMR (150 MHz), MeOH-d_4, 298 K.

Pos.	**δ_C (ppm)**	**δ_H (ppm), m, *J* (Hz)**	**HMBC**	**COSY**	**NOESY**
1	128.0				
2	128.2				
3	140.9				
4	152.7				
5	113.6	6.85, (1H, brs)	7, 20, 19, 3, 4	7, 19, 20	20
6	131.8				
7	31.6	2.99–2.97, (1H, m) 2.57–2.51, (1H, m)	7	7, 8	
8	27.5	2.00–1.95, (1H, m) 1.85–1.80, (1H, m)		8, 9, 7, 7	
9	23.8	1.64–1.58, (1H, m) 1.48–1.41, (1H, m)			
10	40.2	1.85–1.80, (1H, m) 1.55–1.49, (1H, m)		10, 11, 10	
11	69.1	3.91, (1H, m)		12, 10	
12	35.5	2.26–2.20, (1H, m) 1.67–1.62, (1H, m)			
13	27.9	2.87–2.82, (1H, m) 2.04–2.00, (1H, m)	1, 15	12	12, 15
14	132.0				
15	130.6	7.04, (1H, dd, *J* = 2.3, 8.2)	13, 16, 18, 17	16	13, 16
16	117.2	6.78, (1H, d, *J* = 8.2)	2, 14, 17	15	
17	152.1				
18	135.0	7.07, (1H, brs)	13, 16, 2, 15, 18, 17	13	12, 13, 19
19	127.6	6.76, (1H, brs)	7, 5, 19, 1, 6, 3	7, 3	18, 8, 9
20	56.6	3.88, (3H, s)	4		3
Gluc.					
1’	104.8	4.99, (1H, d, *J* = 7.3)	3	2’	4’
2’	75.3	3.38, (1H, m)	1’, 3’	1’, 3’	
3’	71.1	3.20, (1H, m)	4’	4’, 2’	
4’	77.5	3.07, (1H, m)	6’	3’,5’	1’
5’	78.6	3.29, (1H, m)		4’, 5’	
6’	62.6	3.45, (2H, m)		5’	

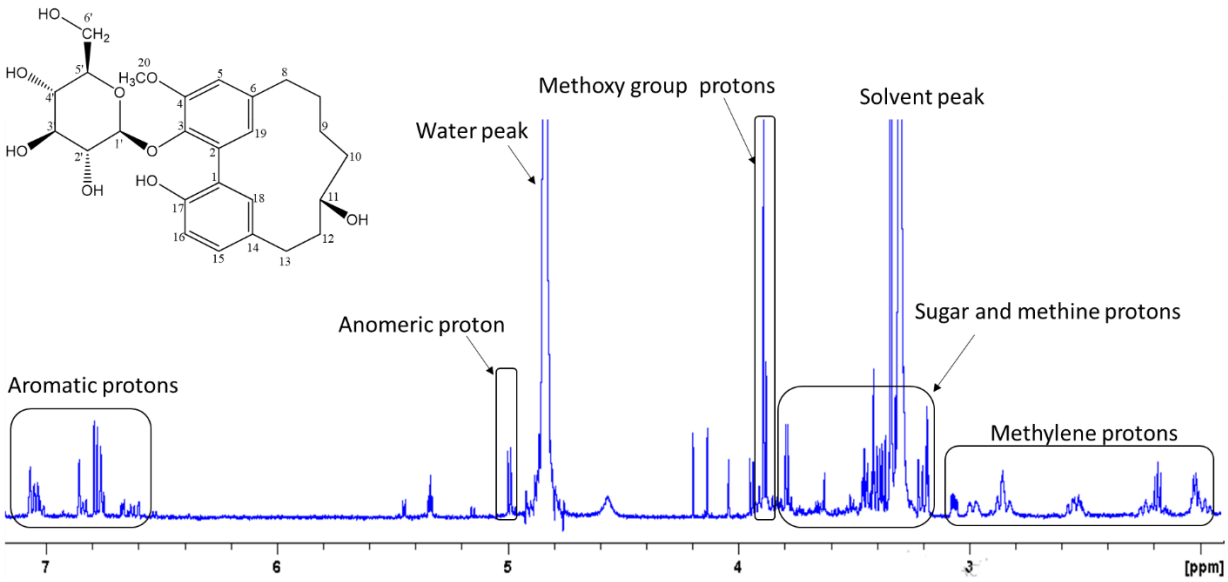

Figure 3.65: ^{1}H NMR spectrum of compound **17** ^{1}H NMR (600 MHz), ^{13}C NMR (150 MHz), MeOH-d$_4$, 298 K.

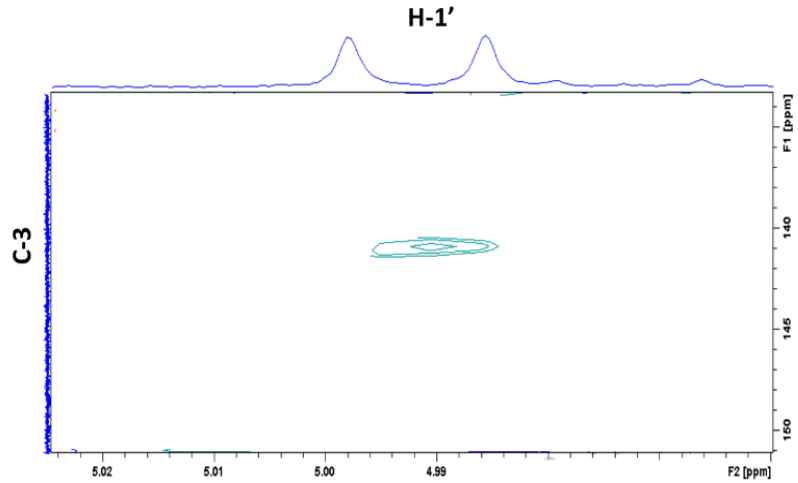

Figure 3.66: Part of the HMBC spectrum of **17** showing a long correlation between anomeric proton H-1' (4.99 ppm) and C-3 (140.9 ppm), a proof of assignment of glycosidic bond to position 3. The carbon signals are not clearly seen due to the low amount of **17**.

Compound 18

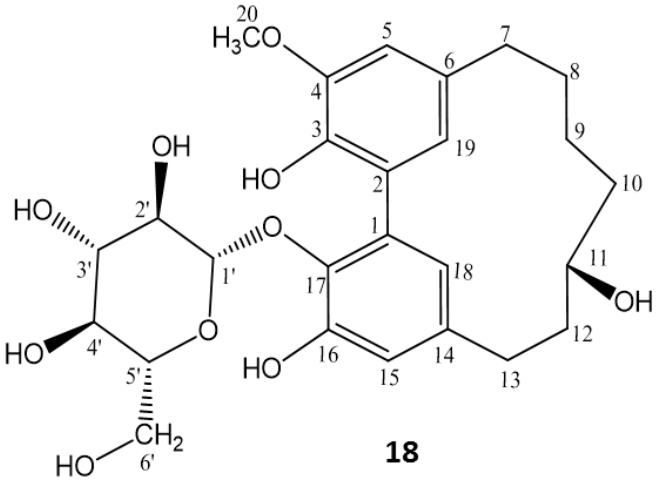

18

Figure 3.67: Structure of salicireneol B: 16-hydroxyjuglanin B 17-*O*-β-D-glucoside **(18)**.

Compound **18 (Figure 3.67)** was isolated as a white amorphous powder with a negative optical rotation $[\alpha]_D^{25}$= -33.6 (c 0.1, MeOH). A purple blue spot was detected on TLC after derivatization with anisaldehyde-sulphuric acid reagent with R_f value of ~ 0.58 **(**mobile phase MP_1, **Figure 3.49)**. Molecular mass of **18** were realized from HRESI-MS ions at *m/z* 505.2078 $[M-H]^-$ and 551.2137 $[M+HCOO^-]$ calculated for molecular formula of $C_{26}H_{34}O_{10}$. The UV spectra (MeOH) of **18** showed absorption maxima at the wavelengths 216, 253, and 298 nm suggestive of biphenyl type of diarylheptanoid[117,171].

The ^{1}H NMR of **18** showed four aromatic protons, at $\delta_{H\text{-}5}$ 7.04 ppm, brs, $\delta_{H\text{-}19}$ 6.87 ppm, brs, $\delta_{H\text{-}18}$ 6.65 ppm, brs and $\delta_{H\text{-}15}$ 5.66 ppm, brs. Furthermore, signals attributed to six aliphatic methylenes were detected between δ_H 0.90 – 2.78 ppm and were assigned to position 7, 8, 9, 10, 12 and 13 **(Table 3.18)**. One methoxy group was observed at δ_H 3.80 ppm, s, 3H, assigned to position 20 and one oxymethine at δ_H 3.05 ppm, m for position 11. A glucopyranosyl moiety was observed at $\delta_{H\text{-}1'}$ 5.00 ppm, d, J = 7.6 Hz and the glycosidic linkage of **18** was elucidated by HMBC experiment. The long range correlation was observed between the anomeric proton (H-1') and the C-17 of the aglycone moiety (δ_H 144.7 ppm). The position of the hydroxyl group at C-11 was deduced from only H-H COSY experiment due to invisible long range correlation signals in the upper field of the HMBC experiment. Finally, the absolute configuration of **18** was achieved as previously described in section **3.3.5.2.1**.

Compound **18** was concluded to be 16-hydroxyjuglanin B 17-*O*-β-D-glucoside, a new compound and named salicireneol B.

Table 3.18: NMR data for compound **18** ^{1}H NMR (600 MHz), ^{13}C NMR (150 MHz), MeOH-d_4, 298 K.

Pos.	δ_C (ppm)	δ_H (ppm), m, *J* (Hz)	HMBC	COSY	NOESY
1	126.2				
2	131.5				
3	144.8				
4	154.0				
5	115.3	7.04, (1H, brs)	7, 19, 2, 6, 3, 4		8, 7, 5, 20, 1', 15
6	137.9				
7	36.2	2.78, (1H, m)		8, 7	18, 13, 7
		2.64, (1H, m)			
8	31.2	1.74, (1H, m)		7	
		1.59, (1H, m)			
9	23.4	1.27, (1H, m)		11, 10	
		1.03, (1H, m)			
10	39.5	1.27,(1H, m)		11	
		0.90, (1H, m)			
11	72.2	3.05, (1H, m)		10, 12	10, 9, 12, 15
12	37.4	1.43, (1H, m)		11	10, 11, 15
13	29.3	2.64, (1H, m)		7, 8	12, 18
		2.60, (1H,m)			
14	136.3				
15	115.2	5.66, (1H, brs)	13, 18, 2, 14, 17, 16	18	10, 9, 12, 13, 11
16	151.6				
17	144.7				
18	122.7	6.64, (1H, brs)	13, 18, 17, 16	15	13, 15
19	124.2	6.87, (1H, brs)	6, 5, 1, 2, 3		5, 7, 8, 9
20	56.4	3.80, (3H, s)	4		5
Glu.					
1'	102.9	5.00, (1H, d, *J* = 7.6)	17	2'	2' 4',5
2'	74.7	3.54, (1H, m)	3', 1'	1'	
3'	77.8	3.49, (1H, m)	4'		
4'	71.1	3.42, (1H, m)	3'		1'
5'	78.0	3.42, (1H, m)	3'		
6'	62.3	3.89, (1H, brd, *J* = 12.3	5', 1'	3'	
		3.71, (1H, dd, *J* = 4.0, 1.8)			

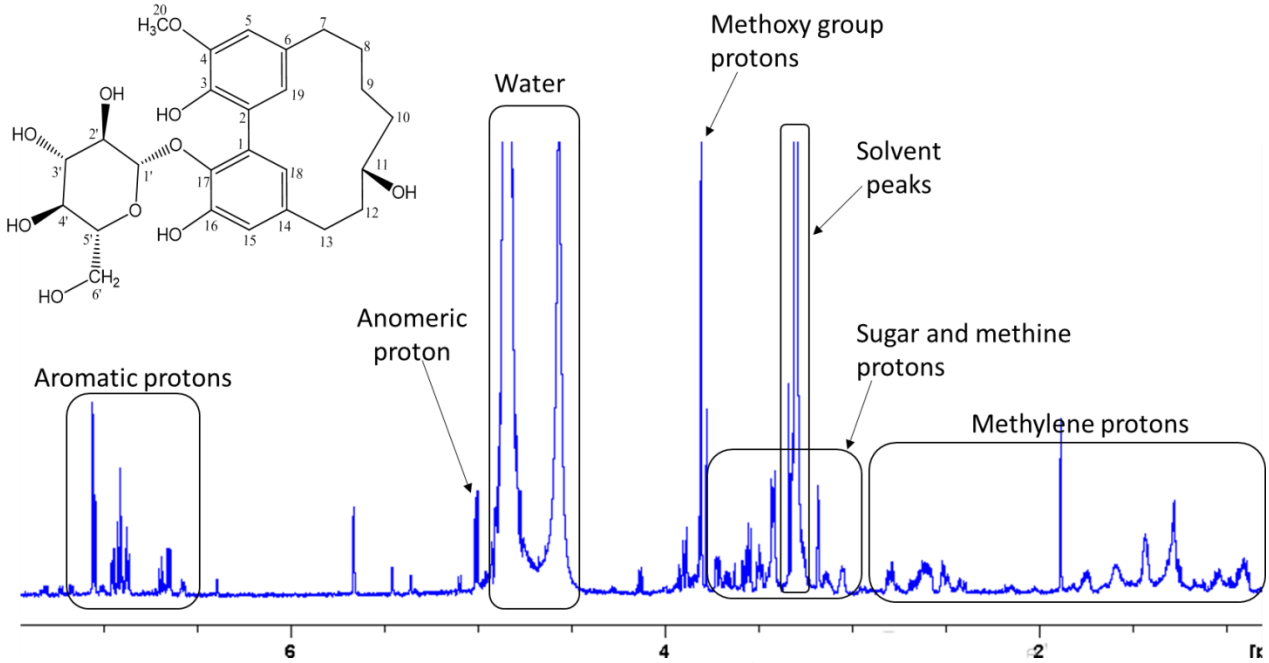

Figure 3.68: ^{1}H NMR spectrum of compound **18** ^{1}H NMR (600 MHz), ^{13}C NMR (150 MHz), MeOH-d_4, 298 K.

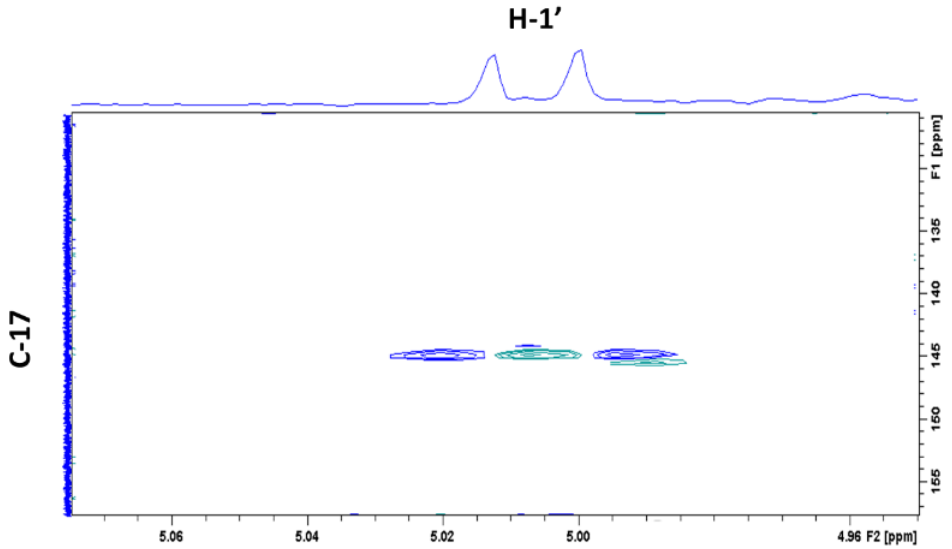

Figure 3.69: Part of the HMBC spectrum of **18** showing a long correlation between anomeric proton H-1' (5.00 ppm) and C-3 (144.8 ppm), a proof of assignment of glycosidic bond to position 17.

3.3.5.2.4 Galloylated cyclic diarylheptanoid glycosides

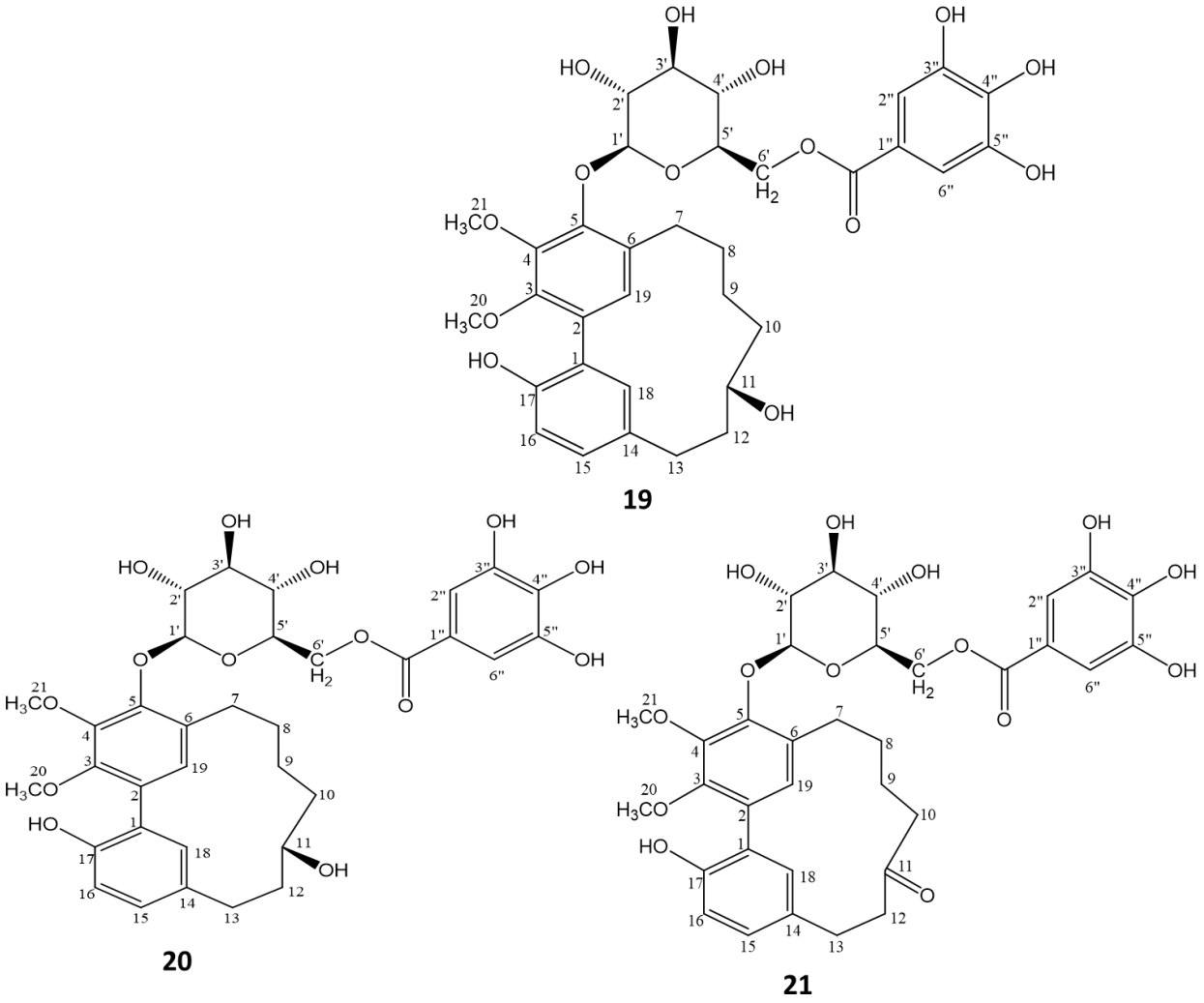

Figure 3.70: Myricanol 5-*O*-β-D-(6'-*O*-galloyl) glucoside (**19** and **20**) and myricanone-5-*O*-β-D-(6'-*O*-galloyl) glucoside **(21)**.

Compounds **19**, **20** and **21 (Figure 3.70)** were isolated and elucidated to be myricanol 5-*O*-β-D-(6'-*O*-galloyl) glucoside (**19** and **20**) and myricanone-5-*O*-β-D-(6'-*O*-galloyl) glucoside **(21)**.

The spectroscopy data of **21** was in agreement with published data by Yoshimura et al.[110]. Confirmation of compound **21** was further supported by the following obtained data: off-white amorphous powder, yellowish-green spot on TLC after derivatization with anisaldehyde-sulphuric acid reagent with R_f value ~ 0.80 (mobile phase MP_1, **Figure 3.49**), ESI-MS exhibited ions at *m/z* 671.23 $[M+H]^+$ in the positive mode and at *m/z* 669.21 $[M-H]^-$ in the negative mode,

calculated for molecular formula of $C_{34}H_{38}O_{14,}$ optical rotation: $[\alpha]_D^{25}$= -44 (c 0.1, MeOH) and UV maxima (MeOH) at wavelengths 213, 255, 280 nm.

Likewise, the data obtained for compound **19** and **20** were in accordance with the proton and carbon NMR data published by Yaguchi et al.[128]. The two compounds were isolated from fraction S2 subfraction F5.C1.5. During the purification step of F5.C1.5 on the silica gel flash chromatography (FL-6), the two compounds exhibit different retention times, compound **19** eluted earlier with methanol/chloroform and compound **20** eluted later in the washing step with methanol. Furthermore, compound **19** was isolated as deep green amorphous powder while compound **20** as yellow amorphous powder. On TLC **(Figure 3.49** and **3.30 C)**, both compounds were detected as purple-blue spots on visualization under visible light (VIS) with different R_f values ~ 0.75 (**19**) and 0.62 (**20**), mobile phase MP_1. On the other hand, the 1D and 2D-NMR data for compound **19** and **20** could not pronounce their differences, as all the obtained spectra data were very similar. Additional characteristics of the two compounds which were also similar are: Mass data, ESI-MS ions at *m/z* 673.24 $[M+H]^+$ in the positive mode and *m/z* 671.23 $[M-H]^-$ in the negative mode, calculated mass of 672 Da and a molecular formula of $C_{34}H_{40}O_{14}$. Optical rotation was $[\alpha]_D^{25}$= -52.7 (**19**) and -33.6 (**20**), (c 0.1, MeOH). UV spectra (MeOH) for both displays absorption maxima at 213, 255 and 298 nm. CD spectra exhibited positive cotton effect in the wave length region of 205-225 nm (**19**) and 203 - 223 nm (**20**), negative cotton effect at 227 - 265 nm, 285 - 305 nm (**19**) and 203 - 223 nm, 285 - 309 nm (**20**) respectively. The CD data of the two compounds concluded that they are 11*R*-configured. Based on the obtained data, a structural difference between **19** and **20** could not be figured out. Further investigations to discover their differences was unachievable due to the acquired low yields for the two compounds.

The 1D and 2D NMR data of compound **19, 20** and **21** are summarized in the below **Table 3.19**.

Table 3.19: NMR data for compound **19** (MeOH-d_4), **20** (MeOH-d_4/$CDCl_3$ - 1/1 (v/v)) and **21** (MeOH-d_4). ^1H NMR (600 MHz), ^{13}C NMR (150 MHz), 298 K.

Pos.	19		20		21	
	δ_C (ppm)	δ_H (ppm), m, *J* (Hz)	δ_C (ppm)	δ_H (ppm), m, *J* (Hz)	δ_C (ppm)	δ_H (ppm), m, *J* (Hz)
1	125.6		126.5		126.4	
2	129.2		129.7		129.8	
3	148.0		149.0		149.0	
4	145.8		146.5		146.7	
5	149.3		149.8		149.9	
6	131.5		131.7		130.0	
7	27.1	2.85-2.82, 1H, m) 2.54-2.49, (1H, m)	27.5	2.88-2.82, (1H, m) 2.57-2.52, (1H, m)	27.8	2.95-2.88, (2H, m)
8	26.4	1.73-1.68, (1H, m) 1.58-1.53, (1H, m)	26.8	1.64-1.57, (1H, m) 1.77-1.69, (1H, m)	25.6	1.88-1.82, (1H, m) 1.67, (1H, m)
9	23.6	1.52-1.48, (1H, m) 1.35-1.31, (1H, m)	24.0	1.51-1.41, (1H, m) 1.34-1.29, (1H, m)	23.4	1.51-1.45, (2H, m)
10	40.0	1.78-1.73, (1H, m) 1.45-1.41, (1H, m)	40.4	1.77-1.69, (1H, m) 1.51-1.41, (1H, m)	44.7	2.64-2.54, (1H, m) 2.27-2.24, m
11	69.0	3.87, (1H, m)	69.4	3.84, (1H, m)	215.0	
12	35.4	2.22-2.16, (1H, m) 1.65-1.61, (1H, m)	35.8	2.25-2.16, (1H, m) 1.64-1.57, (1H, m)	42.2	2.95-2.88, (1H, m) 2.64-2.54, (1H, m)
13	27.8	2.85-2.82, (2H, m)	28.2	2.88-2.82, (2H, m)	27.9	2.85-2.81, (1H, m) 2.64-2.54, (1H, m)
14	131.8		132.0		132.5	
15	130.7	7.03, (1H, brd)	130.5	6.78-6.75, (1H, m)	130.0	7.01, (1H, brd, *J* = 8.2)
16	117.0	6.78, (1H, m)	117.2	6.78-6.75, (1H, m)	117.4	6.75, (1H, d, *J* = 8.2)
17	152.0		152.8		152.9	
18	134.4	7.06, (1H, brs)	135.0	7.04, (1H, brs)	134.0	6.50, (1H, brs)
19	130.1	6.77, (1H, s)	131.0	7.02, (1H, s)	129.9	6.49, (1H, s)
20	61.8	3.85, (3H, s)	61.7	3.86, (3H, s)	62.0	3.84, (3H, s)
21	62.1	3.95, (3H, s)	62.1	3.94, (3H, s)	62.0	3.92, (3H, s)
Glu.						
1’	105.3	4.83, (1H, d, *J* = 7.4)	105.6	4.90, (1H, d, *J* = 7.3)	105.0	5.04, (1H, d, *J* = 6.7)
2’	75.0	3.53-3.47, (1H, m)	75.6	3.50, (1H, m)	75.5	3.51-3.48, (1H, m)
3’	75.1	3.53-3.47, (1H, m)	75.6	3.50, (1H, m)	77.7	3.51-3.48, (1H, m)
4’	71.1	3.53-3.47, (1H, m)	71.6	3.50, (1H, m)	71.7	3.51-3.48, (1H, m)
5’	77.3	3.53-3.47, (1H, m)	77.7	3.50,(1H, m)	75.7	3.51-3.48, (1H, m)
6’	64.0	4.49, (1H, d, *J* = 11.6) 4.40, (1H, dd, *J* = 11.7, 4.4)	64.2	4.46, (1H, brd, *J* = 11.5) 4.38, (1H, brd, *J* = 8.7)	64.8	4.37, (2H, m)

	19		20		21	
	δ_C (ppm)	**δ_H (ppm), m, *J* (Hz)**	**δ_C (ppm)**	**δ_H (ppm), m, *J* (Hz)**	**δ_C (ppm)**	**δ_H (ppm), m, *J* (Hz)**
Gal.						
1''	120.9		120.0		120.2	
2''/6"	109.9	7.01, (2H, s)	109.9	7.01, (2H, s)	110.0	6.98, (2H, s)
3''/5"	145.8		146.7		146.8	
4''	139.2		140.0		139.2	
C=O	167.9		168.5		168.5	

3.3.5.2.5 Cyclic diarylheptanoid di-glycosides

Compounds 22 and 23

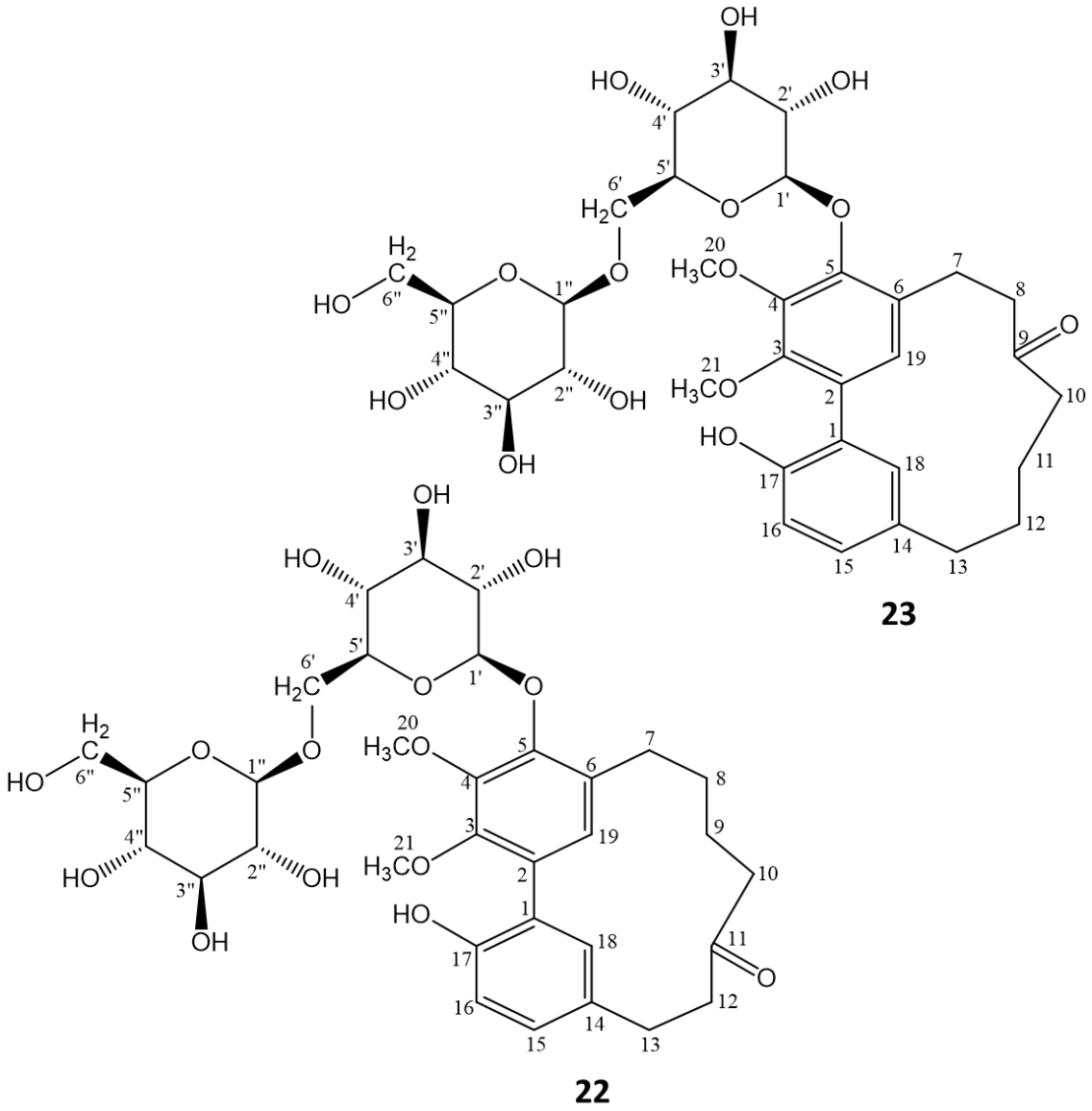

Figure 3.71: Structures of saliciclaireone A: myricanone 5-*O*-β-D-glucopranosyl-(1-6)-β-D-glucopyranoside **(22)** and saliciclaireone B: neomyricanone 5-*O*-β-D-glucopranosyl-(1-6)-β-D-glucopyranoside **(23).**

Compounds **22** and **23 (Figure 3.71)** were identified as new compounds and isolated as white amorphous powder both with negative optical rotation, $[\alpha]_D^{25}$= -51.6 (c 0.1, MeOH) and $[\alpha]_D^{25}$= -43.1 (c 0.1, MeOH) respectively. The two compounds depict yellow-brownish spot on the TLC detected under VIS and fluorescent yellow-brownish under UV 366 nm with the same R_f value of ~ 0.30. HRESI-MS of **22** and **23** exhibited ions at *m/z* 679.2682 $[M-H]^-$ and *m/z* 679.2622 [M-

H]$^-$ with the common molecular formula of $C_{33}H_{44}O_{15}$ and calculated mass of 680 Da. The UV spectra (MeOH) of **22** and **23** displays absorption maxima at 214 250, and 300 nm as well as 214, 250 and 298 nm which is a characteristic of biphenyl cyclic diarylheptanoids[117,171].

The ^{1}H NMR of **22** showed signals at δ_H 3.94 and 3.80 ppm both singlets, integrated for three protons each which were assigned to two methoxy group at C-20 and C-21. Four aromatic protons assigned to position C-15, C-16, C-18 and C-19 of the aglycone. Six methylenes assigned to position C-7, C-8, C-9, C-10, C-12 and C-13. Carbonyl group at δ_C 217.2 ppm assigned to position C-11 was deduced from HMBC experiment due to long range correlation between H-9, H-10, H-12, H-13 and the carbonyl carbon. Further confirmation was achieved from ^{1}H-^{1}H COSY experiment due to observed cross peaks between H-7and H-8, H-8 and H-9, H-9 and H-10, H-12 and H-13.

Two anomeric protons for two glucose moiety observed at $\delta_{H\text{-}1'}$ 4.99 ppm, d, *J* =7.2 Hz and $\delta_{H\text{-}1''}$ 4.28 ppm, d, *J* =7.8 Hz. The position of two glycosidic linkages were elucidated from HMBC experiment. Long-range correlation was observed between anomeric proton (H-1') and C-5 of the aglycone and anomeric proton H-1" to C-6' of the glucose. Therefore, two sugar groups are attached to C-5 of the aglycone and they were confirmed to be two D-glucose (section **3.3.5.2.1**). Hence, the structure of **22** was confirmed to be myricanone 5-*O*-β-D-glucopranosyl-(1-6)-β-D-glucopyranoside (saliciclaireone A).

The carbon data for **23** was found to be similar to the published data of neomyricanone 5-*O*-β-D-glucopyranoside[117] except that compound **23** was found to have two glucose moieties attached to C-5. In the same manner, NMR data of **23** were similar to **22** in terms of having two methoxy groups at position C-20 and C-21, four aromatic protons at position C-15, C-16, C-18 and C-19 and two glucose moiety attached at C-5. The difference between two compounds was observed during assignment of the six methylenes at position C-7, C-8, C-10, C-11, C-12 and C-13 based on proton coupling network from ^{1}H-^{1}H COSY experiment due to cross peaks between H-7 and H-8, H-10 and H-11, H-12 and H-11, H-13 and H-12. Further difference was observed on the HMBC for the assignment of carbonyl carbon position, the long range HMBC correlation was observed between H-7, H-8, H-10 and the carbonyl carbon. Therefore, compound **23** was found to be neomyricanone 5-*O*-β-D-glucopranosyl-(1-6)-β-D-glucopyranoside (saliciclaireone

B). The summarized 1 and 2D NMR data for **22** and **23** can be found in **Table 3.20** and **3.21** respectively.

Table 3.20: NMR data for compound **22.** ^{1}H NMR (600 MHz), ^{13}C NMR (150 MHz), MeOH-d_4, 298 K.

Pos.	δ_C (ppm)	δ_H (ppm), m, *J* (Hz)	HMBC	COSY	ROESY
1	126.7				
2	129.4				
3	146.6				
4	149.2				
5	149.8				
6	131.8				
7	28.4	2.94-2.88, (1H, m)	8, 9, 19, 6, 5	8	18, 9, 1', 19
		2.83-2.72, (1H, m)			
8	25.7	1.90-1.88, (2H, m)	6, 7, 9, 10	9, 7	7, 19
9	22.9	1.72-1.68, (2H, m.)	7, 8, 10, 11	8, 10	7, 10
10	46.2	2.83-2.72, (1H, m.)	9, 8, 11	9	9, 8, 19
		2.68-2.61, (1H, m)			
11	217.2				
12	43.1	2.94-2.88, (1H, m)	11, 14		19, 15, 18, 19
		2.83-2.72, (1H, m)			
13	29.1	2.94-2.88, (1H, m)	11, 14		19, 15, 18, 19
14	133.2				
15	130.2	7.05, (1H, dd, *J* = 2.1, 8.2)	13, 16, 1, 18, 17	16,	13
16	117.5	6.80, (1H, d, *J* = 8.2)	1, 2, 14, 17,	15	15
17	152.8				
18	133.9	6.64, (1H, brs)	13, 16, 17, 19		9, 13, 19
19	130.0	6.57, (1H, s)	1, 2, 7, 18, 3, 4		8, 9, 10, 12
20	62.3	3.94, (3H, s)	3		
21	61.8	3.80, (3H, s)	4		
Sug.					
1'	105.0	4.99, (1H, d, *J* = 7.2)	5', 5	2'	7, 2'
2'	75.4	3.54-3.46, (1H, m)	4', 2', 5', 1'	1'	1', 6'
3'	77.0	3.54-3.46, (1H, m)			
4'	71.0	3.54-3.46, (1H, m)			
5'	77.5	3.44-3.38, (1H, m)		4', 6'	1', 4'
6'	69.5	4.08, (1H, dd, *J* = 1.8, 11.5)	5', 1"	5'	5', 1"
		3.79-3.77, (1H, m)			
1''	104.4	4.28, (1H, d, *J* =7.8)	6', 2'	2"	5", 4", 6'
2''	75.0	3.19-3.16, (1H, m)	5", 1"	33", 1"	1"
3''	77.7	3.30, (1H, m)	4", 2"	2"	
4"	71.4	3.27-3.23, (1H, m)	5", 4"		6", 1"
5"	77.7	3.27-3.23, (1H, m)			
6''	62.6	3.85-3.82, (1H, m)	4", 5"	5"	4", 5"
		3.63, (1H, dd, *J* = 11.9, 5.2)			

Table 3.21: NMR data for compound **23**. ^{1}H NMR (600 MHz), ^{13}C NMR (150 MHz), MeOH-d_4, 298 K.

Pos.	δ_C (ppm)	δ_H (ppm), m, *J* (Hz)	HMBC	COSY	NOESY
1	125.4				
2	129.6				
3	148.3				
4	146.3				
5	148.7				
6	131.9				
7	23.6	3.19, (1H, m)	8, 2, 6, 9	8	19, 6”
		2.99-2.94, (1H, m)			
8	41.8	2.88-2.86, (2H, m)	7, 6, 9	7	7, 9
9	215.8				
10	44.6	2.78-2.72, (1H, m)	9, 12	11	11, 12
		2.68-2.60, (1H, m)			
11	22.7	1.77-1.70, (1H, m)		12, 10	12, 13, 19, 18
12	26.2	1.98-1.95, (1H, m)		11, 13	11, 13, 18
13	31.8	2.78-2.72, (1H, m)		12	11, 12
		2.68-2.60, (1H, m)	11, 12, 14		
14	132.1				
15	130.9	7.00, (1H, d, *J* = 8.2, 2.2)	13, 18, 17	16	13, 16
16	117.4	6.82, (1H, d, *J* = 8.2)	1, 14, 17	15	15
17	152.2				
18	133.7	6.87, (1H, d, *J* = 1.9)	13, 2, 15, 17		11, 12, 13, 19
19	129.5	6.42, (1H, s)	7, 1, 2, 4, 3		11, 8, 7, 18
20	62.1	3.84, (3H, s)	3		
21	62.2	3.95, (3H, s)	4		1’
Sug.					
1’	105.2	4.88, (1H, d, *J* = 7.6)	5	2’	3’
2‘	74.8	3.54-3.51, (1H, m)	6’, 5’, 1’	1’, 3’	
3‘	76.3	3.41-3.38, (1H, m)		2‘/4‘	1', 6‘
4‘	70.5	3.55-3.52, (1H, m)		3‘, 5‘	1', 6‘
5’	77.0	3.48-3.45, (1H, m)	4‘, 2‘		
6’	69.3	4.11, (1H, dd, *J* = 11.2, 2.2)	4‘, 3‘		3‘, 1“
		3.80-3.78, (1H, m)			
1’’	103.8	4.25, (1H, m)	6‘	2“	6“, 2“
2‘‘	74.3	3.24, (1H, m)	4“, 5“, 1“	1“	
3‘‘	77.0	3.22, (1H, m)	4“, 1“, 5“		
4‘‘	70.8	3.27, (1H, m)	4“, 2“, 5“		
5’’	77.2	3.27, (1H, m)	4“, 2“, 5“		
6’’	62.2	3.81, (1H, dd, *J* = 11.9, 2.5)	4“, 5“	5“	4“/5“, 1“
		3.63, (1H, dd, *J* = 11.9, 5.4)			

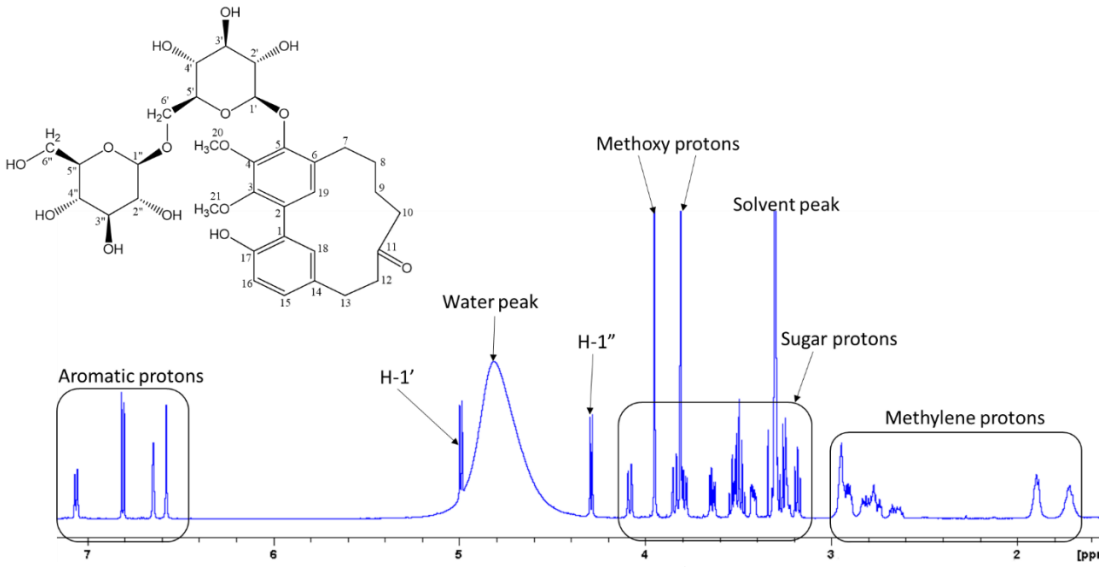

Figure 3.72: ^{1}H NMR spectrum of compound **22**. ^{1}H NMR (600 MHz), ^{13}C NMR (150 MHz), MeOH-d_4, 298 K.

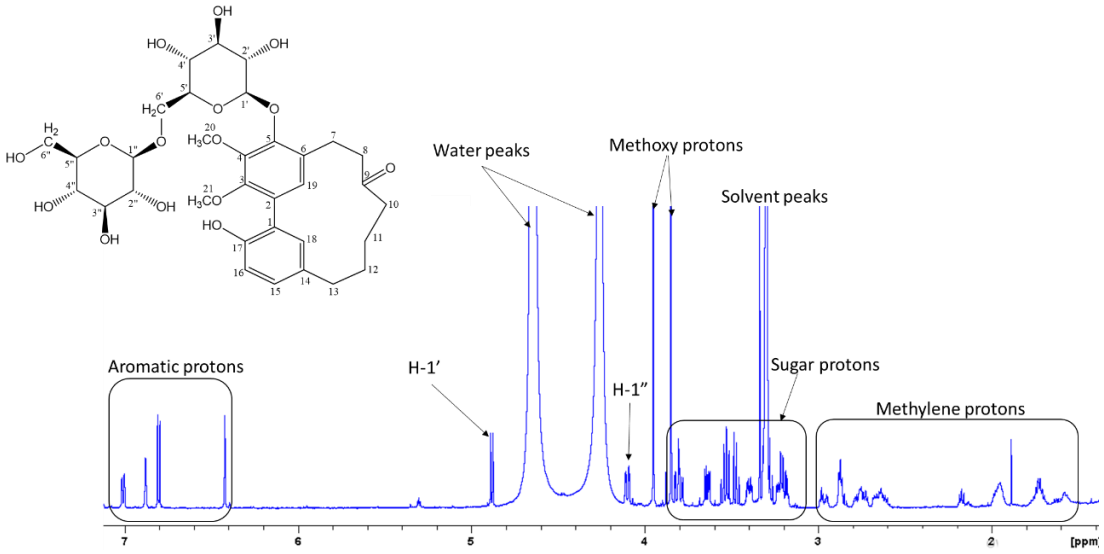

Figure 3.73: ^{1}H NMR spectrum of compound **23**. ^{1}H NMR (600 MHz), ^{13}C NMR (150 MHz), MeOH-d_4, 298 K.

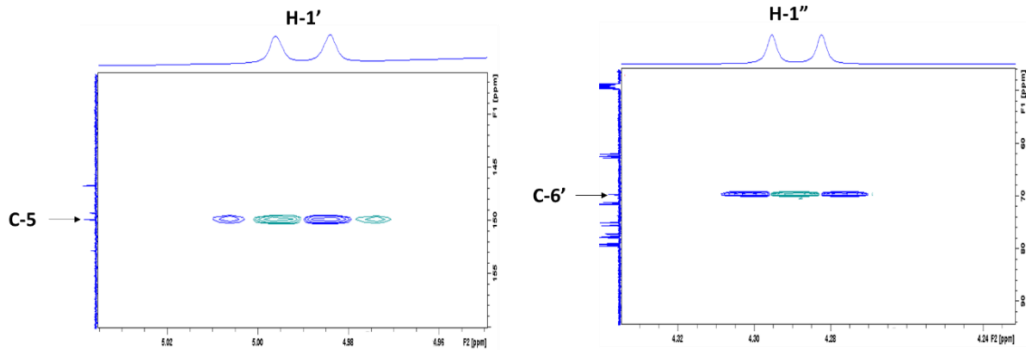

Figure 3.74: Part of the HMBC spectrum showing a long range correlation between anomeric proton H-1’ and C-5 (for the first glucose) and between H-1”and C-6’ (for the second glucose) a proof of attachment of two glucose moieties to position C-5 for compound **22**. (The same was observed for compound **23**).

Compound 24

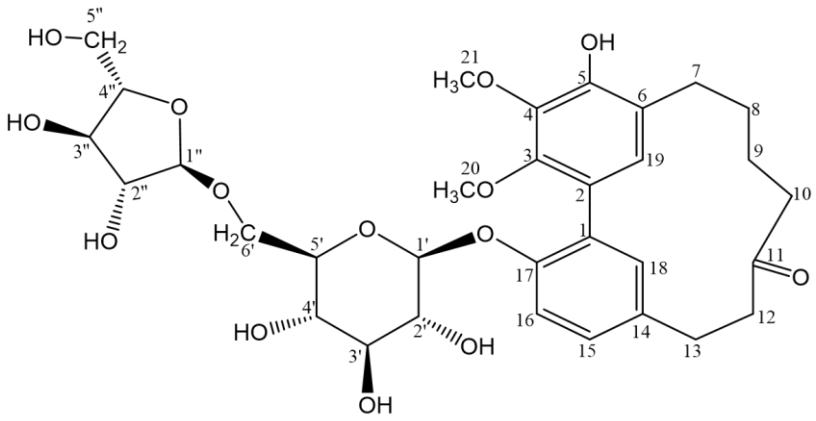

24

Figure 3.75: Structure of saliciclaireone C: myricanone 17-*O*-α-L-arabinofuranosyl-(1-6)-β-D-glucopyranoside **(24)**.

Compound **24 (Figure 3.75)**, a new compound named saliciclaireone C, was isolated as off-white amorphous powder, yellow-brownish spot on TLC visualized under VIS and fluorescent light yellow-greenish under UV 366 nm with R_f value ~ 0.43 (mobile phase MP_1). Optical rotation was $[\alpha]_D^{25}$= -36 (c 0.1, MeOH). The HRESI-MS exhibited ions at *m/z* 649.2509 $[M-H]^-$ in the negative mode consistent with the molecular formula of $C_{32}H_{41}O_{14}$. The UV spectrum (MeOH) showed absorption maxima at the wavelengths 215, 252 and 295 nm, a characteristic of biphenyl type cyclic diarylheptanoid.

The ^{1}H NMR spectrum shows two methoxy groups at δ_H 3.81 and 3.93 ppm singlets, integrating for 3H each, assigned to position C-20 and C-21. Four aromatic protons assigned to position C-15, C-16, C-18 and C-19 of the aglycone. Six methylenes assigned to position C-7, C-8, C-9, C-10, C-12 and C-13. Carbonyl group at δ_C 216.1 ppm was assigned to position C-11 based on HMBC experiment due to long range correlation between $\delta_{H\text{-}10}$ 2.77/2.64 ppm, $\delta_{H\text{-}12}$ 2.93/2.80 ppm, $\delta_{H\text{-}13}$ 2.95 ppm and the carbonyl carbon at δ_C 216.1 ppm. Two anomeric protons observed at $\delta_{H\text{-}1'}$ 4.97 ppm, d, *J* = 7.2 Hz and $\delta_{H\text{-}1''}$ 4.83 ppm, brs, indicating the presence of two sugar moieties with a β-D and α-L-configuration. The position of glycosidic linkages were elucidated from HMBC experiment. Long-range correlation was observed between $\delta_{H\text{-}1}$ 4.97 ppm and C-17 (δ_C 152.7 ppm) of the aglycone as well as $\delta_{H\text{-}1''}$ 4.83 ppm and a C-6' (δ_C 68.0 ppm) of the glucose.

Therefore, it was concluded that, the two sugar groups are attached to C-17 of the aglycone. The NMR signals of the aglycone were similar to those of myricanone (compound **12**).

The attached glycosides were confirmed to β-D-glucopyranoside and *α*-L-arabinofuranoside as described in section **3.3.5.2.1**. The furan ring of the *α*-L-arabinose was concluded based on its carbon chemical shifts as described by Beier and Mundy[174].

Based on the obtained data, compound **24** was identified to be myricanone 17-*O*-α-L-arabinofuranosyl-(1-6)-β-D-glucopyranoside and named saliciclaireone C. The 1D and 2D-NMR data of compound **24** are summarized in **Table 3.22**.

Table 3.22: 1D and 2D NMR data for compound **24**. ^{1}H NMR (600 MHz), ^{13}C NMR (150 MHz), MeOH-d_4, 298 K.

Pos.	δ_C (ppm)	δ_H (ppm), m, *J* (Hz)	HMBC	COSY	NOESY
1	126.5				
2	129.6				
3	146.5				
4	148.9				
5	149.9				
6	127.6				
7	28.2	2.75-2.71, (1H, m)		8	
		2.98-2.94, (1H, m)			
8	25.6	1.92-1.87, (2H, m)		9, 7	19, 7, 9
9	22.9	1.77-1.72, (2H, m)		18, 10	
10	45.8	2.83-2.78, (1H, m)	11, 8	9	7
		2.64-2.58, (1H, m)			
11	216.1				
12	42.7	2.81-2.77, (1H, m)	13, 15, 14, 18, 11		
		2.93, (1H, m)			
13	28.7	2.95, (2H, m)	15, 14, 11, 12		12, 16, 15
14	132.8				
15	129.8	7.03, (1H, dd, *J* = 8.7, 2.9)	13, 14, 18, 17	16	13, 16, 18
16	117.1	6.78, (1H, d, *J* = 8.2)	1, 14, 17	15	15
17	152.7				
18	133.8	6.67, (1H, d, *J* = 2.3)	13, 1, 2, 17		9, 12, 7, 15
19	129.7	6.58, (1H, s)	7, 1, 6, 3, 4, 5		9, 8, 18
20	61.8	3.93, (3H, s)	3		
21	61.6	3.81, (3H, s)	4		
Sug.					
1’	104.9	4.97, (1H, d, *J* = 7.2)	17	2‘	2‘
2’	75.3	3.44, (1H, m)	4‘, 3‘, 1‘	1‘, 4‘	
3’	77.5	3.43, (1H, m)			
4’	75.3	3.44, (1H, m)	4‘, 3‘, 1‘		
5’	76.6	3.38, (1H, m)	3‘		6‘

Pos.	δ_C (ppm)	δ_H (ppm), m, *J* (Hz)	HMBC	COSY	NOESY
6’	68.0	3.96, (1H, dd, *J* = 11.0, 2.1) 3.56, (1H, m)		5’, 6’	5’, 4’
1’’	109.6	4.83, (1H, brs)	6‘, 4“	2“	6‘
2’’	82.8	3.91, (1H, m)	3“	1“, 3“	3“, 4“
3’’	78.6	3.78, (1H, m)	2“	2“	5“
4’’	85.6	3.83, (1H, m)		5“	5”, 3”
5’’	62.7	3.67, (1H, dd, *J* = 11.7, 3.2) 3.58, (1H, m)	4”	5”, 4”	4”

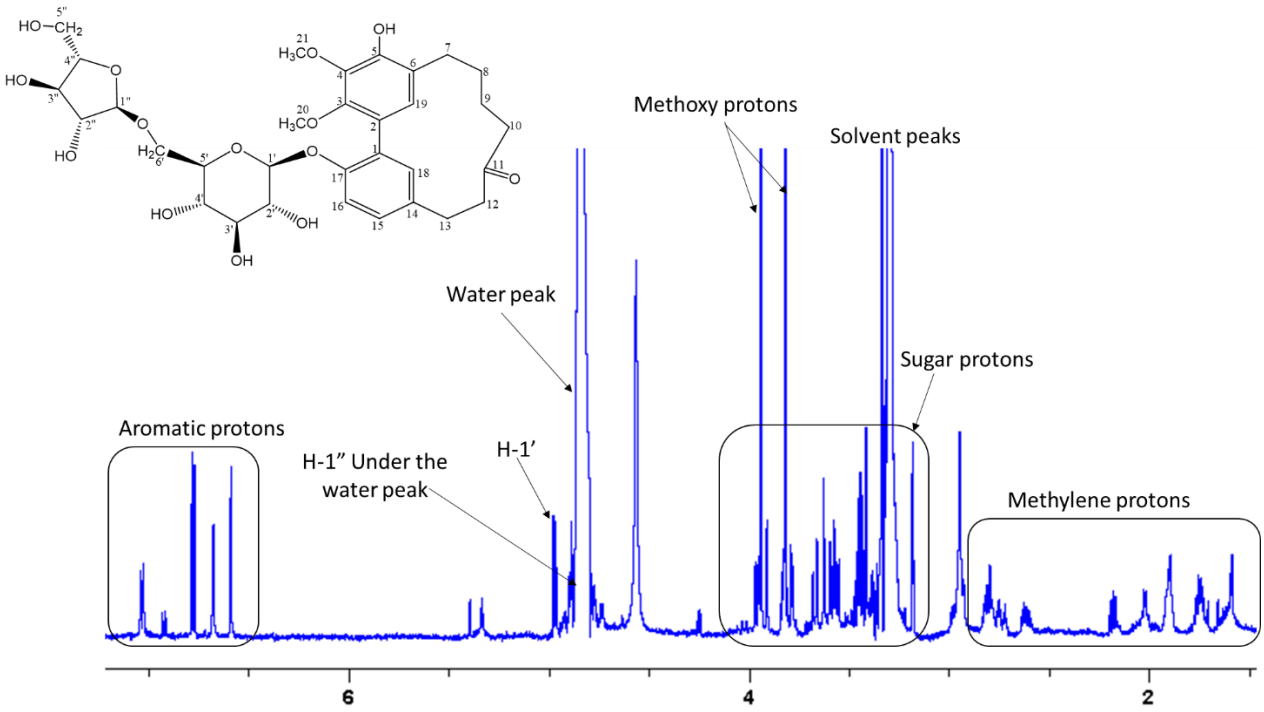

Figure 3.76: ^{1}H NMR spectrum of compound **24**. ^{1}H NMR (600 MHz), ^{13}C NMR (150 MHz), MeOH-d_4, 298 K.

Compounds 25 and 26

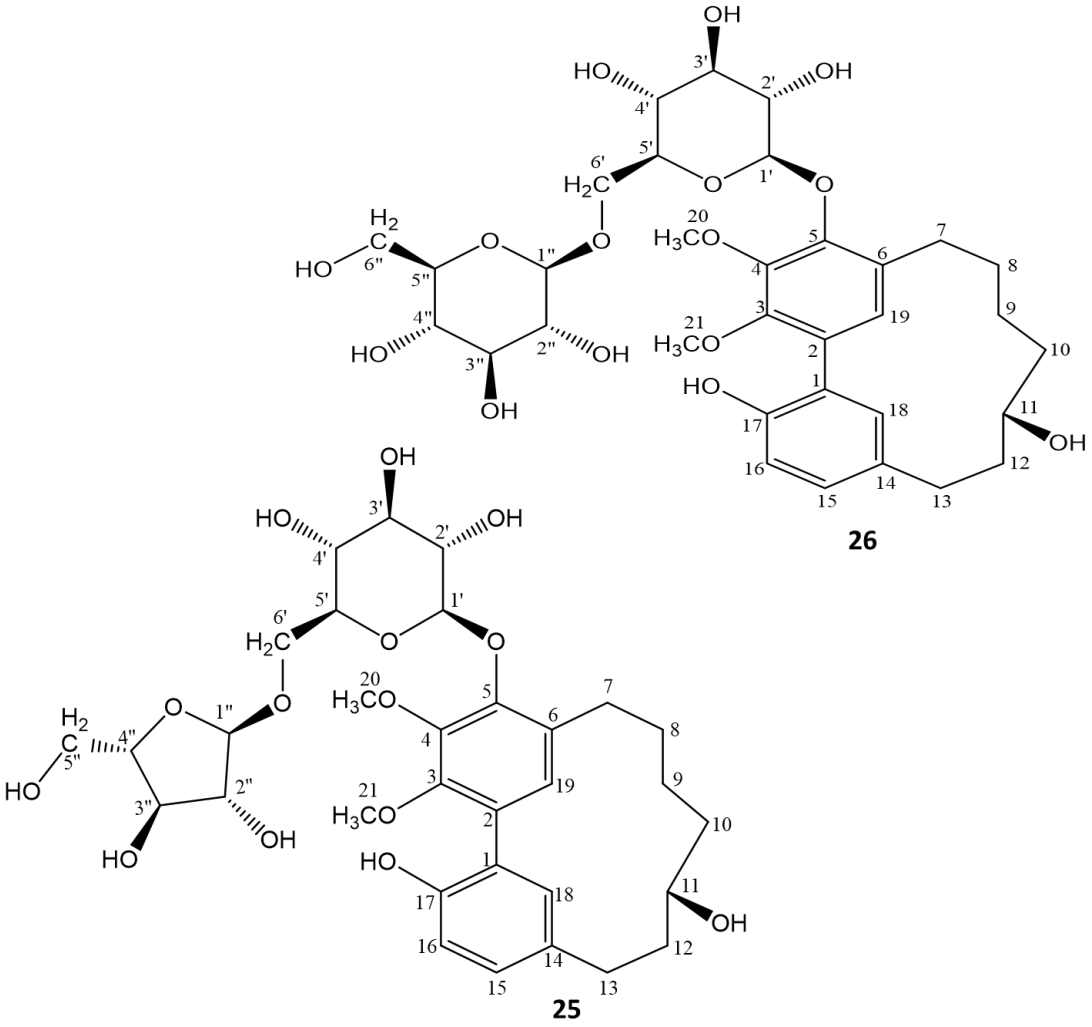

Figure 3.77: Structures of myricanol 5-*O*-α-L-arabinofuranosyl-(1-6)-β-D-glucopyranoside **(25)** and myricanol 5-*O*-β-D-glucopranosyl-(1-6)-β-D-glucopyranoside or myricanol gentiobioside **(26)**.

Compounds **25** (myricanol 5-*O*-α-L-arabinofuranosyl-(1-6)-β-D-glucopyranoside) and **26** (myricanol 5-*O*-β-D-glucopranosyl-(1-6)-β-D-glucopyranoside or myricanol gentiobioside) **(Figure 3.77)** were isolated from S2 subfractions F5.C5 and F5.C7 **(Figure 3.34)**. The structure elucidation of the two compounds were achieved based on obtained spectroscopic data in comparison to literature data by Sakurai et al.[129] **(25)** and Yaguchi et al.[128] **(26)**. The ^{13}C NMR data of the two compounds were similar, their differences were observed in carbon shifts of their sugar moieties. The ^{1}H and ^{13}C NMR data are summarized in **Table 3.23** and other characteristics are listed below.

Compound **25** (myricanol 5-*O*-α-L-arabinofuranosyl-(1-6)-β-D-glucopyranoside): White amorphous powder, purple- blue spot on TLC (mobile phase MP_1, R_f value ~ 0.40) when visualized under VIS and fluorescent blue under UV 366 nm **(Figure 3.49)**. ESI-MS exhibited ions at *m/z* 651.26 $[M-H]^-$ and 1303.5 $[2M–H]^-$ in the negative mode, calculated for molecular formula $C_{32}H_{44}O_{14}$. Optical rotation was $[\alpha]_D^{25}$= -56 (c 0.1, MeOH). UV absorption maxima (MeOH) at the wavelengths 212, 255 and 298 nm.

Compound **26 (**myricanol 5-*O*-β-D-glucopranosyl-(1-6)-β-D-glucopyranoside), a myricanol gentiobioside has the following characteristics: white amorphous powder, purple-blue spot on TLC (R_f value ~ 0.31), ESI-MS, *m/z* 681.27 $[M-H]^-$ in the negative mode, calculated mass = 682 Da and molecular formula of $C_{33}H_{46}O_{15}$, optical rotation value $[\alpha]_D^{25}$= -73 (c 0.1, MeOH), UV absorption maxima (MeOH) at 212, 255 and 298 nm.

Table 3.23: NMR data for compounds **25** and **26**. ^{1}H NMR (600 MHz), ^{13}C NMR (150 MHz), MeOH-d_4, 298 K.

Pos.	**25**		**26**	
	δ_C (ppm)	**δ_H (ppm), m, *J* (Hz)**	**δ_C (ppm)**	**δ_H (ppm), m, *J* (Hz)**
1	126.5		129.7	
2	129.6		126.6	
3	146.5		146.5	
4	149.3		149.4	
5	149.9		149.7	
6	131.3		131.2	
7	27.6	2.97-2.93, (1H, m)	27.5	2.93-2.81, (1H, m)
		2.68-2.63, (1H, m)		2.68-2.63, (1H, m)
8	27.1	1.84-1.79, (2H, m)	27.1	1.94-1.87, (1H, m)
				1.84 – 1.78, (1H, m)
9	24.1	1.59-1.50, (1H, m)	24.0	1.59-1.49, (1H, m)
		1.46-1.40,(1H, m)		1.44-1.40, (1H, m)
10	40.5	1.95-1.88, (1H, m)	40.4	1.84-1.78, (1H, m)
		1.59-1.50, (1H, m)		1.59-1.49, (1H, m)
11	69.4	3.92, (1H, m)	69.2	3.90, (1H, m)
12	35.8	2.27-2.21, (1H, m)	35.7	2.26-2.21, (1H, m)
		1.67-1.61, (1H, m)		1.66-1.62, (1H, m)
13	28.2	2.90-2.82, (2H, m)	28.1	2.93-2.81, (2H, m)
14	132.0		132.0	
15	131.0	7.03, (1H, dd, *J* = 2.1, 8.2)	131.0	7.03, (1H, dd, *J* = 8.2, 1.9)
16	117.3	6.77, (1H, d, *J* = 8.1)	117.3	6.78, (1H, d, *J* = 8.2)
17	153.0		152.8	
18	135.1	7.10, (1H, d, *J* = 1.8)	135.1	7.08, (1H, brs)
19	130.5	6.83, (1H, s)	130.5	6.83, (1H, s)
20	62.1	3.97,(3H, s)	62.1	3.97, (3H, s)
21	61.6	3.89, (3H, s)	61.6	3.88, (3H, s)
Glyc.				
1’	105.4	4.94, (1H, d, *J* = 7.3)	105.1	5.01, (1H, d, *J* = 7.10)
2’	75.7	3.46-3.39, (1H, m)	75.7	3.48-3.43, (1H, m)
3’	76.9	3.46-3.39, (1H, m)	77.8	3.48-3.43, (1H, m)
4’	72.0	3.36-3.33, (1H, m)	71.5	3.48-3.43, (1H, m)
5’	78.0	3.46-3.39, (1H, m)	77.6	3.48-3.43, (1H, m)
6’	68.1	3.94, (1H, m)	69.7	4.07, (1H, brd, *J* = 11.5)
		3.58-3.55, (1H, m)		3.77-3.759, (1H, m)
1’’	109.8	4.82, (1H, brs)	104.5	4.23, (1H, d, *J* = 7.7)
2’’	83.1	3.88, (1H, m)	75.0	3.15-3.09, (1H, m)
3’’	78.8	3.75, (1H, m)	77.9	3.21-3.19, (1H, m)
4’’	85.7	3.84-3.81, (1H, m)	71.5	3.21-3.19, (1H, m)
5’’	62.9	3.65, (1H, m)	77.9	3.15-3.09, (1H, m)
		3.58-3.55, (1H, m)		
6’’			62.7	3.79, (1H, dd, *J* = 11.8, 2.2)
				3.59, (1H, dd, *J* = 5.8, 11.8)

3.3.5.3 Methylated ellagic acid glycosides (MEAG)

Methylated ellagic acid glycosides (MEAG) are derivatives of ellagic acid. They were also isolated from S2 subfractions. The TLC overview of the isolated MEAG is shown in **Figure 3.78**. All isolated MEAG were detected as fluorescent blue spots when visualized under UV 366 nm after spraying with anisaldehyde-sulphuric acid. No detection was observed prior spraying with anisaldehyde-sulphuric acid reagent on the plate and after spraying when visualized under visible light (VIS).

Three MEAG were successfully isolated and their detailed structure elucidation is described in the succeeding subsections. The assignment of ^{1}H and ^{13}C NMR spectra was based on reported literature data of ellagic acid as reference compound. Further to this, the most important tool used for assignment of quaternary carbon signals on the ellagic acid of isolated MEAG was the long range C-H correlation from HMBC experiment. Assignment of position of the methoxy groups and glycoside was deduced from long range HMBC and a NOESY experiment of the particular compound.

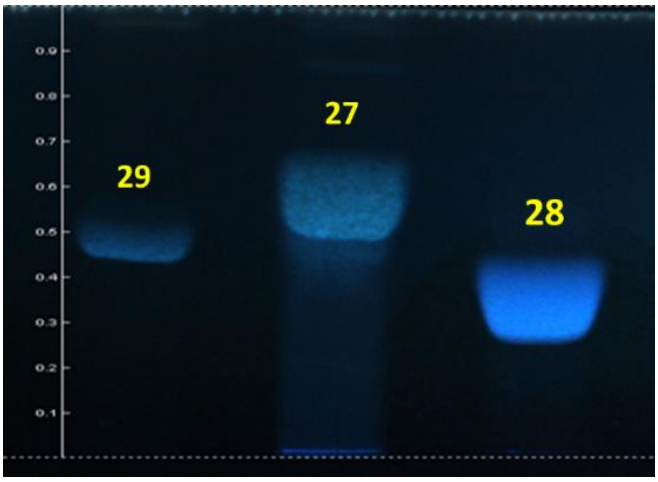

Figure 3.78: NP-TLC overview of the isolated MEAG, compounds **27, 28 and 29**. Mobile phase MP_1. Detection: UV 366 nm. Spraying reagent: anisaldehyde-sulphuric acid.

Compound 27

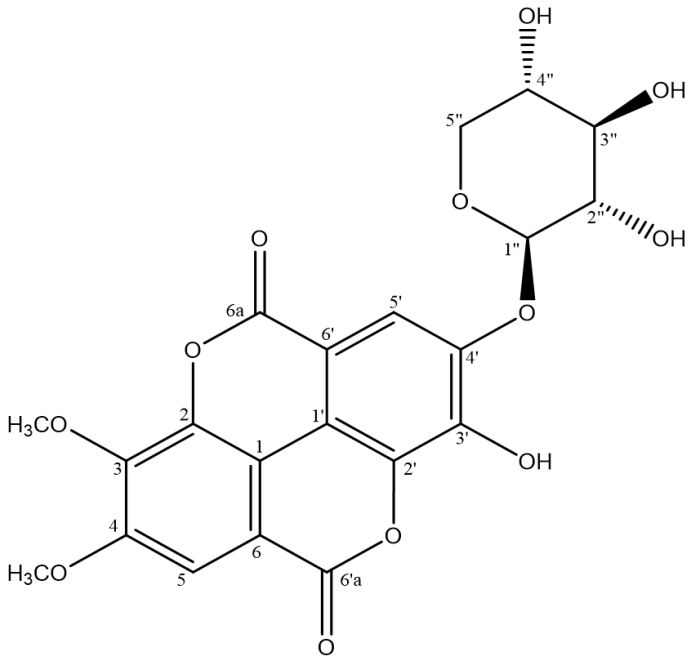

27

Figure 3.79: Structure of myriside: 3,4 di-*O*-methyl ellagic acid 4'-*O*-β-D-xylopyranoside **(27).**

Compound **27 (Figure 3.79)** was identified as 3,4 di-*O*-methyl ellagic acid 4'-*O*-β-D-xylopyranoside, a new MEAG and was given a name myriside**. 27** was isolated as yellowish amorphous powder with $[\alpha]_D^{25}$= -38.3 (c 0.1, MeOH) and it displayed a fluorescent blue spot on TLC with R_f value ~ 0.60 (mobile phase MP_1) after derivatization with anisaldehyde-sulphuric acid reagent **(Figure 3.78)**. The UV spectrum (MeOH) showed absorption maximum at 255.1 nm. The molecular formula of $C_{21}H_{17}O_{12}$ for myriside was achieved based on the HREIS-MS exhibited ions at *m/z* 461.0735 $[M-H]^-$ and 923.1510 $[2M–H]^-$ in the negative mode.

The ^{1}H NMR spectrum of **27** showed two methoxy group protons signals at δ_H 4.10 and 4.01 ppm directly correlated to δ_C 62.0 and 57.1 ppm in the HSQC experiment, and were assigned to position C-3 and C-4. The assignment of methoxy groups to position C-3 and C-4 was determined by the long range HMBC correlation between δ_H 4.10 ppm and $\delta_{C\text{-}3}$ 142.6 ppm, δ_H 4.01 ppm and $\delta_{C\text{-}4}$ 155.6 ppm as well as between δ_H 7.68 ppm and $\delta_{c\text{-}3}$ and $\delta_{c\text{-}4}$. Further hint for the methoxy groups assignment was based on the observed cross peak between $\delta_{H\text{-}5}$ 7.68 ppm and $\delta_{H\text{-}4}$ 4.01 ppm in the NOESY experiment.

Two singlets signals were further observed in the aromatic region at δ_H 7.68 and 7.69 ppm each integrated for one proton. These protons were found to have direct correlation in the HSQC with $\delta_{C\text{-}5}$ 108.0 ppm and $\delta_{C\text{-}5'}$ 113.4 ppm. From the long range correlation HMBC experiment between these two protons and quaternary carbons signals resulted to the assignment of carbon values at position C-1, C-2, C-3, C-4, C-6 and C-6a and their respective primed numbers were achieved.

Anomeric proton signal was observed at $\delta_{H\text{-}1''}$ 4.76 ppm, d, J =7.5 Hz and other four sugar protons signals between δ_H 3.99 - 3.41 ppm, their respective carbon values were obtained in the direct correlation HSQC experiment. Assignment of their positions at C-2'', C-3'', C-4''and C-5'' were based on homonuclear H-H COSY experiment through their proton couplings network. The position of the glycosidic linkage at C-4' was determined by long range correlation HMBC between anomeric proton $\delta_{H\text{-}1''}$ 4.76 ppm and C-4' carbon at δ_C 152.9 ppm. This was further confirmed in the NOESY following observation of cross peak between $\delta_{H\text{-}5'}$ 7.69 ppm and $\delta_{H\text{-}1''}$ 4.76 ppm

Confirmation of sugar type and its absolute configuration was performed as described in **3.3.6.2.1**. The 1D and 2D NMR data of **27** are summarized in **Table 3.24**. Determination of the sugar configuration was achieved as explained in section **3.3.5.2.1**.

Table 3.24: 1D and 2D NMR data for compound **27**. ^{1}H NMR (600 MHz), ^{13}C NMR (150 MHz), MeOH-d_4, 298 K.

Pos.	δ_C (ppm)	δ_H (ppm), m, *J* (Hz)	HMBC	COSY	NOESY/ROESY
1	98.6				
2	139.5				
3	142.6				
4	155.6				
5	108.0	7.68, (1H, s)	1, 6, 3, 4, 6a		4- OMe
6	115.1				
6a	162.2				
1’	98.6				
2’	139.5				
3’	142.6				
4’	152.9				
5’	113.4	7.69, (1H, s)	1’, 6’, 2’, 4’, 6a’		1”
6’	115.6				
6a’	162.5				
3-OCH_3	62.0	4.10, (3H, s)	3		
4- OCH_3	57.1	4.01, (3H, s)	4		5
Sug.					
1’’	104.7	4.76, (1H, d, *J* = 7.5)	5”, 2", 3”, 4’	2’	3”, 2”, 5’
2’’	74.6	3.57-3.53, (1H, m)	3”, 1”, 5”	1’, 3’	
3’’	77.2	3.46-3.40, (1H, m)	3”, 1”, 5”,2”	2’	
4’’	71.1	3.61-3.58, (1H, m)	3”, 5”	3’/5’	
5’’	67.1	3.99, (1H, m)	3”, 1”, 4”	5’, 4’	
		3.46-3.41, (1H, m)			

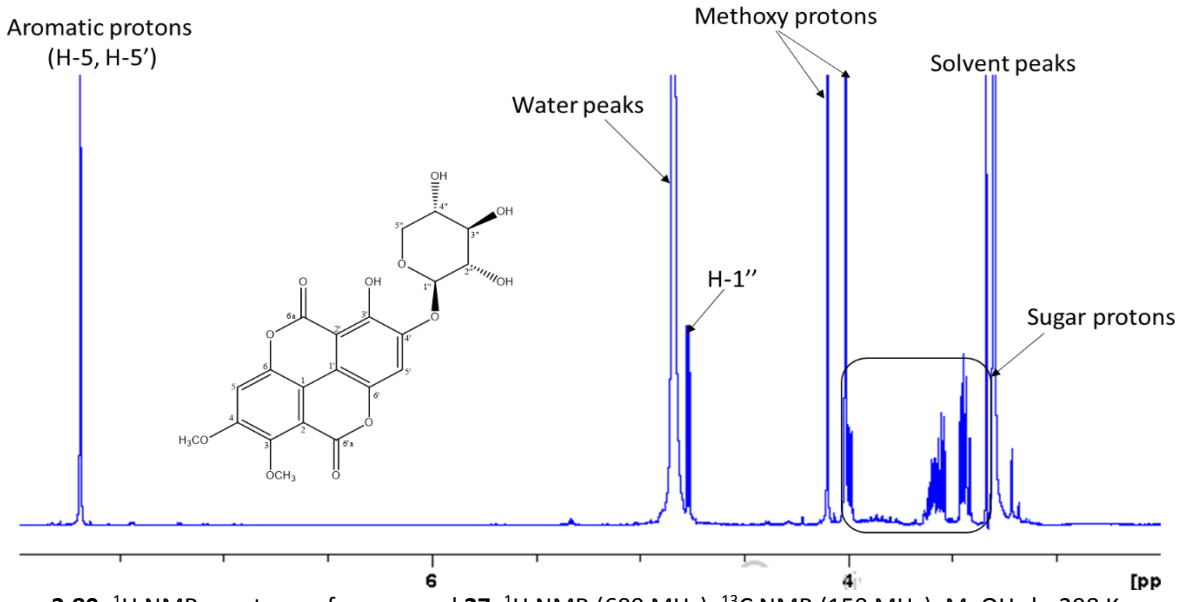

Figure 3.80: ^{1}H NMR spectrum of compound **27**. ^{1}H NMR (600 MHz), ^{13}C NMR (150 MHz), MeOH-d_4, 298 K.

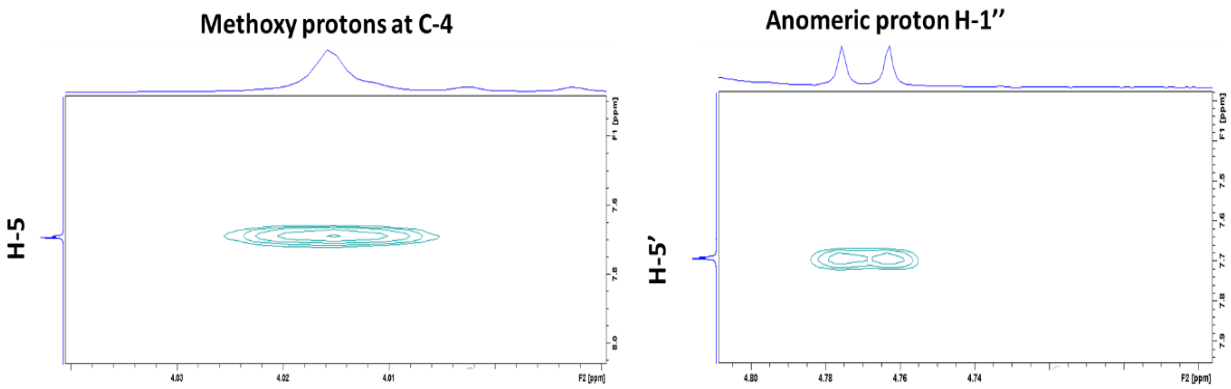

Figure 3.81: NOESY correlation between methoxy protons at position 4 and proton H-5, a proof that they are in neighbouring position. Likewise for the anomeric proton (H-1") and H-5'. The later enabled the assignement of glycosidic linkage at position 4'.

Compounds 28 and 29

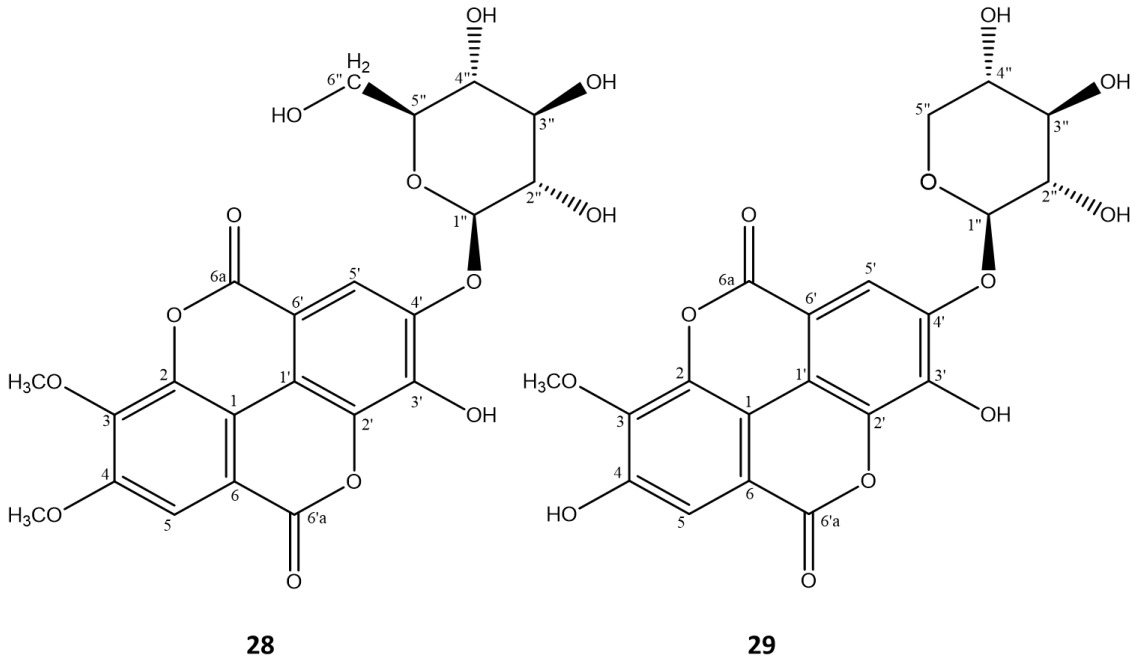

28 **29**

Figure 3.82: Structures of largertannin **(28)** and ducheside A **(29)**.

Compound **28** and **29 (Figure 3.82)** were identified as largertannin (3,4 di-*O*- methyl ellagic acid 4'-*O*- β-D-glucopyranoside) and ducheside A (3-*O*-methyl-ellagic acid 4'-*O*-β-D-xylopyranoside). The isolation and structure elucidation of **29** was reported for the first time by Ye and Yang[175]. The existence of compound **28** was found through searching in SciFinder, unfortunately no reference corresponding to this compound was available. NMR data of **29** was not found for

comparison purposes, though its isolation is reported from few plant species but none of these literature contained the full assignment NMR data of **29**. Therefore, structure confirmation of **28** and **29** was achieved from the following obtained spectroscopic and HRESI-MS data.

NMR data for compounds **28** and **29** were similar to a large extent with those of compound **27** and they both had sugar substitution at C-4'. The difference between **27** and **28** was the attached sugar moiety i.e. D-xylose for **27** and D-glucose for **28**. Moreover, the difference between **27** and **29** was the number of attached methoxy groups i.e. 2 methoxy groups at position C-3 and C-4 for **27** and 1 methoxy group at position C-3 for **29**. Regardless of the above mentioned differences for the three compound, all other obtained 1D and 2D-NMR spectra data were quite similar for the three compounds. The proton and carbon NMR for compounds **28** and **29** is given in **Table 3.25**.

Further characteristics of **28** were: yellowish amorphous powder with optical rotation $[\alpha]_D^{25}$= -24.6 (c 0.1, MeOH) and R_f value of ~ 0.40 **(Figure 3.78)**. Molecular formula of $C_{22}H_{20}O_{13}$ following HREIS-MS exhibited ions at *m/z* 491.0821 $[M-H]^-$ and 983.1733 $[2M–H]^-$ in the negative mode. The UV spectrum (pyridine) showed absorption maximum at 354.9 nm.

Compound **29** was obtained as yellow amorphous powder, $[\alpha]_D^{25}$= -60 (c 0.1, MeOH), R_f value ~ 0.50 **(Figure 3.78)**. HREIS-MS exhibited ions at *m/z* 449.0716 $[M-H]^-$ in the negative mode corresponding to molecular formula of $C_{20}H_{16}O_{12}$.. The UV spectrum (MeOH) showed absorption maximum at 265.0 nm. The sugar configuration was achieved as described in section **3.3.5.2.1**.

Table 3.25: NMR data for compounds **28** and **29**. ^{1}H NMR (600 MHz), ^{13}C NMR (150 MHz), pyridine-d_5, 298 K.

Pos.	**28**		**29**	
	δ_C (ppm)	**δ_H (ppm), m, *J* (Hz)**	**δ_C (ppm)**	**δ_H (ppm), m, *J* (Hz)**
1	114.0		112.2	
2	142.3		142.8	
3	141.8		141.2	
4	154.9		154.2	
5	107.8	7.79, (1H, s)	112.7	8.02, (1H, s)
6	114.8		114.4	
6a	159.7		159.6	
1’	107.6		106.9	
2’	137.7		137.6	
3’	149.4		145.2	
4’	149.4		149.0	
5’	113.7	8.47, (1H, s)	114.2	8.44, (1H,)
6’	114.0		115.7	
6a’	159.2		159.9	
3-OCH_3	61.5	4.12, (3H, s)	61.2	4.17, (3H, s)
4-OCH_3	56.5	3.83, (3H, s)		
Sug.				
1’’	103. 6	5.94, (1H, d, *J* = 7.7)	104.5	5.78, (1H, d, *J* = 6.6)
2’’	74.8	4.28, (1H, t, *J* = 8.1)	74.5	4.30-4.26, (1H, m)
3’’	71.0	4.35, (1H, m)	78.1	4.30-4.26, (1H, m)
4’’	78.4	4.39, (1H, m)	70.8	4.30-4.26, (1H, m)
5’’	79.1	4.14, (1H, m)	67.5	4.41-4.38, (1H, m)
				3.88-3.82, (1H, m)
6”	62.1	4.42, (1H, dd, *J* = 12.0, 4.7)		
		4.54, (1H, dd, *J* = 12.0, 2.2)		

3.3.5.4 Further compounds

Apart from tannins, diarylheptanoids and MEAG, further two compounds (**30** and **31**) were isolated **(Figure 3.83)**. The structure elucidation of **30** and **31** was accomplished as described in the following sections.

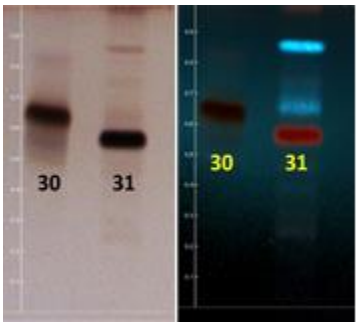

Figure 3.83: NP-TLC overview of the other compounds (**30** and **31**) isolated from fraction S2 of methanolic extract of *M. salicifolia*. Mobile phase MP_1. Detection: VIS **(left)** and UV 366 nm **(right)**. Spray reagent: anisaldehyde-sulphuric acid.

Compound 30

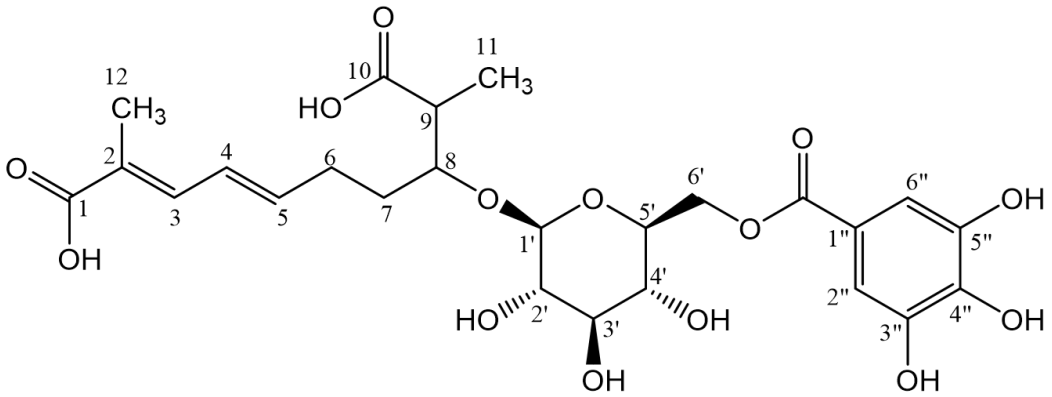

30

Figure 3.84: Structure of 2,9-dimethyl-8-*O*-(6'-O-galloyl)-β-D-glucopyranoside-2,4-dienedioic acid **(30)**.

Compound **30 (Figure 3.84)** was isolated as off-white amorphous powder with optical rotational value $[\alpha]_D^{25}$= -19 (c 0.1, MeOH). HREIS-MS exhibited ions at *m/z* 555.1720 $[M-H]^-$ in the negative mode and *m/z* 557.1862 $[M+H]^+$ in the positive mode , corresponding to molecular formula of $C_{25}H_{32}O_{14}$. The UV absorption maximum (MeOH) was exhibited at 265 nm. On the TLC, **30** displays dark brown spot (R_f value ~ 0.68) following spraying with anisaldehyde-sulphuric acid

reagent and visualized under day light (**Figure 3.83 left,** mobile phase MP_1). The structure elucidation of **30** was achieved with the aid of NMR data summarized in **Table 3.26** and confirmed by the mass and molecular formula obtained from HRESI-MS. From the obtained data it was concluded that **30** contains two double bonds, one sugar and one galloyl moiety. The sugar moiety was deduced to be β-D-glucose as described in section **3.3.5.2.1**. It is the first time the isolation of this compound is reported and its chemical name was deduced to be 2,9-dimethyl-8-*O*-(6'-O-galloyl)-β-D-glucopyranoside-2,4-dienedioic acid.

Table 3.26: 1 and 2D NMR data for compound **30**. ^{1}H NMR (600 MHz), ^{13}C NMR (150 MHz), methanol-d_4, 298 K.

Pos.	**δ_C (ppm)**	**δ_H (ppm), m, *J* (Hz)**	**HMBC**	**COSY**	**NOESY**
1	172.6				
2	126.0				
3	140.2	7.03, (1H, d, *J* = 11.0)	12, 2, 4, 5, 1	12, 4	5, 4
4	128.3	6.25, (1H, dd, *J* = 11.4, 14.9)	6, 2, 3	5, 3	5, 7
5	143.3	5.99-5.94,(1H, m)	6, 9, 3	6, 4	3, 4, 7, 6
6	37.5	2.46-2.40, (1H, m) 1.9-1.93, (1H, m)	11, 9, 8, 4, 5	5	11, 9, 6/7, 5, 4
7	39.1	2.54-2.51, (1H, m) 2.46-2.40, (1H, m)	6, 8, 1', 5, 10	8	8, 6/7, 5, 4
8	81.6	4.10, (1H, brs)	6, 1'	7, 9	11, 9, 2.42, 6/7
9	38.5	1.86, (1H, brs)			11, 7
10	178.0				
11	14.6	0.83, (3H, d, *J* = 6.9).	6, 9, 8	9	
12	12.8	1.79, (3H, s)	1, 4, 3, 5,		
Gluc.					
1'	103.9	4.43, (1H, d, *J* = 7.7)	2', 3', 8	2'	2', 4',3',
2'	75.4	3.19, (1H, m)	5', 1'	1', 3'	
3'	75.4	3.58-3.55, (1H, m)	4', 5' 1'	4'	
4'	72.0	3.38, (1H, m)	6', 4', 2', 3', 5'		
5'	78.1	3.38, (1H, m)	6', 4', 3', 5'		
6'	64.9	4.50, (1H, dd, *J* = 11.7, 2.0) 4.38, (1H, dd, *J* = 11.7, 6.6)	3', 4', C=O		
Gal.					
1"	121.6				
2"/6"	110.3	7.09, (2H, s)	2"/6", 1", 4", 3"/5",2, C=O		
3"/5"	146.5				
4"	139.8				
C=O	168.3				

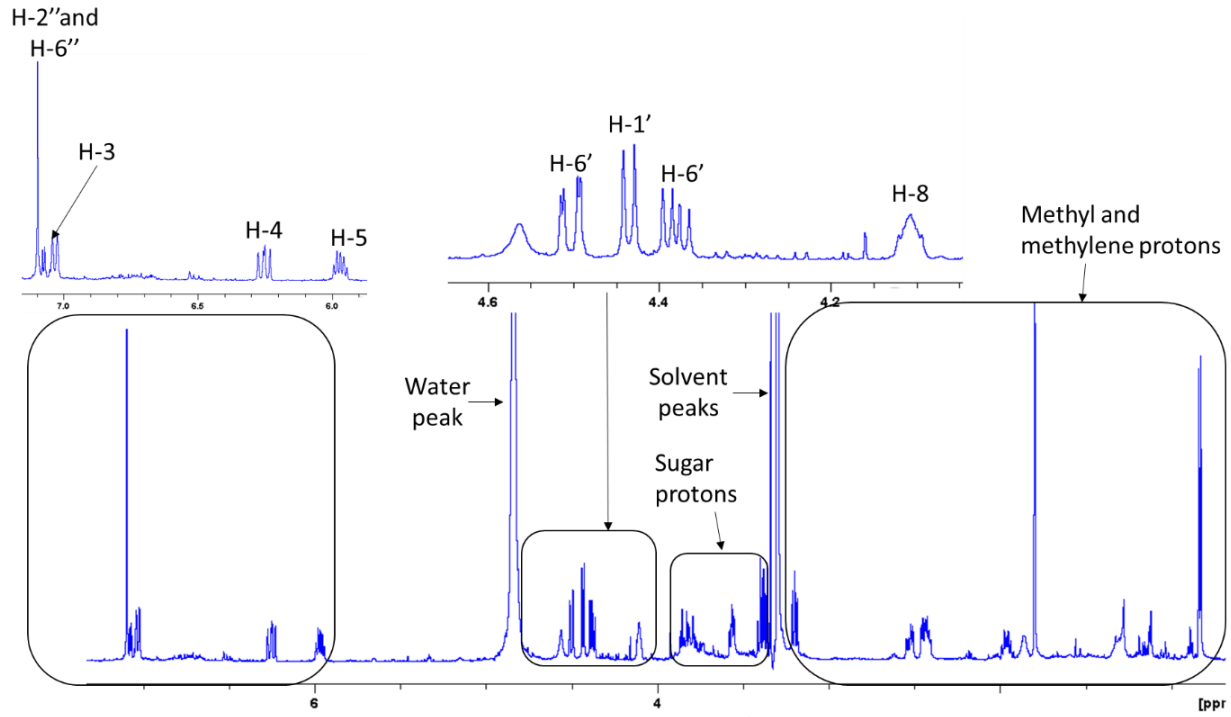

Figure 3.85: ^{1}H NMR spectrum of compound **30**. ^{1}H NMR (600 MHz), ^{13}C NMR (150 MHz), MeOH-d_4, 298 K.

Compound 31

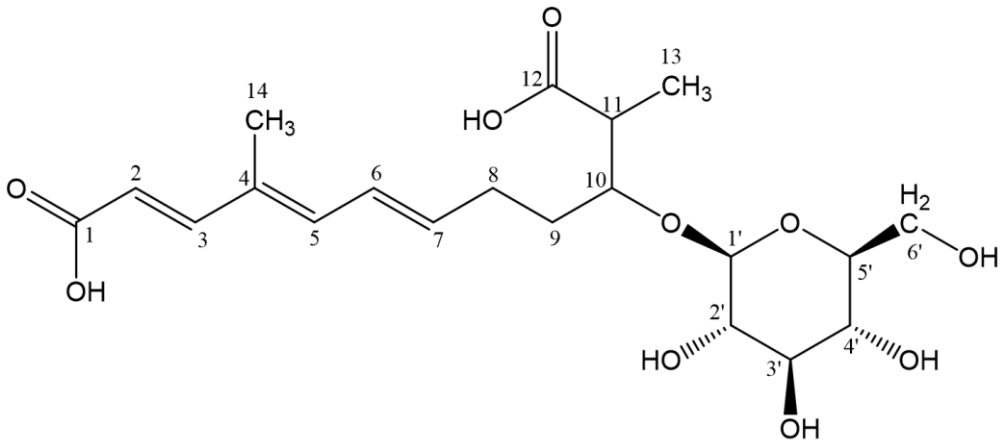

31

Figure 3.86: Structure of 4,11-dimethyl-10-*O*-β-D-glucopyranoside-2,4,6-trienedioic acid **(31)**.

Compound **31 (Figure 3.86)** was isolated as off-white amorphous powder with optical rotation value of $[\alpha]_D^{25}$= -22 (c 0.1, MeOH). On the TLC **31** shows a deep dark brown spot (R_f value ~ 0.58) following spraying with anisaldehyde-sulphuric acid reagent and visualization under visible light (VIS) and a florescent reddish spot under UV 366 nm. In the UV spectrum (MeOH) of

31, absorption maximum was observed at wavelength 295 nm. HREIS-MS exhibited ions at *m/z* 429.1766 $[M-H]^-$ in the negative mode and *m/z* 448.2175 $[M+NH_4]^+$ in the positive mode , corresponding to molecular formula of $C_{20}H_{30}O_{10}$.

The 1D and 2D NMR data of **31** are summarized in **Table 27**. From the obtained spectroscopic data, **31** was concluded to be 4,11-dimethyl-10-*O*-β-D-glucopyranoside-2,4,6-trienedioic acid. In comparison to compound **30**, compound **31** was found to contain no galloyl moiety and possessing longer chain (C-14). Compound **31** is a new compound and is not yet reported in the literature.

Table 3.27: 1 and 2D NMR data for compound **31**. ^{1}H NMR (600 MHz), ^{13}C NMR (150 MHz), methanol-d_4, 298 K.

Pos.	**δ_C (ppm)**	**δ_H (ppm), m, *J* (Hz)**	**HMBC**	**COSY**	**NOESY**
1	172.2				
2	118.8	5.83, (1H, d, *J* = 15.5)	4, 1,	3	11, 3
3	149.9	7.26, (1H, d, *J* = 15.5)	14, 2, 4, 5, 1	2	11, 2, 5
4	132.5				
5	139.8	6.38, (1H, d, *J* = 11.6)	14, 6, 7, 3	11, 6	11, 7, 3
6	128.9	6.49, (1H, dd, *J* = 14.8, 11.3)	8, 4	7, 5	13, 11, 8
7	140.8	6.02, (1H, d, *J* = 7.4)	8, 11, 6, 4, 5	8, 6	13, 8, 5
8	37.1	2.57-2.54, (1H, m) 2.04-1.98, (1H, m)	13, 9, 10, 6, 7	9, 7	13, 7
9	39.2	2.51, (1H, dd, *J* = 15.2, 7.5) 2.43, (1H, dd, *J* = 15.2, 5.4)	10, 12, 11	10	10, 1', 13
10	81.3	4.10, (1H, m)	8, 11, 1', 12	9, 11	13, 11, 9, 1'
11	38.6	1.91-1.89, (1H, m)		10	13, 8, 10
12	178.2				
13	15.0	0.92, (3H, d, *J* = 6.8)	8, 11, 10		11, 8, 9, 10
14	12.5	1.87, (3H, s)	4, 5, 3		2, 6
Gluc.					
1'	103.8	4.39, (1H, d, *J* = 7.7)	5', 10	2'	11, 9, 2', 5', 10
2'	75.4	3.16, (1H, dd, *J* = 8.8, 7.9)	3', 1'	1'	
3'	78.1	3.36, (1H, t, *J* = 8.8)	4', 2'	2'	1'
4'	71.6	3.31, (1H, m)	6', 3'		1'
5'	77.9	3.27-3.25, (1H, m)		6'	
6'	62.8	3.84, (1H, dd, *J* = 11.7, 2.3) 3.68, (1H, dd, *J* = 11.7, 5.2)	4', 3'	5'	5'

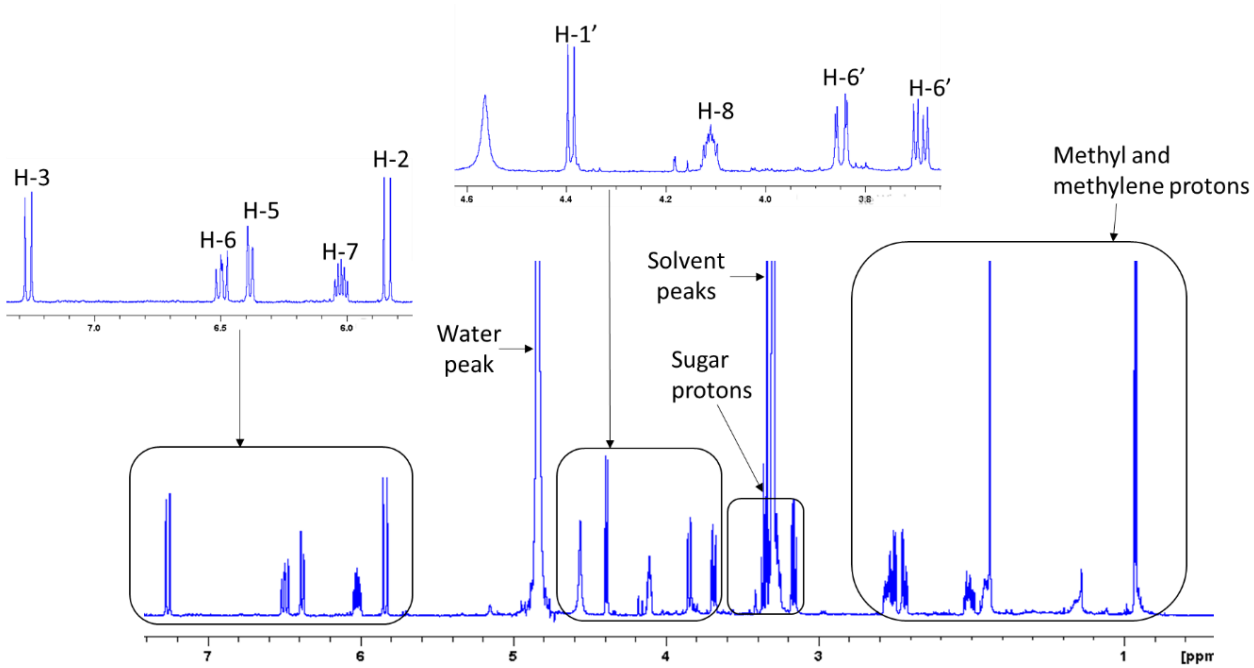

Figure 3.87: ^{1}H NMR spectrum of compound **31**. ^{1}H NMR (600 MHz), ^{13}C NMR (150 MHz), MeOH-d_4, 298 K.

3.4 Summary and discussion of the isolated compounds from *M. salicifolia* bark

3.4.1 Summary on the isolated compounds

Phytochemical characterization of *M. salicifolia* bark methanolic extract resulted in isolation and structure elucidation of 31 compounds. The identified compounds belongs to various groups such as: condensed tannins **(1 - 8)**, hydrolysable tannins **(9)**, cyclic diarylheptanoids **(10 – 26)**, ellagic acid derivatives **(27 – 29)** and others **(30 – 31)**. 10 out of 31 elucidated compounds were identified to be completely new and not to be reported in literature yet. 1 dimeric A-type prodelphinidin **(7)**, 6 cyclic diarylheptanoid glycosides **(16 – 18** and **22 - 24)**, 1 methylated ellagic acid glycoside **(27)** and 2 other compounds **(30** and **31)**. A list of isolated compounds is shown in **Table 3.28**.

Table 3.28: Summary of the isolated compounds obtained from the methanolic extract of *M. salicifolia* bark.

	Compound, amount and status.	**Colour of the amorphous powder**	**Molecular formula**	**Mass (Da)**	**UV. Max. (nm)**	**Optical rotation** (c 0.1, MeOH)
Tannins						
1	gallocatechin (49.0 mg). **KNOWN**	Light orange	$C_{15}H_{14}O_7$	306	270 (MeOH)	+25.06
2	epigallocatechin-3-*O*-gallate (1.1 mg). **KNOWN**	Light orange	$C_{22}H_{18}O_{11}$	458	275 (MeOH)	-96.8
3	prodelphinidin B1: (-)-epigallocatechin-(4β→8)-gallocatechin (2.3 mg). **KNOWN**	Light orange	$C_{30}H_{26}O_{14}$	610	270 (MeOH)	-15.33
4	epigallocatechin-3-*O*-gallate-(4β→8)-gallocatechin (12.5 mg). **KNOWN**	Orange	$C_{37}H_{30}O_{18}$	762	275 (MeOH)	+168
5	epigallocatechin-(4β→8)-gallocatechin 3-*O*-gallate (9.1 mg). **NEW** **(**further proof needed)	Orange	$C_{37}H_{30}O_{18}$	762	275 (MeOH)	+ 220

	Compound, amount and status.	**Colour of the amorphous powder**	**Molecular formula**	**Mass (Da)**	**UV. Max. (nm)**	**Optical rotation** (c 0.1, MeOH)
6	ephedrannin D5: (-)-epigallocatechin-(2β→*O*→7,4β→8)–gallocatechin (6.0 mg). **NEW** to the genus	Orange	$C_{30}H_{24}O_{14}$	608	270 (MeOH)	-82.4
7	myricedin: (+)-gallocatechin-(2β→*O*→7,4β→8)-gallocatechin (0.7 mg). **NEW**	Orange	$C_{30}H_{24}O_{14}$	608	279 (MeOH)	-22.6
8	adenodimerin C: (+)-gallocatechin-3-O-gallate (2β→*O*→7,4β→8)–gallocatechin (3.0 mg). **KNOWN**	Orange	$C_{37}H_{28}O_{18}$	760	275 (MeOH)	+20.5
9	castalagin (1.6 mg). **KNOWN**	Off-white	$C_{41}H_{26}O_{26}$	934	-	+15.6
Cyclic diarylheptanoids						
10	juglanin B-sulphate (1.0 mg). **KNOWN**	Off-white	$C_{20}H_{24}O_7S$	408	254, 300 (MeOH)	-12.5
11	myricanol (30.5 mg). **KNOWN**	White	$C_{21}H_{26}O_5$	358	259.9, 298 (MeOH)	-76.5
12	myricanone (6.6 mg). **KNOWN**	Off-white	$C_{21}H_{24}O_5$	356	259.9, 300 (MeOH)	-26
13	myricanol 5-*O*-β-D-glucose (77.0 mg). **KNOWN**	White	$C_{27}H_{36}O_{10}$	520	216, 255.1, 299 ((MeOH))	-52.4
14	myricanone 5-*O*-β-D-glucose (10.2 mg). **KNOWN**	Off-white	$C_{27}H_{34}O_{10}$	518	254, 280 ((MeOH)	-44
15	myricanol 11-*O*-β-D-xylopyranoside (0.7 mg). **KNOWN**	White	$C_{26}H_{34}O_9$	490	214, 260, 298. (MeOH)	-80.8

	Compound, amount and status.	**Colour of the amorphous powder**	**Molecular formula**	**Mass (Da)**	**UV. Max. (nm)**	**Optical rotation** (c 0.1, MeOH)
16	salicimeckol: 7-hydroxymyricanol 5-*O*-β-D-glucose (2.5 mg). **NEW**	White	$C_{27}H_{36}O_{11}$	536	213, 250, 295 (MeOH)	-56
17	salicireneol A: Juglanin B 3-*O*-β-D-glucoside (0.5 mg). **NEW**	White	$C_{26}H_{34}O_{9}$	490	214, 254 285 (MeOH)	-49
18	salicireneol B: 16-hydroxyjuglanin B 17-*O*-β-D-glucoside. (0.7 mg). **NEW**	White		506	216, 253, 298 (MeOH)	-33.6
19	myricanol 5-*O*-β-D-(6'-*O*-galloyl) glucoside (13.3 mg). **KNOWN**	Deep green	$C_{34}H_{40}O_{14}$	672	213, 255, 298 (MeOH)	-52.7
20	myricanol 5-*O*-β-D-(6'-*O*-galloyl) glucoside (5.8 mg). **KNOWN**	Yellow	$C_{34}H_{40}O_{14}$	672	213, 255, 298 (MeOH)	-33.6
21	myricanone 5-*O*-β-D-(6'-*O*-galloyl) glucoside (3.1 mg). **KNOWN**	Off-white	$C_{34}H_{38}O_{14}$	670	213, 255, 280 (MeOH)	-44
22	saliciclaireone A: myricanone 5-*O*-β-D-glucopranosyl-(1-6)-β-D-glucopyranoside (4.2 mg). **NEW**	Off-white	$C_{33}H_{44}O_{15}$	680	214, 250, 300 (MeOH)	-51.6
23	saliciclaireone B: neomyricanone 5-*O*-β-D-glucopranosyl-(1-6)-β-D-glucopyranoside (0.9 mg). **NEW**	Off-white	$C_{33}H_{44}O_{15}$	680	214, 250, 298 (MeOH)	-43.1
24	saliciclaireone C: myricanone 17-*O*-α-L-arabinofuranosyl-(1-6)-β-D-glucopyranoside (0.9 mg). **NEW**	Off-white	$C_{32}H_{42}O_{14}$	650	215, 252, 295 (MeOH)	-36

	Compound, amount and status.	**Colour of the amorphous powder**	**Molecular formula**	**Mass (Da)**	**UV. Max. (nm)**	**Optical rotation** (c 0.1, MeOH)
25	myricanol 5-*O*-α-L-arabinofuranosyl-(1-6)-β-D-glucopyranoside (2.2 mg). **KNOWN**	White	$C_{32}H_{44}O_{14}$	652	212, 255, 298 (MeOH)	-56
26	myricanol gentiobioside**:** myricanol 5-*O*-β-D-glucopranosyl-(1-6)-β-D-glucopyranoside (2.6 mg). **KNOWN**	White	$C_{33}H_{46}O_{15}$	682	212, 255, 298 (MeOH)	-73
Methylated ellagic acid glycosides (MEAG)						
27	myriside: 3,4 di-*O*-methyl ellagic 4'-*O*-β-D-xylopyranoside (1.9 mg). **NEW**	Yellowish	$C_{21}H_{18}O_{12}$	462	255.1 (MeOH)	-38.3
28	largertannin: 3,4 di-*O*-methyl ellagic acid 4'-*O*-β-D-glucopyranoside (6.0 mg). **NEW** to the genus	Yellowish	$C_{22}H_{20}O_{13}$	492	354.9 (Pyridine)	-24.6
29	ducheside A**:** 3-*O*-methyl-ellagic acid 4'-*O*-β-D-xylopyranoside (18.6 mg). **NEW** to the genus	Yellowish	$C_{20}H_{16}O_{12}$	448	265 (MeOH)	-60
Other compounds						
30	2,9-dimethyl-8-*O*-(6'-O-galloyl)-β-D-glucopyranoside-2,4-dienedioic acid (1.4 mg). **NEW**	Off-white	$C_{25}H_{32}O_{14}$	556	265 (MeOH)	-19
31	4,11-dimethyl-10-*O*-β-D-glucopyranoside-2,4,6-trienedioic acid (0.6 mg) **NEW**	Off-white	$C_{20}H_{30}O_{10}$	430	295 (MeOH)	-22

3.4.2 Determination of absolute configuration of isolated diarylheptanoids

The isolated cyclic diarylheptanoids in this study contained either sugar, hydroxyl, carbonyl or sulphate group at their position 11. Some of these compounds possessed further hydroxyl or sugar (mono or diglycoside) attached to either position 3, 5, or 17. Therefore, determination of absolute configuration for these compounds to provide their full stereochemistry was

inevitable. The absolute configuration of the sugars was achieved through an already established method[140]. Determination of absolute configuration of the aglycone was achieved by CD spectra calculations (performed by Prof. Dr. Thomas Schmidt, Institute of Pharmaceutical Biology and Phytochemistry, University of Münster).

Previously, absolute configuration of diarylheptanoids has been achieved through X-ray crystallography, comparison of optical rotations signs with the already established X-ray structure or by using Mosher's reagent method[123].

Determination of absolute configuration of myricanol isolated from *M. nagi* was achieved via X-ray crystallography of a brominated derivative of myricanol[141]. The said myricanol has optical rotation $[\alpha]_D^{27.5}$= -65.6 (c 3% in $CHCl_3$). From the resulting X-ray crystal structure it was concluded that myricanol was 11*R*-configured. Furthermore, the group recorded CD spectra of myricanol as negative cotton effects at 240, 257 and 290 nm. In another study, Joshi et al.[169] determined the absolute configuration of a racemate myricanol ($[\propto]_D$= 0) isolated from *M. cerifera* also by using X-ray crystallography method. They found that the crystal structure of racemate myricanol contained two independent molecules (+)-*aR*,11*S*-myricanol and (-)-*aS*,11*R*-myricanol whereby the second was similar to that of 11*R*-myricanol obtained by Begley et al.[141].

Following X-ray crystallography performed by the group of Begley[141], several groups afterwards concluded the absolute configuration of myricanol based on the optical rotation sign (negative sign (11*R*) and positive sign (11*S*)). Inoue et al.[186] isolated myricanol from *M. rubra* with $[\propto]_D$ = -62.9. Takaeda et al.[131] isolated myricanol from *M. rubra* with $[\propto]_D$ = -27.6 (c 0.65 in $CHCl_3$). Sun et al.[87] isolated myricanol from *M. esculenta* with$[\propto]_D$ = -64 (c 0.05 in $CHCl_3$). The negative optical rotation of the myricanol from different groups were correlated to 11*R*-configuration obtained by X-ray crystallography of brominated derivative of myricanol[141].

Confirmation of the absolute configuration by comparing the optical rotation signs to that of brominated derivative of myricanol[141] was further used for isolated cyclic diarylheptanoids containing attached glycosides[117,126,128,129], galloylglucoside[110,128] or sulphate[110,112] group. The cyclic diarylheptanoid glycosides were cleaved prior measurement of their optical rotations for comparison. They were concluded to have 11*R*- or 11*S*-configuration due to their negative or positive optical rotations respectively.

In this study, a CD simulation method to determine absolute configuration of cyclic diarylheptanoids (*meta,meta*-bridged biphenyls) containing a chiral centre at position 11 was used. The method is described in the material and methods section **3.2.8.8** and in the results section **3.3.5.2.1**. The optical rotation signs of the isolated cyclic diarylheptanoids in this study were negative with different values **(Table 3.28)**. In addition to that, the recorded experimental CD spectra in **Figure 3.54** (**1 – 12**) showed the negative cotton effect at the region of 231, 255 and 296 nm. Based on the similarities of recorded CD spectra (aglycone and the diarylheptanoid glycosides) it was concluded that there was no effect of an attached glycoside or sulphate group to the aglycone. Additionally, matching of the recorded CD spectra to the calculated CD spectra as shown in **Figure 3.56 C** showed very good match between the two spectra. Hence, based on these calculations the absolute configuration of these compounds was confirmed to be 11*R*- and very predominantly *Sa*-configured. The presence of a smaller amount of the *Ra* atropisomer in the conformational equilibrium of these compounds was also concluded due to the observed perfect match of recorded CD spectra to the calculated CD spectra of the equilibrium mixture of *R,Sa* (97%) and *R,Ra* (3%) **(Figure 3.56 D)**.

The obtained absolute configuration of natural myricanol in this study matches very well to the one achieved by X-ray in the group of Begley[141]. However, in this study the established CD calculation of myricanol was further used as a reference and a non-destructive method to determine the absolute configuration of isolated diarylheptanoids containing glycosides or sufate groups. The method used is reliable as the obtained results were in agreement to the published crystal structure. It should also be noted that this method was used to determine the absolute configuration of the *meta,meta*-bridged biphenyls with chiral centre at position 11. There was no sample to prove if the same method can also be applied for the cyclic diarylheptanoids of the *meta,para*- diphenyl ether type as well as for the ones without chiral centre at position 11.

3.4.3 Comparison of isolated compounds from *M. salicifolia* and other plant species

3.4.3.1 Tannins

Isolation of tannins from *Myrica* species has been limitedly reported. However, reisolation of some of these reported tannins was achieved also in *M. salicifolia*. The reisolated compounds are gallocatechin **(1)**, epigallocatechin-3-*O*-gallate **(2)**, adenodimerin C **(8)** and castalagin **(9)**. The existing literature data on previously reported tannins **(Table 3.29)** provide evidence of the taxonomic relationship between *M. salicifolia* and other *Myrica* species.

In addition to that, five prodelphinidins (compounds **3** – **7**) which have not been previously reported in the genus *Myrica* were isolated in this study **(Table 3.29)**. This is the first time that, prodelphinidin B1 (epigallocatechin-(4β→8)-gallocatechin) **(3)**, epigallocatechin 3-*O*-gallate-(4β→8)-gallocatechin **(4)**, epigallocatechin–(4β→8)–gallocatechin 3-*O*-gallate **(5)**, ephedrannin D5 (epigallocatechin (2β→O→7,4β→8)–gallocatechin) **(6)** and myricedin ((+)-gallocatechin-(2β→*O*→7,4β→8)-gallocatechin) (**7**) are reported to the genus *Myrica*.

The isolation of proanthocyanidins from *M. salicifolia* was preceded by a tedious period of searching for the right chromatographic separation method. The same challenge of complex chromatographic separation of proanthocyanidins due to their vast occurrence as similar isomeric oligomers in plant sources is often reported in literature. This could be an answer as to why there are limited literature reports on isolation of individual proanthocyanidins from the genus *Myrica* despite the reported high contents of tannins in the bark of *Myrica* species[87,106]. Such a high content of tannins was also observed in the bark of *M. salicifolia* already after Sephadex® LH-20 fractionation, where 162.46 g of crude methanolic extract yielded a proanthocyanidin polymer fraction of 96.45 g (59.4%) and three further fractions (S4-S7) containing tannins **(Figure 3.25)**.

3.4.3.2 Cyclic diarylheptanoids

The isolation and identification of cyclic diarylheptanoids **(10 - 26)** from the crude methanolic extract of *M. salicifolia* bark further showed its relation to other *Myrica* species. Several cyclic diarylheptanoids have been reported from other *Myrica* species and some of these compounds

were also isolated in this study **(Table 3.29)**. Myricanol **(11)** and myricanone **(12)** are the two cyclic diarylheptanoids which are frequently reported in almost all *Myrica* species that have been phytochemically investigated. Some authors are suggesting that both compounds can be used as chemotaxonomic markers of the genus *Myrica*[71,135]. **Table 3.29** contains a summary of the isolated cyclic diarylheptanoids from *M. salicifolia* which have been also isolated from other *Myrica* species.

Additionally, six cyclic diarylheptanoids glycosides **(16-18**, **21-23)** are reported for the first time in the genus *Myrica*. The new isolated diarylheptanoids have slight variations from already described ones in term of position of the glycosidic linkage, number and position of hydroxyl groups, position of keto group as well as number and type of attached sugar moieties. Salicimeckol (7-hydroxymyricanol 5-*O*-β-D-glucoside, **16**), a new cyclic diarylheptanoid, was found to be similar to myricanol 5-*O*-β-D-glucoside **(13),** a known compound[117,126,128]. However, the observed difference between the two was the attachment of an extra hydroxyl group to position 7 of salicimeckol**.** Salicireneol A (juglanin B 3-*O*-β-D-glucoside, **17**) was observed to be similar to juglanin B[172,173] with exception of attachment of a glucose moiety at position 3 of the juglanin B. Moreover, NMR data of saliciclaireone A (myricanone 5-*O*-β-D-glucopranosyl-(1-6)-β-D-glucopyranoside, **22**) and saliciclaireone B (neomyricanone 5-*O*-β-D-glucopranosyl-(1-6)-β-D-glucopyranoside, **23**) were resembling the known structures of myricanone 5-*O*-β-D-glucopyranoside[117,126] and neo myricanone 5-*O*-β-D-glucopyranoside[117] except that the two compounds were found to contain an extra glucose moiety in each. Saliciclaireone C (myricanone 17-*O*-α-L-arabinofuranosyl-(1-6)-β-D-glucopyranoside, **24**) were similar to known compound **(25)** myricanol 5-*O*-α-L-arabinofuranosyl-(1-6)-β-D-glucopyranoside[129], but **24** was found to contain a glycosidic linkage at position 17 and a keto group instead of hydroxyl group at position C-11 of the aglycone.

3.4.3.3 Methylated ellagic acid glycosides (MEAG)

Three methylated ellagic acid glycosides (**27 – 29**) were isolated from *M. salicifolia*. However, to date, there is no literature data describing the existence of these compounds in the genus *Myrica*. There is also limited literature data describing their isolation from other plants.

Therefore, this is the first time myriside (3,4 di-*O*-methyl ellagic 4'-*O*-β-D-xylopyranoside **27**), largertannin (3,4 di-*O*-methyl ellagic acid 4'-*O*-β-D-glucopyranoside **28)** and ducheside A (3-*O*-methyl-ellagic acid 4'-*O*-β-D-xylopyranoside **29)** are reported in *Myrica.*

The identification of these three compounds was challenging as they tend to change solubility over time. Some of the isolated compounds which are believed to be MEAG could not be dissolved in any of the solvent just as little in the NMR solvents. This made their identification and structure elucidation impossible, hence they are not reported in this thesis. The solubility of myriside (**27**) was achieved in deuterated methanol, thereafter its identification and structure elucidation was successfully done. Compounds **28** and **29** were totally dissolved in the deuterated methanol in the first place, but within a few minutes they precipitated. Their identification and structure elucidation by 1D and 2D NMR measurement was achieved after dissolving them in deuterated pyridine and shaking the mixture in the water bath at 40 ^{o}C until a clear solution was achieved. The cause of the solubility change of the MEAGs was not investigated in this study. However, the solubility change of these compounds causes the difficulty in their isolation, purification and identification. This could also be a reason to the scarcity of literature data not only from *Myrica* but also from other plant species. The solubility change problems for methyl ellagic acid glycosides were also reported by Hillis and Yazaki[176]. However, they also did not investigate the underlying mechanism.

Table 3.29: Reported literature on the isolation of the known compounds isolated from *M. salicifolia.*

Isolated compound		Other *Myrica* species	Other plant species
Tannins			
1	gallocatechin	*M. gale*[107], *M. rubra*[106]	Green tea[143], *Salix purpurea*[162], *Trifolium repens*[144], *Catha edulis*[177] to mention a few.
2	epigallocatechin -3-*O*-gallate	*M. nagi*[87], *M. rubra*[117,178]	Green tea[143], etc.
3	prodelphinidin B1 (epigallocatechin-(4β→8)-gallocatechin	NONE	*Cistus incanus*[154], *Lotus pedunculatus*[155], *Catha edulis*[177], *Stryphnodendron adstringens*[153]
4	epigallocatechin 3-*O*-gallate-(4β→8)-gallocatechin	NONE	*Cistus incanus*[154], *Hamamelis virginiana*[157]
5	epigallocatechin–(4β→8)–gallocatechin 3-*O*-gallate	NONE	NONE
6	ephedrannin D5 (epigallocatechin (2β→O→7, 4β→8)–gallocatechin	NONE	*Ephedra sinica*[160]
8	adenodimerin C (gallocatechin-3-O-gallate (2β→O→7,4β→8)–gallocatechin)	*M. adenophora*[109]	NONE
9	castalagin	*M. esculenta*[87]	*Quercus robur*[166,167], *Quercus petraea*[179,180], *Castanea sativa*[181,182], *Anogeissus leiocarpus*[91], *Eugenia grandis*[183]
Cyclic diarylheptanoids			
10	juglanin B-sulphate	*M. rubra*[110,112]	NONE
11	myricanol	*M. rubra*[117,128], *M. cerifera*[119], *M. nagi*[141,184], *M. arborea*[126], *M. esculenta*[87], *M. nana*[185], *M. adenophora*[109]	NONE
12	myricanone	*M. rubra*[117,128], *M. nagi*[141,184], *M. esculenta*[87], *M. nana*[185], *M. gale*[125], *M. adenophora*[109]	NONE
13	myricanol 5-*O*-β-D-glucose	*M. rubra*[117,128], *M. arborea*[126]	NONE
14	myricanone 5-*O*-β-D-glucose	*M. rubra*[117]	NONE
15	myricanol 11-*O*-β-D-xylopyranoside	*M. rubra*[128], *M. arborea*[126], *M. adenophora*[109]	NONE

Isolated compound		**Other *Myrica* species**	**Other plant species**
19	myricanol 5-*O*-β-D-(6'-*O*-galloyl) glucoside	*M. rubra*[128]	NONE
20	myricanol 5-*O*-β-D-(6'-*O*-galloyl) glucoside	*M. rubra*[128]	NONE
21	myricanone 5-*O*-β-D-(6'-*O*-galloyl) glucoside	*M. rubra*[128]	NONE
25	myricanol 5-*O*-α-L-arabinofuranosyl-(1-6)-β-D-glucopyranoside	*M. rubra*[129]	NONE
26	myricanol 5-*O*-β-D-glucopranosyl-(1-6)-β-D-glucopyranoside or myricanol gentiobioside	*M. rubra*[128]	NONE
Methylated ellagic acid glycosides (MEAG)			
28	largertannin (3,4 di-*O*-methyl ellagic acid 4'-*O*-β-D-glucopyranoside)	NONE	SciFinder could not provide a reference from which largertannin was isolated
29	ducheside A (3-*O*-methyl-ellagic acid 4'-*O*-β-D-xylopyranoside)	NONE	*Duchesnea indica*[175]

3.5 Conclusion

M. salicifolia bark is a common potent medicinal plant part used as a drug in Maasai community of north-eastern Tanzania. However, phytochemical characterization up to a point of individual isolated compounds as well as pharmacological studies to scientifically prove its medicinal effectiveness are scarce. For this reason, crude methanolic extract of *M. salicifolia* bark was subjected to phytochemical investigation. This resulted in isolation of 31 compounds belonging to different compound classes such as proanthocyanidins, ellagitannins, cyclic diarylheptanoids, methylated ellagic acid glycosides and others (section **3.4.1**). The isolation of compounds was not focused to a specific group of compounds but on every possible compound for documentation and also for scientific back up of the plant phytochemical composition. Besides, it was observed that the methanolic extract of *M. salicifolia* contained mainly proanthocyanidins and cyclic diarylheptanoids in large quantity compared to other compound classes.

Moreover, a method to determine absolute configuration of the isolated cyclic diarylheptanoids of *meta,meta*-bridged biphenyls type having chiral centre at position 11 by using CD calculation was established. The method was established by help of Prof. Dr. Thomas Schmidt from Institute of Pharmaceutical Biology and Phytochemistry, University of Münster.

In addition, the phytochemical composition of *M. salicifolia,* demonstrated the taxonomic relationship of the plant with other reported *Myrica* species. The taxonomic relationship was deduced from comparison of isolated *M. salicifolia* compounds to the same compounds reported from other *Myrica* species (section **3.4.2**). Furthermore, the existence of a new class of compounds, methylated ellagic acid glycosides (MEAG), to the genus *Myrica* was discovered.

Finally, there is still a great number of compound to discover and elucidate from *M. salicifolia* bark that were not achieved in this study. Among the encountered challenges were, the presence of too many compounds with low amount in the non-tannin fractions S1-S3 **(Figure 3.18)**. Therefore, for further thorough analysis and isolation of non-tannins compounds from the *M. salicifolia* bark in the future, a higher amount of the starting bark material for the extraction is absolutely recommended.

4 Summary and future recommendation

In this study, an ethnopharmacological survey was conducted in Arusha and Manyara regions of north-eastern Tanzania. The objective of the survey was a detailed investigation and documentation of commonly used Maasai medicinal plants in the area. A total of 65 consented traditional medicinal practitioners (TMPs) were interviewed. Information was collected by using a semi structured questionnaire interview. Four commonly used medicinal plants were investigated, namely *Myrica salicifolia* (Myricaceae), *Pappea capensis* (Sapindaceae), *Flacourtia indica* (Salicaceae) and *Vangueria apiculata* (Rubiaceae). Documentation on plant parts used, drug preparation, traditional medicinal uses, drug administration and overdose management was achieved. A number of diseases were reported to be cured by the four plants. The most mentioned diseases to be treated by *M. salicifolia* were gonorrhoea (81%) and running nose (73%). *P. capensis* was mainly used for the enhancement of libido (89%) and to treat blood loss (72%). *F. indica* was applied to treat fever (92%), malaria (90%) and jaundice (87%). The most mentioned applications for *V. apiculata* were eye infection (73%) and diarrhoea (66%). Moreover, all four plants were reported to cure further disorders and diseases like joints pain, back pain, gouts, diarrhoea, stomach upset, etc. Furthermore, the survey revealed that barks and roots were the most utilized plant parts. Drug administration was observed not to be uniform, in terms of concentration, time and dose.

Phytochemical investigation of a crude methanolic extract of *M. salicifolia* bark was performed following its documented ethnopharmacological survey data. The phytochemical investigation resulted in isolation of 34 compounds belonging to different compounds classes: 8 proanthocyanidins, 1 ellagitannin, 17 cyclic diarylheptanoids, 3 methylated ellagic acid glycosides and 5 further compounds. 10 of the isolated compounds from *M. salicifolia* were identified to be completely new, not described in the literature yet. Additionally, the existence of a new class of compounds to the genus *Myrica* was also discovered, the so called methylated ellagic acid glycosides (MEAG). It was further noticed that the methanolic extract of *M. salicifolia* contained mainly proanthocyanidins and cyclic diarylheptanoids in large quantity compared to other compound classes. Moreover, taxonomic relationship of *M. salifolia* to other

reported *Myrica* species was demonstrated by the compounds isolated from *M. salicifolia.* Some of the compounds were also reported from other *Myrica* species, for example myricanol (**11**) and myricanone (**12**). These two compounds are found in almost every *Myrica* species which has been phytochemically investigated.

Finally, the objective of the work was accomplished to a great extent, however further investigations are recommended for the future.

Due to time constraints, the isolated compounds were not investigated for their pharmacological activities. However, existing literature data on *in-vitro* and/or *in-vivo* biological activity of the mentioned classes of compounds isolated from other plants species and also from *Myrica* provide a preliminary indication of a healing potential of this plant.

To provide scientific confirmation of the healing potential of *M. salicifolia* bark, prospective i*n-vitro* and/or *in-vivo* pharmacological investigations of the isolated compounds should be conducted by using assays which adhere to the diseases claimed to be treated by *M. salicifolia* bark.

Also further phytochemical investigation of *M. salicifolia* bark should be conducted to achieve the complete phytochemical composition of the bark. The future phytochemical investigation should focus on the non-polar extracts (dichloromethane and ethylacetate extracts) which could not be investigated in this research work. But also the polar extracts (methanol 100% and methanol 50% extract) should be further processed. In the methanolic fraction are still a great number of compounds not isolated as they were found in very small amounts. In addition, there are further compounds that would have a good yield, but due to time limitations they were not isolated yet.

Moreover, phytochemical and pharmacological investigations of the remaining three medicinal plants *F. indica, P. capensis and V. apiculata* should be performed in the same way as for *M. salicifolia*.

Lastly, dissemination of the results is essential and should be done to increase awareness of the four medicinal plants. This should be done in Arusha and Manyara regions, where the ethnopharmacological survey was conducted, but also in all other parts of Tanzania. Moreover,

results dissemination should be done in different languages in such a way that every Tanzanian would understand and be in position to utilize the knowledge whenever in need.

5 References

(1) Tanzania National Bureau of Statistics http://www.nbs.go.tz/ (accessed 10, 2015).

(2) JICA. Poverty Profile United Republic of Tanzania. Executive Summary. **2006**.

(3) Levitan, J. Investing in Rural People in the United Republic of Tanzania. **2014**.

(4) Nahashon, N. Conservation of Wild-Harvested Medicinal Plant Species in Tanzania. Chain and Consequence of Commercial Trade on Medicinal Plant Species, Geotryckeriet, Uppsala University, Uppsala, 2013.

(5) Mahunnah, R. L. A.; Mshigeni, K. E. Tanzania's Policy on Biodiversity Prospecting and Drug Discovery Programs. *Journal of Ethnopharmacology* **1996**, *51*, 221–228.

(6) Mhame, P. P.; Nyigo, V. A.; Mbogo, G. P.; Wiketye, V. E.; Kimaro, G.; Mdemu, A. The Management of HIV/AIDS-Related Conditions Using a Traditional Herbal Preparation in Tanzania. **2004**.

(7) WHO. National Policy on Traditional Medicine and Regulation of Herbal Medicine. **2005**.

(8) Institute of Traditional medicine, Muhimbili University of Health and Allied Sciences-MUHAS http://www.muchs.ac.tz/index.php/academics/muhas-institutes/110-itm (accessed 10, 2015).

(9) Mhame, P. P. The Role of Traditional Knowledge (TK) in the National Economy: The Importance and Scope of TK, Particularly Traditional Medicine in Tanzania. **2000**.

(10) Swai, R. E. A. Utilisation and Commercialisation of Medicinal Tree Products in Tanzania. **2003**.

(11) Gessler, M. C.; Msuya, D. E.; Nkunya, M. H. H.; Schär, A.; Heinrich, M.; Tanner, M. Traditional Healers in Tanzania: Sociocultural Profile and Three Short Portraits. *Journal of Ethnopharmacology* **1995**, *48*, 145–160.

(12) Planning; policy department. Annual Health Statistical Abstract. **2006**.

(13) Wenzel, T. L. Western and Traditional Medicine Use Practices in Shirati, Tanzania. **2011**.

(14) Rukia, A. K. Use of Medicinal Plants for Human Health in Udzungwa Mountains Forests: A Case Study of New Dabaga Ulongambi Forest Reserve Tanzania. *Journal of Ethnobiology and Ethnomedicine* **2007**, *3*, 1–4.

(15) WHO. Legal Status of Traditional Medicine and Complementary/Alternative Medicine: A Worldwide Review. **2001**.

(16) Ministry of Health, T. The National Traditional and Birth Attendants Implementation Policy. **1999**.

(17) Fratkin, E. 1996. Traditional Medicine and Concepts of Healing among Samburu Pastoralists of Kenya. *Journal of Ethnobiology* **1996**, *16*, 63–97.

(18) Kiringe, W. J. A Survey of Traditional Health Remedies Used by the Maasai of Southern Kaijiado District, Kenya. *Ethnobotany Research and Applications* **2006**, *4*, 61–73.

(19) Maundu, P.; Berger, D.; Saitabau, C.; Nasieku, J.; Kipelian, M.; Mathenge, S.; Morimoto, Y.; Robert, H. Ethnobotany of the Loita Maasai. Towards Community Management of the Forest of the Lost Child Experiences from the Loita Ethnobotany. **2001**.

(20) Cox, P. A.; Balick, M. The Ethnobotanical Approach to Drug Discovery. *Scientific American* **1994**, *270*, 82–87.

(21) Sankan, S. S. *The Maasai*; Nairobi. East Africa Literature Bureau: Nairobi, Kenya, 1971.

(22) Fedders, A.; Salvadori, C. *Peoples and Cultures of Kenya*; Transafrica, Nairobi / Rex Collings, London, 1979.

(23) Sindiga, I. Indigenous Medical Knowledge of the Maasai. *Indigenous Knowledge and Development Monitor* **1994**, *2*, 16–18.

(24) Sindiga, I. Ethnomedicine and Health Care in Kenya. **1992**.

(25) Burford, G.; Rafiki, M. Y.; Ngila, L. O. The Forest Retreat of Orpul: A Holistic System of Health Care Practiced by the Maasai Tribe of East Africa. *Journal of Alternative and Complementary Medicine* **2001**, *7*, 547–551.

(26) Holford-Walker, A. F. Herbal Medicines and Drugs Used by the Maasai, 1951.

(27) Wambugu, S. N.; Mathiu, P. M.; Gakuya, D. W.; Kanui, T. I.; Kabasa, J. D.; Kiama, S. G. Medicinal Plants Used in the Management of Chronic Joint Pains in Machakos and Makueni Counties, Kenya. *Journal of Ethnopharmacology* **2011**, *137*, 945–955.

(28) Kokwaro, J. O. *Medicinal Plants of East Africa*; 2nd ed.; Kenya Literature Bureau: Nairobi, Kenya, 1993.

(29) Maundu, P.; Tengnèas, B.; Birnie, A.; Muema, N. *Useful Trees and Shrubs for Kenya*; 2nd Edition.; World Agroforestry Centre, 2005.

(30) Kokwaro, J. *Medicinal Plants of East Africa*; Kenya literature Bureau: Nairobi, Kenya, 1976.

(31) Polhill, R. M.; Verdcourt, B. *Flora of Tropical East Africa. Myricaceae*; Beentje, H. J. and Smith, S. A. L., Ed.; Balkema, A. A. / Rotterdam, 2000.

(32) Mbuya, L. P.; Msanga, H. P.; Ruffo, C. K.; Birnie, A.; Tengnas, B. *Useful Trees and Shrubs for Tanzania. Identification, Propagation and Management for Agricultural and Pastoral Communities.*; SIDA regional conservation Unit, RSCU, 1994.

(33) Hedberg, I.; Hedberg, O.; Madati, P. J.; Mshigeni, K. E.; Mshiu, E. N.; Samuelsson, G. Inventory of Plants Used in Traditional Medicine in Tanzania. II. Plants of the Families Dilleniaceae-Opiliaceae. *Journal of Ethnopharmacology* **1983**, *9*, 106–112.

(34) Kisangau, D. P.; Lyaruu, H. V. M.; Hosea, K. M.; Cosam, C. J. Use of Traditional Medicines in the Management of HIV/AIDS Opportunistic Infections in Tanzania: A Case in the Bukoba Rural District. *Journal of Ethnobiology and Ethnomedicine* **2007**, *3*, 1 – 8.

(35) Getahun, A. Some Common Medicinal and Poisonous Plants Used in Ethiopian Folk Medicine. **1976**.

(36) Kamatenesi-Mugisha, M.; Oryem-Origa, H. Traditional Herbal Remedies Used in the Management of Sexual Impotence and Erectile Dysfunction in Western Uganda. *African Health Sciences* **2005**, *5*, 40–49.

(37) Geyid, A.; Abebe, D.; Debella, A.; Makonnen, Z.; Aberra, F.; Teka, F.; Kebede, T.; Urga, K.; Yersaw, K.; Biza, T.; *et al.* Screening of Some Medicinal Plants of Ethiopia for Their Anti-Microbial Properties and Chemical Profiles. *Journal of Ethnopharmacology* **2005**, *97*, 421–427.

(38) Njung'e, K.; Muriuki, G.; Mwangi, J. W.; Kuria, K. A. M. Analgesic and Antipyretic Effects of *Myrica salicifolia* (Myricaceae). *Phytotherapy Research* **2002**, *16 Suppl 1*, 73–74.

(39) Davies, H. D.; Verdcourt, B. *Floral of Tropical East Africa. Sapindaceae*; Beentje, H. J. and Whitehouse, M. A., Ed.; Balkema, A. A/ Rotterdam, 1998.

(40) Chettleborough, J.; Lumeta, J.; Magesa, S. Community Use of Non Timber Forest Products. A Case Study from the Kilombero Valley. **2000**.

(41) Moshi, M. J.; Otieno, D. F.; Mbabazi, P. K.; Weisheit, A. Ethnomedicine of the Kagera Region, North Western Tanzania. Part 2: The Medicinal Plants Used in Katoro Ward, Bukoba District. *Journal of Ethnobiology Ethnomedicine* **2010**, *6*, 19.

(42) Kaingu, C. K.; Oduma, J. A.; Kanui, T. I. Practices of Traditional Birth Attendants in Machakos District, Kenya. *Journal of Ethnopharmacology* **2011**, *137*.

(43) Musila, W.; Kisangau, D.; Muema, J. Conservation Status and Use of Medicinal Plants by Traditional Medical Practitioners in Machakos District, Kenya. **2004**.

(44) Medicinal uses of plants Found in KNR www.knra.co.za/workinggroups/medicinal-uses.htm (accessed 12, 2012).

(45) Mulaudzi, R. B. Pharmacological Evaluation of Medicinal Plants Used by Venda People against Venereal and Related Diseases, University of KwaZulu-Natal, 2012.

(46) Hines, D. A.; Eckman, K. Indigenous Multipurpose Trees for Tanzania: Uses and Economic Benefits to the People. **1993**.

(47) Orwa, C. A. M.; Kindt, R.; Jamnadass, R. S. A. *Flacourtia indica*: Agroforestry Database: A Tree Reference and Selection Guide. **2009**.

(48) Kota, G. C.; Karthikeyan, M.; Kannan, M.; Rajasekar. *Flacourtia indica* (Burm. F.) Merr.-A Phytopharmacological. *International Journal of Research in Pharmaceutical and Biomedical Sciences* **2012**, *3*, 78–81.

(49) Nadkarni, K. M. *Indian Meteria Medica*; 2nd ed.; Ramdas Bhatkal: prakashan pvt.ltd, Mumbai, 1927; Vol. 1.

(50) Rajasekaran, K. *The Ayurvedic Pharmacopoeia of India*; 1st ed.; National Institute of Science Communication: New delhi India, 1999; Vol. IV.

(51) Tyagi, S. N.; Rakshit, S. A.; Raghvendra, A. S.; Patel, B. D. In Vitro Antioxidant Activity of Methanolic and Aqueous Extract of *Flacourtia indica* Merr. *American-Eurasian Journal of Scientific Research* **2011**, *5*, 201–206.

(52) Bhaumik, P.; Guha, K.; Biswas, G.; Mukherjee, B. (-) Flacourtin a Phenolic Glucoside Ester from *Flacourtia indica*. *Phytochemistry* **1987**, *11*, 3090–3091.

(53) Kaou, A. M.; Leddet, V. M.; Canlet, C.; Debrauwer, L.; Hutter, S. Antimalarial Compounds from the Aerial Parts of *Flacourtia indica* (Flacourtiaceae). *Journal of Ethnopharmacology* **2010**, *130*, 272–274.

(54) Nazneen, M.; Mazid, A.; Kundu, J. K.; Bachar, S. C.; Begum, F.; K., D. B. Protective Effects of *Flacourtia indica* Aerial Parts Extracts against Paracetamol Induced Hepatotoxiciy in Rats. *Journal of Taiba Univesity of Science* **2009**, *2*, 1–6.

(55) Tyagi, S.; Singh, M.; Singh, D.; Yadav, I.; Singh, S.; Mansoori, M. H. Anti-Asthmatic Potential of *Flacourtia indica* Merr. *African Journal of Basic and Applied Sciences* **2011**, *3*, 201 – 204.

(56) Ruffo, C. K.; Birnie, A.; Tengnäs, B. Edible Wild Plants of Tanzania. **2002**.

(57) Flora Zambesiaca http://apps.kew.org/efloras/fz/intro.html (accessed 10, 2015).

(58) Field Guide to the Moist Forest Trees of Tanzania. http://www.york.ac.uk/res/celp/webpages/projects/ecology/tree%20guide/introduction.htm (accessed 10, 2015).

(59) Useful Tropical plants http://tropical.theferns.info/viewtropical.php?id=Vangueria+apiculata (accessed 10, 2015).

(60) Moshi, M. J.; Otieno, D. F.; Mbabazi, K. P.; Weisheit, A. The Ethnomedicine of the Haya People of Bugabo Ward, Kagera Region, North Western Tanzania. *Journal of Ethnobiology and*

Ethnomedicine **2009**, *5*, 1–5.

(61) Ssegawa, P. and K. J. M. Medicinal Plant Diversity and Uses in the Sango Bay Area, Southern Uganda. *Journal of Ethnopharmacology* **2007**, *113*, 521–540.

(62) Kokwaro, J. O. *Medicinal Plants of East Africa*; 3rd ed.; University of Nairobi Press: University of Nairobi, 2009.

(63) Hamill, F. A.; Apio, S.; Mubiru, N. K.; Bukenya-Ziraba, R.; Mosango, M.; Maganyi, O. W.; Soejarto, D. D. Traditional Herbal Drugs of Southern Uganda, II: Literature Analysis and Antimicrobial Assays. *Journal of Ethnopharmacology* **2003**, *84*, 57–78.

(64) Kamatenesi, M. M.; Oryem, O. H. Medicinal Plants Used to Induce Labour during Childbirth in Western Uganda. *Journal of Ethnopharmacology* **2007**, *109*, 1–9.

(65) Malocho, W. N. Arusha Region Social Economic Profile. **1998**.

(66) Huguet, V.; Gouy, M.; Normand, P.; Zimpfer, J. F.; Fernandeza, M. P. Molecular Phylogeny of Myricaceae: A Reexamination of Host–symbiont Specificity. *Molecular Phylogenetics and Evolution* **2005**, *34*, 557–568.

(67) Yanthan, M.; Misra, A. K. Molecular Approach to the Classification of Medicinally Important Actinorhizal Genus *Myrica*. *Indian journal of biotechnology* **2013**, *12*, 133–136.

(68) Herbert, J. New Combinations and a New Species in *Morella* (Myricaceae). *Novon* **2005**, *15*, 293–295.

(69) Herbert, J. Systematic and Biography of Myricaceae, University of St Andrews, 2004.

(70) Sun, C.; Huang, H.; Xu, C.; Li, X.; Chen, K. Biological Activities of Extracts from Chinese Bayberry (*Myrica rubra* Sieb. et Zucc.): A Review. *Plant Foods for Human Nutrition* **2013**, *68*, 97–106.

(71) Silva, B. J.; Seca, A. M.; Barreto, M. C.; Pinto, D. C. Recent Breakthroughs in the Antioxidant and Anti-Inflammatory Effects of *Morella* and *Myrica* Species. *International Journal of Molecular Sciences* **2015**, *16*, 17160–17180.

(72) Kirtikar, K. R.; Basu, B. D. *Indian Medicinal Plants*; 2nd ed.; International Book Distributors: New Delhi, India, 1999; Vol. 3.

(73) Nadkarni's, K. M. *Indian Materia Medica*; 3rd ed.; Popular Prakashan Pvt Ltd: Mumbai, India, 2002; Vol. 1.

(74) Laloo, R. C.; Kharlukhi, S.; Jeeva, S.; Mishra, B. P. Status of Medicinal Plants in the Disturbed and the Undisturbed Sacred Forest of Meghalaya, Northeast India: Population Structure and Regeneration Efficacy of Some Important Species. *Current Science* **2006**, *90*.

(75) Panthari, P.; Kharkwal, H.; Kharkwal, H.; Joshi, D. D. Myrica Nagi: A Review on Active Constituents, Biological and Therapeutic Effects. *International Journal of Pharmacy and*

Pharmaceutical Science **2012**, *4*, 38–42.

(76) Kumar, A.; Rana, A. C. Pharmacognostic and Pharmacological Profile of Traditional Medicinal Plant: *Myrica nagi*. *International Research Journal of Pharmacy* **2012**, *3*.

(77) Hoffmann, D.; Hoffmann, F. N. *Medical Herbalism: The Science and Practice of Herbal Medicine*; Inner Traditions/Bear & Company: Vermont, VT, USA, 2003.

(78) Schmidt, E.; Lotter, M.; McCleland, W. *Trees and Shrubs of Mpumalamga and Kruger National Park*; Jacana Publishers: Johannesburg, South Africa, 2002.

(79) Ashafa, A. O. T. Medicinal Potential of *Morella serata* (Lam.) Killick (Myricaceae) Root Extracts: Biological and Pharmacological Activities. *BMC Complementary and Alternative Medicine* **2013**, *13*, 163.

(80) Chantrill, B. H.; Coulthard, C. E.; Dickinson, L.; Inkley, G. W.; Morris, W.; Pyle, A. H. The Action of Plant Extracts on a Bacteriophage of *Pseudomonas Pyocyanea* and on Influenza A Virus. *Journal of General Microbiology* **1952**, *6*, 74–84.

(81) Small, E. *North American Cornucopia: Top 100 Indigenous Food*; Plants CRC Press: New York: NY, USA, 2014; Vol. p. 669.

(82) Gross, G. G. *Plant Polyphenols. Synthesis, Properties, Significance*; Hemingway, Richard W. and Laks, Peter E, Ed.; Plenum Press: New York, 1992; pp. 43 –44.

(83) Salminen, J. P.; Ossipov, V.; Loponen, J.; Haukioja, E.; Pihlaja, K. Characterisation of Hydrolysable Tannins from Leaves of *Betula pubescens* by High-Performance Liquid Chromatography-Mass Spectrometry. *Journal of Chromatography A* **1999**, *864*, 283–291.

(84) Vermerris, W.; Nicholson, R. *Phenolic Compound Biochemistry*; Springer, 2008.

(85) Haslam, E.; Cai, Y. Plant Polyphenols (vegetable Tannins): Gallic Acid Metabolism. *Natural Product Reports* **1994**, *11*, 41–66.

(86) Porter, L. J. Flavans and Proanthocyanidins. In *Flavonoids Advances in Research since 1986*; Harborne, J. B., Ed.; Chapman and Hall, 1994; pp. 23–55.

(87) Sun, D.; Zhao, Z.; Wong, H.; Foo, L. Y. Tannins and Other Phenolics from *Myrica esculenta* Bark. *Phytochemistry* **1988**, *27*, 579– 583.

(88) Fernandes, A.; Fernandes, I.; Cruz, L.; Mateus, N.; Cabral, M.; de Freitas, V. Antioxidant and Biological Properties of Bioactive Phenolic Compounds from *Quercus suber* L. *Journal of Agricultural and Food Chemistry* **2009**, *57*, 11154–11160.

(89) Taguri, T.; Tanaka, T.; Kouno, I. Antimicrobial Activity of 10 Different Plant Polyphenols against Bacteria Causing Food-Borne Disease. *Biological and Pharmaceutical Bulletin* **2004**, *27*, 1965—1969.

(90) Vilhelmova, N.; Jacquet, R.; Quideau, S.; Stoyanova, A.; Galabov, A. S. Three-Dimensional Analysis of Combination Effect of Ellagitannins and Acyclovir on Herpes Simplex Virus Types 1 and 2. *Antiviral Research* **2011**, *89*, 174–181.

(91) Shuaibu, M. N.; Pandey, K.; Wuyep, P. A.; Yanagi, T.; Hirayama, K.; Ichinose, A.; Tanaka, T.; Kouno, I. Castalagin from A*nogeissus leiocarpus* Mediates the Killing of Leishmania in Vitro. *Parasitology Research* **2008**, *103*, 1333–1338.

(92) Fu, Y.; Qiao, L.; Cao, Y.; Zhou, X.; Liu, Y.; Ye, X. Structural Elucidation and Antioxidant Activities of Proanthocyanidins from Chinese Bayberry (*Myrica rubra* Sieb. et Zucc.) Leaves. *Plos One* **2014**, *9*, e96162.

(93) Zhang, Y. L.; Kong, L. C.; Yin, C. P.; Jiang, D. H.; Jiang, J. Q.; He, J.; Xiao, W. X. Extraction Optimization by Response Surface Methodology, Purification and Principal Antioxidant Metabolites of Red Pigments Extracted from Bayberry (*Myrica rubra*) Pomace. *LWT - Food Science and Technology* **2013**, *51*, 343–347.

(94) Aron, P. M.; Kennedy, J. A. Flavan-3-Ols: Nature, Occurrence and Biological Activity. *Molecular Nutritional and Food Research* **2008**, *52*, 79 – 104.

(95) Tatsuno, T.; Jinno, M.; Arima, Y.; Kawabata, T.; Hasegawa, T.; Yahagi, N.; Takano, F.; Ohta, T. Anti-Inflammatory and Anti-Melanogenic Proanthocyanidin Oligomers from Peanut Skin. *Biological and Pharmaceutical Bulletin* **2012**, *35*, 909–916.

(96) Karioti, A.; Sokovic, M.; Ciric, A.; Koukoulitsa, C.; Bilia, A. R.; Skaltsa, H. Antimicrobial Properties of *Quercus ilex* L. Proanthocyanidin Dimers and Simple Phenolics: Evaluation of Their Synergistic Activity with Conventional Antimicrobials and Prediction of Their Pharmacokinetic Profile. *Journal of Agricultural and Food Chemistry* **2011**, *59*, 6412–6422.

(97) Janecki, A.; Kolodziej, H. Anti-Adhesive Activities of Flavan-3-Ols and Proanthocyanidins in the Interaction of Group A-Streptococci and Human Epithelial Cells. *Molecules* **2010**, *15*, 7139–7152.

(98) Sen, C. K.; Khanna, S.; Gordillo, G.; Bagchi, D.; Bgchi, M.; Roy, S. Oxygen, Oxidants, and Antioxidants in Wound Healing. An Emerging Paradigm. *Annals of the New York Academy of Sciences* **2002**, *957*, 239–249.

(99) Schmidt, C. A.; Murillo, R.; Heinzmann, B.; Stefan L.; Wray, V.; Merfort, I. Structural and Conformational Analysis of Proanthocyanidins from *Parapiptadenia rigida* and Their Wound-Healing Properties. *Journal of Natural Products* **2011**, *74*, 1427–1436.

(100) Song, X.; Siriwardhana, N.; Rathore, K.; Lin, D.; Wang, H. C. R. Grape Seed Proanthocyanidin Suppression of Breast Cell Carcinogenesis Induced by Chronic Exposure to Combined 4-(methylnitrosamino)-1-(3-Pyridyl)-1-Butanone and Benzo[a]pyrene. *Molecular Carcinogenesis* **2010**, *49*, 450–463.

(101) Yokozawa, T.; Cho, E. J.; HumPark, C.; Kim, J. H. Protective Effect of Proanthocyanidin against against Diabetic Oxidative Stress. *Evidence-Based Complementary and Alternative Medicine.*

2012, 1–11.

(102) Kim, K. K.; Singh, A. P.; Singh, R. K.; DeMartino, A.; Brard, L.; Vorsa, N. L.; Lange, T. L. S.; Moore, R. G. Anti-Angiogenic Activity of Cranberry Proanthocyanidins and Cytotoxic Properties in Ovarian Cancer Cells. *International Journal of Oncology* **2012**, *40*, 227–235.

(103) Zhao, M.; Yang, B.; Wang, J.; Liu, Y.; Yu, L. M.; Jiang, Y. M. Immunomodulatory and Anticancer Activities of Flavonoids Extracted from Litchi (Litchi Chinensis Sonn) Pericarp. *International Immunopharmacology* **2007**, *7*, 162–166.

(104) Beecher, G. R. Proanthocyanidins: Biological Activities Associated with Human Health. *Pharmaceutical Biology* **2004**, *42*, 2 – 20.

(105) Santos, B. C.; Scalbert, A. Proanthocyanidins and Tannin-like Compounds-Nature, Occurrence, Dietary Intake and Effects on Nutrition and Health. *Journal of the Science of Food and Agriculture* **2000**, *80*, 1094–1117.

(106) Nonaka, I. G.; Muta, M.; Nishioka, I. Myricatin, a Galloyl Flavanonol Sulfate and Prodelphinidin Gallates from *Myrica rubra*. *Phytochemistry* **1983**, *22*, 237 –241.

(107) Santos, S. C.; Waterman, P. G. Condensed Tannins from *Myrica gale*. *Fitoterapia* **2000**, *71*, 610–612.

(108) Yang, L. L.; Chang, C. C.; Chen, L. G.; Wang, C. C. Antitumor Principle Constituents of *Myrica rubra* Var. Acuminata. *Journal of Agricultural and Food Chemistry* **2003**, *51*, 2974–2979.

(109) Ting, Y. C.; Ko, H. H.; Wang, H. C.; Peng, C. F.; Chang, H. S.; Hsieh, P. C.; Chen, I. S. Biological Evaluation of Secondary Metabolites from the Roots of *Myrica adenophora*. *Phytochemistry* **2014**, *103*, 89–98.

(110) Yoshimura, M.; Yamakami, S.; Amakura, Y.; Yoshida, T. Diarylheptanoid Sulfates and Related Compounds from *Myrica rubra* Bark. *Journal of Natural Products* **2012**, *75*, 1798–1802.

(111) Lv, H.; She, G. Naturally Occurring Diarylheptanoids - A Supplementary Version. *Records of Natural Products* **2012**, *6*, 321–333.

(112) Kim, H. H.; Oh, M. H.; Park, K. J.; Heo, J. H.; Lee, M. W. Anti-Inflammatory Activity of Sulfate-Containing Phenolic Compounds Isolated from the Leaves of *Myrica rubra*. *Fitoterapia* **2014**, *92*, 188–193.

(113) Morihara, M.; Sakurai, N.; Inoue, T.; Kawai, K. I.; Nagai, M. Two Novel Diarylheptanoid Glucosides from *Myrica gale* Var. Tomentosa and Absolute Structure of Plane-Chiral Galeon. *Chemical and Pharmaceutical Bulletin* **1997**, *45*, 820–823.

(114) Malterud, K. E.; Anthonsen, T.; Hjortas, J. 14-Oxa-[7.1]-Metapara-Cyclophanes from *Myrica gale* L., a New Class of Natural Products. *Tetrahedron Letters* **1976**, *17*, 3069 – 3072.

(115) Lv, H.; She, G. Naturally Occuring Diarylheptanoids. *Natural Product Communications* **2010**, *5*, 1687 – 1708.

(116) Akazawa, H.; Fujita, Y.; Banno, N.; Watanabe, K.; Kimura, Y.; Manosroi, A.; Manosroi, J.; Akihisa, T. Three New Cyclic Diarylheptanoids and Other Phenolic Compounds from the Bark of *Myrica rubra* and Their Melanogenesis Inhibitory and Radical Scavenging Activities. *Journal of Oleo Science* **2010**, *59*, 213–221.

(117) Tao, J.; Morikawa, T.; Toguchida, I.; Ando, S.; Matsuda, H.; Yoshikawa, M. Inhibitors of Nitric Oxide Production from the Bark of *Myrica rubra*: Structures of New Biphenyl Type Diarylheptanoid Glycosides and Taraxerane Type Triterpene. *Bioorganic and Medicinal Chemistry* **2002**, *10*, 4005–4012.

(118) Wang, J.; Dong, S.; Wang, Y.; Lu, Q.; Zhong, H.; Du, G.; Zhang, L.; Cheng, Y. Cyclic Diarylheptanoids from *Myrica nana* Inhibiting Nitric Oxide Release. *Bioorganic and Medicinal Chemistry* **2008**, *16*, 8510–8515.

(119) Jones, J. R.; Lebar, M. D.; Jinwal, U. K.; Abisambra, J. F.; Koren, J.; Blair, L.; O'Leary, J. C.; Davey, Z.; Trotter, J.; Johnson, A. G.; *et al.* The Diarylheptanoid (+)-aR, 11S-Myricanol and Two Flavones from Bayberry (*Myrica cerifera*) Destabilize the Microtubule-Associated Protein Tau. *Journal of Natural Products* **2011**, *74*, 38–44.

(120) Ishida, J.; Kozuka, M.; Wang, H. K.; Konoshima, T.; Tokuda, H.; Okuda, M.; Mou, X. Y.; Nishino, H. Antitumor-Promoting Effects of Cyclic Diarylheptanoids on Epstein–Barr Virus Activation and Two-Stage Mouse Skin Carcinogenesis. *Cancer Letters* **2000**, *159*, 135 –140.

(121) Ohta, S.; Sakurai, N.; Kamogawa, A.; Yaguchi, Y.; Inoue, T.; Shinoda, M. Protective Effects of the Bark of *Myrica rubra* Sieb. et Zucc. On Experimental Liver Injuries. *Yakugaku zasshi : Journal of the Pharmaceutical Society of Japan* **1992**, *112*, 244–252.

(122) Matsuda, H.; Yamazaki, M.; Matsuo, K.; Asanuma, Y.; Kubo, M. Anti-Androgenic Activity of *Myrica* Cortex-Isolation of Active Constituents from Bark of *Myrica rubra*. *Biological and Pharmaceutical Bulletin* **2001**, *24*, 259–263.

(123) Matsuda, H.; Morikawa, T.; Tao, J.; Ueda, K.; Yoshikawa, M. Bioactive Constituents of Chinese Natural Medicines. VII.1) Inhibitors of Degranulation in RBL-2H3 Cells and Absolute Stereo Structures of Three New Diarylheptanoid Glycosides from the Bark of *Myrica rubra*. *Chemical and Pharmaceutical Bulletin.* **2002**, *50*, 208—215.

(124) Malterud, K. E.; Anthonsen, T. 13-Oxomyricanol, a New [7.0]-Metacyclophane from *Myrica nagi*. *Phytochemistry* **1980**, *19*, 705–707.

(125) Nagai, M.; Dohi, J.; Morihara, M.; Sakurai, N. Diarylheptanoids from *Myrica gale* Var. Tomentosa and Revised Structure of Porson. *Chemical and Pharmaceutical Bulletin* **1995**, *43*, 1674 – 1677.

(126) Tene, M.; Wabo, H. K.; Kamnaing, P.; Tsopmo, A.; Tane, P.; Ayafor, J. F.; Sterner, O. Diarylheptanoids from *Myrica arborea*. *Phytochemistry* **2000**, *54*, 975–978.

(127) Wang, J. F.; Zhang, C. L.; Lu, Q.; Yu, T. F.; Zhong, H. M.; Long, C. L.; Cheng, Y. X. Three New Diarylheptanoids from *Myrica nana*. *Helvetica Chimica Acta* **2009**, *92*, 1594 – 1599.

(128) Yaguchi, Y.; Sakurai, N.; Nagai, M.; Inoue, T. Constituents of *Myrica rubra*. III.1) Structures of Two Glycosides of Myricanol. *Chemical Pharmaceutical Bulletin* **1988**, *36*, 1419–1424.

(129) Sakurai, N.; Yaguchi, Y.; Hirakawa, T.; Nagai, M.; Inoue, T. Two Myricanol Glycosides from *Myrica rubra* and Revision of the Structure of Isomyricanone. *Phytochemistry* **1991**, *30*, 3077 3079.

(130) Yu, Y. F.; Lu, Q.; Guo, L.; Mei, R. Q.; Liang, H. X.; Luo, D. Q.; Cheng, Y. X. Myricananone and Myricananadiol: Two New Cyclic _Diarylheptanoids_ from the Roots of *Myrica nana*. *Helvetica Chimica Acta* **2007**, *90*, 1691 – 1696.

(131) Takaeda, Y.; Fujita, T.; Shingu, T.; Ogimi, C. Studies on the Bacterial Gall of *Myrica rubra*: Isolation of a New [7,0]-Metacyclophan from the Gall and DL-B-Phenyllactic Acid from the Culture of Gall-Forming Bacteria. *Chemical Pharmaceutical Bulletin* **1987**, *35*, 2569–2573.

(132) Spínola, V.; Llorent-Martínez, E. J.; Gouveia, S.; Castilho, P. C. *Myrica faya*: A New Source of Antioxidant Phytochemicals. *Journal of Agricultural and Food Chemistry* **2014**, *62*, 9722–9735.

(133) Banola, A.; Semwal, D. K.; Semwal, S.; Rawat, U. Flavonoid Glycoside from *Myrica esculenta*. *Journal of the Indian Chemical Society* **2009**, *86*, 535–536.

(134) Sakurai, N.; Yagushi, Y.; Inoue, T. Triterpenoids from *Myrica rubra*. *Phytochemistry* **1987**, *26*, 217 – 219.

(135) Tene, M.; Tane, P.; Connolly, J. D. Triterpenoids and Diarylheptanoids from *Myrica arborea*. *Biochemical Systematics and Ecology* **2009**, *36*, 872–874.

(136) Schlage, C.; Mabula, C.; Mahunnah, R. L. A.; Heinrich, M. Medicinal Plants of the Washambaa (Tanzania): Documentation and Ethnopharmacological Evaluation. *Plant Biology* **2000**, *2*, 83–92.

(137) Teklay, A.; Abera, B.; Giday, M. An Ethnobotanical Study of Medicinal Plants Used in Kilte Awulaelo District, Tigray Region of Ethiopia. *Journal of Ethnobiology and Ethnomedicine* **2013**, *9*, 65.

(138) Kefalew, A.; Asfaw, Z.; Kelbessa, E. Ethnobotany of Medicinal Plants in Ada'a District, East Shewa Zone of Oromia Regional State, Ethiopia. *Journal of Ethnobiology and Ethnomedicine* **2015**, *11*, 25.

(139) Czochanska, Z.; Foo, L. Y.; Newman, R. H.; Porter, L. J. Polymeric Proanthocyanidins. Stereochemistry, Structural Units, and Molecular Weight. *Journal of Chemical Society Perkin* **1980**, *I*, 2278–2286.

(140) York, W. S.; Hantus, S.; Albersheim, P.; Darvill, A. G. Determination of the Absolute Configuration of Monosaccharides by NMR Spectroscopy of Their per-O-(S)-2-Methylbutyrate Derivatives. *Carbohydrate Research* **1997**, *300*, 199–206.

(141) Begley, M. J.; Campbel, R. V. M.; Crombie, L.; Tuck, B.; Whiting, D. A. Constitution and Absolute Configuration of Metameta-Bridged, Strained Biphenyls from *Myrica nagi*; X-Ray Analysis of 16-Bromomyricanol. *Journal of the Chemical Society* **1971**.

(142) Lou, H.; Yamazaki, Y.; Sasaki, T.; Uchida, M. and T. H.; Oka, S. A-Type Proanthocyanidins from Peanut Skins. *Phytochemistry* **1999**, *51*, 297–308.

(143) Davis, A. L.; Cai, Y.; Davies, A. P.; Lewis, J. R. 'H and 13C NMR Assignments of Some Green Tea Polyphenols. *Magnetic Resonance in Chemistry* **1996**, *34*, 887–890.

(144) Foo, L. Y.; Lu, Y.; Molan, A. L.; Woodfield, D. R.; McNabb, W. C. The Phenols and Prodelphinidins of White Clover Flowers. *Phytochemistry* **2000**, *54*, 539–548.

(145) Nonaka, G. I.; Kawahara, O.; Nishioka, I. Tannins and Related Compounds. XV.1) A New Class of Dimeric Flavan-3-ol Gallates Theasinensin A and B, and Proanthocyanidin gallate From Green Tea Leaf. (1). *Chemical and Pharmaceutical Bulletin* **1983**, *31*, 3906–3914.

(146) Porter, L. J.; Newman, R. H.; Foo, L. Y.; Wong, H.; Hemingway, R. W. Polymeric Proanthocyanidins. ^{13}C N.M.R. Studies of Procyanidins. *Journal of the Chemical Society, Perkin Transaction* **1982**, *1*, 1217–1221.

(147) Yutaka, A. Y.; Shoji, T.; Kawahara, N.; Kamakura, H.; Kanda, T.; Goda, Y.; O. Structural Characterization of a Procyanidin Tetramer and Pentamer from the Apple by Low-Temperature NMR Analysis. *Tetrahedron Letters* **2008**, *49*, 6413–6418.

(148) Botha, J. J.; Ferreira, D.; Roux, D. G. Condensed Tannins. Circular Dichroism Method of Assessing the Absolute Configuration at C-4 of 4-Arylflavan-3-Ols, and Stereochemistry of Their Formation from Flavan-3,4-Diols. *Journal of the Chemical Society, Perkin Transaction* **1978**, *I*, 698–700.

(149) Botha, J. J.; Young, D. A.; Ferreira, D.; Roux, D. G. Synthesis of Condensed Tannins. Part 1. Stereoselective and Stereospecific Syntheses of Optically Pure 4-Arylflavan-3-Ols, and Assessment of Their Absolute Stereochemistry at C-4 by Means of Circular Dichroism. *Journal of the Chemical Society, Perkin Transaction* **1981**, *1*, 1213–1219.

(150) Barrett, M. W.; Klyne, W.; Scopes, P. M.; FIetcher, A. C.; Porter, L. J.; Haslam, E. Plant Proanthocyanidins. Part 6. Chiroptical Studies. Part 95. Circular Dichroism of Procyanidins. *Journal of the Chemical Society, Perkin Transaction* **1979**, *1*, 2375–2377.

(151) Slade, D.; Ferreira, D.; Marais, J. P. J. Circular Dichroism, a Powerful Tool for the Assessment of Absolute Configuration of Flavonoids. *Phytochemistry* **2005**, *66*, 2177–2215.

(152) Lee, M. W.; Morimoto, S.; Nonaka, G. I.; Nishioka, I. Flavan-3-Ol Gallates and Proanthocyanidins from *Pithecellobium lobatum*. *Phytochemistry* **1992**, *31*, 2117–2120.

(153) De Mello, J. P.; Petereit, F.; Nahrstedt, A. Flavan-3-ols and Prodelphinidins from *Stryphnodendron adstringens*. *Phytochemistry* **1996**, *41*, 807–813.

(154) Danne, A.; Petereit, F.; Nahrstedt, A. Proanthocyanidins from *Cistus incanus*. *Phytochemistry* **1993**, *34*, 1129–1133.

(155) Foo, L. Y.; Lu, Y.; Mcnabb, W. C.; Waghorn, G.; Ulyatt, M. J. Proanthocyanidins from *Lotus pedunculatus*. *Phytochemistry* **1997**, *45*, 1689–1696.

(156) Fletcher, A. C.; Porter, L. J.; Haslam, E.; Gupta, R. K. Plant Proanthocyanidins. Part 3.l Conformational and Configurational Studies of Natural Procyanidins. *Journal of the Chemical Society, Perkin Transaction* **1977**, *1*, 1628–1637.

(157) Hartisch, C.; Kolodziej, H. Galloylhamameloses and Proanthocyanidins from *Hamamelis virginiana*. *Phytochemistry* **1996**, *42*, 191–198.

(158) Cronje, A.; Burger, J. F. W.; Brandt, E. V.; Kolodziej, H.; Ferreira, D. Assessment of 3,4 Trans and 3,4-Cis Relative Configurations in the a-Series of (4,8)-Linked Proanthocyanidins. *Tetrahedron Letters* **1990**, *31*, 3189–3792.

(159) Bilia, A. R.; Morelli, I.; Hamburger, M.; Hostettmann, K. Flavans and A-Type Proanthocyanidins from *Prunus prostrata*. *Phytochemistry* **1996**, *43*, 887–892.

(160) Zang, X.; Shang, M.; Xu, F.; Liang, J.; Wang, X.; Mikage, M.; Cai, S. A-Type Proanthocyanidins from the Stems of *Ephedra sinica* (Ephedraceae) and Their Antimicrobial Activities. *Molecules* **2013**, *18*, 5172–5189.

(161) Jones, W. T.; Broadhurs, R. B.; Lyttletton, J. W. The Condensed Tannins of Pasture Legume Species. *Phytochemistry* **1976**, *15*, 1407–1409.

(162) Jürgenliemk, G.; Petereit, F.; Nahrstedt, A. Flavan-3-ols and Procyanidins from the Bark of *Salix purpurea* L. *Pharmazie* **2007**, *62*, 231–234.

(163) Qa'dan, F.; Petereit, F.; Nahrstedt, A. Prodelphinidin Trimers and Characterization of a Proanthocyanidin Oligomer from *Cistus albidus*. *Pharmazie* **2003**, *58*, 416–419.

(164) Eberhardt, T. L.; Young, R. A. Conifer Seed Cone Proanthocyanidin Polymers: Characterization by 13C NMR Spectroscopy and Determination of Antifungal Activities. *Journal of Agricultural and Food Chemistry* **1994**, *42*, 1704–1708.

(165) Sun, D.; Wong, H.; Foo, L. Y. Proanthocyanidin Dimers and Polymers from *Quercus dentata*. *Phytochemistry* **1987**, *26*, 1825–1829.

(166) Herve Du Penhoat, C. L. M.; Michon, V. M. F.; Ohassan, A.; Shuyun, P.; Scalbert, A.; Gage, D. Roburin A, a Dimeric Ellagitannin from Heartwood of *Quercus robur*. *Phytochemistry* **1991**, *30*, 329–332.

(167) Puech, J. L.; Mertz, C.; Michon, V.; Guerneve, C. L. Evolution of Castalagin and Vescalagin in Ethanol Solutions. Identification of New Derivatives. *Journal of Agricultural and Food Chemistry* **1999**, *47*, 2060–2066.

(168) Matsuo, Y.; Wakamatsu, H.; Omar, M.; Tanaka, T. Reinvestigation of the Stereochemistry of the C-Glycosidic Ellagitannins, Vescalagin and Castalagin. *Organic Letters* **2015**, *17*.

(169) Joshi, B. S.; Pelletier, S. W.; Newton, M. G.; Lee, D.; McGaughey, G. B.; Puar, M. S. Extensive 1D, 2D NMR Spectra of Some [7.0] Metacyclophanes and X-Ray Analysis of (+/-)-Myricanol. *Journal of Natural Products* **1996**, *59*, 759–764.

(170) Eliel, E. L.; Wilen, S. H.; Mander, L. N. *Stereochemistry of Organic Compounds*; John Wiley and sons, Ed.; New york, 1994; pp. 1120 – 1121.

(171) Inoue, T. Constituents of *Acer nikoense* and *Myrica rubra*. On Diarylheptanoids. *Yakugaku Zasshi* **1993**, *113*, 181–197.

(172) Liu, J. X.; Di, D. L.; Wei, X. N.; Han, Y. Cytotoxicity Diarylheptanoids from Pericaps of Walnuts (*Juglans regia*). *Planta Medica* **2008**, *74*, 754 – 759.

(173) Yang, H.; Sung, S. H.; Kim, J.; Kim, Y. C. Neuroprotective Diarylheptanoids from the Leaves and Twigs of *Juglans sinensis* against Glutamate-Induced Toxicity in HT22 Cells. *Planta Medica* **2011**, *77*, 841–845.

(174) Beier, R. C.; Mundy, B. P. Assignment of Anomeric Configuration and Identification of Carbohydrate Residues by 13C NMR: Arabino- and Ribopyranosides and Furanosides. *Journal of Carbohydrate Chemistry* **1984**, *3*, 253–266.

(175) Ye, L.; Yang, J. S. New Ellagic Glycosides and Known Triterpenoids from *Duchesnea indica* Focke. *Yao Xue Xue Bao* **1996**, *31*, 844–848.

(176) Hills, W. E.; Yazaki, Y. Properties of Some Methylellagic Acids and Their Glycosides. *Phytochemistry* **1973**, *12*, 2963– 2968.

(177) Sattar, E. A.; El-Olemy, M. M.; Elhag, H.; El-Domiaty, M. M.; Mossa, J. S.; Petereit, F.; Nahrstedt, A. Flavan-3-Ols and Prodelphinidins from *Catha edulis*. *Scientia Pharmaceutica* **1999**, *67*, 159–165.

(178) Yang, H.; Ye, X.; Liu, D.; Chen, J.; Zhang, J.; Shen, Y.; Yu, D. Characterization of Unusual Proanthocyanidins in Leaves of Bayberry (*Myrica rubra* Sieb. et Zucc.). *Journal of Agricultural and Food Chemistry* **2011**, *59*, 1622–1629.

(179) König, M.; Scholz, E.; Hartmann, R.; Lehmann, W.; Rimpler, H. Ellagitannins and Complex Tannins from *Quercus petraea* Bark. *Journal of Natural Products* **1994**, *57*, 1411–1415.

(180) Viriot, C.; Scalbert, S.; Lapierre, C.; Moutounets, M. Ellagitannins and Lignins in Aging of Spirits in Oak Barrels. *Journal of Agricultural and Food Chemistry* **1993**, *41*.

(181) Mayer, W.; Seitz, H.; Jochims, J. C. Die Struktur Des Castalagins. *Liebig's Annalen der Chemie* **1969**, *721*, 186–193.

(182) Lampire, O.; Mila, S.; Raminosoa, M.; Michon, V.; Du penhoat C. H.; Faucheur, N.; Laprevote, O.; Scalbert, A. Polyphenols Isolated from the Bark of *Castanea sativa* Mill. Chemical Structures and Auto-Association. *Phytochemistry* **1998**, *38*, 623 –631.

(183) Nonaka, G. I.; Ishimaru, K.; Watanabe, M.; Nishioka, I.; Yamauchi, T.; Wan, A. S. C. Tannins and Related Compounds. LI (i) Elucidation of the Stereochemistry of the Triphenoyl Moiety in Castalagin and Vescalagin, and Isolation of 1-O-Galloyl Castalagin from *Eugenia grandis*. *Chemical and Pharmaceutical Bulletin* **1987**, *35*, 217 –220.

(184) Malterud, K. E.; Anthonsen, T. 13-Oxomyricanol, a New [7.0]-Metacyclophane from *Myrica nagi*. *Phytochemistry* **1980**, *19*, 705 – 707.

(185) Yu, Y. F.; Lu, Q.; Guo, L.; Mei, R. Q.; Liang, H. X.; Luo, D. Q.; Cheng, Y. X. Myricananone and Myricananadiol: Two New Cyclic "Diarylheptanoids" from the Roots of *Myrica nana*. *Helvetica Chimica Acta* **2007**, *90*, 1691– 1696.

(186) Inoue, T.; Arai, Y.; Nagai, M. Diarylheptanoids in the Bark of *Myrica rubra* Sieb. et Zucc. *Yakugaku Zasshi* **1984**, *104*, 37–41.

6 Appendix

6.1 Plant samples and voucher specimen collection sites

Plant name	Region	Area of collection	Parts collected	Elev. (m)	Southings	Eastings
M. salicifolia	Arusha	Ngorongoro Conservation Area (Mokilali village), Repeater area	Stems, roots, leaves	2958	3.26998	35.43458
	Arusha	Arusha National Park, Miriakamba area	Roots, stems	2600	3.23539	36.78986
	Arusha	Monduli mountains area	Roots, bark, leaves	2188	3.2338	36.48629
	Kilimanjaro	Kilimanjaro National Park, Londorosi area	Stems, roots, leaves	2925	2.97628	37.1943
P. capensis	Arusha	Ngorongoro Conservation Area, Mishili village, Londolo area.	Roots, bark, leaves	1728	3.00993	35.53213
	Kilimanjaro	Uparo village, Kawawa road area	Roots, stems	888	3.37588	37.45669
	Arusha	Monduli Juu, Amairete village.	Bark, roots, leaves	1783	3.1418	36.2303
	Arusha	Lake Duluti Catchment forest reserve	Stems	1287	3.3911	36.78811
F. indica	Arusha	Nkoanenkole Catchment forest reserve	Roots, bark, leaves, stems	1383	3.32902	36.8601
	Kilimanjaro	Kikavu area near Weruweru village	Roots, bark, leaves, stems	926	3.32359	37.21609
V. apiculata	Arusha	Ngorongoro Conservation Area, Kitete wild life corridor	Stems, roots, leaves, bark	1778	3.20849	35.88888
	Arusha	Monduli Juu, Amairete village	Stems, roots, leaves	1772	3.25198	36.3912
	Arusha	Ngongongare village	Leaves, stems, roots	1385	3.31336	36.87664
	Kilimanjaro	Kikavu area near Weruweru village	Roots, bark, stems, leaves	926	3.32359	37.21609

6.2 Location of the interviewed TMPs

TMP	Gender	Age (Yrs)	Ethnical group	Region	District	Village	Elev. (m)	Southings	Eastings
1	M	59	Maasai	Arusha	Monduli	Emairete	1773	3.23862	36.38392
2	M	Elder	Maasai	Arusha	Monduli	Emairete	1816	3.25839	36.40024
3	M	Elder	Maasai	Arusha	Monduli	Emairete	1767	3.1536	36.24017
4	F	Elder	Maasai	Arusha	Monduli	Mti Mmoja	1387	3.41442	36.34145
5	F	Elder	Maasai	Arusha	Monduli	Mti Mmoja	1393	3.41611	36.27681
6	F	Elder	Maasai	Arusha	Monduli	Mti Mmoja	1411	3.40319	36.3166
7	M	68	Maasai	Arusha	Monduli	Mswakini juu	1055	3.62871	36.04805
8	M	71	Maasai	Arusha	Monduli	Mswakini juu	1087	3.66769	36.05683
9	M	Elder	Maasai	Arusha	Monduli	Esilalei	1076	3.48274	36.00033
10	F	89	Maasai	Arusha	Monduli	Lemiyoni	1099	3.56462	36.11232
11	M	74	Maasai	Arusha	Monduli	Makuyuni	1071	3.55265	36.09772
12	M	57	Maasai	Arusha	Monduli	Lokisale	1487	3.76241	36.42029
13	F	55	Maasai	Arusha	Monduli	Bwawani	1234	3.55982	36.59927
14	M	65	Maasai	Arusha	Monduli	Engaruka chini	805	2.99626	35.99886
15	M	85	Maasai	Arusha	Monduli	Engaruka Juu	886	2.99432	35.9734
16	F	Elder	Maasai	Arusha	Monduli	Selela	1051	3.21441	35.95958
17	M	Elder	Maasai	Arusha	Ngorongoro	Osinoni	1774	3.36267	35.09418
18	F	50	Maasai	Arusha	Ngorongoro	Enduleni	1687	3.22101	35.26678
19	F	50	Maasai	Arusha	Ngorongoro	Olerobi	2402	3.24484	35.48767
20	M	57	Maasai	Arusha	Ngorongoro	Olerobi	2487	3.20961	35.45918
21	F	52	Maasai	Arusha	Ngorongoro	Nainokanoka	2603	3.02535	35.69004
22	M	63	Maasai	Arusha	Ngorongoro	Nainokanoka	2603	3.02831	35.69046
23	M	Elder	Maasai	Arusha	Ngorongoro	Erkepus	1813	3.11943	35.68994
24	F	58	Maasai	Arusha	Ngorongoro	Erkepus	2368	3.11195	35.68204
25	F	Elder	Maasai	Arusha	Ngorongoro	Nakurro	2461	2.95734	35.70001

TMP	Gender	Age (Yrs)	Ethnical group	Region	District	Village	Elev. (m)	Southings	Eastings
26	F	Elder	Maasai	Arusha	Ngorongoro	Aleilalei	2421	2.9437	35.69836
27	F	Elder	Maasai	Arusha	Ngorongoro	Ngoile	1319	3.36626	35.48332
28	M	Elder	Maasai	Arusha	Ngorongoro	Oloipiri	2002	2.04288	35.43497
29	M	Elder	Maasai	Arusha	Ngorongoro	Sakala	2032	2.07235	35.60486
30	M	Elder	Maasai	Arusha	Ngorongoro	Masurumunyi	1212	2.5051	35.60578
31	M	65	Sonjo	Arusha	Ngorongoro	Samunge	1362	2.15496	35.70259
32	M	Elder	Sonjo	Arusha	Ngorongoro	Digodigo	1295	2.14626	35.73663
33	M	Elder	Maasai	Arusha	Ngorongoro	Engarasero	658	2.61299	35.8793
34	M	78	Maasai	Arusha	Ngorongoro	Engarasero	673	2.61638	35.87821
35	F	56	Maasai	Arusha	Ngorongoro	Engarasero	658	2.61299	35.8793
36	F	Elder	Maasai	Manyara	Simanjiro	Narakauo	1487	4.17542	36.50721
37	F	Elder	Maasai	Manyara	Simanjiro	Narakauo	1428	4.23035	36.49099
38	F	Elder	Maasai	Manyara	Simanjiro	Njiro	1361	4.46151	37.205
39	F	Elder	Maasai	Manyara	Simanjiro	Njiro	1339	4.45857	37.19987
40	F	Elder	Maasai	Manyara	Simanjiro	Laangai	1321	4.26816	37.2086
41	F	Elder	Maasai	Manyara	Simanjiro	Narosoito	1332	4.44078	37.20198
42	M	55	Muarusha	Manyara	Simanjiro	Namalulu	1407	4.34789	36.95582
43	F	50	Maasai	Manyara	Simanjiro	Sukuro	1456	4.03829	36.54712
44	F	Elder	Maasai	Manyara	Simanjiro	Sukuro	1473	4.01962	36.53444
45	M	Elder	Muarusha	Manyara	Simanjiro	Terrat	1406	3.88659	36.59645
46	F	80	Maasai	Manyara	Simanjiro	Terrat	1427	3.88068	36.58871
47	F	Elder	Maasai	Manyara	Simanjiro	Loswaki	1398	3.86568	36.61665
48	M	Elder	Maasai	Manyara	Simanjiro	Ngage	647	4.16888	37.4818
49	M	Elder	Maasai	Manyara	Simanjiro	Loiborsoit B	644	4.33889	37.46945
50	F	Elder	Maasai	Manyara	Simanjiro	Landanai	1174	4.0781	37.13743
51	M	Elder	Maasai	Manyara	Simanjiro	Naberera	1447	4.20551	36.93122
52	F	Elder	Maasai	Manyara	Simanjiro	Rotiana	1450	4.15155	36.82554
53	M	Elder	Maasai	Manyara	Simanjiro	Kitwai A	1120	4.70308	37.05108

TMP	Gender	Age (Yrs)	Ethnical group	Region	District	Village	Elev. (m)	Southings	Eastings
54	M	Elder	Maasai	Manyara	Simanjiro	Loibosiret	1358	4.2174	36.37105
55	M	77	Maasai	Manyara	Simanjiro	Emboreet	1518	3.97654	36.43325
56	F	60	Maasai	Manyara	Simanjiro	Loibosoit A	1576	3.88093	36.43081
57	M	Elder	Maasai	Manyara	Kiteto	Ndedo	1021	4.87433	36.78964
58	M	Elder	Maasai	Manyara	Kiteto	Ndaleta	1618	5.22357	36.49631
59	F	Elder	Maasai	Manyara	Kiteto	Mbigiri	1269	5.32589	37.02747
60	M	Elder	Maasai	Manyara	Kiteto	Kibaya	1469	5.31535	36.56672
61	F	Elder	Maasai	Manyara	Kiteto	Loolera	1257	5.36553	37.24114
62	M	Elder	Maasai	Manyara	Kiteto	Loolera	1287	5.39836	37.22775
63	M	Elder	Maasai	Manyara	Kiteto	Lembapuli	1241	5.38875	37.26522
64	M	Elder	Maasai	Manyara	Kiteto	Namelok	1646	5.39669	36.51591
65	M	Elder	Maasai	Manyara	Kiteto	Irkiushibor	1114	4.78977	36.38186

Note:

Elder = older TMP, looks older than 50 years but did not know his/her age

F = female TMP

M = male TMP

Elev. = elevation

Yrs = years

6.3 Reported medicinal uses of the four plants

Plant name	Diseases treated	Number of TMPs responding on particular disease	Total number of responding TMPs	%
M. salicifolia	Gonorrhoea	53	65	81.54
	Running nose/Flue	48	65	73.85
	Back pains	43	65	66.15
	Sinus headache	40	65	61.54
	Severe cough	36	65	55.38
	Joint pains	31	65	47.69
	Immunity boosting	30	65	46.15
	Abdominal pains	13	65	20
	Pneumonia	11	65	16.92
	Gouts	10	65	15.38
	Urination problems	10	65	15.38
	Fever	8	65	12.31
	Tonsillitis	5	65	7.69
	Colic	4	65	6.15
	Liver problems	2	65	3.08
	Diarrhoea	2	65	3.08
	Tuberculosis	2	65	3.08
	Malaria	2	65	3.08
P. capensis	Libido	58	65	89.23
	Blood loss	47	65	72.30
	Joint pains	45	65	69.23
	Back pains	38	65	58.46
	General body strength	33	65	50.77
	Abdominal pains	21	65	32.31
	Malaria	20	65	30.77
	Bile oversecretion	16	65	24.61
	Stomach upset	15	65	23.08
	Diarrhoea	15	65	23.08
	Gouts	12	65	18.46
	STDs	9	65	13.85
	Appetizer	8	65	12.31
	Urination problems	7	65	10.77
	Fever	4	65	6.154
	Colic	4	65	6.154

Reported medicinal uses of the four plants continued

Plant name	Diseases treated	Number of TMPs responding on particular disease	Total number of responding TMPs	%
F. indica	Fever	60	65	92.31
	Malaria	59	65	90.77
	Jaundice	57	65	87.69
	Enlarged spleen	56	65	86.15
	Joint pains	49	65	75.38
	Pneumonia	48	65	73.84
	Stomach upset	45	65	69.23
	Difficulty in breathing	45	65	69.23
	Back pains	43	65	66.15
	Gouts	33	65	50.77
	Mastitic breasts	32	65	49.23
	Asthma	27	65	41.54
	Dizziness	24	65	36.92
	Body strength	23	65	35.38
	Urination problems	22	65	33.85
	Diarrhoea	14	65	21.54
	STDs	13	65	20.00
	Bile oversecretion	4	65	6.15
	Phlegmon	2	65	3.08
	Burn wounds	2	65	3.08
V. apiculata	Eye infection/Sticky eyes	48	65	73.85
	Diarrhoea	43	65	66.15
	Stomach upset	42	65	64.62
	Reduced milk secretion	33	65	50.77
	General body strength	30	65	46.15
	Joint pains	24	65	36.92
	Back pains	17	65	26.15
	Gouts	12	65	18.46
	Malaria	12	65	18.46
	Lungs pain	6	65	9.23

6.4 Plant parts used

	M. salicifolia		***P. capensis***		***F. indica***		***V. apiculata***	
Plant part	**Number of responding TMPs**	***%***	**Number of responding TMPs**	***%***	**Number of responding TMPs**	***%***	**Number of responding TMPs**	***%***
Roots	53	81.5	48	73.8	60	92.3	58	89.2
Bark	60	92.3	52	80	44	67.7	14	21.5
Stems	18	27.7	19	29.2	23	35.4	30	46.1
Leaves	0	0	0	0	0	0	48	73.8

6.5 Plants collection and storage, remedies preparations, dosage, application form and application time

Plant	Plant parts collection and storage	Remedies preparation	Dosage	Application form	Application time
M. salicifolia	**Roots, stems and bark:** are collected from the wild, the outer dirty part is removed, the remaining part is sun dried, crushed and stored in a plastic bag or tightened glass or plastic containers. **Leaves:** The *V. apiculata* leaves are collected, dried, crushed and then stored in tightened containers.	**For all four plants:** **1.** Crushed (fresh/dried) plant parts are infused in warm water, thoroughly stirred and left to stand for a few hours before utilization. **2**. Crushed plants parts, drug decoctions and drug infusions, are mixed with boiling soup of either beef/goat/ lamb fatty meat, left to boil for several minutes, thoroughly stirred and consumed while warm. **3**. One teaspoon of crushed plant part roots/bark/stem is mixed in a boiling tea with milk, left to boil for a few minutes, then filtered and consumed. **4**. Powdered plant material is mixed with water, boiled, followed by addition of 2 spoons of ghee and filtered.	Depends on body weight. 250 – 1000 mL of remedy is taken in the morning and in the evening. Less is taken by children and pregnant women (about 250 mL).	Oral, inhalation.	Morning, afternoon and evening. Taken after meal.
P. capensis			No specific dose, but dose adapted to specific patients e. g. 250 mL for children, 500 mL for women and 1 L for men. Remedy is, taken 2 to 3 times a day until recovery.	Oral.	Preferably morning and in the evening, few minutes before meal. Can also be taken at any time.
F. indica			No specific dosage.	Oral.	Morning and/or evening. After or before meal time.
V. apiculata		*V. apiculata* leaves are placed in warm water, stirred, left for several hours, filtered then used to wash sticky eyes/ infected eyes. Another way of preparation is decoction, where by fresh or dried leaves are boiled with water, cooled, filtered and then utilized. **Note:** preparation for the bark, roots and stems, is described above.	No specific dosage.	Oral, bathing / washing infected eyes.	Morning and/or evening. After or before meal time.